CHROMATOGRAPHIC SEPARATION OF CARBOHYDRATES

A Thesis Submitted

by

Elnur Kamal Eldin Abusabah (M.Sc.)

for the Degree of Doctor of Philosophy

DEPARTMENT OF CHEMICAL ENGINEERING
UNIVERSITY OF ASTON IN BIRMINGHAM

April 1983

TO

SALWA AND ALL MY FAMILY

SUMMARY

The general theories of chromatography are reviewed. Also the theories concerning the chromatographic separation of sugar mixtures are presented and examples of industrial applications reported.

The general performance of zeolites, anion and cation exchange resins for the separation of carbohydrate mixtures using batch analytical techniques have been evaluated.

A Semi-Continuous Countercurrent Chromatographic Refiner (SCCR4) unit which has twelve 25.4 mm internal diameter stainless steel columns each of 750 mm length was used to separate feedstocks of either synthetic equimolar mixtures of fructose and glucose or inverted sucrose. The unit was packed with a cation cross-linked polystyrene resin in the calcium form. Fructose products of 93% purity and 2.0%w/v solids concentration were achieved. An intercolumn hold-up of 7% prevented higher purities being obtained.

An unexpected and significant shift in the location of the average column concentration profiles was found depending on which feedstock was used.

A larger SCCR7 unit with twelve 54 mm internal diameter stainless steel columns each of 750 mm length was constructed and packed with an anion exchange resin in the bisulphite form. The unit was used to separate either fructose and glucose mixtures or inverted sucrose at different operating conditions. Fructose and glucose products of 99% purity were achieved. Also for the first time with an SCCR unit fructose products with up to 12% w/v solids concentration were obtained. It was also found that there was no shift in the location of the concentration profiles depending on whether fructose and glucose or inverted sucrose mixtures were separated. Unlike the cation resin which was found to be very stable, the anion resin required frequent regeneration.

A theoretical model based on the plate equilibrium concept has been adapted to simulate the performance of the SCCR7 unit. Equilibrium data obtained at infinite dilution were used in the simulation. An approximate agreement between the experimental results and the model predictions was found.

A thesis submitted by Elnur Kamal Eldin Abusabah, M.Sc., to the Faculty of Engineering at the University of Aston in Birmingham, for the Degree of Doctor of Philosophy.

April 1983

Key Words: Chromatography, Continuous, Fructose, Glucose, Ion Exchange

ACKNOWLEDGEMENTS

The author is grateful to the following:

Professor G.V. Jeffreys and the Department of Chemical Engineering for making available the facilities for research.

Professor P.E. Barker, who supervised the work, for his help and guidance throughout this project.

Dr. G.A. Irlam for his helpful suggestions.

The former and present fellow members of the Separation and Purification Research Group for many helpful discussions.

The University of Gezira, Sudan, for the provision of a Scholarship.

Finally and above all, to my wife Salwa, for her encouragement and sustainment.

CONTENTS

LIST OF FIGURES

LIST OF TABLES

CHAPTER ONE

INTRODUCTION

Chromatography as an analytical tool is credited to a Russian botanist, Tswett, who gave it the name chromatography because it was initially used to separate plant pigments of different colours. However, most of the development and advances in the technique were made by Martin and Synge (1) who in the 1940s developed the concept of partition chromatography and in 1952, Martin and James (2) introduced gas-liquid chromatography.

Chromatography has been used primarily as a separation and isolation method. Unlike other physical and chemical methods, chromatography is intended to separate many component mixtures in a single step. The use of the technique in general analytical procedures for qualitative and quantitative identification of mixtures has increased significantly in the last few years. The powerful separating capacity of chromatography arises from the fact that even very fine structural differences within the molecular species, such as different isotopic composition, stereoisomerism, cis-trans isomerism or optical activity may give rise to chromatographic mobility.

Many industries appreciate the importance of chromatographic separation methods. Commercial scale plants are installed by food, petrochemical and cosmetic industries. Examples of these applications are the Finnsugar process (3) and the Südzucker process (4)

for desugarizing molasses. The Parex process (5) is used for the separation of p-xylene and the Sarex process (6) for the separation of sugars.

The future outlook of the current nutritive sweeteners market would indicate continued increases in the consumptions of sweeteners. This is because of population increases and changes in lifestyle throughout the world. These changes would prompt the development of means to supplement the classical sweetener, sucrose. The ideal substitute to sucrose is fructose which is the sweetest natural sugar and is contained in the sucrose molecule together with an isomer, glucose. Traditionally, fructose has been obtained from sucrose syrup produced by the cane and beet industries. This syrup when hydrolysed with mineral acids, yields an equimolar mixture of fructose and glucose. The mixture is then separated by chemical and physical methods to isolate pure fructose.

In 1970, Clinton Corn Processing Company, U.S.A. started to market a High Fructose Corn Syrup (HFCS) containing 71% sugar solids of which 50% w/w was glucose, 42% w/w fructose and 8% w/w higher saccharides (7). This syrup had a sweetness comparable with sucrose. The syrup is produced by the enzymic depolymerization and hydration of starch-based carbohydrates such as corn, rice and potatoes. Currently 40% of the sweetener market in the U.S.A. is supplied by HFCS. The same demand is for a similar syrup which could be obtained from rice in Japan. However, in Europe due to EEC

Agricultural Policy the introduction of high fructose syrup has been delayed and the full use was restricted in the past decade.

When the corn syrup generated a demand as a sweetener for soft drinks, tinned fruit, jam, baking, sweets and dairy products, much interest was then directed towards developing processes to enrich the proportion of fructose in the syrup. HFCS with 55-90% w/w fructose contents is now marketed in the U.S.A. This sweetener has advantages over sucrose since it is obtained from cheaper carbohydrate sources like corn and is much sweeter than sucrose. This is important for diabetics and weight-conscious people who require sweetness but less calories. Moreover the syrup can be stored without the danger of microbial growth (7).

Since 1967 large-scale separations of fructose from glucose have been performed in chromatographic columns packed with sulphonated co-polymer cationic resins in the calcium form. This ionic form is known to make a weak complex with fructose (8) which results in a preferential retardation of fructose, while glucose is carried through with the mobile phase. Most commercial scale processes in this respect employ repetitive batch chromatography. Notable examples of these processes are the Finnsugar and Südzucker mentioned before and the Boehringer-Mannheim process (8) and the Colonial Sugar Refining Co. process (9). Although continuous chromatography is more efficient in utilizing the entire resin volume and is more economical in terms

of energy and time, the majority of the applied processes are thought to be batchwise.

However, current reports (5,10,11) indicate that industrial interest is growing in continuous chromatographic processes. In the Department of Chemical Engineering, University of Aston in Birmingham, work has been continuing for several years on developing an efficient Semi-Continuous Countercurrent Chromatographic Refiner (SCCR). The historical development of these units for liquid chromatographic separations is summarised in Table 1.1. Although these units can be used for the separation of a wide range of mixtures, they have more recently been used for the separation of carbohydrates.

Since this work is a continuation of the previous researchers work on developing SCCR units for the separation of carbohydrates the set objectives are:

1. To modify an existing SCCR4 unit to improve the purity, concentration and rate of throughput of the products. This is because the maximum throughput obtained by the previous researcher Chuah (14) was only 75 gm/hr at a purity of 92% and a fructose product concentration of only 2.0% w/v.

2. Another objective is to investigate alternative packing materials like the inorganic molecular sieves, zeolites, and anion exchange resins. The latter seem attractive since in contrast to

TABLE 1.1 DEVELOPMENT OF SCCR UNITS FOR LIQUID CHROMATOGRAPHIC CARBOHYDRATES SEPARATION

Unit	Researcher Year	Columns Material	Packing Form	Systems
SCCR4	Ching (12) 1978	10(750x25.4)mm Glass	Zerolit 225 Ca^{2+}	Fructose/Glucose Separation
SCCR5	England (13) 1979	10(750x50.8) mm Stainless Steel	Silica Gel (gpc)	Dextran Fractionation
SCCR4	Chuah (14) 1980	12(750x25.4) mm Stainless Steel	Zerolit 225 Ca^{2+}	Fructose/Glucose Dextran Separation
SCCR6	Gould (15) 1981	10(750x108) mm Stainless Steel	Zerolit 225 Ca^{2+}	Fructose/Glucose Dextran Separation

the cation exchange resins which have been used by the previous researchers, they retard glucose and hence fructose emerges first and in higher concentration (16).

3. To investigate the possibility of using the SCCR unit to handle cheap sources of sugar mixtures such as sucrose or even molasses which is a by-product of the sugar refining industry.

4. To adapt an existing computer model (14) to simulate the performance of the modified SCCR unit under different operating conditions of flowrates, concentration and temperature.

CHAPTER TWO

LITERATURE SURVEY

2.0 SCOPE

The relevant literature to this research work is reviewed in the following two chapters. In the first chapter the general theory of chromatography is given together with the development and scaling up of equipments for liquid chromatographic processes.

The second chapter is devoted mainly to the chromatographic separation of carbohydrates. In this chapter the theory behind sugar separation is reported and some examples of industrial chromatographic processes are described.

2.1 THE DEVELOPMENT OF CONTINUOUS LIQUID CHROMATOGRAPHY

2.1.1 Introduction

Chromatography is a separation method whereby individual chemical compounds which are originally present in a mixture are separated by the selective process of distribution between two heterogeneous phases. These two phases are known respectively as the mobile and stationary phases. The stationary phase is the dispersed medium. It usually has a relatively large surface area through which the mobile phase is allowed to flow. The greater affinity of a particular solute for the stationary phase, the longer it will be retained in the system. However, the

elution of the solute depends on its equilibrium distribution coefficient, K_d, defined by:

$$K_d = \frac{q}{c} \quad \text{..... (2.1)}$$

where q = concentration of the solute in the stationary phase

and c = concentration of the solute in the mobile phase

2.2 CLASSIFICATION OF CHROMATOGRAPHIC METHODS

It is common to classify chromatographic separations in terms of three different categories. These are process techniques, retention mechanisms and the nature of the mobile and stationary phases, which are discussed below.

2.2.1 Process Techniques

According to the early work of Tiselius (17) there are three different process techniques namely, elution development, displacement and frontal analysis.

Elution development is shown in Fig. 2.1a. Here a pulse of sample is introduced into the top of the column bearing the stationary phase. A solvent then flows through the column, conveying the constituents in the sample. The different constituents transfer back and forth between the mobile and stationary phases. Because of mass transfer limitations the bands (peaks) of different components broaden as well as separate as they go down the column (18).

Fig. 2.1a Elution Development Chromatography

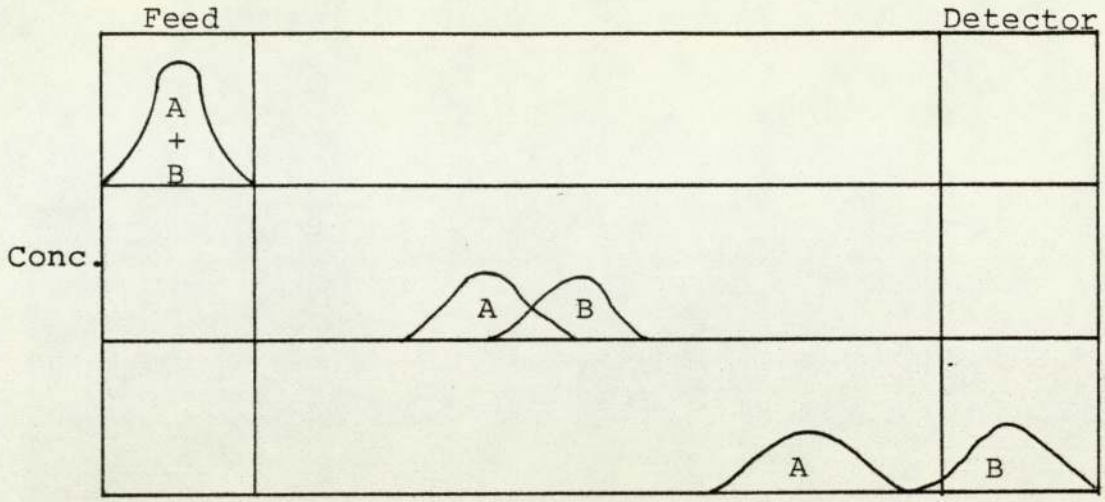

Fig. 2.1b Displacement Development Chromatography

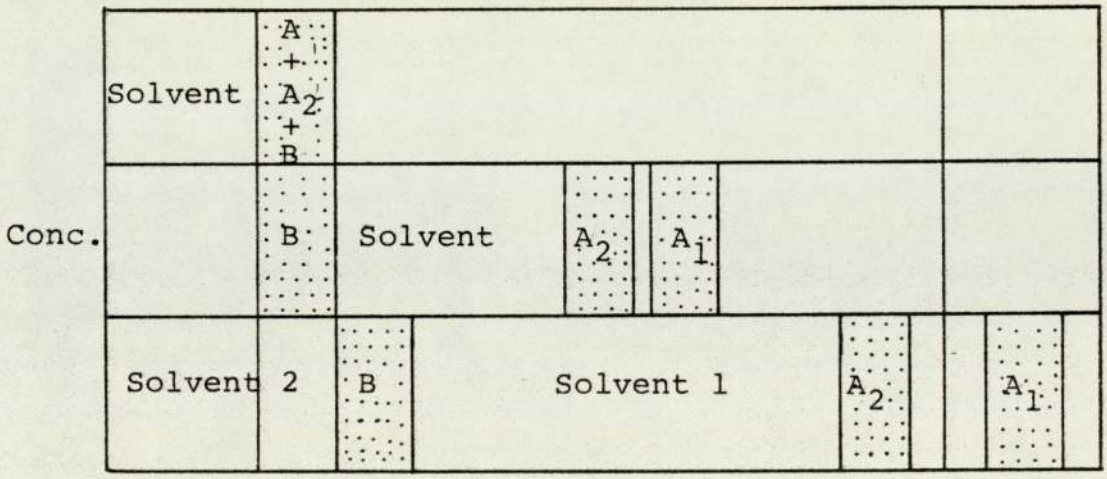

Fig. 2.1c Frontal Analysis Chromatography

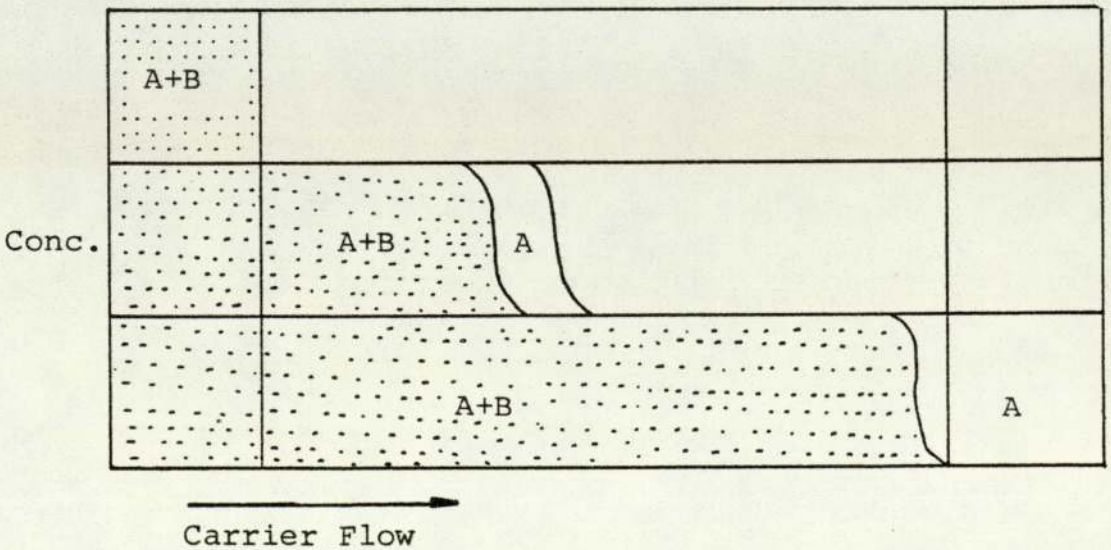

Displacement development is shown in Fig. 2.1b. It is similar to elution development. The only difference is that in this case one or more solvents are used which are more strongly held by the stationary phase than the components of the sample pulse. Hence the solvents displace the sample constituents.

Frontal analysis may be regarded as an integral form of elution development. Here the mixture to be separated is introduced as a step change rather than a pulse. The mixture continues to flow in after the change to it as a feed has been made. In Fig. 2.1c, component B is more strongly held by the stationary phase than A, so that A proceeds ahead of B. This technique gives a zone of pure A, but because of the sustained feed of mixture, cannot give a zone of B free of A.

2.2.2 Mechanisms of Retention

The velocity of migration of the solute components down a chromatographic bed is a function of the equilibrium distribution between the two phases. If a component favours the stationary phase it will migrate slower than that favouring the mobile phase. The means of achieving this differential migration is referred to as "the mechanism of retention". There are generally four types of retention mechanism, ion-exchange, exclusion, partition and adsorption as shown in Fig. 2.2.

Ion-exchange, which is based on selective ionic

Fig. 2.2 Classification of Chromatographic Processes

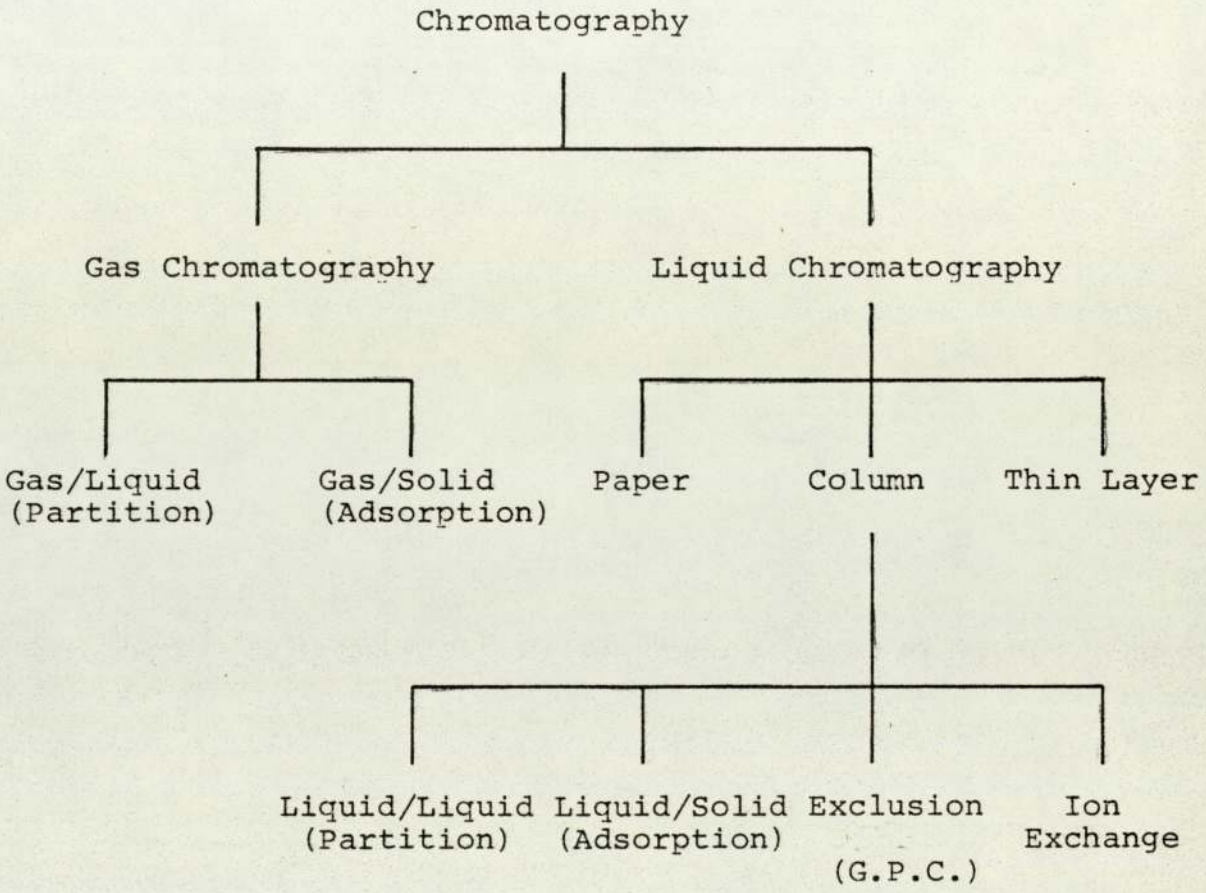

attractions between variously charged sample constituents and ionized chromatographic resins. The separation essentially involves exchange of ions between the resin and the sample constituents.

Exclusion, where the separation results because of the differences in the size of solute molecules. The stationary phase contains pores of molecular dimensions. An example is gel permeation chromatography (g.p.c.) where smaller molecules enter the stationary gel and are therefore retarded more.

Partition, where the separation is affected by the absorption of the solutes on an inert solid support coated with a liquid stationary phase.

Adsorption, where the separation is brought about by weak associations between the solutes and the active sites within the stationary phase. Such associations may be physical (physi-sorption) if the heat of reaction is between 15-20 kcal $mole^{-1}$ (19) or chemical (chemi-sorption) if the heat of reaction is between 20-30 kcal $mole^{-1}$ and do not involve the exchange of ions.

King (18) introduced two unconventional mechanisms which are: membrane permeation, where solutes are separated on the basis of their abilities to permeate through a thin membrane and reversible chemical reaction, where the solutes react to different extents, but reversibly, with the elements of the stationary phase. An example is affinity chromatography where certain chemical ligands are immobilized on the stationary phase and react selectively with the species

to be separated.

2.2.3 Nature of Stationary and Mobile Phases

Further classification of chromatographic methods is according to the type of mobile and stationary phase also shown in Fig. 2.2. Gas chromatography encompasses those methods in which the mobile phase is a gas, while liquid chromatography those in which the mobile phase is a liquid. The different stationary phases used give rise to the names liquid-solid and liquid-liquid chromatography.

In adsorption chromatography, the mobile phase is called the desorbent, and the stationary phase is the adsorbent. Adsorbents are solids having desirable characteristics. The conventional adsorbents used in chromatography are silica gel, aluminia, synthetic magnesium silicate and activated charcoal (20). Desirable characteristics of adsorbents include high capacity and selectivity for the material to be adsorbed together with chemical inertness to the desorbent and physical stability. Further requirements are good packing quality and completely reversible adsorption. These requirements are discussed later in Section 2.2.3.4.

Currently ion exchangers are widely used in adsorption chromatography (3,5,8). It is important to distinguish between the use of ion exchangers in ion exchange chromatography and in adsorption chromatography. In the latter case ion exchangers are essentially used as adsorbents during the actual

chromatographic separation. Their use as ion exchange materials in adsorption chromatography is limited to the initial stage when charging the ion exchangers to the desired ionic form or when it becomes necessary to regenerate the bed.

Two types of ion exchangers are used in adsorption chromatography. These are the inorganic ion exchangers and the synthetic ion exchange resins. Both types are discussed below.

2.2.3.1 Ion Exchangers as Adsorbents

Ion exchangers are solids which can exchange their mobile ions for ions of equal charge from the surrounding medium. The resulting ion exchange is reversible and stoichiometric with the displacement of one ionic species by another on the exchanger. Ion exchangers are either cation exchangers or anion exchangers depending on whether they have affinity for cations or anions. The principle of the ion exchange process can be demonstrated by considering the transit of a solute through a cation exchanger bed. The solute ion will tend to exchange with the mobile cation of the exchanger as follows:

$$R - H^+ + ION^+ \rightleftharpoons R - ION^+ + H^+$$

The forward process is called adsorption and the reverse process is called desorption. The equilibrium of the process is governed by the concentration of the solute ions and is generally expressed in terms of the distribution coefficient. A similar process for an

anionic exchanger and an anionic solute can be illustrated by:

$$R - Cl^- + ION^- \rightleftharpoons R - ION^- + Cl^-$$

Ion exchangers are widely used in industrial, medical and analytical fields. Such uses include the treatment of water, purification of sugars and extraction of rare metals like gold, platinum and uranium from ores, metal plating-baths and leaching solutions (20).

The most common type of ion exchangers that have gained significance in chromatographic processes is the synthetic ion exchange resin. In addition, the inorganic ion exchangers, commonly known as molecular sieves or zeolites, have aroused great interest because of their sound mechanical, thermal and chemical properties. The nature of these two types and their use as adsorbents in chromatographic processes are discussed below.

2.2.3.2 Inorganic Ion Exchangers

Inorganic ion exchangers were the first materials on which ion exchange processes were studied (20). Among the naturally occurring exchangers, aluminosilicates, known as zeolites have gained importance as cation exchangers. Currently zeolites with controlled properties are prepared synthetically. These synthetic zeolites, or molecular sieves, are crystalline sodium aluminium silicates.

Basically synthetic zeolites consist of three dimensional frameworks of SiO_4 and AlO_4 tetrahedra.

The tetrahedra are cross-linked by sharing oxygen atoms so that the ratio of oxygen atoms to the total atoms of aluminium and silicon is equal to two (21). The electrovalency of each tetrahedron containing aluminium is balanced by the inclusion of a metallic ion. The spaces between the tetrahedra are occupied by water. When the zeolites are activated by heating, the dehydration results in crystals interlaced with channels of molecular dimensions that offer very high surface areas for adsorption of foreign molecules.

The basic formula for synthetic zeolites is:

$$\frac{M_2}{n}O : Al_2O_3 : wSiO_2 : yH_2O$$

where

M = a metallic cation, normally Na^+

n = the valency

w = any value between 2.0-6.0

and y = any value up to 9

The mole ratio of silica to alumina, i.e.

$$\frac{wSiO_2}{Al_2O_3}$$

distinguishes two important types of zeolites, zeolite-X and zeolite-Y. These two zeolites have identical formulae except that zeolite-X has the value of $w = 2.5 \pm 0.5$ and zeolites-Y has w between 3 and 6 (21). The value of y depends on the degree of hydration of the crystals. The cation, M, predominant ly sodium, occupies the exchangeable cationic sites in the zeolites and may be replaced with other cations in

cation exchange processes.

An important feature of zeolites, other than ion exchanging, is molecular sieving. During the manufacturing process, the pore sizes of the zeolites are precisely controlled. A typical zeolite-A has a pore size of 5×10^{-8}m while zeolite-X and -Y have pore sizes of 10×10^{-8}m.

Zeolites are used as adsorbents in chromatographic processes because of the following favourable properties. Zeolites can be tailored to provide a wide range of selectivities. This is because of the three possible compositional variations of zeolites, namely the structure, the silica to alumina ratio and the nature of the exchangeable cation. Crystalline zeolites offer good kinetics because of the uniformity of structure. This means that the adsorption and desorption operations are completely reversible. In terms of chromatographic processes this implies the absence of tailing and less band broadening. Other properties of zeolites are chemical and physical stability and good packing quality. Zeolites are stable to heat treatment up to $500^{\circ}C$ (22).

Zeolites are used as molecular sieves for the separation of normal paraffins from branched-chain paraffinic and olefinic hydrocarbons. The most extensive use of zeolites in this respect is for the separation of paraxylene from mixtures of C_8 aromatics (23). Universal Oil Products (UOP) pioneered the use of zeolites for the separation of sugars. They reported

bench scale experiments for the separation of fructose and glucose mixtures by certain zeolites charged with selected types of cations (6,24,25).

2.2.3.3 Synthetic Ion Exchange Resins

Ion exchange resins are solid insoluble high molecular weight polyelectrolytes. The macromolecules of these resins consist of a three-dimensional network with large numbers of attached ionizable groups. These matrices are produced by polymerization of styrene cross-linked with itself and with divinyl-benzene (20). Fixed ions or functional groups are firmly and chemically bound to the matrices. The exchangeable ions are called counterions and the channels enclosed in the matrix are called pores.

Ion exchange resins are divided into four categories, strongly acidic and weakly acidic cation exchangers, and strongly basic and weakly basic anion exchangers. Strongly acidic exchangers contain sulphonic acid ($-SO_3^-H^+$) groups at their active sites, while weakly acidic exchangers contain carboxylic ($-COO^-H^+$) groups. On the other hand, strongly basic anion exchangers have quaternary ammonium groups ($-CH_2N^+(CH_3)_3Cl^-$), while weakly basic resins have functional groups such as ($-N^+H(R_2)Cl^-$) (26).

2.2.3.4 Properties of Ion Exchange Resins

Before choosing any resin as an adsorbent, some properties which determine the resin capacity, equilibrium

and kinetic behaviour must be examined. Such properties are reviewed below.

Capacity is the most important property which is essential to determine quantitatively how many counterions can be taken up by an exchanger. It is expressed in milliequivalents per gram (meq/g) of H^+, with respect to cation exchangers, and Cl^-, with respect to anion exchangers. The capacity is measured by the following formula (20).

$$\text{Capacity (meq/g)} = \frac{\text{Vol } (cm^3) \times \text{Nor}}{\text{Wt (gms)} \times \text{Sol}} \times 1000 \quad \ldots (2.2)$$

Where Vol and Nor are th volume and normality of the reagent that contains the exchangeable ions and Wt is the weight of the wet resin and Sol is the solid contents of the wet resin.

Selectivity is the degree of adsorption of a particular ion from the solute by the exchange resin. At low concentrations, all exchangers have greater affinity for polyvalent ions than monovalent ones in accordance with the following selectivity sequence (20).

$$Na^+ < Ca^{++} < La^{+++} < Th^{++++}$$

In the case of ions of identical valency, the selectivity increases with increasing atomic number thus

$$Li^+ < Na^+ < K^+ < Rb^+$$

$$Mg^{++} < Ca^{++} < Sr^{++} < Ba^{++}$$

$$F^- < Cl^- < Br^- < I^-$$

However, the selectivity for H^+ and OH^- ions depends on the strength of the acid or the base formed between the functional group of the resin and the H^+ or OH^- ions. The selectivity is determined quantitatively by the selectivity coefficient, β, which is defined by:

$$\beta = \frac{X_A/Y_A}{X_B/Y_B} \quad \ldots\ldots\ldots\ldots\ldots\ldots\ldots\ldots \quad (2.3)$$

where X_A and Y_A are the concentrations of the ion A in the solute and resin respectively and X_B and Y_B are the corresponding concentrations of the ion B.

Cross-linking is the degree of spatial interlinkage. Commercial resins usually contain 2-12% divinylbenzene as a cross-linking agent. Resins with a low degree of cross-linking are soft and mechanically unstable while resins with a high degree of cross-linking are hard and brittle with increased sensitivity to osmotic influences. The capacity of the resin is inversely proportional to the degree of cross-linking. A high degree of cross-linking decreases the moisture content of the resin and more importantly, it decreases the extent of swelling.

The swelling effect of the resin is the change in the volume that takes place during the transition of resin from one solvent to another. When the resin is surrounded by a dilute solution, the ions concentration inside the resin bead is much higher than in the solution and therefore there is a considerable osmotic effect trying to decrease the internal concentration by taking up the solvent. The extent of swelling depends on the surrounding medium, the nature of the

resin matrix and particularly the degree of cross-linking, the nature and concentration of the ionic group and the type of counterion (20).

Other important characteristics of resins are the particle and pore sizes. These will affect the flowrate and homogeneity of the chromatographic columns (27). In column processes small spherical particles with small range of size distribution are preferred since they offer a large contact area and thus high efficiency. On the other hand, small particles lead to higher pressure drops according to Kozeny's (28) equation for spherical particles:

$$\Delta P = \frac{180(1-\varepsilon)^2 u.l.v}{\varepsilon^2 d_p^2} \quad \ldots\ldots\ldots\ldots\ldots\ldots \quad (2.4)$$

where

ΔP is the pressure drop

d_p is the particle size

l is the column length

u is the fluid viscosity

v is the fluid velocity

ε is the porosity

The stability and attrition of a resin are determined by its resistance under various chemical and physical conditions. Chemical stability is manifested by the resistance of the functional group to oxidation. The sulphonic acid groups of strong cation exchange resins of the styrene type hardly change under the influence of pH or temperature. Strong anion exchange resins, on the other hand, tend

to suffer irreversible degradation and loss of capacity on ageing processes. Even oxygen in the air has a very strong action on anionic resins. Kunin (29) explained this phenomenum as an attack of oxygen on a weak link of the resin to form a peroxide and a free radical. The reaction then continues by a free radical chain, thus:

$$ROOH \rightarrow RO + HO^-$$

$$RO^- + R'H \rightarrow ROH + R'$$

$$HO^- + R'H \rightarrow H_2O + R'$$

where R and R' are aliphatic radicals.

These oxidation attacks are referred to as "auto-oxidation" and they are enhanced by the presence of iron or copper which act as catalysts (20).

Under high temperatures, resins undergo spontaneous thermal decomposition. Cation exchange resins are more stable under these conditions than anion exchange resins. Usually resin manufacturers indicate the highest operating temperatures together with acceptable pH ranges.

To complete this section on various types of chromatographic methods, the following part will be devoted to the mathematical models which have been formulated to describe the performance of these chromatographic processes.

2.3 CHROMATOGRAPHIC MODELS AND DEFINITIONS

Most research work on chromatography has been focussed on the batch mode. Parameters have been defined and models postulated to describe and measure the separation efficiency of chromatographic methods. The most important of these are the retention, resolution and column efficiency as discussed below.

2.3.1 Retention

A fundamental parameter in elution chromatography is the retention volume, V_R. It is defined as the total volume of the mobile phase that must pass through the chromatographic bed to elute the sample. A related parameter is the retention time, t_R, which is the retention volume divided by the flow rate of the mobile phase.

Kirkland (26) defined the relation between the retention volume, V_R, and the distribution coefficient, K_d, by:

$$V_R = V_M + K_d.V_s \quad \ldots\ldots\ldots\ldots\ldots\ldots \quad (2.5)$$

where

V_M and V_s are the total mobile phase and stationary phase volumes respectively.

Although this model has been developed for gel permeation chromatography, it has been generalised by Kirkland for other chromatographic processes. Audebert (30) defined a retention volume where gel permeation and adsorption both take a cumulative part as:

$$V_R = V_M + K_g.K_a.V_s \quad \ldots\ldots\ldots\ldots\ldots\ldots \quad (2.6)$$

where

K_g and K_a are distribution coefficients related to gel permeation and adsorption chromatography respectively. If one of these mechanisms is insignificant then it is omitted.

Another retention parameter is the capacity factor, k, defined by:

$$k = K_d \cdot \frac{V_s}{V_M} \quad \ldots\ldots\ldots\ldots\ldots\ldots\ldots \quad (2.7)$$

which is a measure of the time that the solute spends in the stationary phase, relative to the time in the mobile phase.

2.3.2 Resolution

The resolution, R_s, is a measurement of the degree of separation. It is defined by

$$R_s = 2\left(\frac{t_{R2} - t_{R1}}{W_1 + W_2}\right) \quad \ldots\ldots\ldots\ldots\ldots\ldots \quad (2.8)$$

where

t_{R_1} and t_{R_2} are the retention time for components 1 and 2, and W_1 and W_2 are band widths of components 1 and 2 determined by the intersection of the tangents at the inflection points of the Gaussian curve (peaks) with the base line as shown in Fig. 2.3. Equation (2.8) assumes that the peaks are symmetrical. Usually the peak width for a Gaussian band is taken as equal to 4σ, where σ is the standard deviation of the Gaussian function, then equation (2.8) can be written as

Fig. 2.3 A Chromatogram of Elution Chromatography

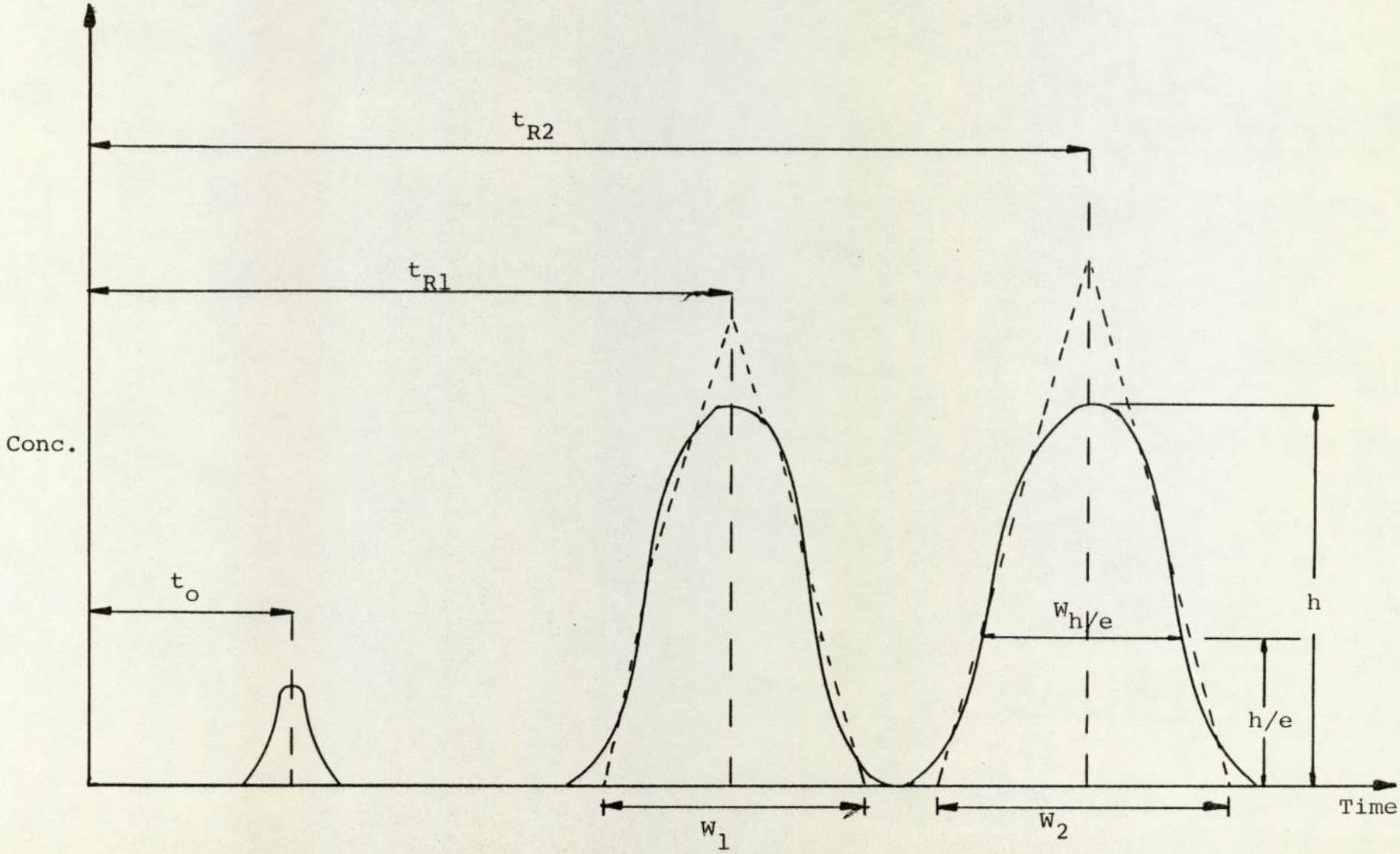

$$R_s = \left(\frac{t_{R_2} - t_{R_1}}{4\sigma}\right) \quad \ldots\ldots\ldots\ldots\ldots\ldots\ldots\ldots \quad (2.9)$$

Equations (2.8) and (2.9) indicate that the effectiveness of separation in chromatography depends on two important requirements. First, a disengagement of band centres ($t_{R_2} - t_{R_1}$) must be obtained through differences in migration rates of individual solutes. The control of migration rates is related to thermodynamic equilibrium. The second requirement is that the band widths ($W_1 + W_2$) must be kept narrow and compact to avoid overlapping. Dynamics of band broadening or, zone spreading, will be discussed in the following section.

A further model which relates the resolution, R_s, to retention and efficiency was developed by Purnell (31).

$$R_s = \frac{1}{4}\left(\frac{\alpha-1}{\alpha}\right)\left(\frac{k}{1+k}\right)N^{\frac{1}{2}} \quad \ldots\ldots\ldots\ldots\ldots\ldots\ldots\ldots \quad (2.10)$$

where α is the relative retention or separation factor

$$\alpha = \frac{K_{d_2}}{K_{d_1}} \quad \ldots\ldots\ldots\ldots\ldots\ldots\ldots\ldots\ldots\ldots\ldots\ldots \quad (2.11)$$

and N is the number of theoretical plates associated with the more retarded solute. Since N is directly proportional to the length of the column, it can be seen that to double the value of R_s, the column length must be increased by a factor of four. A chromatographic separation is generally considered to be adequate if $R \geq 1$ and complete if $R \geq 1.5$ (23).

2.3.3 Band Broadening

The narrowness of the chromatographic band is a crucial parameter for the effectiveness of separation. Obviously the narrower the band, the higher the resolving power of the column and the less the band will overlap. The mechanism of band broadening, previously known in the literature as "zone spreading" or "column dispersion" (32) is frequently studied. If a solute is introduced as a narrow band on the top of the column, it will be subjected to a number of statistical and kinetic events during the ensuing dynamic flow process. These events, associated with diffusion spreading, non-uniformity of flow and the rate at which the sample molecules are redistributed from one phase to another, are all responsible for broadening the band (33). The contribution of these factors to band broadening is strongly dependent on the rate of the solute transport through the system. The narrowness of the band reflects important column characteristics, such as the geometry of the column, nature as well as size of the packing particles, packing uniformity, and amount of stationary phase.

The development of concepts and mathematical expressions for band broadening has been one of the major theoretical and practical challenges of chromatography. These concepts and theories are reported by Giddings (33). The most popular of these theories are the theoretical plate concept and the rate theory.

2.3.3.1 The Theoretical Plate Concept

This model was developed by Martin and Synge (1). It was the earliest attempt to describe chromatography in a mathematical manner. The model is applied to chromatography by considering the column to be made up of a series of equal connected plates, each containing both stationary and mobile phases in equilibrium. Further assumptions are that the distribution coefficient is constant and independent of the concentration and the diffusion of the solute in the axial direction is neglected. The flow of the mobile phase is considered as discontinuous.

The mathematical expression of the plate theory indicates that the peak shape is that of a Poisson distribution, and in the limit of large plate numbers the band is Gaussian thus

$$C = C_o \exp\{-(V_M - V_R)^2 / 2\sigma^2\} \quad \ldots\ldots\ldots\ldots\ldots \quad (2.12)$$

where

C is the solute concentration

C_o is the concentration at the peak

V_R is the retention volume

V_M is the mobile phase volume

and σ^2 is the peak variance in units of volume

Since the variance of the band is the measure of the band width, the square root of the variance or the standard deviation, σ, is proportional to the width of the peak, W. Usually the width of the peak

is taken as equal to 4σ. Equation (2.12) can be written in terms of the plate number, N thus

$$C = C_o \exp\{-N(V_M - V_R)^2/V_R)\} \quad \ldots\ldots\ldots\ldots\ldots\ldots \quad (2.13)$$

Therefore the relation between the variance and the plate number is given by

$$N = \frac{V_R^2}{\sigma^2} = \frac{16V_R^2}{W^2} = \frac{L^2}{\sigma^2} \quad \ldots\ldots\ldots\ldots\ldots\ldots\ldots\ldots \quad (2.14)$$

N is regarded as a measure of the band broadening relative to the distance of migration and therefore the larger the plate number N, the less the band broadens and the more efficient is the system.

From a practical point of view it is not easy to measure the band width at the base line. Glueckauf (34) has related the elution time and the variance of the band to N. He selected a reference point to measure the band width defined by the height of the peak maximum, h, divided by the 'e', the base of natural logarithms, thus

$$N = 8\left(\frac{t_R}{W_{h/e}}\right)^2 \quad \ldots\ldots\ldots\ldots\ldots\ldots\ldots\ldots \quad (2.15)$$

where $W_{h/e}$ is the band width measured at a height equal to the peak maximum divided by e, as shown in Fig. 2.3.

Another parameter which is a natural product of the plate model, is the plate height, H, or the Height Equivalent to the Theoretical Plate, HETP, defined by

$$H = \frac{d\sigma^2}{dL} \quad \ldots\ldots\ldots\ldots\ldots\ldots\ldots\ldots\ldots\ldots \quad (2.16)$$

and for a uniform column,

$$H = \frac{\sigma^2}{L} = \frac{L}{N} \quad \ldots\ldots\ldots\ldots\ldots\ldots\ldots\ldots\ldots\ldots \quad (2.17)$$

H is also an efficiency parameter, the lower value of H the better the system.

Although the plate theory is widely accepted for comparing column efficiencies, it fails to account for kinematic processes occurring within the bed. The model does not indicate directly the relationship between the band broadening and the mobile phase velocity or the support particle size or the uniformity of the particle packing.

2.3.3.2 The Rate Theories

The rate theory was developed by Lapidus and Amundson (35). The theory incorporates mass transfer and longitudinal diffusion terms into the model. The model was further developed by van Deemter et al (36) to accommodate axial diffusion and finite rate of mass transfer. In the simplest form the model defines the plate height, H by:

$$H = A + \frac{B}{V} + C'_m V + C'_s V \quad \ldots\ldots\ldots\ldots\ldots\ldots\ldots \quad (2.18)$$

where

A = eddy diffusion term

B = longitudinal diffusion term

C'_m and C'_s = resistances to mass transfer in mobile and stationary phases respectively

and V = mobile phase velocity

Equation (2.18) implies that the terms contributing to the plate height are independent of one another. Giddings (37) proposed a coupling theory to link the resistance to mass transfer in the mobile phase and eddy diffusion. The general form of the Giddings equation is

$$H = \frac{B}{V} + C'_s V + \left(\frac{1}{A} + \frac{1}{C'_m V}\right)^{-1} \quad \ldots\ldots\ldots\ldots\ldots\ldots \quad (2.19)$$

Equation (2.19) suggests that the overall contribution to the plate height of the two coupled terms is smaller than their individual sum.

Generally the rate theory models relate the experimental parameters to the efficiency. The plate height, H, depends explicitly on the mobile phase velocity, on the nature and amount of the stationary phase, on the support particle size and the geometry of the packing and on the diffusion of the solute on both phases.

2.4 SCALING UP OF CHROMATOGRAPHIC PROCESSES

In the previous sections some theories of chromatography have been discussed. The early use of chromatography was as an analytical tool and therefore all the theories were related to small scale batch processes. When chromatographic processes proved to be viable, the scaling up of these processes to preparative

and commercial scale became of interest. The scaling up is associated with many problems such as the fluid flow pattern in large diameter columns, the effect of increased sample size and concentration and the effect of increased fluid velocities. The nature of these problems have been reviewed elesewhere (12). In this section some practical approaches to these problems will be discussed.

A typical analytical column may be 6 mm in diameter and 250 mm in length. The obvious approach to scaling up such a process is to use a larger column and the next step is to use a longer column or multiple columns in parallel arrangement. In the early stage of development the introduction of large diameter column was not wholly successful. Poor separation and excessive dilution of the eluted components made the application uneconomical.

When the liquid was introduced into the top of a large diameter column the front moved downwards at a rate different from that of the bulk of the liquid. This caused the concentration along the same radial plane to vary because of the uneven velocity profile which subsequently broadened the band. Giddings (37) showed that the efficiency of the column decreases with increase in diameter of the column. He suggested an additional term, H_c, to be added to the van Deemter equation (2.18) to account for this. The modified equation for height of the theoretical plate is:

$$H = A + \frac{B}{V} + C_s V + H_c \quad \ldots\ldots\ldots\ldots\ldots\ldots \quad (2.20)$$

and

$$H_c = G \frac{r_c^2 V^2}{\gamma D_m} \quad \ldots\ldots\ldots\ldots\ldots\ldots\ldots\ldots \quad (2.21)$$

where

G = constant

r_c = column radius

V = mobile phase velocity

γ = radial Labyrinth factor

D_m = diffusivity of the solute in the mobile phase

The practical solution of the problems associated with large diameters was approached by Badour (38) with the introduction of transverse baffles within the column. These baffles were used to induce lateral flow of the liquid. Lauer et al (39) introduced units for radial mixing and divided the column into several sections.

The introduction of built-in structures like baffles and mixers within the column made it difficult to backwash or regenerate the column packing. A different approach reported by Melaja (40) was tried by the Japanese who saturated the column with the solution to be separated and used counter-current flow in order to avoid disturbances caused by density gradients. The Melaja (40) approach to these problems was to use a baffle-free cylindrical container with distributors for supplying solution uniformally to the top of the column.

The next step towards production scale was the repeated feed injection method. This was a technique

where feed charges were regularly injected at set time intervals. These time intervals were calculated such that overlapping of bands was avoided. Although repetitive feed injection can improve batch chromatography, it has been established for all separation processes that the continuous mode allows better column utilization. The continuous mode of chromatographic process and its development is discussed in the following section.

2.5 CONTINUOUS MODE CHROMATOGRAPHY

The increased potential throughputs offered by continuous counter-current mode operations relative to batch co-current mode are illustrated by Fig. 2.4 in which the idealised solute concentration profiles obtained for a binary separation are compared (41). If high purity products are to be collected in repetitive batch processes, then the overlapped region Y-Z in Fig. 2.4a has to be recycled. Fig. 2.4b shows that for a continuous counter-current mode the solutes need only be partially resolved within the column to permit the collection of pure products. Here the entire power of the column is used to effect this partial resolution. In addition to greater throughputs and high product purities, continuous mode operations are normally more economical in terms of time and energy. All of these factors prompted many workers to develop chromatographic systems to work in the continuous mode.

Modern equipment for continuous chromatographic operation has been developed through four stages.

Fig. 2.4 Concentration Profiles for a) Repetitive Batch and b) Continuous Countercurrent

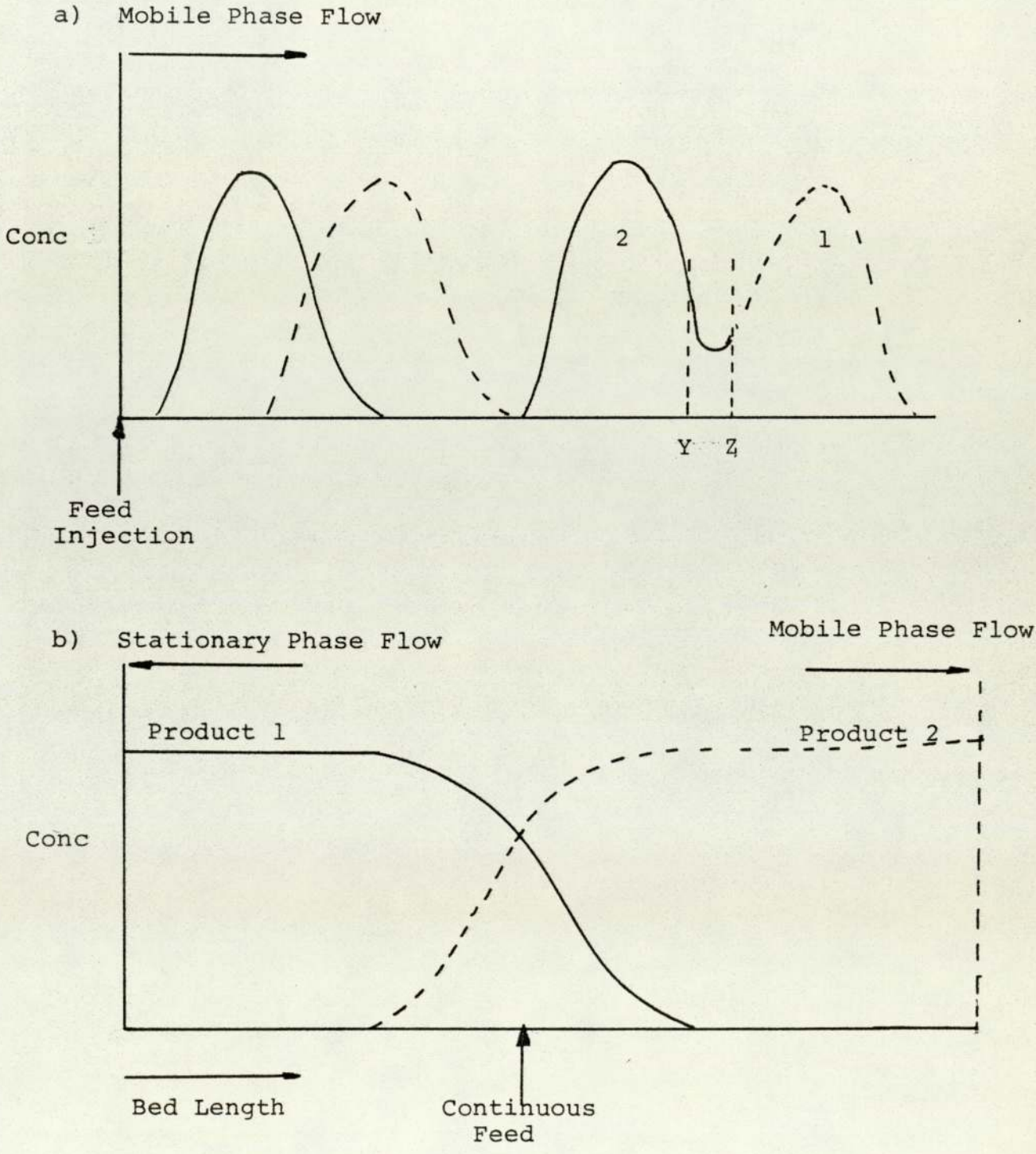

(1) Moving bed systems

(2) Moving column systems

(3) Moving feed point systems

(4) Simulated moving bed systems

2.5.1 Moving Bed Systems

In the case of moving bed systems, the packings flow under gravity counter-current to the mobile phase. The feed mixture is pumped into the centre of the column as shown in Fig. 2.5. The least strongly adsorbed fraction is carried upward to exit at the top of the column while the more strongly adsorbed fraction is carried down the column.

A typical apparatus of this kind was used by Barker and Critcher (42) to separate an azeotropic mixture of benzene and cyclohexane. Because of the bed movement, the packing quality is uneven and deteriorates due to attrition.

2.5.2 Moving Column Systems

Equipment with moving columns was developed to overcome the problems associated with moving bed systems. This used the rotation of a series of columns past fixed inlet and outlet ports against the direction of flow of the mobile phase, as shown in Fig. 2.6. Barker, Hatt and Somers (43) used such equipment for the separation of carbohydrates like glucose and starch, and also for the fractionation of dextran polymers. The major problem with moving column systems is to

Fig. 2.5 Apparatus for Moving Bed Systems

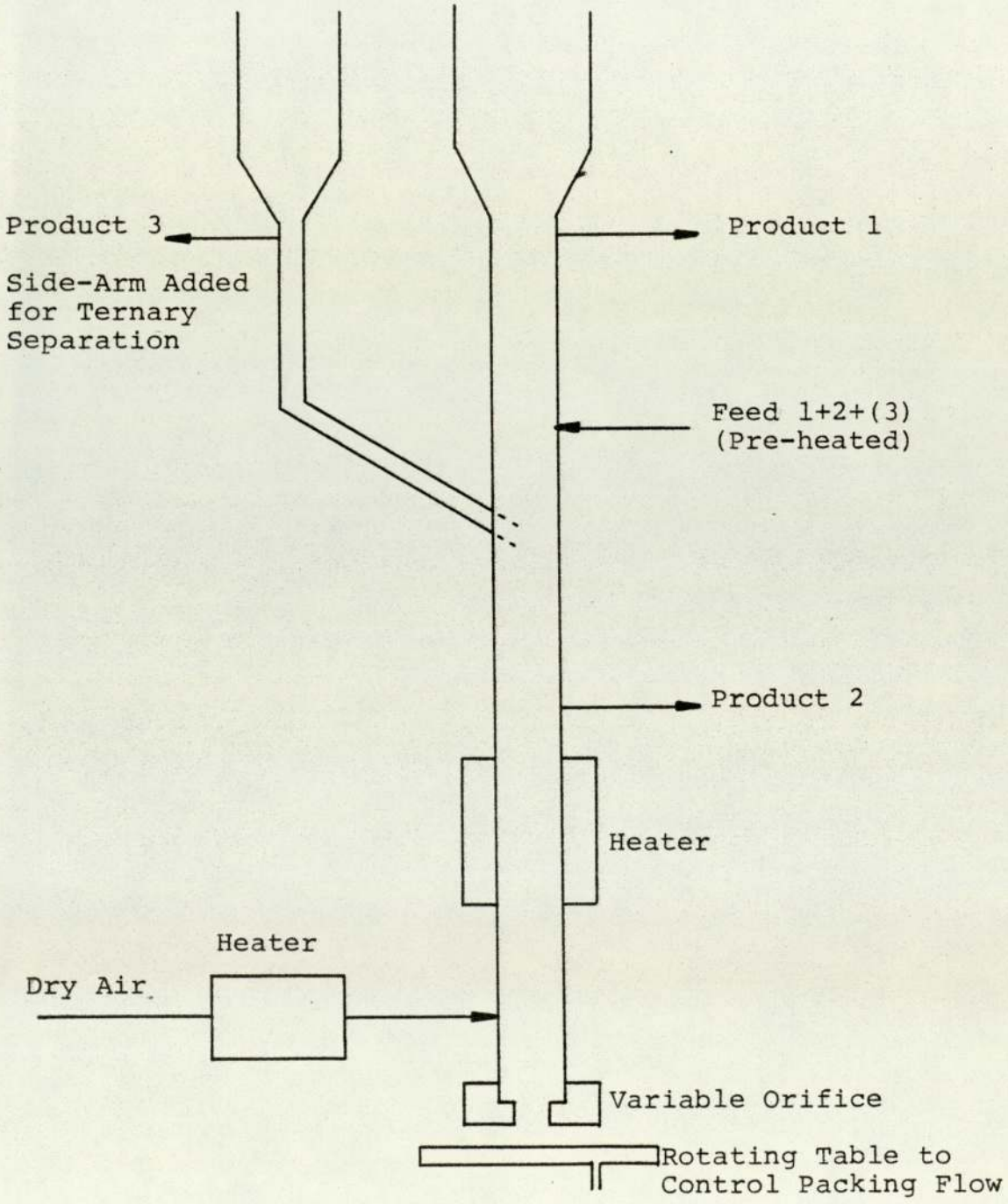

Fig. 2.6 Apparatus for Moving Column Systems

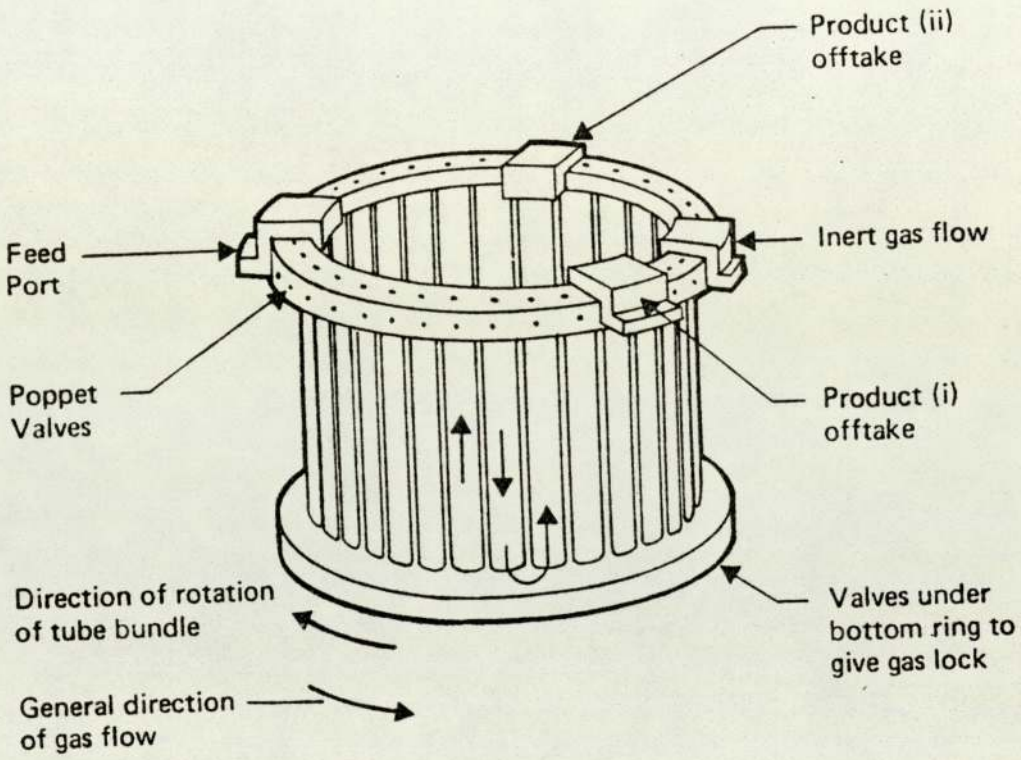

achieve a reliable mechanical seal between the static ports and the moving columns.

2.5.3 Moving Feed Point Systems

Moving feed point chromatography is intermediate between conventional preparative batch chromatography and simulated counter-current systems in complexity and efficiency. The technique was developed by Wankat (44) who studied the techniuqe theoretically with equilibrium models. Fig. 2.7 shows a typical moving feed point system used by Wankat and Oritz (45) to separate dextran 2000 from cobalt chloride in water. The system utilized a continuous flow of solvent into the top of a series of columns. The feed was introduced as a long pulse. The first portion of this pulse was introduced into the first column while the second portion was input to the second column and so on. Switching of the feed position was done automatically by a rotary valve which was controlled by a switching timer. The switching was timed so that the average velocity that the feed ports were switched were between the velocities of elution of the least and the more strongly adsorbed solutes.

From the experimental results obtained by Wankat and Oritz they considered that the moving feed system could produce separations with higher resolution in less time for the same throughput than a conventional batch system.

Fig. 2.7 Apparatus for Moving Feed-Point Systems

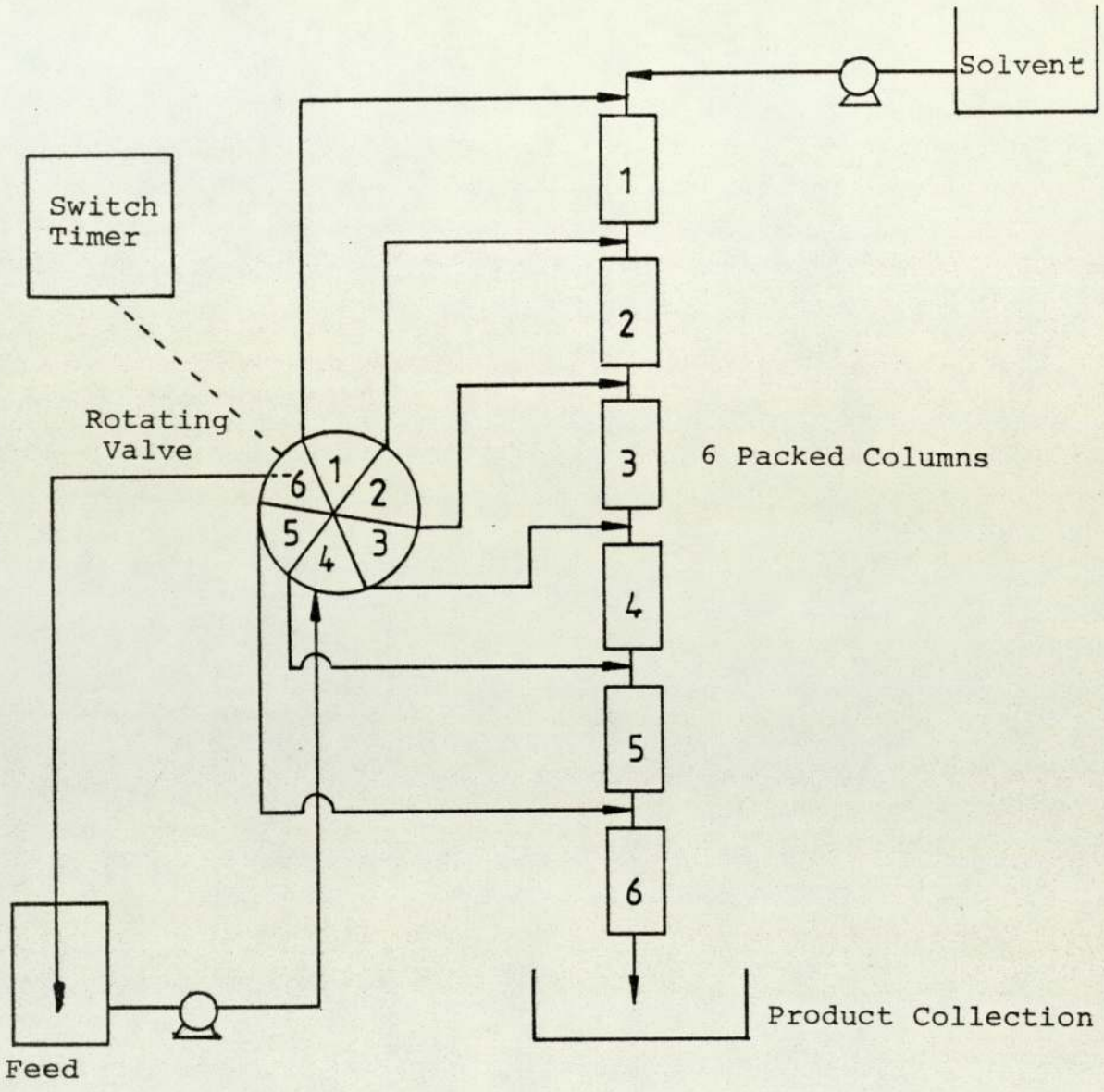

Although the moving feed point technique is related to the simulated counter-current technique, it does not utilize the adsorbent bed as effectively as a counter-current or simulated counter-current technique since there are time periods when the adsorbent in part of the system is doing no separation.

2.5.4 Simulated Moving Bed Systems

Universal Oil Product (UOP), U.S.A. developed a simulated moving bed process known as the Sorbex technique (46). Here the movement of the bed is simulated by holding the bed stationary and periodically alternating the positions at which a stream of liquid enters or leaves the column. Fig. 3.5 illustrates a process for the separation of mixtures of fructose and glucose using this technique.

Later Szepesey (47) proposed a scheme in which a switching valve was centrally mounted on a rotary PTFE disc. Rotation of the valve altered the relative position of the inlet and outlet ports to a stationary series of columns. In such a manner the counter-current columns movement is simulated. The Szepesey design still relies upon the rotary seal.

Barker and Deeble (48) designed a moving port apparatus whereby all the moving parts were eliminated except for the operation of valves of proven reliability to direct the various flows. The prototype equipment was made of twelve 76 mm internal diameter columns connected in series to form a closed loop. The equipment

was used for the separation of the binary halocarbon mixtures.

Ching (12) used a similar flow scheme in constructing a similar unit for the separation of carbohydrates. The largest reported unit in this respect was that constructed by Gould (15) to separate carbohydrates. This unit had ten columns each of 650 mm length and 108 mm diameter.

The apparatus designed and used for part of this research work uses a similar flow scheme and will be discussed later.

CHAPTER THREE

PRODUCTION AND SEPARATION OF SUGARS

3.1 INTRODUCTION

It is intended in this introduction to outline some properties which have a direct effect on the production and separation of glucose and fructose.

Glucose is the commonest monosaccharide, occurring free in juice of fruits and in honey. Abundant sources of glucose are starch, maltose and cellulose, which when hydrolysed all yield glucose (49). Fructose is another common monosaccharide frequently found with glucose in fruits. The hydrolysis of sucrose (common sugar) yields equimolar mixtures of fructose and glucose. Glucose and fructose are both soluble in water and although fructose is also soluble in ethers and alcohols, glucose is only slightly soluble in alcohols (49). Fructose is strongly laevorotatory (50) with a specific rotation of $(\alpha)_D^{20} = -132.2^o$ in water while glucose is dextrorotatory with $(\alpha)_D^{20} = 52.7^o$. This is why fructose is sometimes called laevoluse and glucose is called dextrose.

The formula of both sugars is $C_6H_{12}O_6$ but from the open chain forms of the two sugars shown in Figs. 3.1 and 3.2, it can be seen that glucose is an aldohexose as it contains the aldehyde group (CHO), and fructose is a ketohexose as it contains the carbonyl group (C=O). Fig. 3.1 shows three stable forms of glucose namely the open chain and the two pyranose forms α-D-and β-D-glucopyranose. In aqueous solution

Fig. 3.1 Different Forms of Glucose in Solution

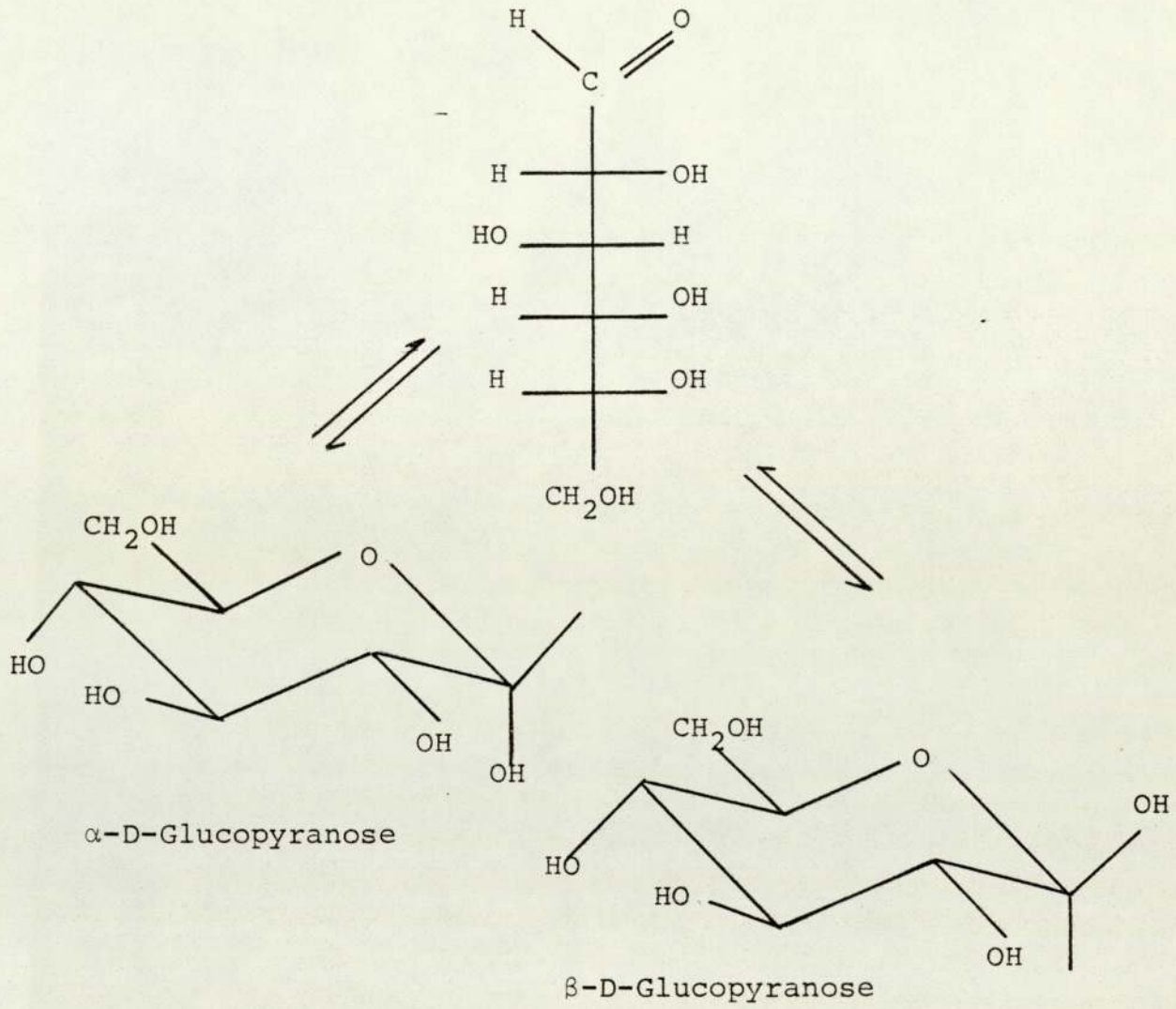

the equilibrium between these three forms is about one-third of α-D-glucopyranose and two-thirds β-D-glucopyranose with a very small amount of the open chain form (50). Fig. 3.2 shows the stable forms of fructose in solution. The equilibrium between these forms is a function of the temperature and the concentration of the solution (51). For example a 50% w/v solution at 23°C will contain 75% of the β-D-fructopyranose form, 21% of the β-D-fructofuranose form and 4% of α-D-fructopyranose.

Further properties of fructose which are related to its use as a sweetener in food industries are discussed in the next section.

3.2 IMPORTANCE OF FRUCTOSE AS A SWEETENER

During the last two decades since fructose has been industrially produced, it has become a substitute sweetener for sucrose in various food products. Although it is unlikely that fructose could ever completely replace sucrose, its use is expected to expand rapidly. At the present time high fructose syrups are used as sweeteners in foods such as confectionery and beverages. In the medical field pure fructose is important as a quick source of energy for patients who must be fed intravenously. Fructose has the following properties which favour it as sweetener in spite of its higher cost over sucrose.

Fructose is twice as sweet as sucrose (7). Sweetness is defined as the perception of the basic sweet taste (52). It is assessed by a panel of trained

Fig. 3.2 Different Forms of Fructose in Solution

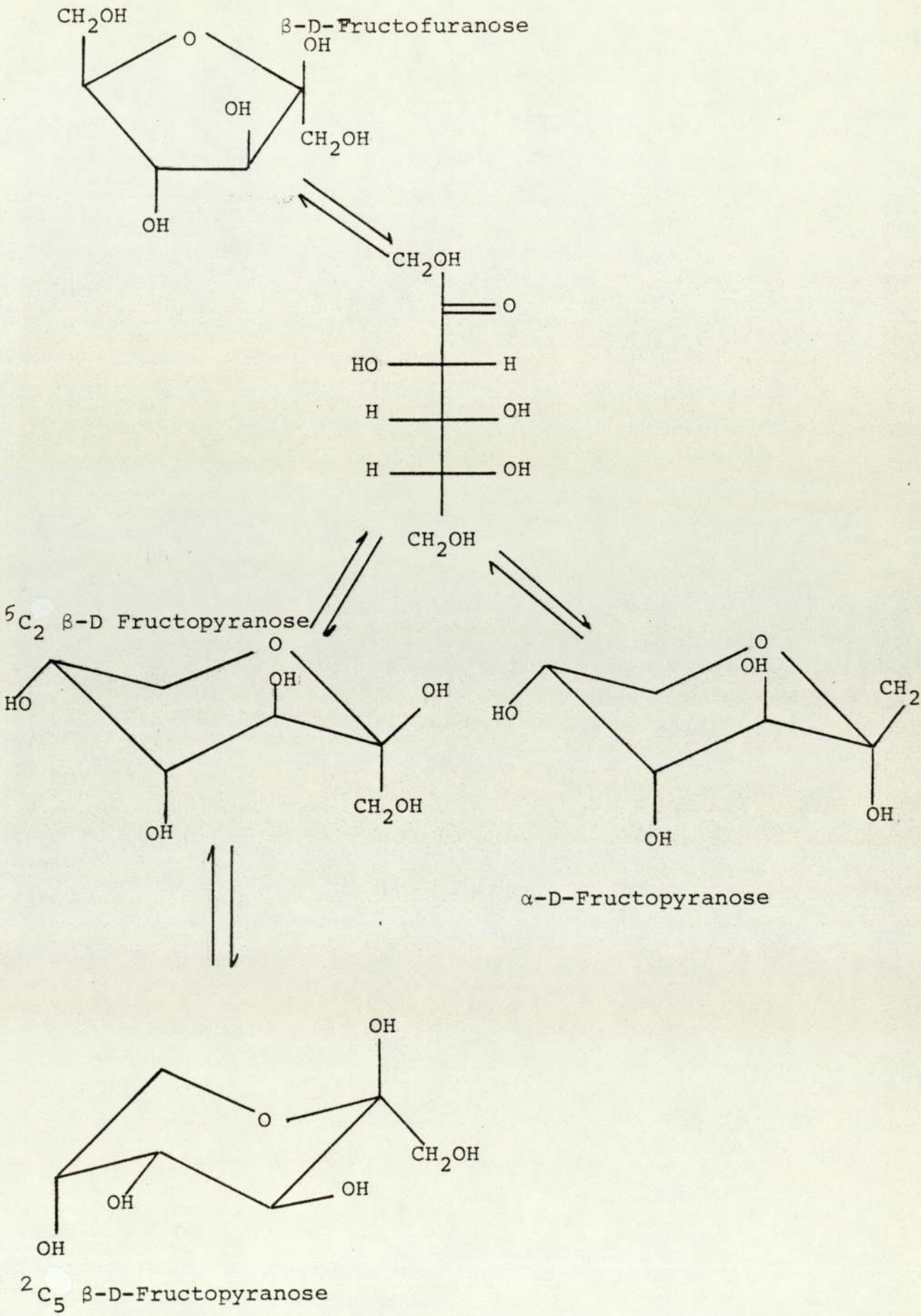

judges under controlled conditions. Sucrose is taken as a basis for sweetness assessment. Also fructose has been shown to have a synergistic sweetening effect with other sugars. The sweetness of a mixture of 33% w/w fructose and 67% w/w sucrose is the same as that of pure fructose, and a 99.7% w/w fructose solution with 0.3% w/w saccharin is 3-4 times as sweet as pure sucrose solution (52).

Fructose is highly water soluble. A saturated aqueous solution of fructose contains 78.9% w/v of fructose at 20°C while that of sucrose at the same temperature is 66.6% w/v. Also the viscosities of fructose solutions are lower than those of sucrose solutions. For example the viscosity of a 60% w/v fructose solution at 20°C is 0.034 kg m^{-1} sec^{-1} while that of an equivalent sucrose solution is 0.058 kg m^{-1} sec^{-1} (53). The solubility and viscosity of fructose solutions are important since fructose is used in the liquid phase as a sweetener.

Moreover, the calorific value of fructose is 3.7 kcal kg^{-1} while that of sucrose is 4.0 kcal kg^{-1}. Since fructose is sweeter than sucrose, this means that one gets more sweetness for less calories by taking fructose. This is important for diabetics and weight conscious people.

These considerations highlight the importance of developing processes for the production of commercial quantities of fructose at desired purities and at competitive prices. Fructose exists widely in nature. For example, almost one-half of the dry constituents

of honey is fructose and most fruits contain between 5 and 6% by weight fructose. However methods for isolating high purity fructose are difficult (53). Three methods are practiced in industry to produce fructose with varying purities and from different sources. These methods are:

(1) hydrolysis of inulin

(2) enzymatic conversion of glucose

(3) hydrolysis of sucrose

Hydrolysis of inulin is the earliest industrial method for the production of relatively pure fructose. Inulin is a polysaccharide extracted from the tubers and roots of Jerusalem artichokes and dahlias. The molecular weight of inulin is approximately 5000 which corresponds to a chain of 30 fructoses as shown by the structural formula of inulin in Fig. 3.3. The use of this method to produce fructose never gained significant importance in industry and has now been completely discontinued (53). The reason for this is that there is no readily available large scale source of inulin.

The other two methods are widely used for production of fructose. They are discussed below.

3.2.1 Enzymatic Production of High Fructose Corn Syrup (HFCS)

Several countries, who in the past have imported large quantities of raw sugars for further processing, have in recent years been developing alternative sucrose supplies from starches. Starch is an abundant source

Fig. 3.3 Structural Formula for Inulin

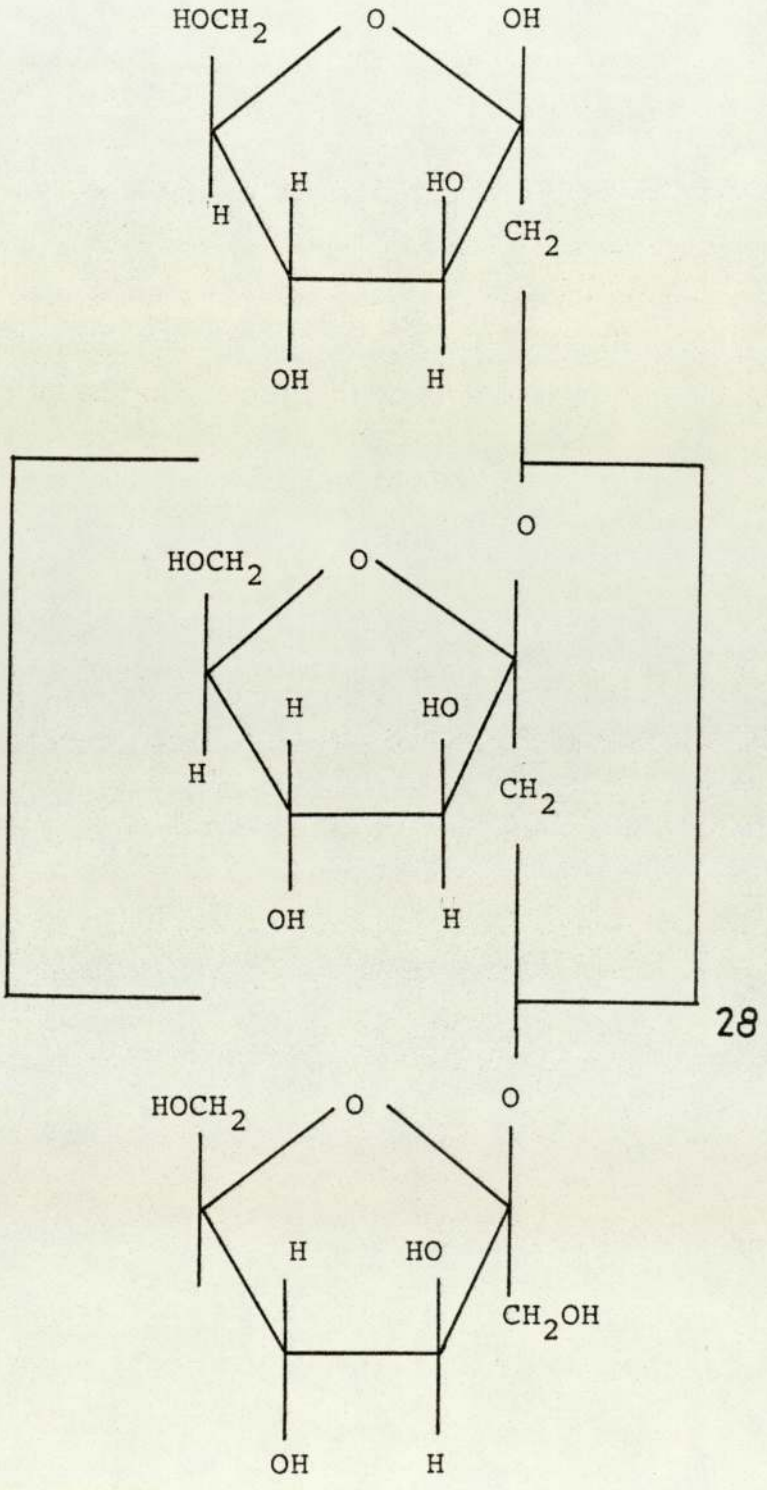

28

of glucose which can then be isomerized to fructose. Starch is obtained from vegetables like maize in the U.S.A., potatoes in the more temperate parts of the world, and rice in Japan. The enzymatic isomerization of sugars has been practiced since the late 1930s (12). Saccharifying enzymes were used to hydrolyse starch into glucose and the glucose was subsequently allowed to be partially isomerized with the enzyme isomerase to fructose. The mechanism of fructose isomerization is the rearrangement of a glucose molecule in an equilibrium reaction brought about by the isomeraze enzyme. It involves intermolecular proton transfer between adjacent carbon atoms in the sugar molecule. Fig. 3.4 illustrates such a transformation.

The first successful isomerization of glucose to fructose was carried out in 1957 by Marshall and Kooi (54), using a microbial enzyme obtained from Pseudomonous Hydrophila. In 1970 the Clinton Corn Processing Company of the U.S.A. became the first company to produce commercial scale High Fructose Corn Syrup (HFCS) based on the work of Takasaki (55). Five years later, I.C.I. Agricultural Division, U.K., reached an agreement with KSH of Holland to supply immobilized enzymes to process 200,000 tons of starch per annum at their refinery in Tilbury (7). Due to EEC restrictions, the refinery is now only processing 40,000 tons per annum of the syrup.

A typical HFCS syrup produced by an isomerization process is a water-white, odourless and rather viscous

FIG. 3.4 ISOMERIZATION OF GLUCOSE INTO FRUCTOSE

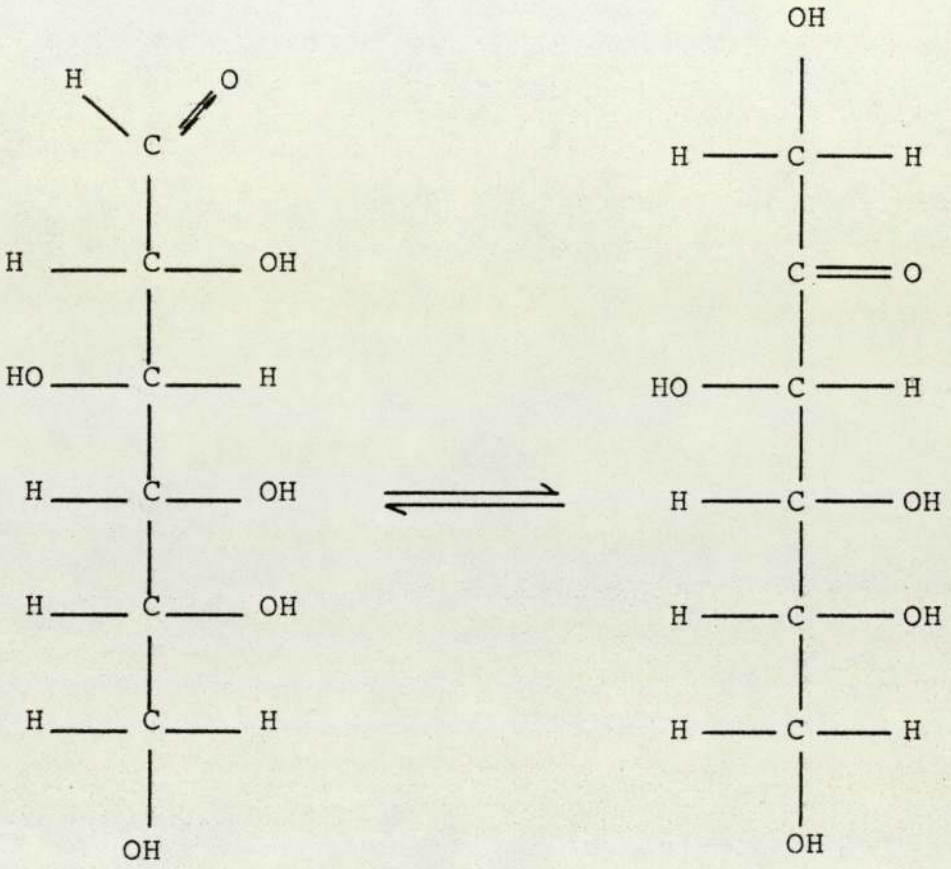

liquid containing 70% by weight solids. The solids are 42% by weight fructose, 55% glucose and 3% higher saccharides. Further separation processes are necessary to remove the glucose and concentrate the fructose before using this syrup as a sweetener.

One typical process for producing HFCS is the Sarex Process (56). This process has been recognised with an Honours Award for food processing systems in 1979. Some features of this process are described below.

3.2.1.1 The Sarex Process for HFCS

The Sarex Process was originally developed by UOP for the separation of hydrocarbons in the petrochemical industries (23). The process was adapted by ADM Corn Sweeteners, U.S.A., for the production of HFCS.

The production sequence of HFCS is shown as a block diagram in Fig. 3.5 and the separation unit is detailed in Fig. 3.6. Normally 42% HFCS is continuously charged into a single adsorption column via a distributing rotary valve. At the same time desorbent water is added through different parts of the rotary valve. The Sarex Process is simulating the movement of the stationary adsorbent by changing inlet and outlet ports to correspond with the appropriate liquid composition. This is accomplished by a specifically timed stepping of the rotary valve through which all the four primary streams pass. The column operates as a closed loop

Fig. 3.5 Production Sequence of HFCS

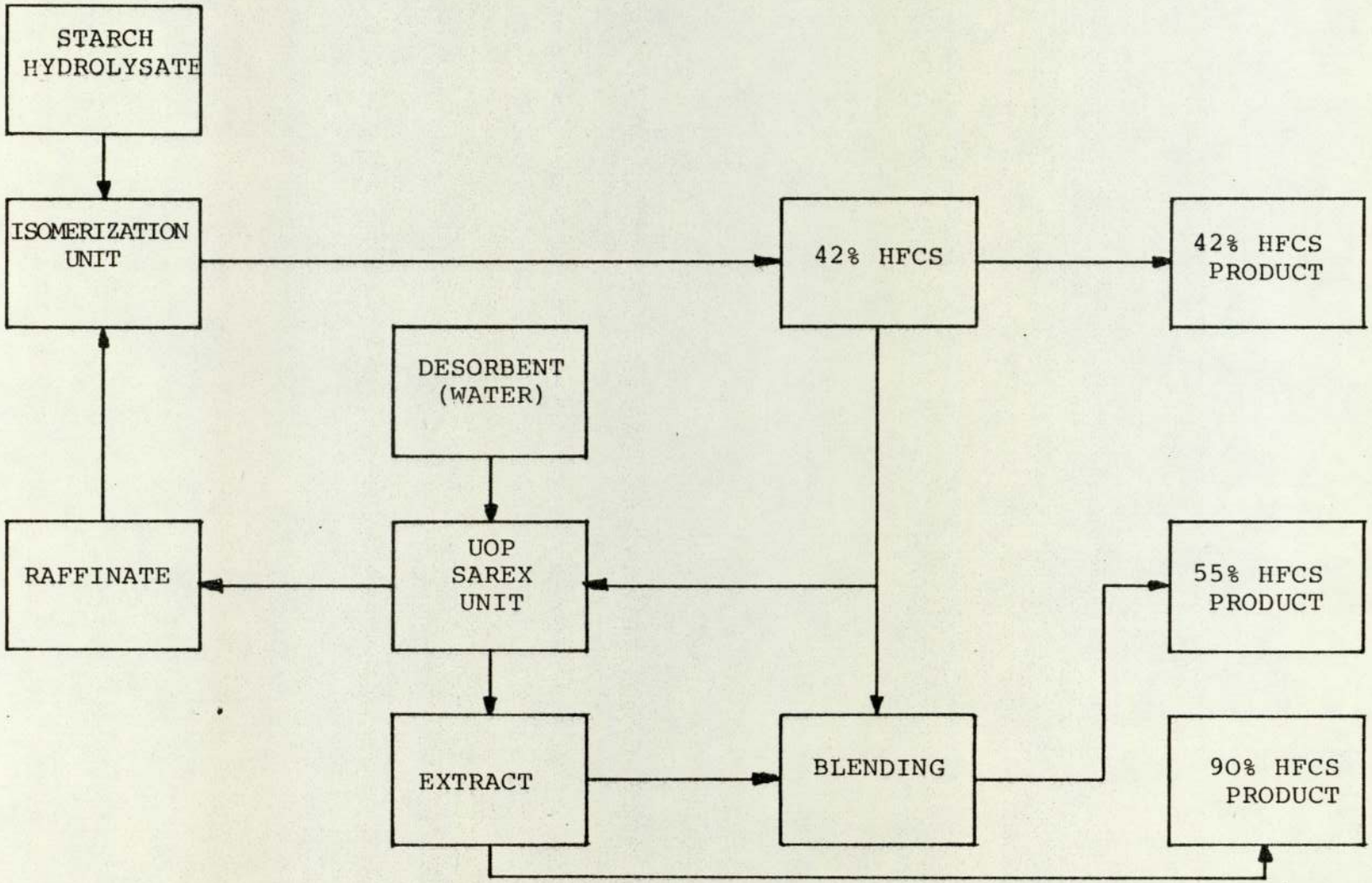

Fig. 3.6 The Sarex Process Flowsheet

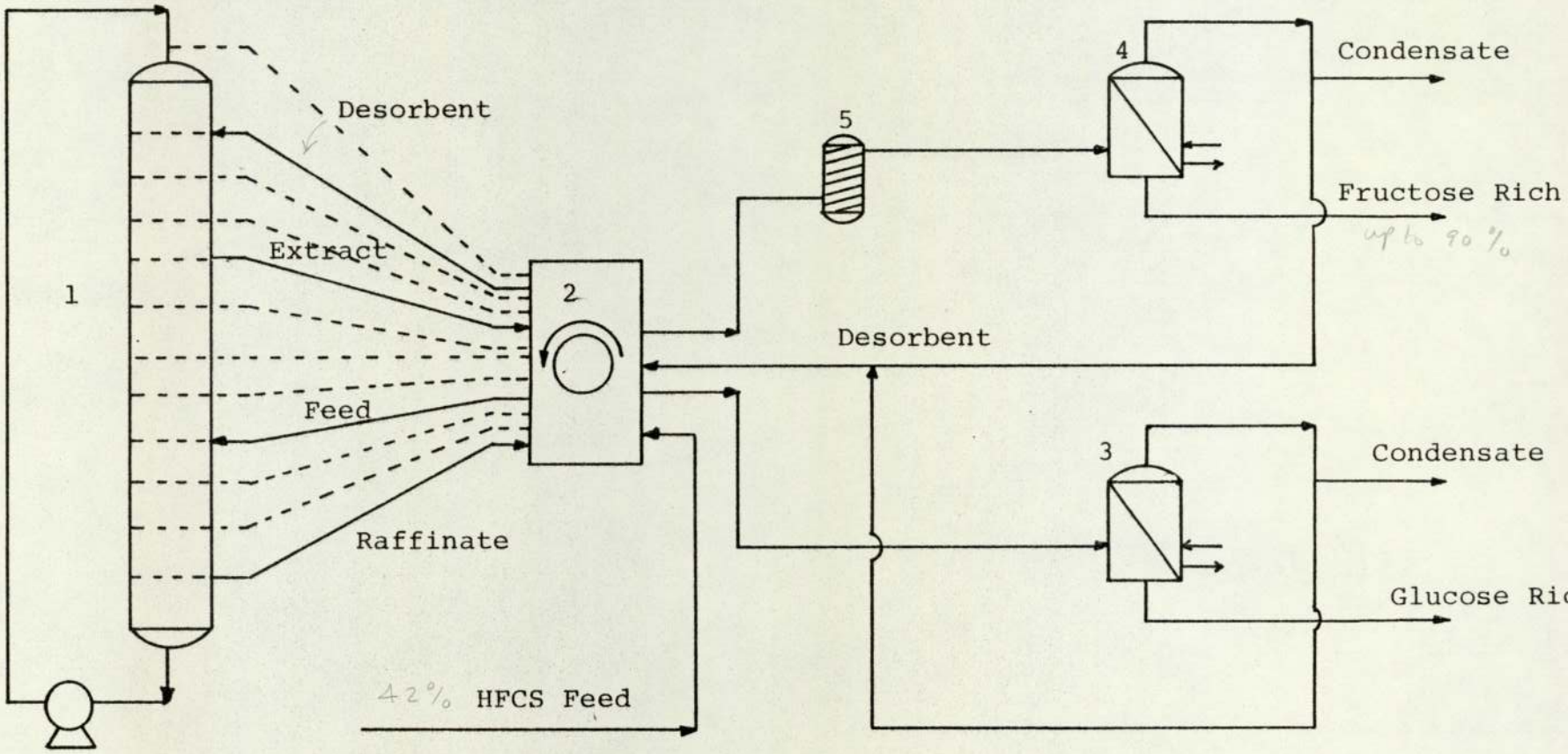

1. Adsorbent Chamber
2. Rotary Valve
3. Raffinate Evaporator
4. Extract Evaporator
5. Ion Exchanger

through a pump, which provides a positive flow of liquids from the bottom to the top of the adsorbent column. The extract (high purity fructose) and the raffinate (high purity glucose) streams are removed separately from different sections of the column continuously. Products from the process are purified by ion-exchange then concentrated by evaporation. The extract contains in excess of 90% of the original fructose in the feed and at more than 90% purity. The raffinate, which is mainly glucose, is recycled to the glucose isomerization channel for production of more 42% HFCS.

3.2.2 Hydrolysis of Sucrose

The structure of sucrose as illustrated by Fig. 3.7 shows that it contains one molecule of fructose and one molecule of glucose. On hydrolysis the molecule of sucrose breaks into an equimolar mixture of fructose and glucose. Hydrolysis of sucrose, sometimes known as inversion since the products are the invert sugars fructose and glucose, is an old practice. In fact the hydrolysis of sucrose and the precipitation of fructose was developed as early as 1847 (53).

Sucrose can be hydrolysed by either acid or resin treatment.

1. Acid Treatment. The sucrose solution is heated with a dilute acid such as hydrochloric, sulphuric or acetic. However, heat treatment of sugars is undesirable since it may cause thermal

Fig. 3.7 Structure of Sucrose (α-D-Glucopyranosyl-β-D-Fructofuranoside)

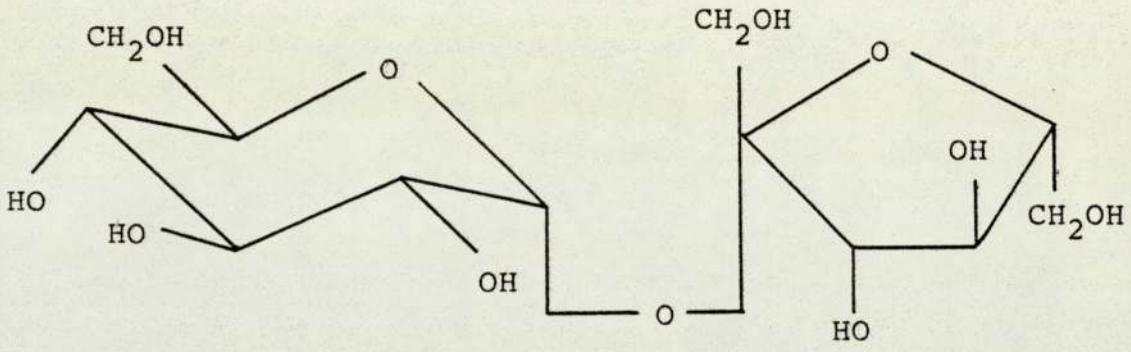

degradation of the sugars (57).

2. Resin Treatment. The inversion can be carried out very simply on a cation exchange resin in the H^+ form. Cation exchange resins with a low number of cross linkages are usually used for the inversion so as to facilitate the penetration of the resin beads by the solute.

Industrially the sucrose solution is percolated through a strongly acid cation exchange resin (58). The inversion is controlled by varying the temperature or the percolation speed. The regeneration of the resin is carried out by dilute hydrochloric or sulphuric acid.

The advantage of the resin treatment is that both inversion and separation of the products can be carried out simultaneously in the same bed. This is possible if the original resin in the H^+ form is treated with a 10% w/v calcium chloride solution at room temperature. Such treatment will leave up to 30% of the H^+ ions unreplaced by the Ca^{2+} ions. The H^+ ions will then effect the inversion of the sucrose and the Ca^{2+} ions will effect the separation of fructose and glucose (8).

Although pure sucrose solution is an ideal starting material to yield a fructose and glucose mixture on hydrolysis, significant economic advantages are obtained if the sucrose is supplied to the process in the form of a by-product of the cane and/or beet sugar refineries. One of the most readily available and cheap by-product of sugar refineries is the viscous liquid known as

molasses, which contains a significant portion of dissolved sucrose. Molasses contains between 13 and 15% w/w of the total sugars originally present in the beet or cane (59). The other constituents of molasses are organic matters such as amino acids and colouring pigments, and metallic ions such as Mg^{2+}, Ca^{2+} and K^{+} ions. The sugar constitutes up to 66% w/w of the solid contents of the molasses.

Some reports (3,16) indicate the possibility of carrying out all of the processes of desugarizing the molasses, then hydrolysing the sucrose and separating the invert products by chromatographic means.

Since the product of hydrolysis of sucrose or the enzymatic isomerization of glucose is always a mixture of fructose and glucose, this mixture needs further separation to produce pure sugars. Two methods are used to separate the fructose and glucose mixture. The conventional method is by the chemical precipitation of one of the sugars, and a novel approach is to use a chromatographic technique. These two methods are discussed below with special emphasis on the chromatographic technique.

3.3 CHEMICAL SEPARATION OF FRUCTOSE/GLUCOSE MIXTURES

The chemical separation technique involves the precipitation of fructose with an alkaline earth metal. The technique takes advantage of the fact that the fructose complexes with the alkaline earth metals, are less soluble in water than the corresponding

complexes of glucose. One process relying on this technique is based on adding calcium hydroxide to precipitate the fructose as a calcium salt. This insoluble salt is then separated by filtration. An acid, usually phenol is added to decompose the salt. Then the fructose is concentrated and finally crystallized from the solution.

Another process is based on the oxidation of glucose with bromine or iodine to form gluconic acid, followed by the separation of fructose which is not oxidised. The fructose produced by such chemical precipitation techniques does not meet modern industrial standards (60). For example even at low temperatures colouration of the precipitated fructose indicates that the sugar is chemically degraded.

3.4 CHROMATOGRAPHIC SEPARATION OF FRUCTOSE/GLUCOSE MIXTURES

The sugar industry has been the first to use ion exchange resins in its manufacturing process (58). Ion exchange resins have been used in sugar refineries for decolourising and purifying syrups. However, the use of ion exchange resins as chromatographic adsorbents, rather than ion exchangers, for sugar separation is relatively new. The earliest reported use of the chromatographic separation of sugars is by Samuelson and Sjöstrum (61) in 1952.

Currently chromatographic methods are widely used in analytical and large scale separation of fructose

and glucose mixtures. Both types of cationic and anionic exchangers can be used as adsorbents as discussed below.

3.4.1 Separation by Cationic Exchangers

In 1962 three consecutive U.S. patents appeared to describe processes for separating fructose from glucose. The first one by Serbia (62) illustrated a method based on feeding a solution containing a mixture of fructose and glucose into a column packed with a cation exchange resin in the calcium salts. In a second patent, Leferve (63) suggested barium and strontium instead of calcium. Also Leferve (64) described the use of Dowex 50W-X4 in the silver salts. All of these processes are limited to analytical applications. Their commercial importance was not appreciated. In 1967 Boehringer et al (8) were granted a British patent. They claimed a process for the separation of mixtures of fructose and glucose using a 50% w/w sucrose solution as a feed. The process used the cation exchange resin Dowex 50W-X4 which had been charged to the Ca^{2+} form, with a 10% w/v calcium chloride solution at room temperature. This treatment of the resin was claimed to leave some of the H^{+} ions unreplaced by the Ca^{2+} ions. The Boehringer process utilized six glass columns 150 mm in diameter and with a total separating length of 9 metres. The eluent flow rate was between 0.6-1.2 $m^3 hr^{-1}$. The patent stated that the degree of separation

was virtually the same whether the starting material was a sucrose solution or a mixture containing fructose and glucose. The process used repeated feed injection and recycling of contaminated products. The separation was performed at 60°C.

An equally important process which was disclosed at the same time as the Boehringer process, was that of the Colonial Sugar Refining Co. (9). The process used Dowex 50W-X4 in the Ca^{2+} form for the separation of the fructose and glucose mixture at 60°C. The resin bed was 1.8m long and the system was operated in a co-current batch mode with various recycles. The collected products differed in purity and concentration. One fructose-rich product fraction had a concentration of 29% w/w solids of which 82% was fructose.

In the late 1970s chromatographic separation of fructose from sugar mixtures was attempted using zeolites (24,25). In 1977 two different U.S. patents were granted to Odawara et al (65) and Neuzil et al (24). The Odawara process, which was assigned to Toray Industries, Inc. described the separation of a mixture of fructose and glucose using zeolite X and zeolite Y in the K^{+}, Ba^{2+}, Sr^{2+} and Ca^{2+} forms. Two years later Odawara et al (11) disclosed a process for continuous separation of a mixture of fructose and glucose. The process utilized a simulated counter-current flow system. They claimed that the system was capable of being operated at temperature ranges from 10 to 100°C and at linear flow rates of

up to 72 m hr^{-1}. Bieser et al (6) consider that the performance of the zeolites is superior to that of the commercially available resins. When packing the Sarex equipment (section 3.2.1.1) with an inorganic adsorbent they obtained a 94% w/w pure fructose product from HFCS which originally had 41.1% w/w fructose, 51.8% w/w glucose and 7.1% w/w higher saccharides.

The theory behind the chromatographic separation in all the cases mentioned above is that fructose makes a weak complex with the metallic ions on contact and it is therefore retarded. Since the glucose does not complex with the ions, it emerges first. The complex formation of fructose and metals is the subject of the next section.

3.4.1.1 Sugar Complexes with Metal Ions

Research work on the complex formation of different cations and sugars has been going on since the ninteenth century. The results of this work have been comprehensively compiled by Lippman (66) and Vogel et al (67). Relatively new research on the subject conducted by Saltman and Charely (68) has shown by dialysis experiments that Ca^{2+}, Ba^{2+}, Mg^{2+} and Sr^{2+} ions form soluble compounds in aqueous alkaline solution with the sugars, galactose, arabinose, maltose, lactose and fructose. Further proof of the existence of sugar complexes with metal ions was conducted by Charley and Saltman (68). They showed

that the absence of any precipitation of alkaline earth metal hydroxide when an aqueous solution of fructose and alkaline earth salt is made alkaline by adjusting the pH to 12, is supporting evidence for the existence of sugar complex with metal ions.

Although these studies have provided sufficient evidence of the existence of such complexes, the chemical formulae and the favourable conditions for the complex formation is still hypothetical. The most important hypothesis on this subject is that of Angyal (69), reviewed below.

3.4.1.2 The Angyal Hypothesis

The most important work in this area was conducted by Angyal (69,70,71,72). In a recent report, Angyal et al (73) suggested that, "in solution a sugar forms a reasonably strong complex with cations if it contains a sequence of an axial, an equatorial and an axial hydroxyl group on a six-membered ring, or a sequence of three cis-hydroxyl groups on a five membered ring". Fig. 3.8a shows a Cis and Trans arrangement and Fig. 3.8b shows conformational behaviour of a six-membered ring illustrating the terms equatorial and axial arrangement of bonds. Bonds which are parallel to the axis C3 are termed axial while those which on projection towards C-axis describe tetrahedral angles with it are termed equatorial (50). Angyal concluded that it is reasonable to expect that, in the crystalline complex of sugars

Fig. 3.8a Cis and Trans. Arrangement of the CH_2OH Group

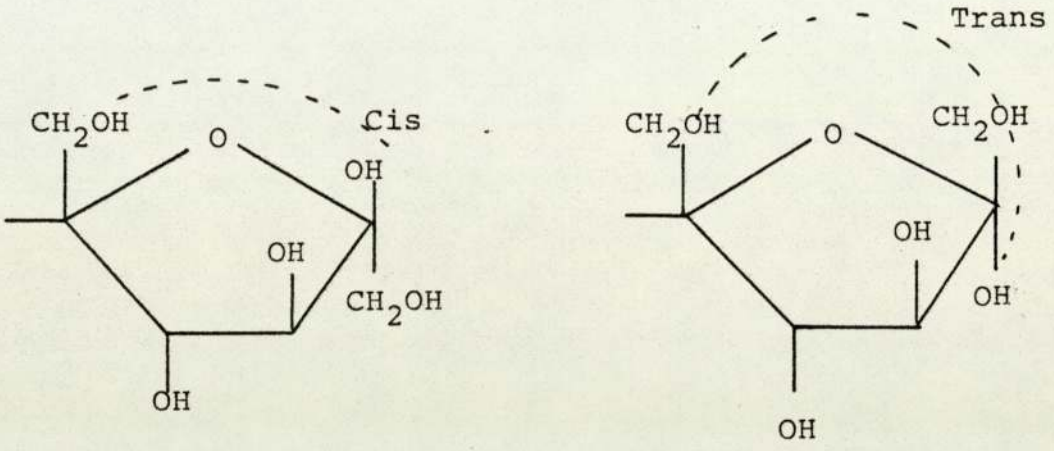

Fig. 3.8b Conformational Behaviour of a Pyranoid Ring

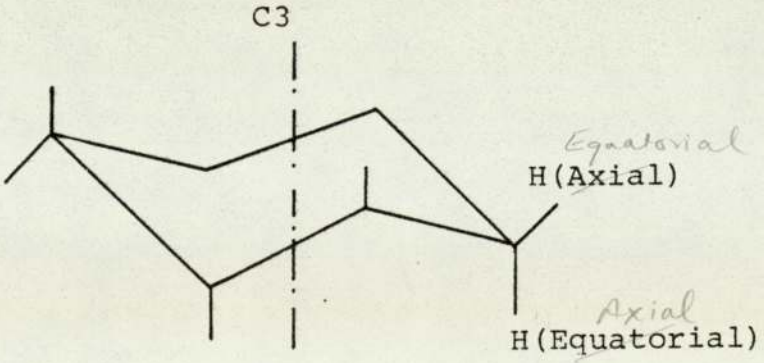

the cation would be found co-ordinated to the same three oxygen atoms. This has been proved in four cases investigated by X-ray crystallographic analysis. These complexes are β-D-mannofuranose.$CaCl_2.4H_2O$, methyl β-D-mannofuranoside.$CaCl_2.3H_2O$, methyl α-D-glycero-D-gulo-heptopyranoside.$CaCl_2.H_2O$, and epi-inositol.$SrCl_2.H_2O$

According to the Angyal hypothesis, only $^2C_5$-β-D-fructopyranose is expected to form a complex with cations since it has an axial-equatorial-axial hydroxide group arrangement. On the other hand, glucose is not expected to form any complex with cations since in none of its different forms shown in Fig. 3.1 does it contain such a favourable arrangement.

Rendleman (74) proposed that a basic metal oxide or hydroxide can complex with the sugar molecule directly through the hydroxyl groups. Continuing with this assumption, the calcium complex of fructose may be

$CaC_6H_{10}O_6$ or

$C_6H_{11}O_6Ca(OH)$

Rendleman's proposition was based on the work of Mackenzie and Quin (75). They suggested that in the compounds of reducing sugars with calcium hydroxide, the calcium is united with the hydroxyl group at C-1, possibly in the form

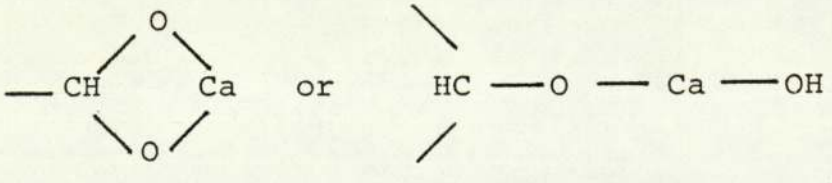

3.4.1.3 Large Scale Chromatographic Separation Processes

It was mentioned before that chromatographic separation methods are widely used in industry for the separation of sugars. The two patented processes of Boehringer and the Colonial Sugar Co. are examples of pilot plant processes. The Sarex process for HFCS is an example of a large scale chromatographic separation process. The Finnsugar process (3) and the Südzucker process (4) which will be briefly reviewed below, are also typical industrial applications of large scale chromatographic separation processes.

3.4.1.4 The Finnsugar Process

The Finnish Sugar Co. Ltd. of Kantvik, Finland, started applying chromatographic separation processes to desugarise molasses in the 1950s. At the present time the company has the largest chromatographic plant for desugarising molasses in the world. In its newest plant, Finnsugar has installed ten columns designed to treat 1.25×10^5 kg of molasses daily to produce 2.5×10^4 to 4×10^4 kg of crystal sugar.

The actual separation process is essentially the same for cane and beet molasses. A certain amount of pretreated molasses is fed evenly by distributors to the top of the column as shown in Fig. 3.9. The molasses is followed by the eluent, water, that moves plugwise down through the resin bed under the influence of gravity. The resin is a cationic exchanger in alkali metal form. During the downflow, the molasses

Fig. 3.9 The Finnsugar Batch Process

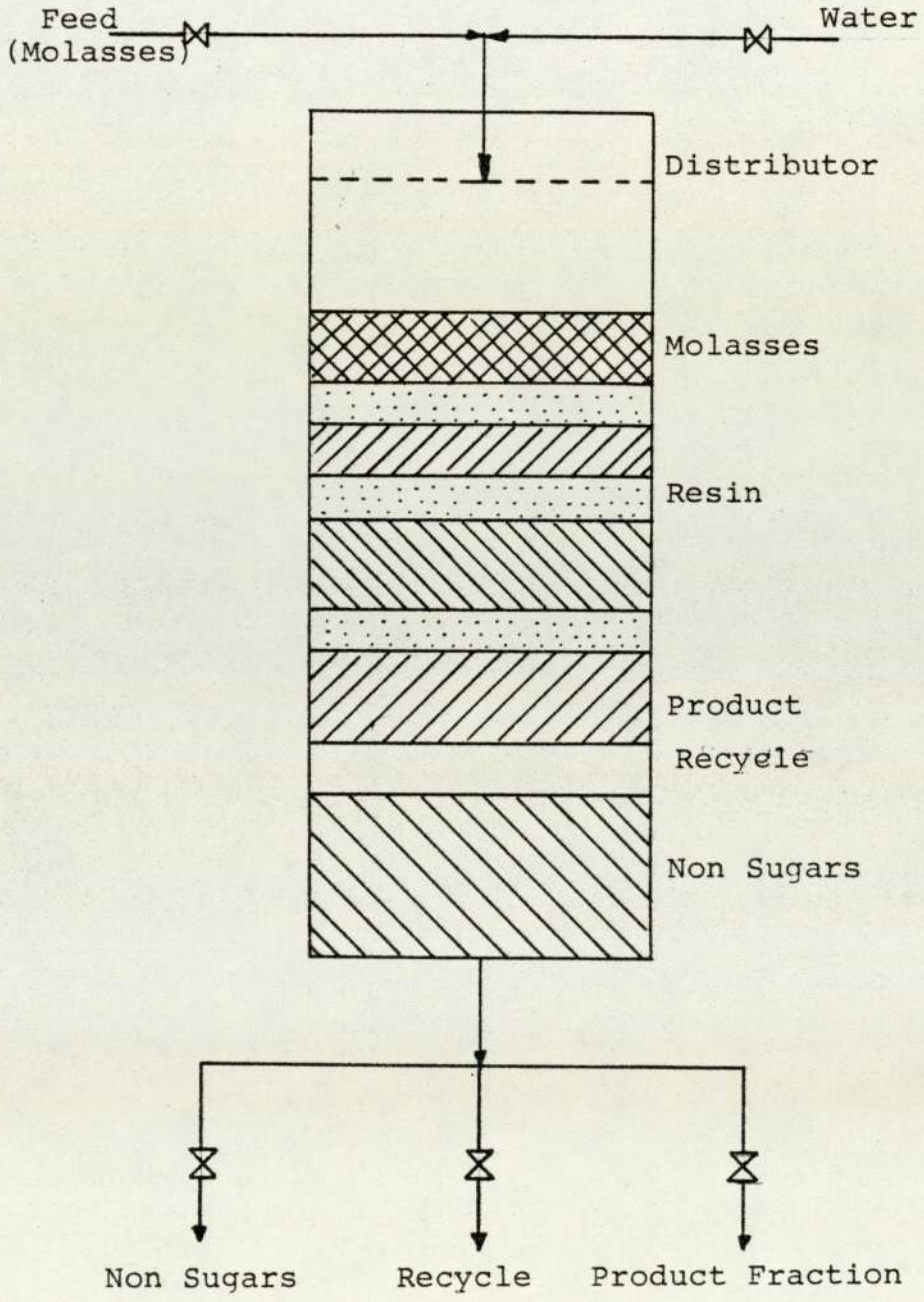

is separated into different fractions as shown in Fig. 3.9. As the feed molasses passes through the resin bed, the sucrose and the other carbohydrates are adsorbed by the resin and their passage through the column is delayed. The ionised components of the molasses are not adsorbed and pass through the resin unhindered. As the feed solution reaches the column outlet, the non-sugar fraction emerges first, followed by the sucrose fraction and the last to appear are the invert sugars. After this fraction the non-sugar fraction of the next molasses batch follows and a new cycle begins. Between the product fractions, mixtures of low concentration and purity are collected separately, recycled to the starting point of the main process and used for diluting the feed molasses.

The process is a repetitive batch one with several successive batches in the same column simultaneously. Column operation is automated and controlled by a microprocessor which controls the feed, eluent and recycle. The yield of sucrose from the molasses depends on the quality of the desired product. If crystalline sugar is required then yields of up to 90% of the original sugar in the molasses are possible. However higher yields of sugar are possible for lower purity.

Unlike beet molasses, cane molasses needs intensive pretreatment before being fed to the column. This is because of the cane molasses' composition which gives it high turbidity. Such pretreatment

includes operations like heating, pH-adjustment, decantation and filtration. This pretreatment is necessary to protect the resin from being fouled.

3.4.1.5 The Südzucker Process

The other process for desugarisation of molasses is the Südzucker process of Süddeutsche Zucker AG., Obrigheim, Germany. The Südzucker pilot plant shown in Fig. 3.10 incorporates three columns each 6 metres in length and a metre in diameter, with a total resin bed volume of 13.4 m^3. The upper half of the first column is filled with a special resin which has a high affinity for calcium ions and does not undergo any change in volume during regeneration. Since this resin acts as a filter, there is no need to pretreat cane molasses prior to loading. The adsorbent is a strongly acid cation exchange resin, Lewatit TSW 40 manufactured by Bayer AG., Leverkusen. It is used in the calcium form. Water which is made slightly alkaline with calcium oxide is used as eluent. The plant is operated at a temperature of 90^{o}C and a linear flow rate of 2.05 m hr^{-1}. Molasses containing 50% w/w dry matter is loaded into the column. The volume of each batch is 6% of the bed volume. The sequence in which the different components of the molasses are eluted is firstly the colouring matters of the molasses then the higher saccharides, the sucrose and finally the different amino-acids. The effluent streams are continuously monitored by

Fig. 3.10 The Südzucker Process

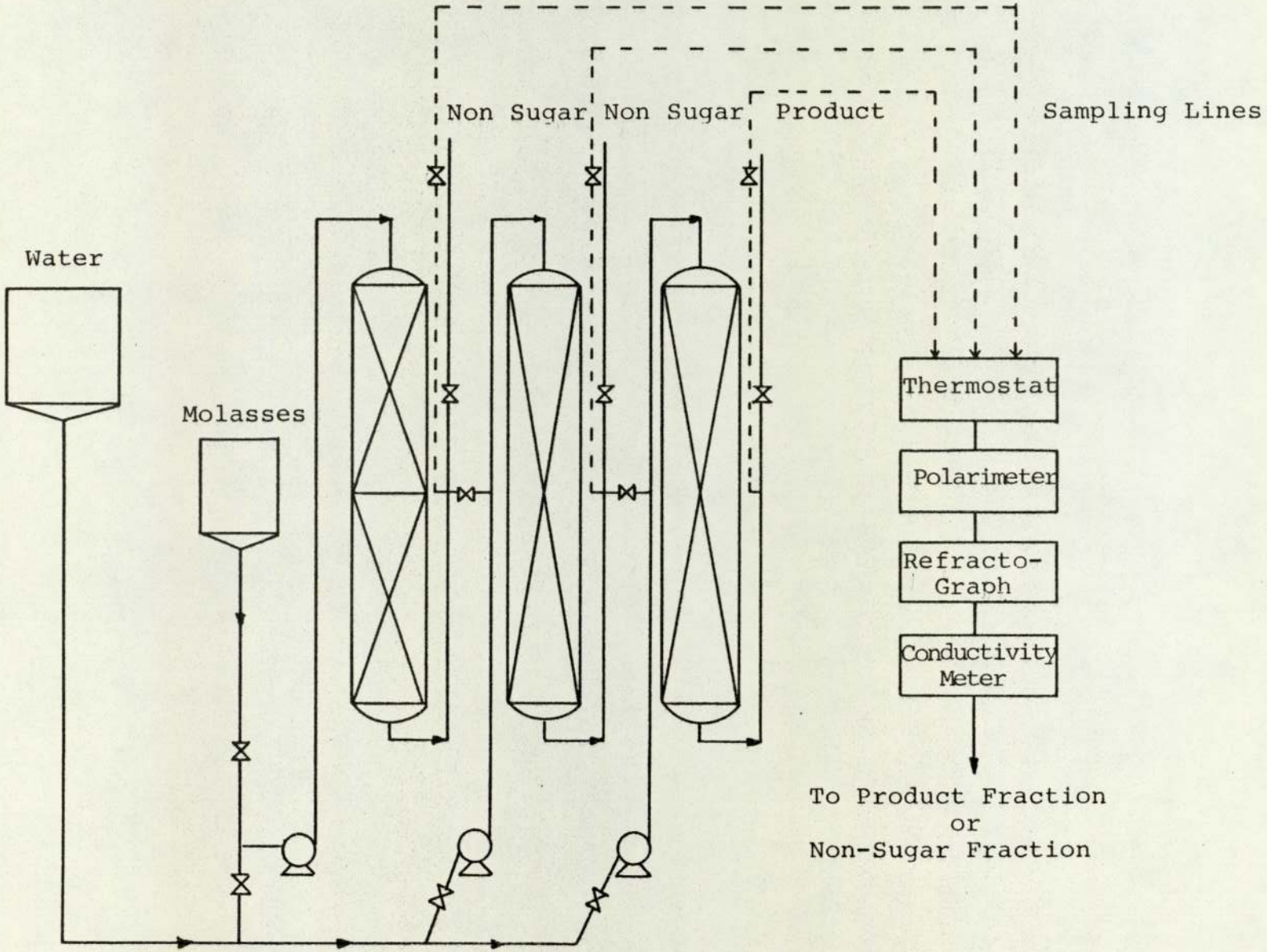

detectors as shown in Fig. 3.10.

The process is claimed to produce 10 to 11% w/v dry matter product with purity of over 90% for a 95% w/w yield of the sugar originally present in the molasses.

3.4.2 Separation by Anionic Exchangers

The first report on the separation of sugars with anion exchange resins was by Samuelson and Sjöstrum (61). They adsorbed monosaccharides on an anion exchange resin in the bisulphite form at a high ethanol concentration and separated the sugars by elution with gradually lower ethanol concentration. Lindberg and Glessor (76) used a small column of 5 mm diameter and 320 mm long packed with an anion exchange resin in the bisulphite form to separate mixtures of aldoses from each other and from ketoses. They succeeded in isolating very pure fructose, glucose and galactose from commercial products. In 1974 Takasaki was granted a U.S. patent (16) for the separation of fructose from mixtures of sugars. The process used an anion exchange resin Dowex 1-X8 (supplied by the Dow Chemicals, U.S.A.) in the bisulphite and sulphite forms. An important comment made by the authors was that the separation was improved with increase of temperature.

A literature survey revealed no report on an existing industrial process for the separation of fructose and glucose using an anion exchange resin. This is probably because of the instability of such

exchangers discussed in Section 2.5.1.1.

The theory behind the separation of sugars on anion exchange resin in the bisulphite form is that although both fructose and glucose make complexes with bisulphites, the glucose complex is more stable as discussed in the following section.

3.4.2.1 Sugar Complexes with Bisulphites

The reaction of sugars with the bisulphite ions is an established fact in analytical chemistry (78). The reaction of the carbonyl group (C=O) with the bisulphite is the basis for the determination of many aldehydes and ketones. When an aldehyde or a ketone is contacted with sulphurous acid or a bisulphite salt, it forms an α-hydroxyl-sulphonic acid such as

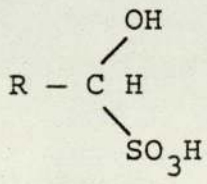

This acid derivative or its salt dissociates into its components in aqueous solutions. The extent of the dissociation depends on the strength of the bond and is a function of temperature and the concentration of the solution. The equilibrium reaction could be as follows.

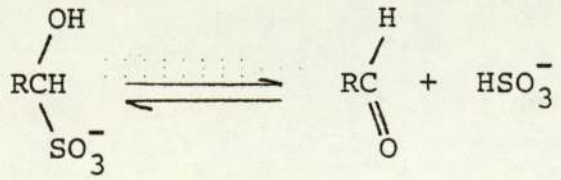

The strength of the bonding between the sugars and the bisulphite ions was determined by paper electrophoresis. Paper electrophoresis is a technique by which a separation of particles or macromolecules is brought about by differential migration due to an electric field (18). Paper electrophoresis of various sugars in an aqueous solution of bisulphites showed that ketohexoses did not migrate while aldohexoses migrated at various rates with glucose being the slowest. This implies that fructose, which is a ketohexose, has little or no tendency to form a stable bisulphite complex, while glucose forms a stable complex with the bisulphite ions. Ferrier and Collins (50) suggest a scheme for this complex path as follows.

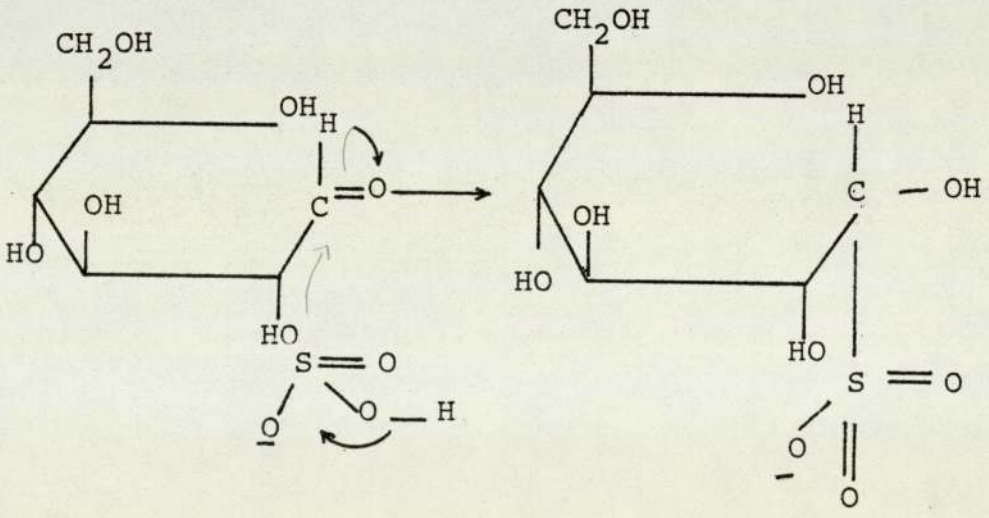

CHAPTER FOUR

DESIGN AND CONSTRUCTION OF THE SCCR7 UNIT

4.1 PRINCIPLE OF OPERATION OF THE SCCR UNIT

The principle of operation of the SCCR unit is schematically illustrated in Figs. 4.1a, b, c. A mixture of two components 1 and 2 is fed into the system at port D. The less strongly adsorbed component 1 is preferentially moved towards the product 1 off-take port A. A section of the closed loop is isolated by locks T and TT. An independent purge liquid stream enters at port E and exits with the strongly adsorbed component 2 from port B. Fig. 4.1a represents the distribution of the two components within the system soon after start-up. In Fig. 4.1b, all the port functions have been advanced one position in the direction of the mobile phase flow. This port advancement results in a simulated movement of the packing in a direction counter-current to the direction of the mobile phase flow. The rate of advancement of the ports must be less than the velocity of the less strongly adsorbed component 1. Component 2 is retained preferentially on the packing while component 1 emerges from port A. Fig. 4.1c shows the fully established operating conditions of the unit.

Figs. 4.2a,b,c demonstrate how the simulated counter-current mode is achieved without physically moving the packing. Here three successive switch

Fig. 4.1 Principles of Operation of the SCCR Unit

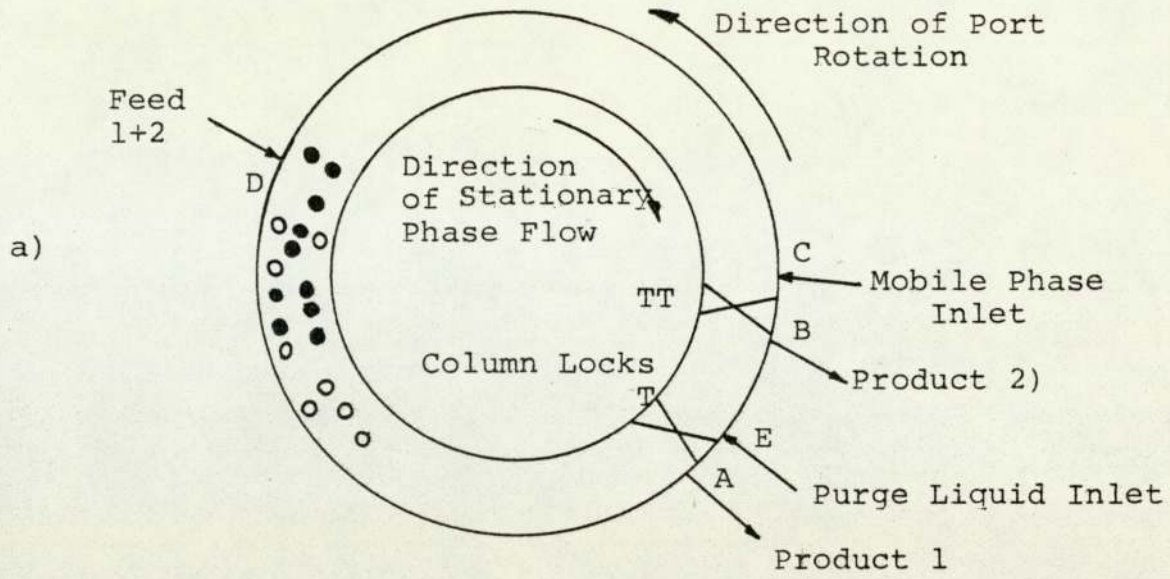

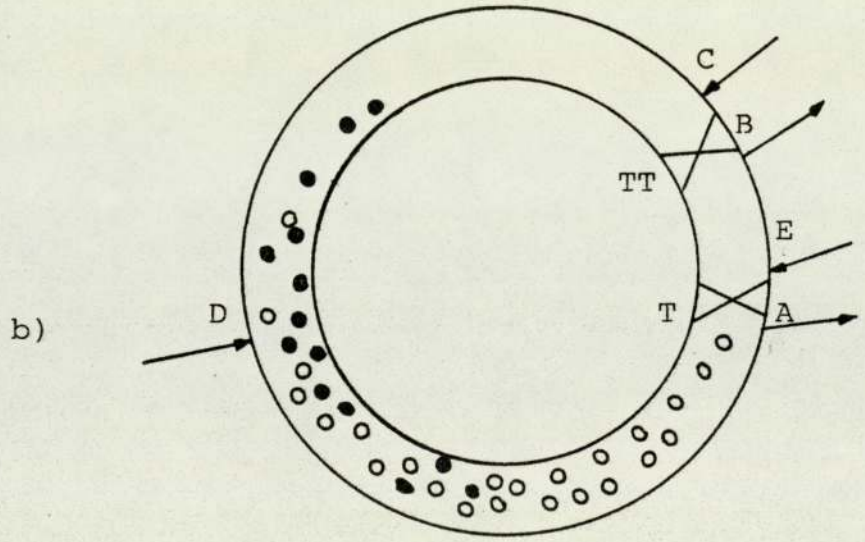

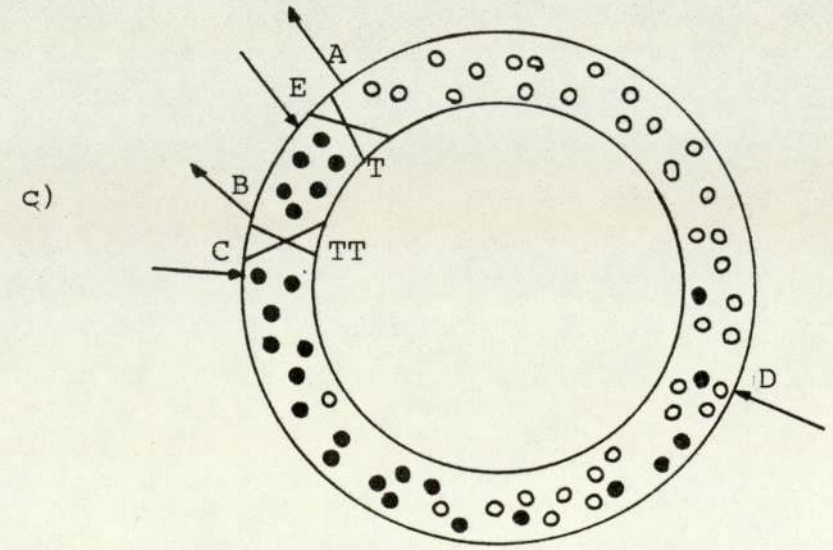

Fig. 4.2 Sequencing Operation of the SCCR Unit

a) Switch One Column 1 is Isolated

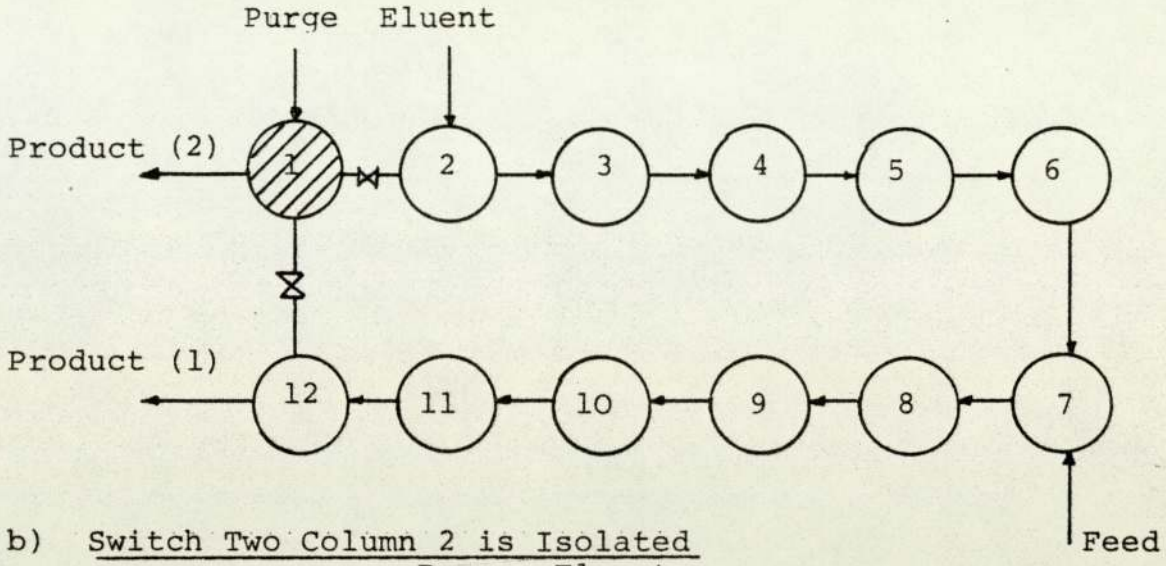

b) Switch Two Column 2 is Isolated

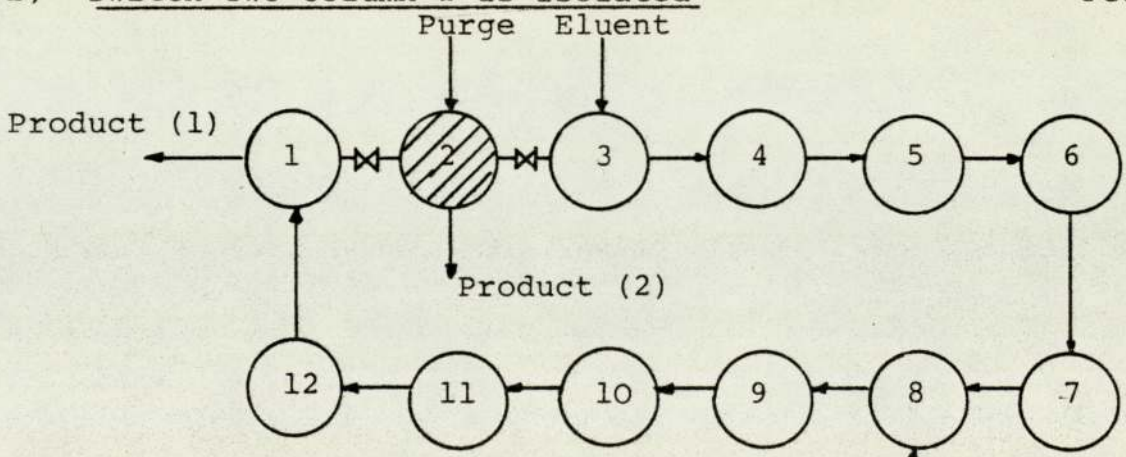

c) Switch Three Column 3 is Isolated

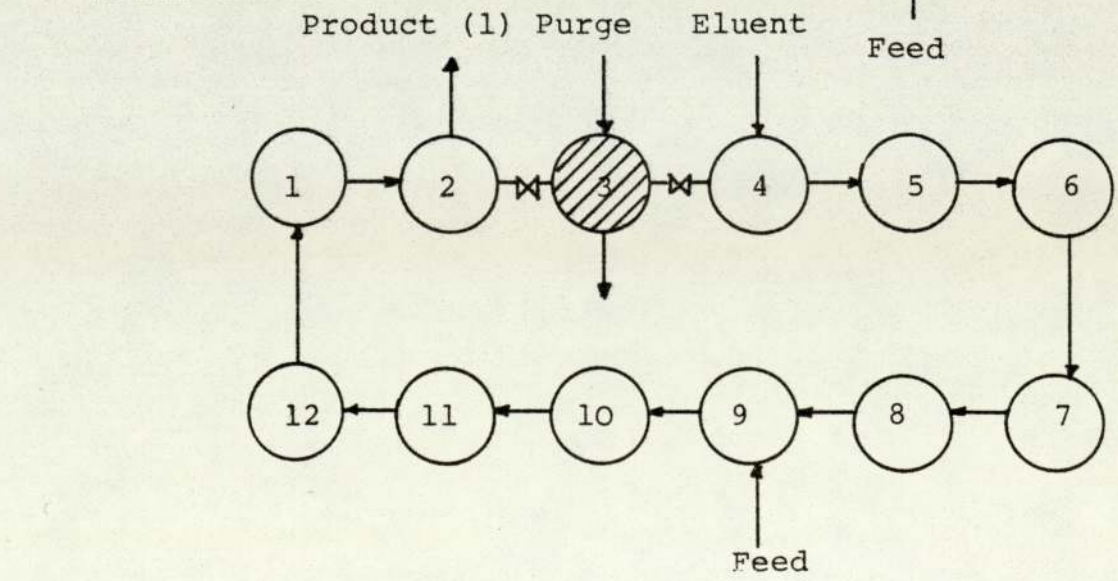

periods are represented for the SCCR unit with twelve columns. It can be seen that seven valves need be opened or closed simultaneously. These valves are the feed, mobile phase and purge inlets, two product outlets and two column isolation locks. Fig. 4.2a represents the first switch period where column 1 is isolated and purged for product 2. The eluent enters at column 2, the feed at column 7 and product 1 is issuing from column 12. The next switch period is represented by Fig. 4.2b, where the purge is advanced by one step to column 2, the eluent to column 3 and the feed to column 8. Product 1 in this case is issuing from column 1. A similar advancement of the functions in the third switch period is shown by Fig. 4.2c.

4.2 DESCRIPTION OF THE SCCR4 UNIT

Fig. 4.3 is a photograph of the SCCR4 Unit. It was originally constructed by Ching (12) and modified by Chuah (14) who reported the unit in full detail .

The separation section had twelve stainless steel columns 25.4 mm (1") in internal diameter and 750 mm long. The columns were packed with a cation exchange resin Zerolit 225 SRC 14 supplied by Diamond Shamrock Polymer Ltd., Middlesex. The particle size range of the resin was 150-300 μm, with 8% cross-linkage. The resin was charged to the column in the calcium (Ca^{2+}) form. A pneumatic compression device was incorporated to counter the swelling and contraction

FIG. 4.3 PHOTOGRAPH OF THE SCCR4 UNIT

A = Packed Column

B = Valves

C = Constant Temperature Enclosure

D = Midget Cylinder

E = Control Box

F = Pulsation Dampener

G = Pneumatic Lines

H = Feed Reservoir

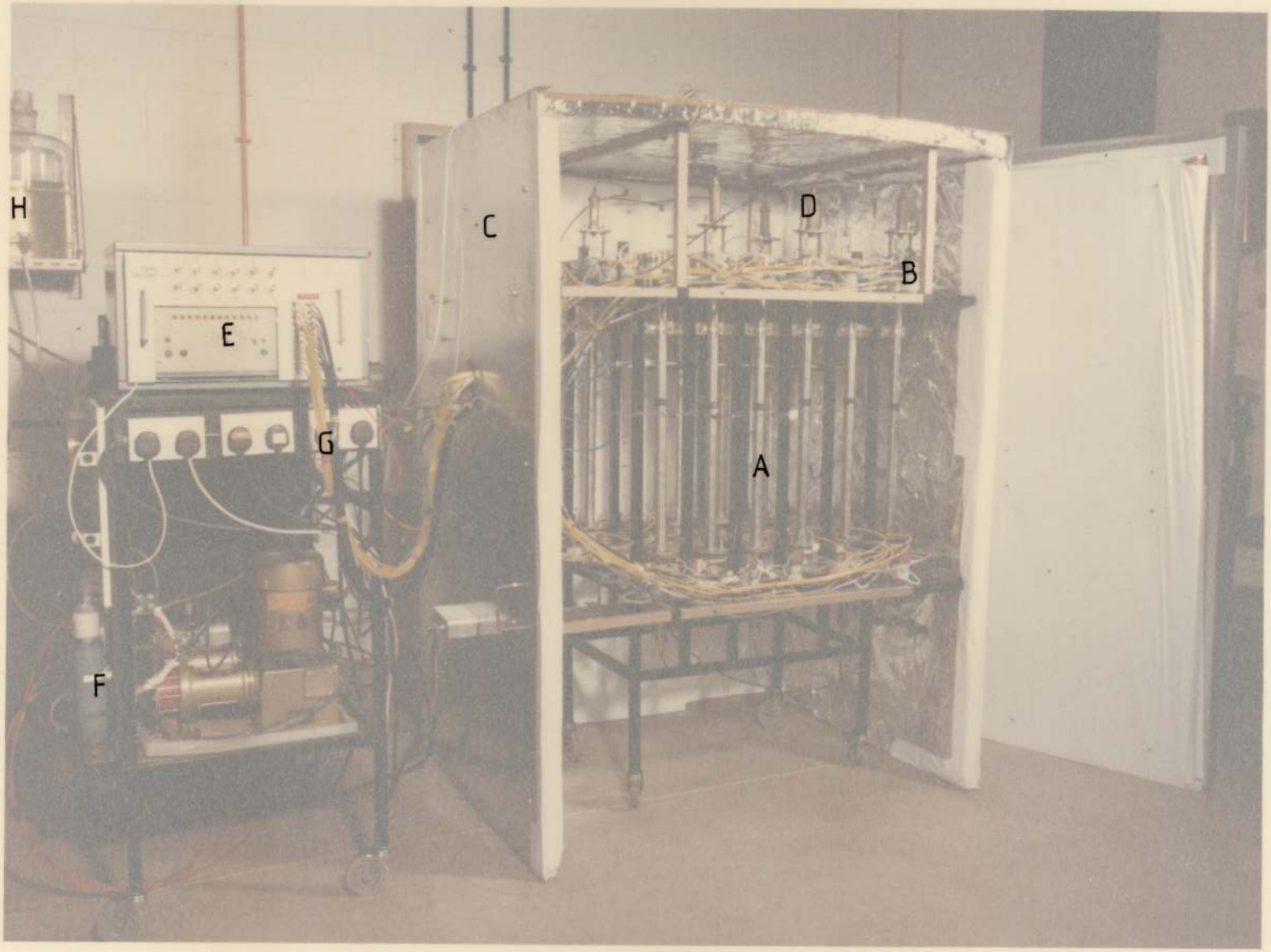
H
C
D
B
E
G
A
F

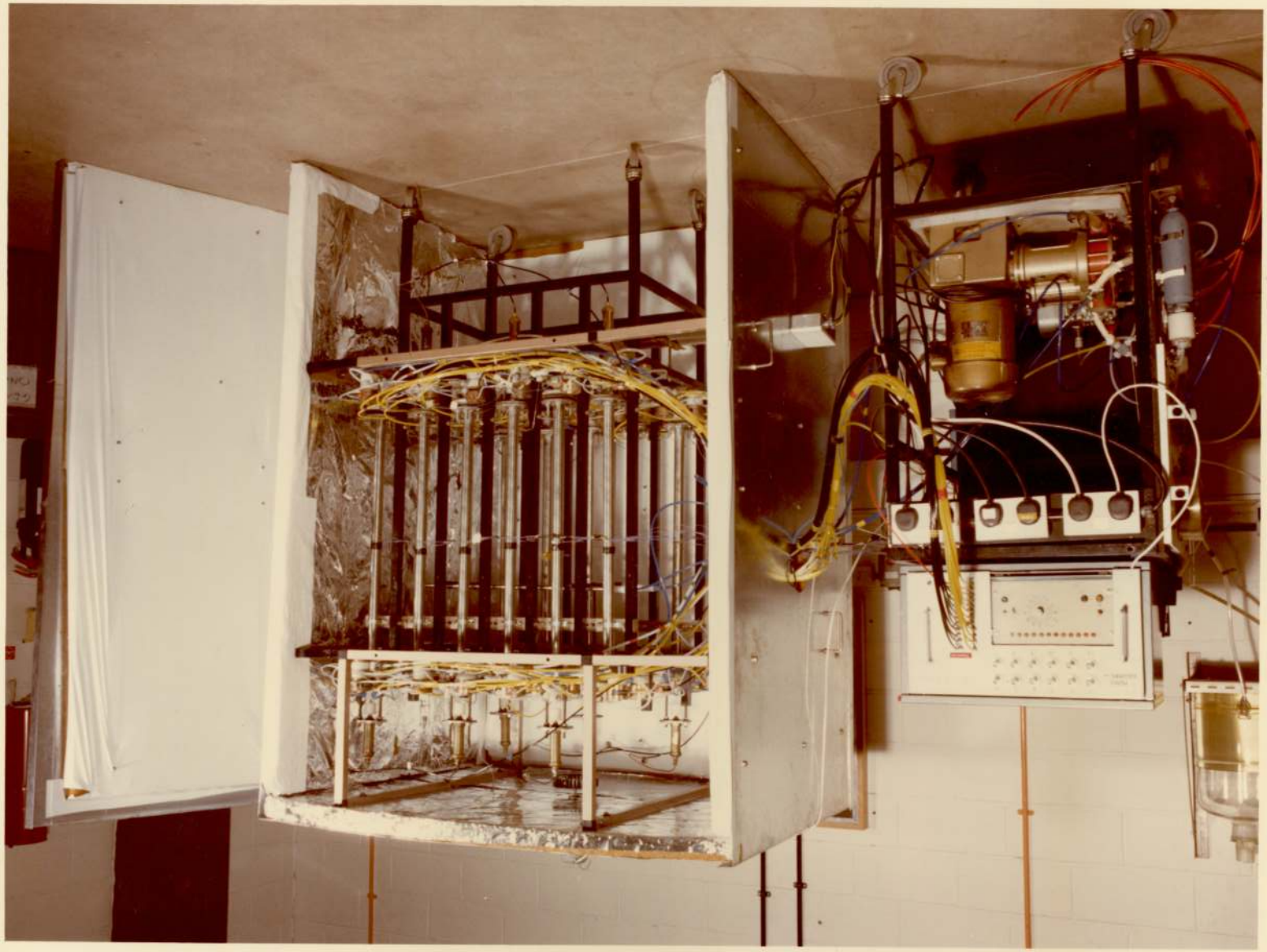

of the resin. Midget cylinders were mounted at the inlet of the columns on top of plunger devices. These cylinders were connected in a closed loop via 3 mm internal diameter nylon tubing to an air supply of 240 kNm^{-2}.

Six pneumatic valves were connected to each column for the feed, eluent and purge inlets, two product outlets and a liquid transfer valve to an adjacent column. The function of these valves was governed by a pneumatic control system which is described in Section 4.2.2.

The columns were mounted on a mobile frame and surrounded by a constant temperature enclosure. The enclosure was constructed from galvanised steel sheets lagged with 50 mm thick glass fibre pads. The enclosure was heated by a U-shaped, 5.0 kW fin heater supplied by Eltron Ltd, London. The hot air was circulated by a fan placed at the centre top of the enclosure.

The temperature of the enclosure and of the liquid inside the columns was measured by a network of Nickel-Chrome thermocouples. The thermocouples were placed mid-way along each column, in the transfer lines between the columns and in the feed, the eluent and the purge lines. The other terminals of the thermocouples were connected to a multi-point switch. Temperatures were displayed as millivolt potentials on a proportional digital controller. The thermocouples and the digital controller were supplied by

Diamond Control Ltd.

Other features of the SCCR4 unit are described below.

4.2.1 Pretreatment and Handling of Liquids

Deionised water was used to elute and purge the SCCR4 unit. As shown in Fig. 4.4 water was drawn by gravity from the elevated reservoir to a 1.2×10^{-1} m^3 plastic tank. From the tank water flowed through a solenoid valve into a 7.5×10^{-2} m^3 glass aspirator used to preheat the eluent and purge before being pumped to the SCCR4 unit. The aspirator was jacketed with two electric heaters of 5.0 kW and 2.0 kW. Both heaters were used at the start to boost the temperature to the required value. Then during operation only the 2.0 kW heater, which was connected to a thermostat, was used to maintain the required temperature.

An elevated 2.0×10^{-2} m^3 glass aspirator was used as a feed reservoir. From the reservoir, the feed flowed under gravity through a 25.4 mm internal diameter glass column to the pump. The column was wrapped with a tape heater to preheat the feed. The tape heater was linked to a fine temperature controller.

Each liquid line had a flow measurement device, a Bourdon pressure gauge and a safety relief valve. In addition, the purge and eluent lines each had a pulsation dampener. These pulsation dampeners were made from stainless steel and nitrile rubber diaphragms.

Fig. 4.4 Flow Diagram of the SCCR4 Unit

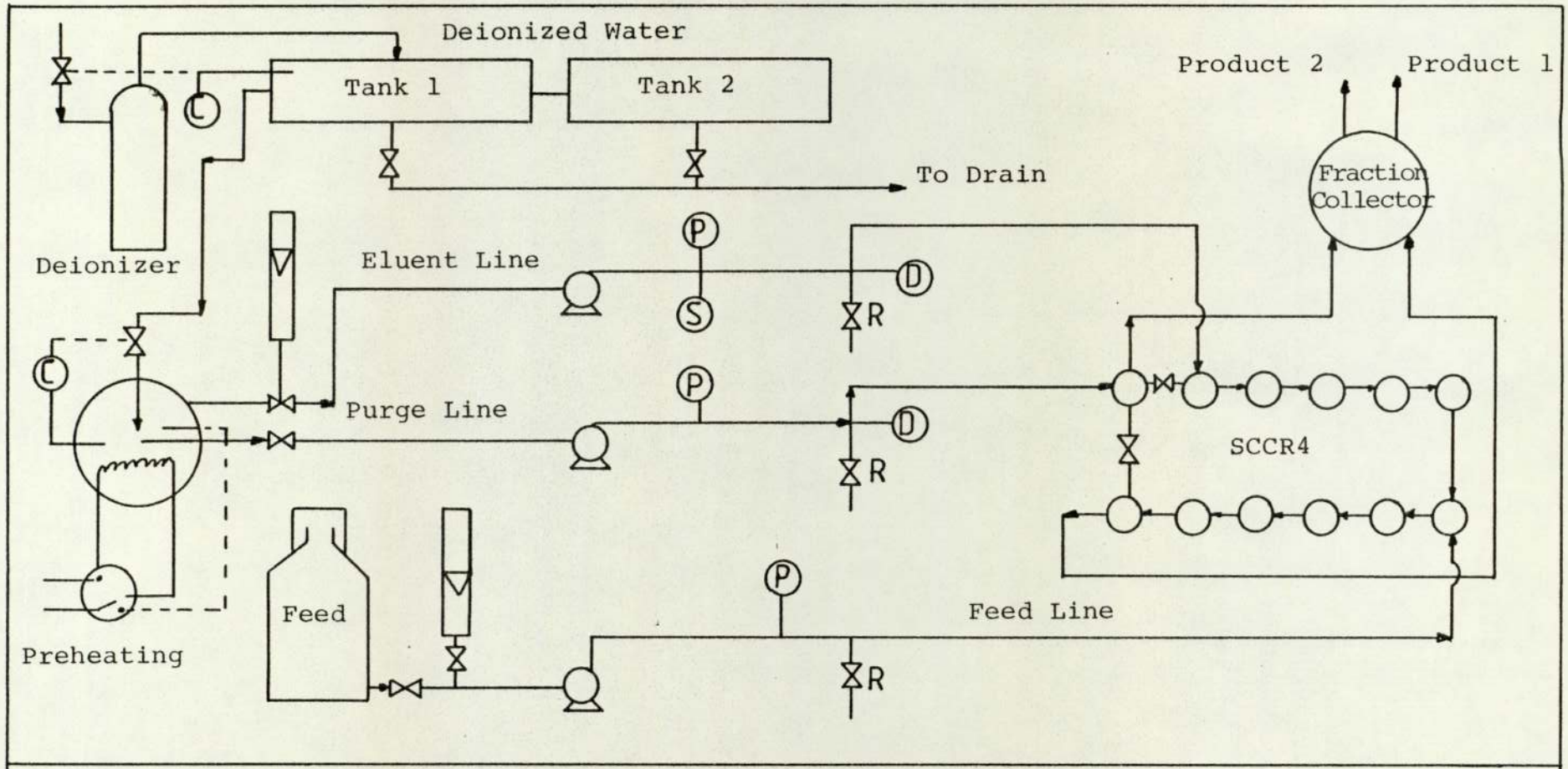

They were used to ensure smooth flow of fluids under high flow rates.

Two pumps, supplied by Metering Pumps Ltd., London, were used for pumping the process liquids. A series II MPL micrometering pump was used to pump the feed and eluent. This pump had three heads rating at 10 cm^3min^{-1}, 20 cm^3min^{-1} and 40 cm^3min^{-1}. The purge was pumped by a K-series metering pump with two plastic heads of different types. One was a positive displacement piston head to give high pressure at low flow rate up to 100 cm^3min^{-1}, and the other was a diaphragm head for low pressure and high flow rates up to 2000 cm^3min^{-1}.

4.2.2 The Pneumatic Control System

Double acting pneumatically controlled poppet valves were used to control the flow of liquids into and out of the columns. Fig. 4.5 is a photograph of one of these valves together with its different parts. A total of 72 poppet valves were fitted to the SCCR4 unit. Normally the valves were closed due to a bias pressure of 240 kNm^{-2} constantly applied to the lower side of the diaphragm. When an actuating pressure of 550 kNm^{-2} was applied to the upper side of the diaphragm the valve was opened for liquid flow.

The poppet valves were controlled by a pneumatic control system. The control mechanism consisted of a number of solenoid valves activated individually by a rotating cam mechanism. Twelve of these solenoid

They were used to ensure smooth flow of fluids under high flow rates.

Two pumps, supplied by Metering Pumps Ltd., London, were used for pumping the process liquids. A series II MPL micrometering pump was used to pump the feed and eluent. This pump had three heads rating at 10 cm^3min^{-1}, 20 cm^3min^{-1} and 40 cm^3min^{-1}. The purge was pumped by a K-series metering pump with two plastic heads of different types. One was a positive displacement piston head to give high pressure at low flow rate up to 100 cm^3min^{-1}, and the other was a diaphragm head for low pressure and high flow rates up to 2000 cm^3min^{-1}.

4.2.2 The Pneumatic Control System

Double acting pneumatically controlled poppet valves were used to control the flow of liquids into and out of the columns. Fig. 4.5 is a photograph of one of these valves together with its different parts. A total of 72 poppet valves were fitted to the SCCR4 unit. Normally the valves were closed due to a bias pressure of 240 kNm^{-2} constantly applied to the lower side of the diaphragm. When an actuating pressure of 550 kNm^{-2} was applied to the upper side of the diaphragm the valve was opened for liquid flow.

The poppet valves were controlled by a pneumatic control system. The control mechanism consisted of a number of solenoid valves activated individually by a rotating cam mechanism. Twelve of these solenoid

FIG. 4.5 PHOTOGRAPH OF THE POPPET VALVE

A = Assembled Valve

B = Upper Diaphragm Chamber

C = Lower Diaphragm Chamber

D = Neoprene Rubber Diaphragm

E = Liquid Inlet Chamber

F = Liquid Outlet Chamber

G = Poppet and Stem

H = Viton Rubber Gasket

I = Valve Base

J = Diaphragm Backing Plates

K = Diaphragm Assembly Components

L = Adjustment Nut

M = Viton O-Ring

N = Thrust Washer

O = 4x2BA Cheese Head Body Screws

P = 6x4BA Cap Screws

VALVE

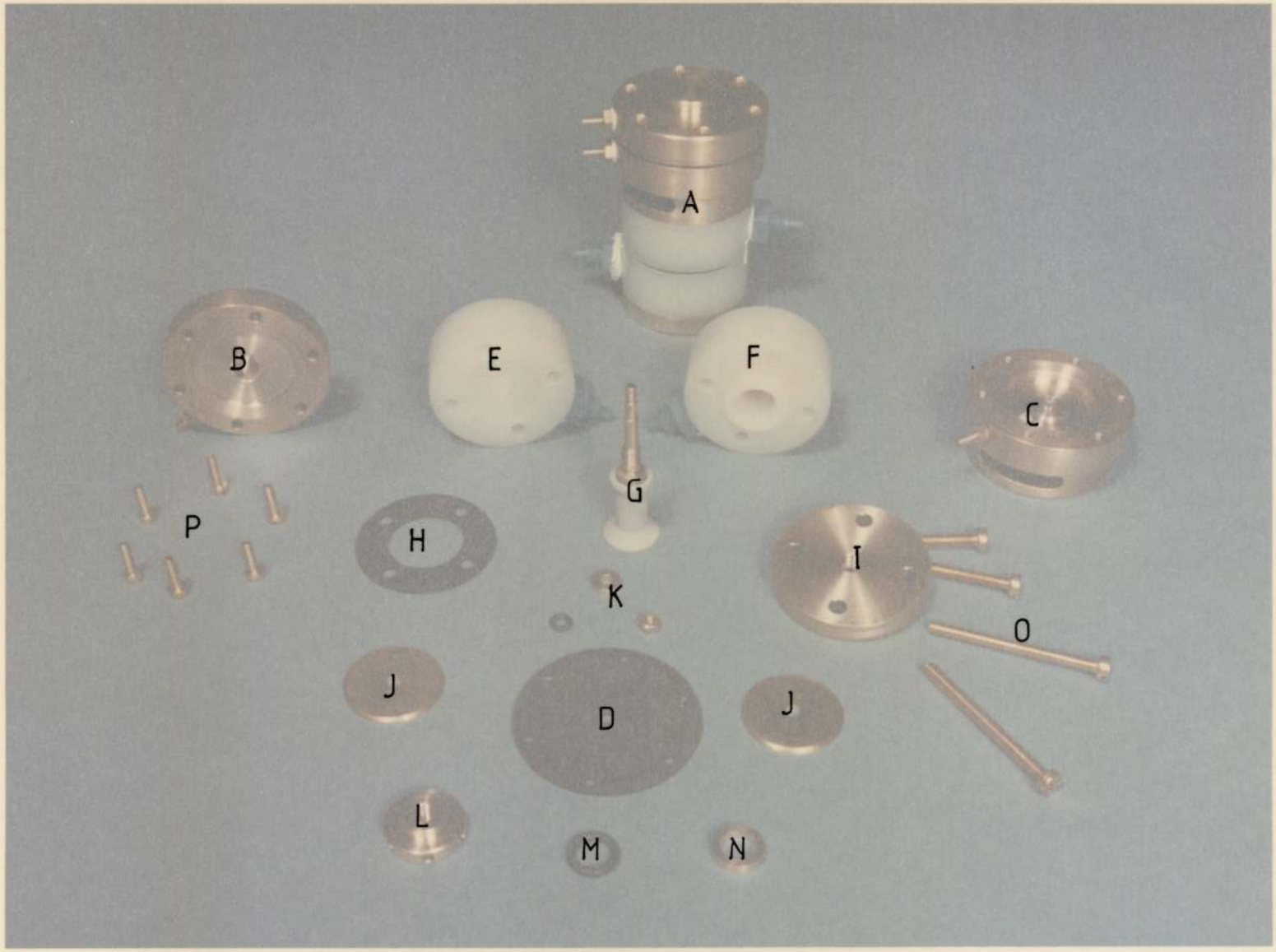

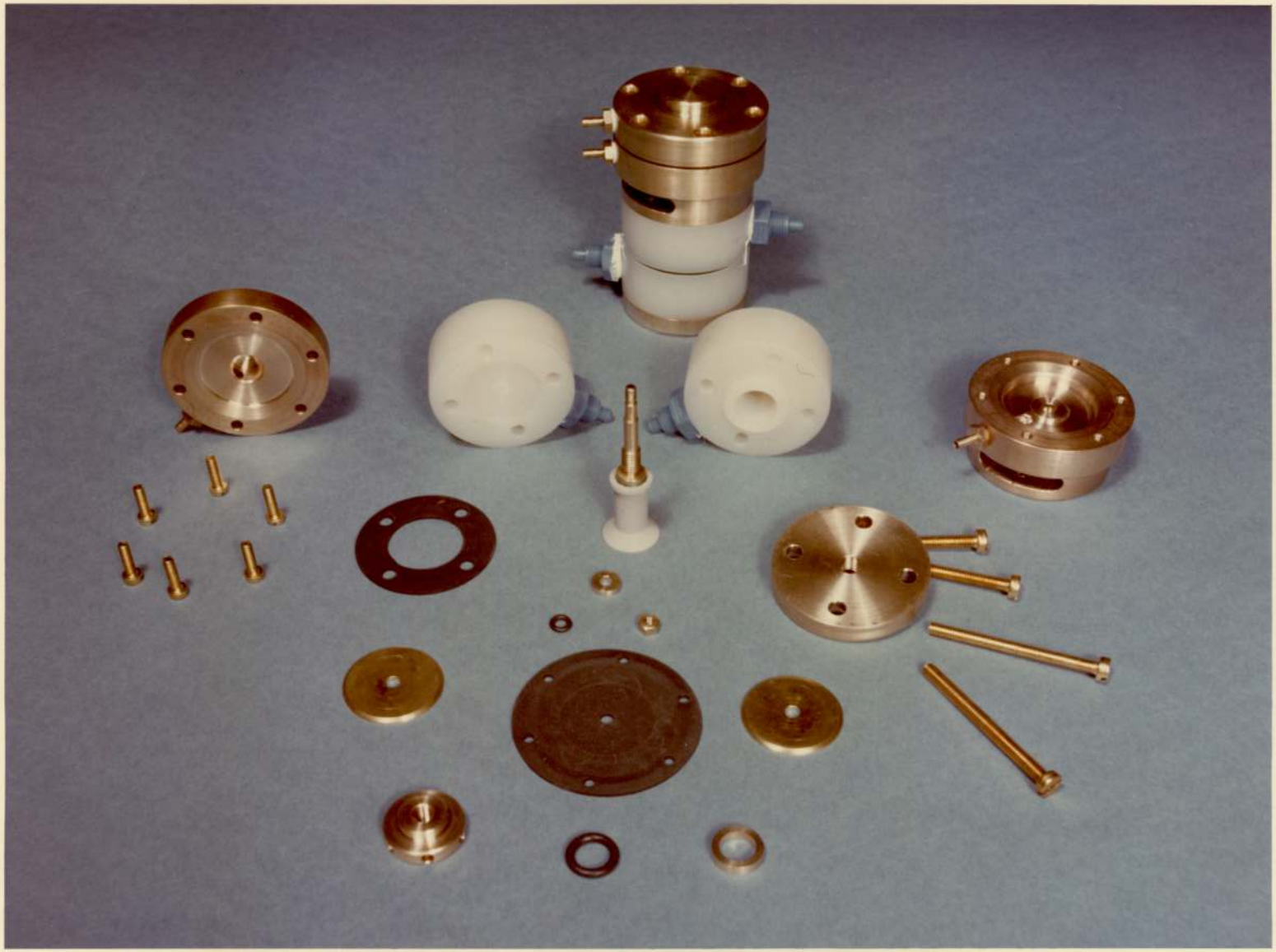

valves were set corresponding to the twelve columns such that each solenoid valve would directly activate the transfer valves to isolate the corresponding column. The solenoid valves were each linked to double return valves to activate the appropriate feed, eluent and purge inlets and two product outlets. One possible arrangement is illustrated by Fig. 4.6 and table 4.1 shows the sequence of the valve settings.

A digital timer was incorporated into the cam unit to control the rotating mechanism which in turn opened and closed the solenoid valves at a fixed time period. The timer was set at a fixed time period and at the end of that period a signal was triggered causing the cam unit to rotate by 30^{o}. The next set of valves were then activated, and so on.

The compressed air was supplied by an air compressor and a stand-by air cylinder. The supply was divided into bias and actuating streams whose pressures were controlled to 240 kNm^{-2} and 550 kNm^{-2} respectively by a regulator. The bias line was branched and led directly to the poppet valves described above and the midget cylinders while the actuating line was led to the control unit. Nylon tubing of 3.0 mm internal diameter was used for the pneumatic lines. The pneumatic distribution network from the air supply to the control unit and the poppet valves is illustrated by Fig. 4.7.

Fig. 4.6 A Schematic Diagram of the Control Box

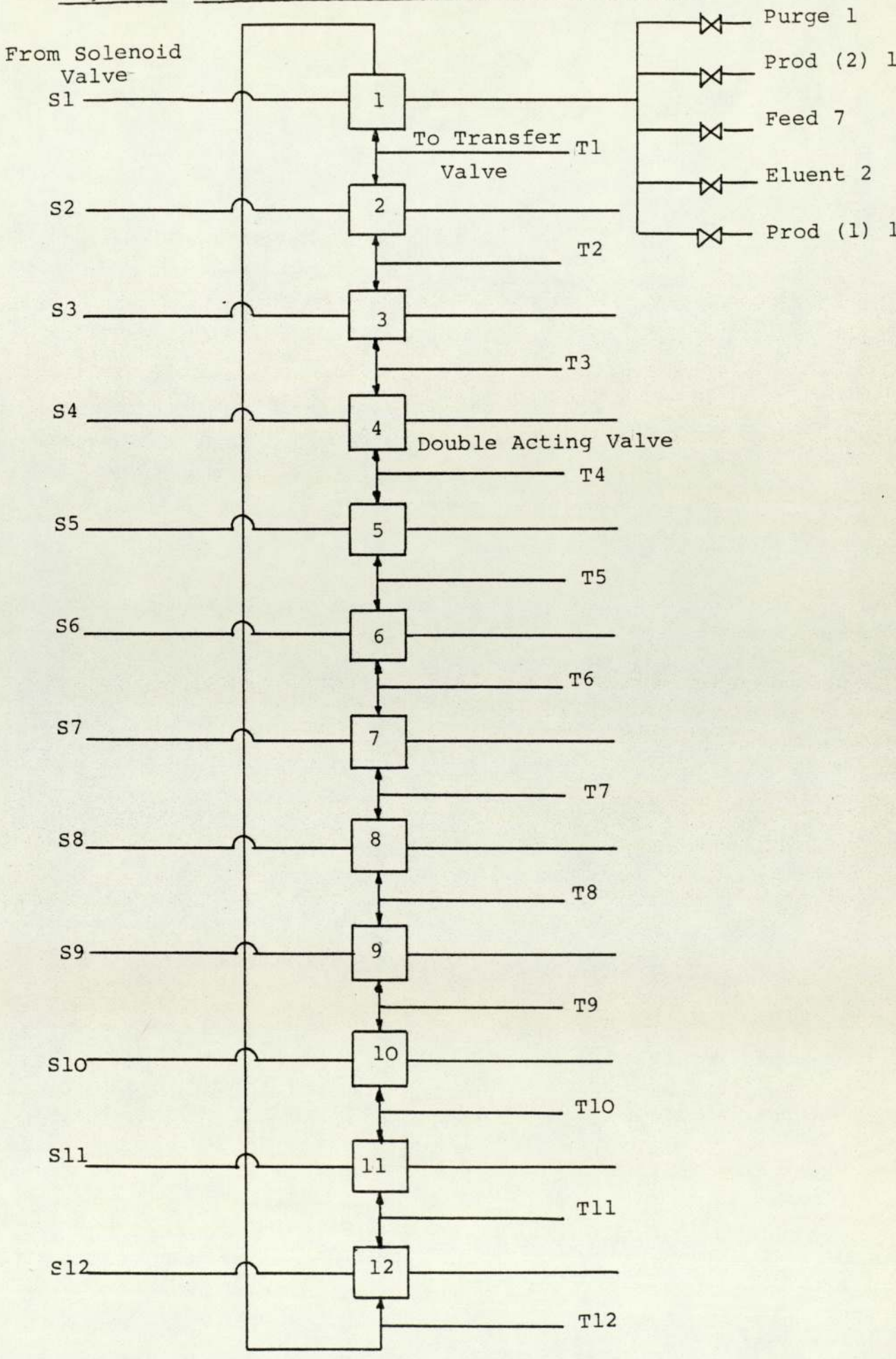

TABLE 4.1 SEQUENCES OF VALVE SETTINGS

Switch Number	Valves Activated						
	Open					Close	
	Purge	Eluent	Feed	Product 1	Product 2	Transfer	Transfer
1	1	2	7	12	1	1	12
2	2	3	8	1	2	2	1
3	3	4	9	2	3	3	2
4	4	5	10	3	4	4	3
5	5	6	11	4	5	5	4
6	6	7	12	5	6	6	5
7	7	8	1	6	7	7	6
8	8	9	2	7	8	8	7
9	9	10	3	8	9	9	8
10	10	11	4	9	10	10	9
11	11	12	5	10	11	11	10
12	12	1	6	11	12	12	11

Fig. 4.7 Schematic Diagram of the Pneumatic Network

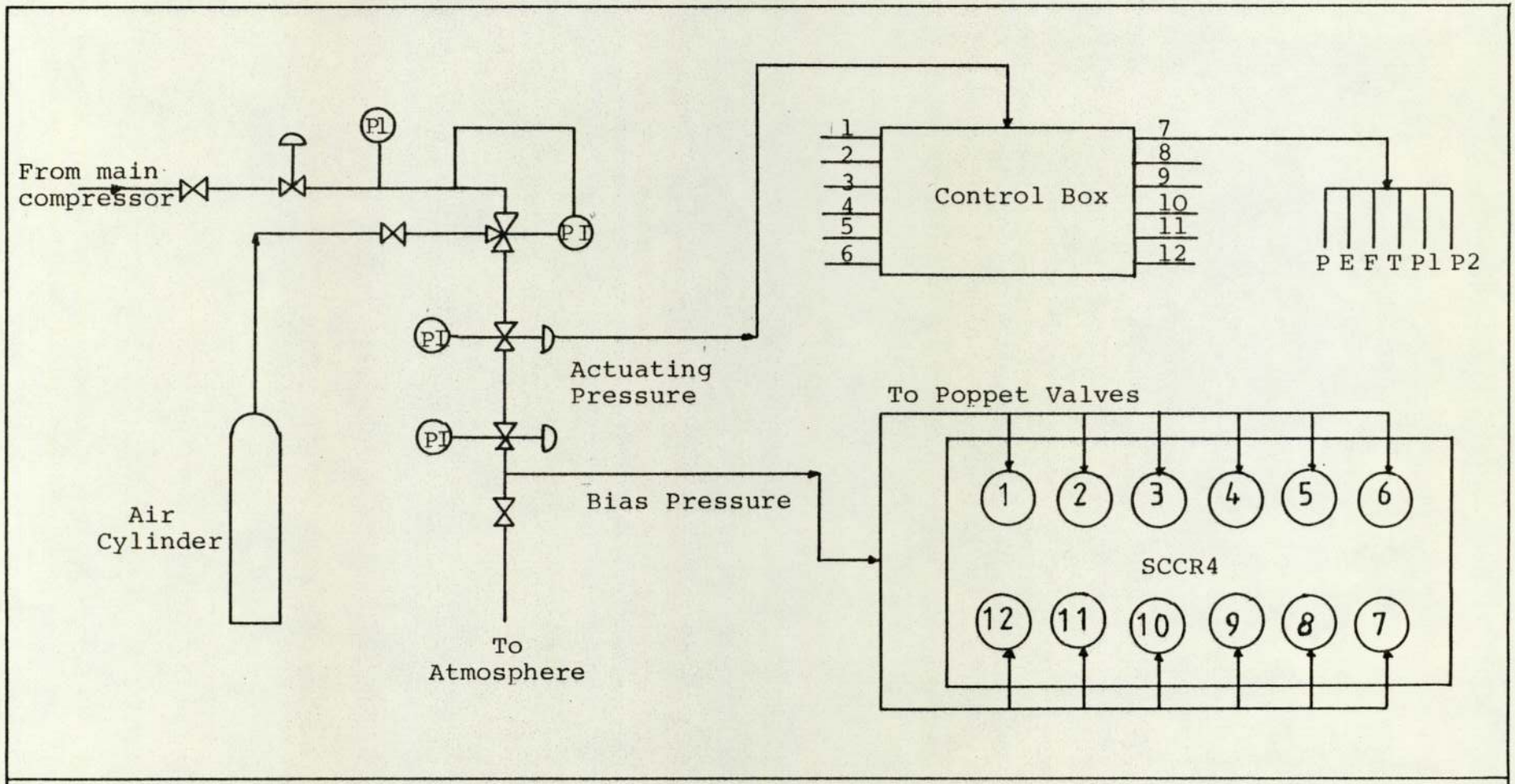

Key: P: Purge E: Eluent T: Transfer Pl: Product 1 P2: Product 2 PI: Press Indicator

4.2.3 Safety Devices

Two safety devices were incorporated on the liquid lines. One was a pressure relief valve and the other was a level controller.

The maximum pressure drop in any part of the process was not expected to exceed 1040 kNm^{-2}. In order to protect the unit against higher pressure drops due to blockage in any line of the process fluids, pressure relief valves supplied by Hoke International Ltd., were placed in the feed, eluent and purge lines. The feed and eluent pressure relief valves were set to 1040 kNm^{-2}. Since the pressure drop in the purge line was expected to be very small and in order to protect the diaphragm of the K-series pump which was used for purging, the purge pressure relief valve was set to 275 kNm^{-2}.

The water was supplied to the preheater aspirator through 10 mm internal diameter tubing. A solenoid valve was connected in line with the tubing just beneath the tank. The solenoid valve was activated by a liquid level controller supplied by Fisons Ltd. When the water in the aspirator reached the upper predetermined level, the controller switched off the solenoid valve. When the water dropped to the lower level, the controller opened the solenoid valve to allow water to flow to the aspirator.

Two safety devices were also incorporated in the air line. One was a relief valve which was set at 700 kNm^{-2}. The other was a differential switch valve. The switch valve was placed in the line connecting

the main air compressor and the standby air cylinder. The air was usually supplied to the SCCR4 unit from the compressor. In cases of failure of the compressor, and as soon as the pressure fell to 480 kNm^{-2}, the switch valve switched the air supply from the compressor to the standby air cylinder.

4.3 MODIFICATION OF THE SCCR4 UNIT

The highest purity recorded by Chuah (14) when using the SCCR4 unit to separate mixtures of fructose and glucose was 92% at a throughput of 75 gms/hour. Therefore it was thought from the start of the research programme that the SCCR4 could be further developed to increase the product purity and the throughput so that the unit could be industrially viable.

The inter-column hold-up volume, i.e. dead volume, was found to be 6-7% of the total liquid volume in the columns. The major contributorsto the hold-up liquid were the poppet valves which controlled the liquid flow in and out of the columns. There was also a small hold-up in the lines. Two alternatives were considered to reduce this high hold-up volume. The first one was to change the valves for ones having small hold-up volume. The second was to increase the columnsize thus decreasing the ratio of the hold-up volume to the total liquid. The latter alternative seemed more economically attractive and furthermore offered the opportunity of scaling up the unit to give higher throughputs. Other modifications to the SCCR4 are described in the following sections.

4.4 GENERAL DESCRIPTION OF THE SCCR7 UNIT

The modified unit was designated SCCR7. Fig. 4.8 is a photograph of the unit. The unit used the same ancilliary equipment described for the SCCR4. These were the pumps, the liquid reservoirs and preheaters, the constant temperature enclosure and the flow rate and temperature measuring devices. The pneumatic control system and the poppet valves were the same as those used in the SCCR4. However before installing the poppet valves they were individually tested for leakage under 1040 kNm^{-2} pressure and any defective valve was repaired. The liquid and pneumatic lines were replaced by new ones of the same size as used for the SCCR4.

The columns were all replaced by larger columns with hydraulic compression devices as described in Section 4.4.1. The new columns were packed with an anion exchange resin Duolite A113 supplied by Dia-prosim Ltd., Pontyclun, Glamorgan, Wales. The particle size range of the resin was 150-300 μm and was 4% cross-linked. The resin was charged in the bisulphite (HSO_3^-) form. Two Super-carbon filters provided by Millipore (U.K.) Ltd. were placed in the deionised water line between the water reservoir and the plastic tank. These filters were capable of retaining impurities of size greater than 6 μm. They were used to protect the anion resin from mechanical fouling by organic matter which might not be removed by the deioniser.

FIG. 4.8 PHOTOGRAPH OF THE SCCR7 UNIT

A = Packed Columns with Sample Points

B = Valves

C = Constant Temperature Enclosure

D = Control Box

E = Digital TImer

F = Pulsation Dampener

G = Pneumatic Lines

H = Metering Pump

I = Pressure Sensitive Switch

SCCR7

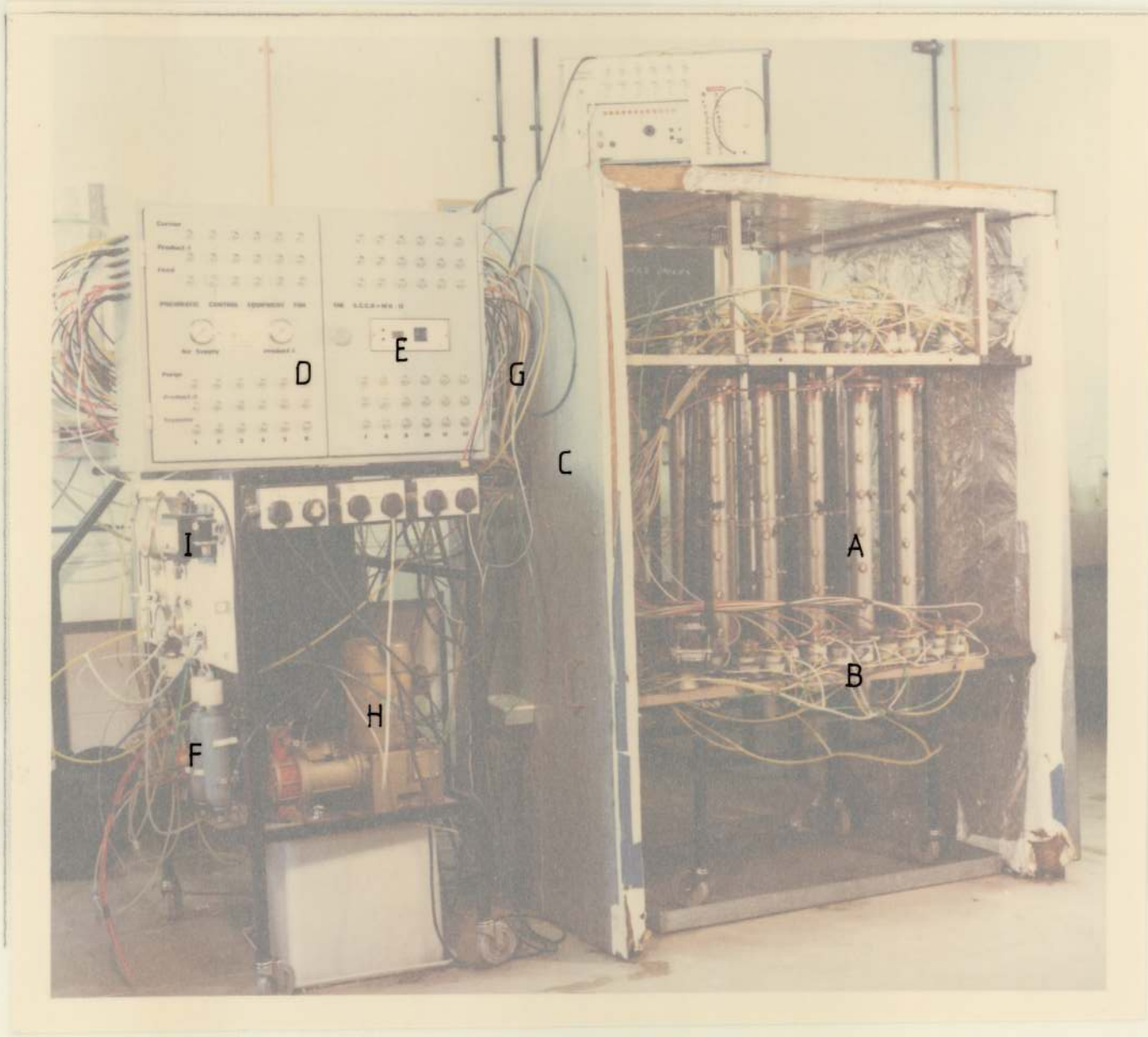

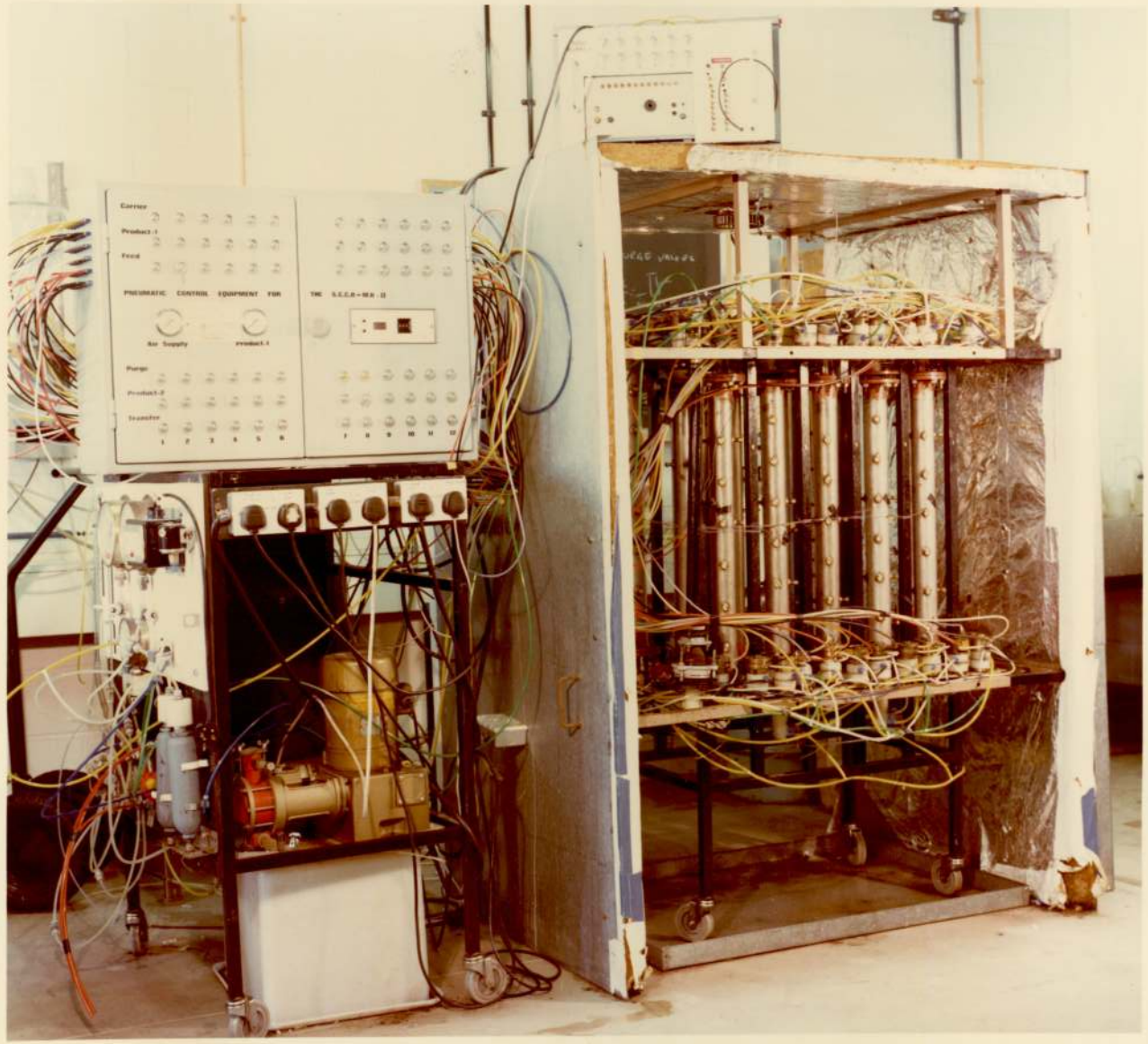
Carrier
Product-1
Feed
PNEUMATIC CONTROL EQUIPMENT FOR
Air Supply
Product-1
Purge
Product-2
Transfer

A further safety device was incorporated into the SCCR7 unit. This was a low pressure sensing switch which is described in Section 4.4.3.

4.4.1 The Columns

The twelve columns were fabricated from type 321 seamless stainless steel tube. Each column was 54 mm internal diameter and 750 mm overall length. The design was according to B.S.5500 : 1976 for pressure vessels.

Fig. 4.9 shows the top part of one of the columns with its inlet fittings. The dimensions and material of construction of various parts are listed with the figure. The inlet assembly consisted of an inlet head with four ports and a compression plunger. The ports were tapped to accommodate 6.4 mm Festo fittings to which the feed, eluent, purge and transfer lines were connected. Liquid channels of 3.0 mm diameter were drilled through the head, the plunger and the piston. To ensure an even velocity profile of the liquid entering the column a perforated polypropylene distributor was placed beneath the piston. A fine polypropylene mesh was used to prevent the packing resin from blocking the liquid ducts.

Fig. 4.10 shows the lower part of one of the columns with all the outlet fittings. The outlet assembly consisted of two parts, a stainless steel mesh and an outlet head. The stainless steel mesh was used to retain the resin. The head had three ports fitted with Festo fittings. Two of the ports were connected to the

Part List of Fig. 4.9

1. Stainless steel tube 750 x 54 mm
2. Neoprene gasket 2 mm thick
3. Polypropylene piston 54 x 50 mm
4. Stainless steel rod 130 x 19 mm
5. Polypropylene inlet head 65 x 40 mm (with 4 ports)
6. Stainless steel sleeve 45 x 20 mm
7. Dowty O-rings No. 200-830-4470
8. Sample points 20 mm x ⅛ BSP
9. Mild steel flanges
10. Polypropylene mesh 100 µm
11. Dowty O-rings No. 200-113-4470, 22·7 mm outer diameter
12. Polypropylene inlet ports 12.7 mm x Tap ¼ BSP
13. Polypropylene distributor
14. Polypropylene retaining ring

Fig. 4.9 The Inlet Assembly of the SCCR7 Column

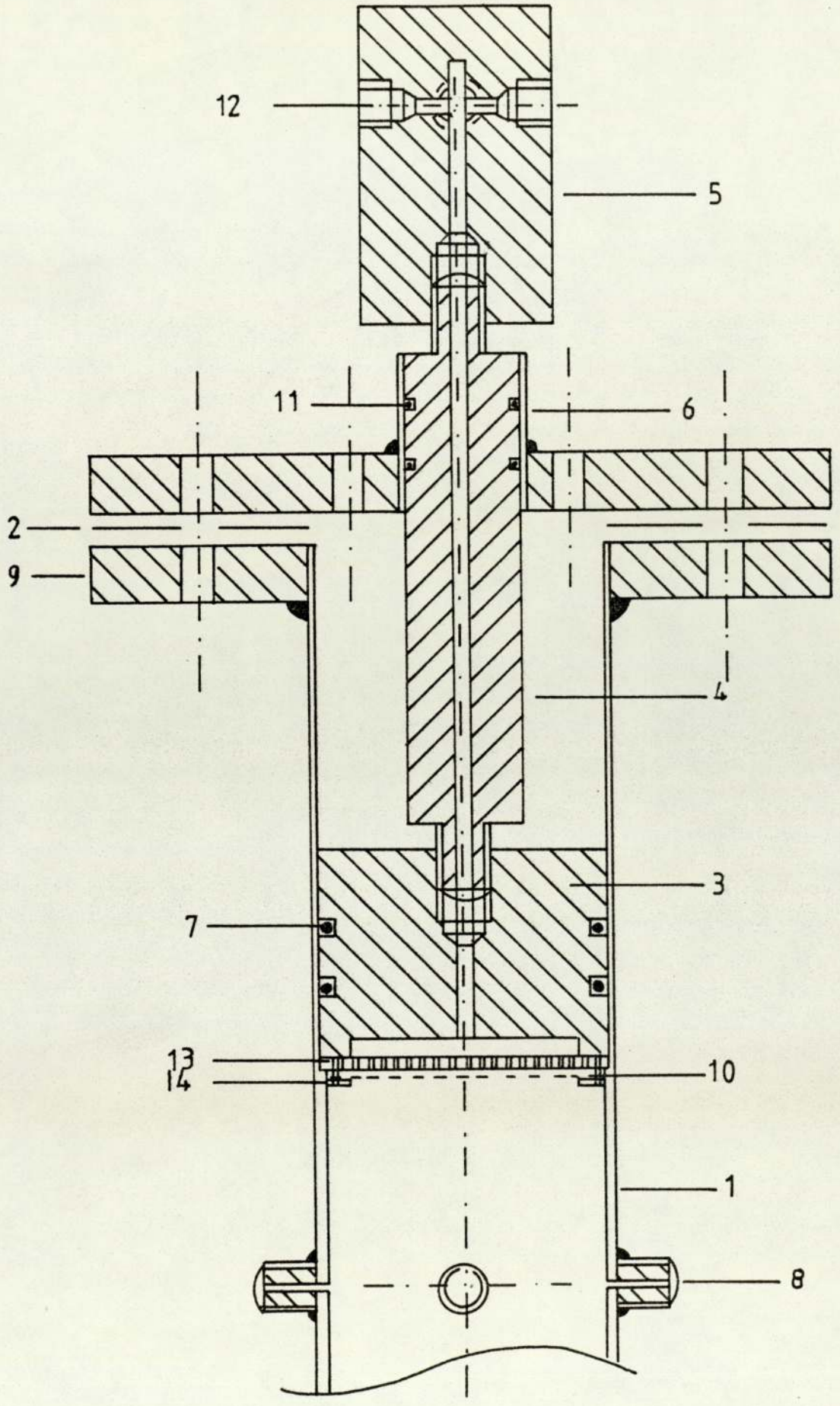

Part List of Fig. 4.10

1. Stainless steel tube 750 x 54 mm
2. Mild steel flanges 130 x 10 mm
3. Sample points
4. Neoprene gasket 2 mm thick
5. Neoprene gasket 2 mm thick
6. Polypropylene outlet head 70 x 38 mm (with 3 ports)
7. Stainless steel mesh 100 µm
8. Outlet ports 12.7 mm x ¼ BSP

Fig. 4.10 The Outlet Assembly of the SCCR7 Column

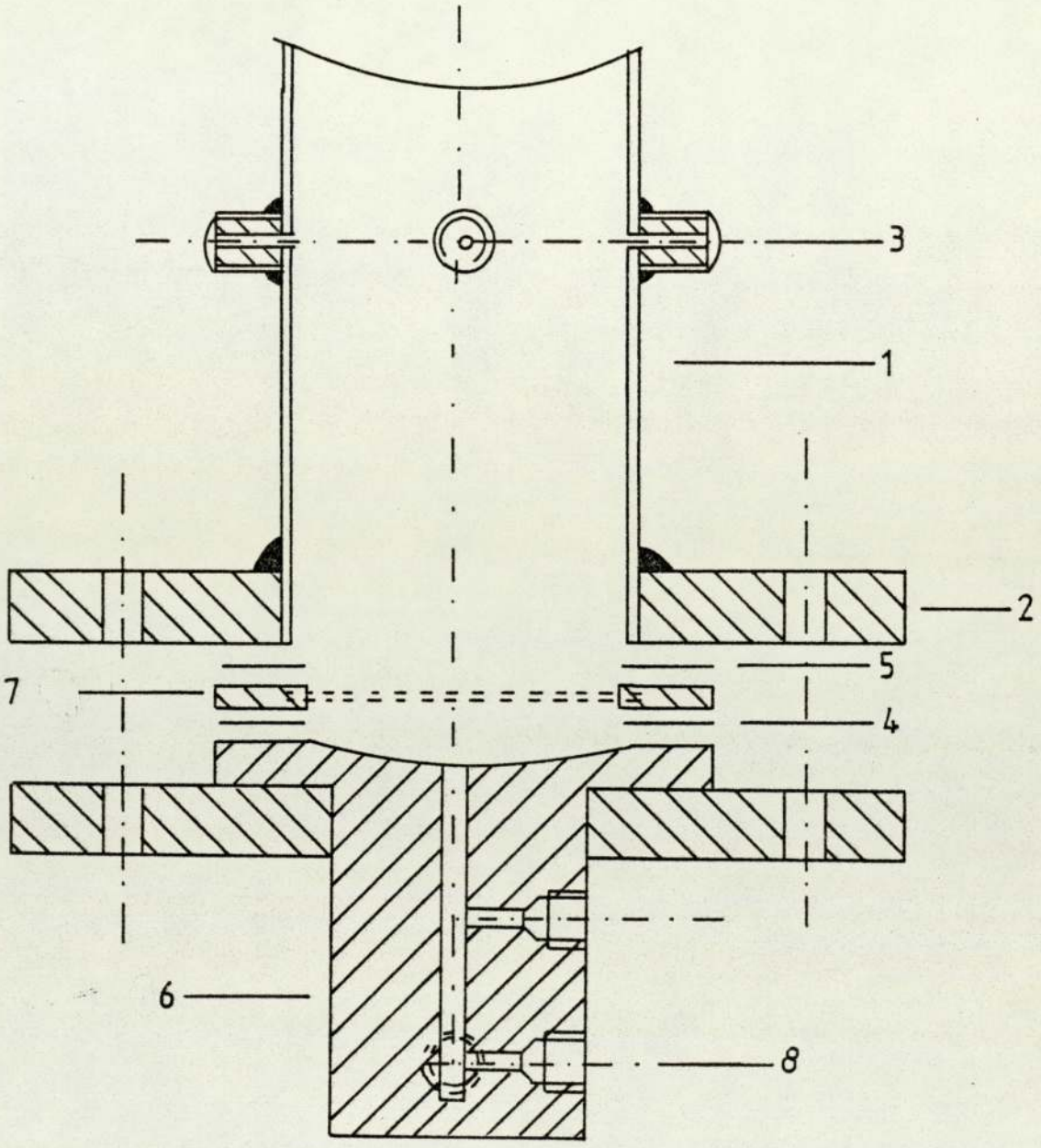

product lines and the third port was connected to a transfer line. To ease the escape of the liquid from the bed through the outlet, a 3^{o} cone was turned on the inside face of the outlet block as shown in Fig. 4.10. The mesh and the head were separated by a neoprene gasket and clamped to the mild steel flange.

Each column had sample points along its length and around the diameter. These sample points were stainless steel rods with 2.0 mm holes drilled through them. The rods were welded to the column as shown in Figs. 4.9 and 4.10. The rod ends were plugged with silicone rubber septa. The septa were held in position by simplifix nuts. When taking samples from the column, hypodermic needles were inserted through the septa to the inside of the column.

4.4.2 The Hydraulic Compression Device

In order to counteract any expansion or contraction of the packing resin during operation a dynamic hydraulic device was incorporated. A similar device had already been incorporated successfully in a larger SCCR Unit (15).

The piston and the rod as shown in Fig. 4.9 were the moving parts of the device. One end of the rod was screwed to the piston and the other end was fitted with O-rings provided by Dowty, Cheltenham, Glos., and passed through a stainless steel sleeve welded to the upper flange. Two O-rings were fitted to the piston to seal on to an accurately machined surface of 100 mm length at the top of the column. This was necessary

to allow the movement of the piston and still maintain the seal between the hydraulic fluid and the packed bed.

Deionised water was introduced to fill the compression compartment through an inlet at the top of the flange and air was bled out via a 6 mm gas tap. The compression compartments of all the columns were linked together with 3 mm nylon tubes to form a closed loop.

4.4.3 Pressure Sensor Device

The SCCR7 was designed to operate continuously. Therefore safety devices were incorporated to prevent hazards especially during the night when the unit was working unattended. These safety devices included a low pressure sensor in addition to the high pressure relief valves and the liquid level controller which had already been used for the SCCR4 unit.

The low pressure sensor device was included in the unit to avoid overflowing of the process liquids caused by failure inside the unit, if for example a valve leaks or a tube bursts or a connector breaks. The pressure sensor was constructed by the department's electronic workshop. The main part of the sensor was a pressure sensitive switch shown in Fig. 4.11. Terminal 1 of the switch was connected to the main electric supply and terminal 2 was connected to a distribution board. The electricity supply to this distribution board could be connected manually by pressing a button on the distribution board, or automatically by applying pressure to the spring, S. The pressure required to activate the

Fig. 4.11 Pressure Sensitive Switch

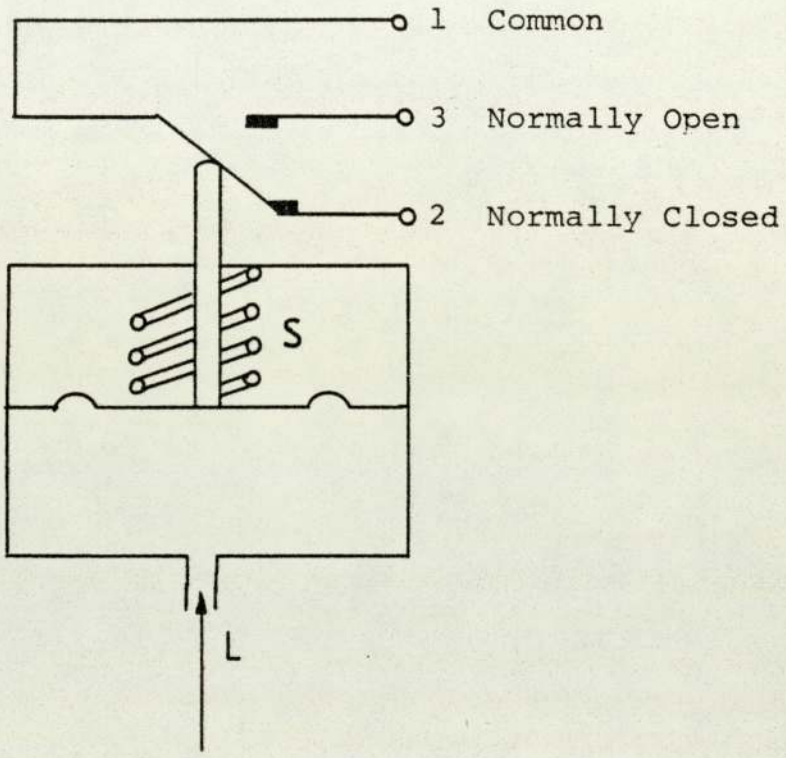

pressure sensive switch was adjustable. Normally that pressure was set to 40 kNm^{-2}. A stream from the eluent line was introduced to the pressure switch diaphragm at L. The electric terminals of the pumps, the liquid preheater and the level controller were all connected to the distribution board.

At the start, the sensor was activated manually by pressing the button, when the eluent pressure built up to the pressure pre-set on the sensor, the sensor was then activated and controlled these functions as long as the eluent pressure was equal to or higher than the pre-set pressure.

In cases of leakage, the eluent pressure dropped and consequently the sensor was deactivated and the pumps, the liquid preheater and the level controller functions were all switched off.

CHAPTER 5

ANALYTICAL WORK USING A BATCH COLUMN

5.1 OBJECTIVES

Considerable analytical batch work has been carried out to investigate the separating capacity of a wide range of packing materials. The performance of different packing materials was compared under different operating conditions of temperature and flow rate. The object was to choose an appropriate material with which to pack the SCCR7 unit for the separation of mixtures of fructose and glucose.

5.2 PACKING MATERIALS INVESTIGATED

Three types of packing materials were studied, inorganic packings and cationic and anionic synthetic resins. Table (5.1) lists these packings together with their relevant properties.

Two of the cationic resins have already been applied on commercial scale units. Dowex 50W-X4, was reported to be used by the Boehringer process (8) and Lewatit TSW 40, was used in the Südzucker process (4). The Zerolit 225 was used to pack pilot plant units by Ching (12), Chuah (14) and Gould (15). The references to the use of anion resins and inorganic packings have been obtained from literature.

TABLE 5.1 PROPERTIES OF VARIOUS PACKING MATERIALS

Packing	Type	Form	Size BS Mesh	Cross-Linking	Capacity Wet(meq/ml)	Max. Temp. ^{o}C	pH-Range
Zeolite 13X (Inorganic)	Cationic	Ba^{2+}	15-35	-	-	500	1-14
Zerolit 225	Cationic	Ca^{2+}	50-100	8	2.0	140	1-14
Dowex 50W-X4	Cationic	Ca^{2+}	50-100	4	1.7	140	1-14
Lewatit TSW-40	Cationic	Ca^{2+}	50-100	4	-	140	1-14
Dowex 1-X8	Anionic	HSO_3^-	50-100	8	1.4	80	1-14
Amberlite CG-400	Anionic	HSO_3^-	100-200	8	1.4	80	1-14
Duolite A113	Anionic	HSO_3^-	50-100	4	1.2	80	1-14

5.2.1 The Treatment of the Packings

The cation exchange resins were all supplied in the sodium (Na^+) form. It was desired to change the resins to the calcium (Ca^{2+}) form to effect the fructose/glucose separation. The procedure for charging the resins was as follows.

Equation (2.2) was used to calculate the quantities of reagents needed. A weighed quantity of the resin was treated with a measured quantity of 10% HCl to replace the Na^+ ions by H^+ ions. Then the resin was washed and contacted at room temperature with a solution of 10% w/v $CaCl_2$ to finally convert it to the Ca^{2+} form.

The anion exchange resins were supplied in the chloride (Cl^-) form. The resin was first treated with a solution of 5% w/v NaOH to replace Cl^- with OH^- ions. Then after the resin was washed, it was finally charged to the bisulphite (HSO_3^-) form by addition of a measured amount of 10% w/v $NaHSO_3$ solution.

A different procedure was followed in charging the zeolites. These were supplied in pellets of 1.5-3.0 mm length. They were first ground and then sieved. The particles between (300-600) μm were retained. Since both zeolites 5A and 13X were provided in the Na^+ form, they were contacted with a much larger amount of the salt of the desired cation, for example $BaCl_2$ was used for zeolite 13X and $CaCl_2$, NaCl and KCl for zeolite 5A. The treatment was carried out at 100°C for an hour. Then the zeolite was filtered, washed and dried (21).

5.2.2 Packing Technique and Sample Loading

Fig. 5.1 shows the column used for this investigation together with its fittings. The glass column was 1030 mm long and 9.7 mm internal diameter. It was surrounded by a constant temperature water jacket.

The slurry packing technique and sample loading procedure as reported by Ching (12) was adopted in this work. The range of the detection unit used restricted the volume and concentration of the sample. Throughout the analytical work 50 µl of solute with a concentration of 1500 ppm was injected into the column.

The constant temperature was maintained by a thermostatically controlled heating bath.

5.3 THE DETECTION UNIT

The detection technique employed for the batch work was colorimetry, and the detection unit was a Technicon-Autoanalyser. The unit was designed to produce a chromophore with an optical density proportional to the sample concentration.

The reagent used throughout the analytical work was prepared by adding a 0.07% w/v solution of the biochemical L-cysteine hydrochloride to 86% w/v sulphuric acid. This reagent was used to determine the total concentration of carbohydrates in the sample. The reagent produced a yellow chromophore. The optical density of carbohydrates was measured at a wavelength of 420 nm.

Fig. 5.2 shows the assembly of the Technicon-Autoanalyser. It consisted of a proportionating pump,

Fig. 5.1 The Analytical Column

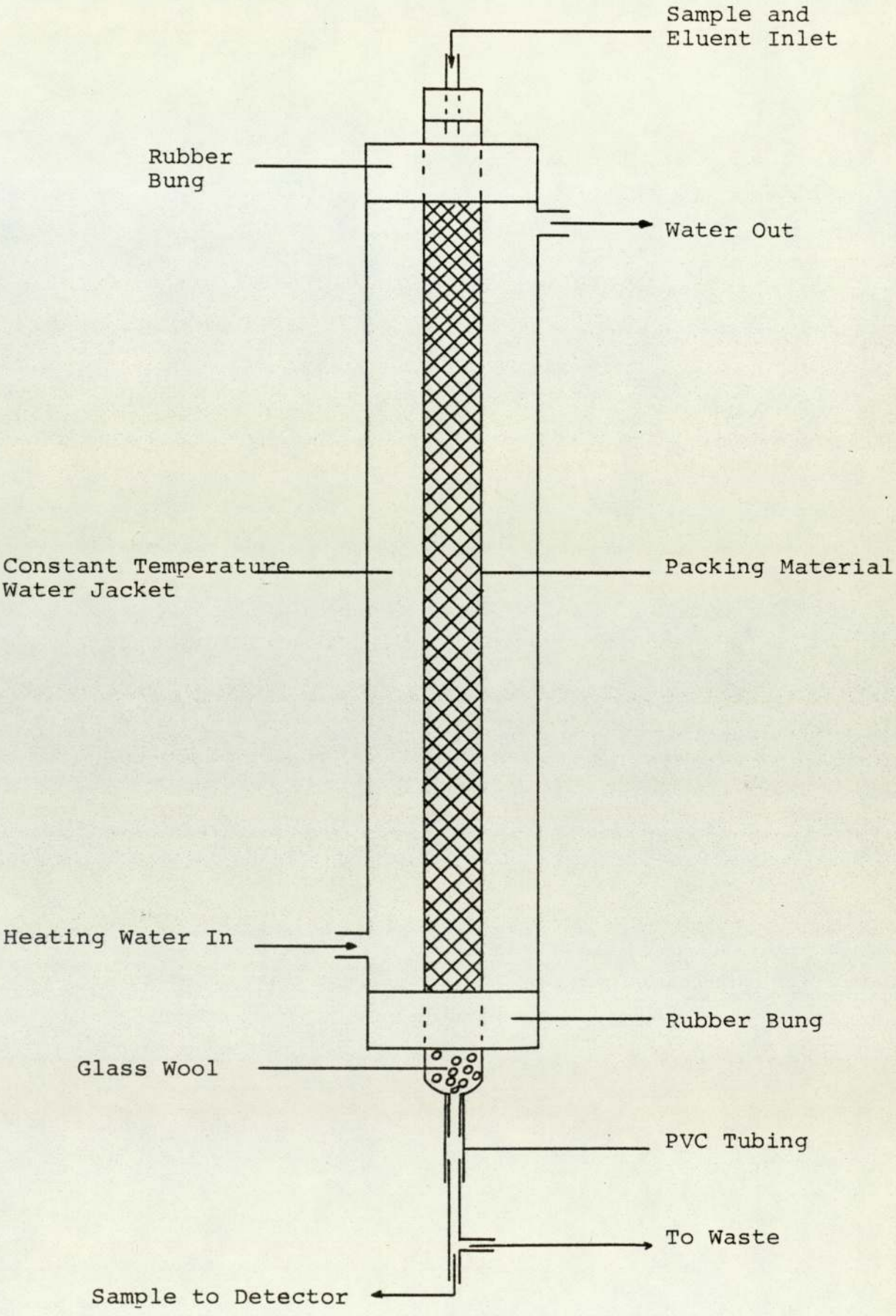

Fig. 5.2 Technicon Auto-Analyser

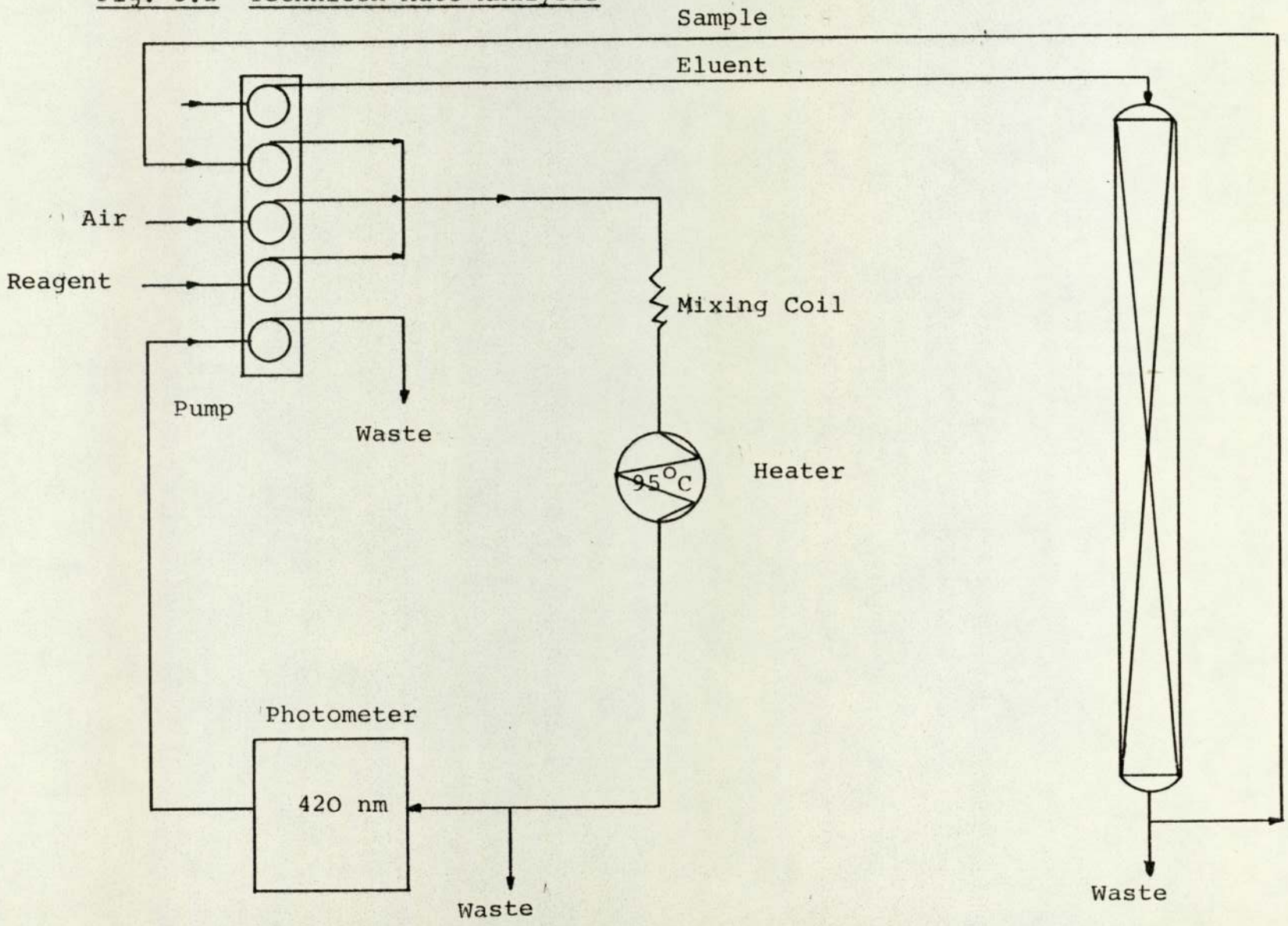

a heating oil bath, a photo-cell, a colorimeter and a chart recorder. The multi-channel proportionating pump was used to meter the sample and reagent streams. The pump functioned on a peristaltic principle where the flow rate was governed by the size of the tubes used. The air stream was used to separate portions of the combined reagent and sample stream before entering the heating bath. That was necessary to minimise back-mixing.

5.4 RESULTS AND DISCUSSION

5.4.1 Determination of Separation Capacity

The chromatograms obtained from different packings were used to determine the relative distribution coefficient, K_d and the resolution, R_s. Equation (2.15) was used to calculate HETP to compare column efficiencies.

Rearranging equation (2.5) gives

$$K_d = \frac{V_R - V_M}{V_S} \quad \ldots\ldots\ldots\ldots\ldots\ldots\ldots\ldots \quad (5.1)$$

but $$V_S = V_T - V_M \quad \ldots\ldots\ldots\ldots\ldots\ldots\ldots\ldots \quad (5.2)$$

where V_T is the total column volume.

Combining (5.1) and (5.2) gives

$$K_d = \frac{V_R - V_M}{V_T - V_M} \quad \ldots\ldots\ldots\ldots\ldots\ldots\ldots\ldots \quad (5.3)$$

If a mixture of dextran, fructose and glucose is eluted through a packing and provided that the packing pores are too small to allow dextran molecules to pass through, then the dextran emerges first by a gel

permeation mechanism. Then, depending on the nature of the ionic charge, either fructose or glucose is chemi-sorbed and thus retarded to emerge last of the three solutes.

Since dextran is neither retarded by chemi-sorption or gel permeation, then its retention volume, V_D, represents the volume of the mobile phase, i.e.

$$V_M = V_D \quad \ldots\ldots\ldots\ldots\ldots\ldots\ldots\ldots \quad (5.4)$$

From equations (5.3) and (5.4), the distribution coefficient, K_d^F, for fructose is

$$K_d^F = \frac{V_F - V_D}{V_T - V_D} \quad \ldots\ldots\ldots\ldots\ldots\ldots\ldots \quad (5.5)$$

and the distribution coefficient K_d^G, for glucose is

$$K_d^G = \frac{V_G - V_D}{V_T - V_D} \quad \ldots\ldots\ldots\ldots\ldots\ldots\ldots \quad (5.6)$$

where V_F and V_G are the retention volume of fructose and glucose respectively.

The resolution, R_s, was defined by equation (2.8). For a binary separation of fructose and glucose.

$$R_s = \frac{2(t_F - t_G)}{W_F + W_G} \quad \ldots\ldots\ldots\ldots\ldots\ldots\ldots \quad (5.7)$$

Examples of the results obtained for these quantities for different packings are presented against ranges of temperature and flow rate in Table (5.2).

Graphs of K_d, R_s and HETP against temperatures and flow rates are plotted in Figs. (5.3-5.11) to compare performances of the packing materials.

TABLE 5.2 PERFORMANCE OF DIFFERENT PACKING MATERIALS

Packing (Form)	Temp. ^{o}C	Flow Rate ($cm^3 min^{-1}$)	Elution Volume (cm^3)			Distribution Coefficient		Resolution R_s	HETP (mm)	
			V_D	V_G	V_F	K_d^G	K_d^F		w.r.t. Glucose	w.r.t. Fructose
Zeolite 13X (Ba^{2+})	20	0.2	56.6	56.6	83.8	0	2.50	1.19	4.59	6.34
Zerolit 225 (Ca^{2+})	20	0.2	30.3	40.9	59.1	0.31	0.81	1.36	4.10	6.60
Dowex 50W (Ca^{2+})	20	0.2	28.8	41.7	61.6	0.33	0.85	1.37	6.20	7.40
Lewatit TSW (Ca^{2+})	20	0.2	32.5	43.0	60.8	0.30	0.81	1.35	3.72	6.54
Dowex 1-X8 (HSO_3^-)	60	0.2	27.3	66.4	47.8	0.94	0.51	1.31	4.20	2.70
Amberlite CG (HSO_3^-)	60	0.2	32.5	65.1	50.0	0.92	0.50	1.38	4.00	3.21
Duolite A113 (HSO_3^-)	60	0.2	27.3	65.7	49.2	0.98	0.54	1.34	4.12	2.50

5.4.2 Effect of Temperature on K_d and R_s

Figs. (5.3,5.4) show that both K_d^F and R_s decrease with increase of temperature for the cation exchangers, Dowex 50W-X4 and Lewatit TSW40. In this case the peak of the more retarded solute, fructose, was brought nearer to the glucose peak with increase of temperatures, and therefore the separating capacity of the packing decreased.

Different behaviour was noticed for the anion exchange resins, Amberlite CG-400, Dowex 1-X8 and Duolite A113. In this case the resolution, R_s, can be seen in Fig. 5.6 to increase with increase of temperature. K_d^G as shown in Fig. 5.5 was virtually constant for temperatures above 40°C, but for temperatures below 30°C higher values for K_d were obtained. It was noticed that at low temperature the band of the more retarded solute, glucose, did not emerge as a true Gaussian curve, and in fact it emerged as a plateau as shown in Fig. 5.7. This might explain the low values of R_s at low temperatures.

5.4.3 Effect of Temperatures on Column Efficiency

For all types of packing materials under investigation, it was found that the column efficiency increased with increase of temperature. This was demonstrated by the smaller values of HETP with respect to the retarded solute, i.e. fructose for cation exchangers and glucose for anion exchangers, as shown in Fig. 5.8. Increase of temperature generally decreases the

Fig. 5.3 Effect of Temperature on K_d^F for Cation Exchange Resins at 0.2 $cm^3 min^{-1}$

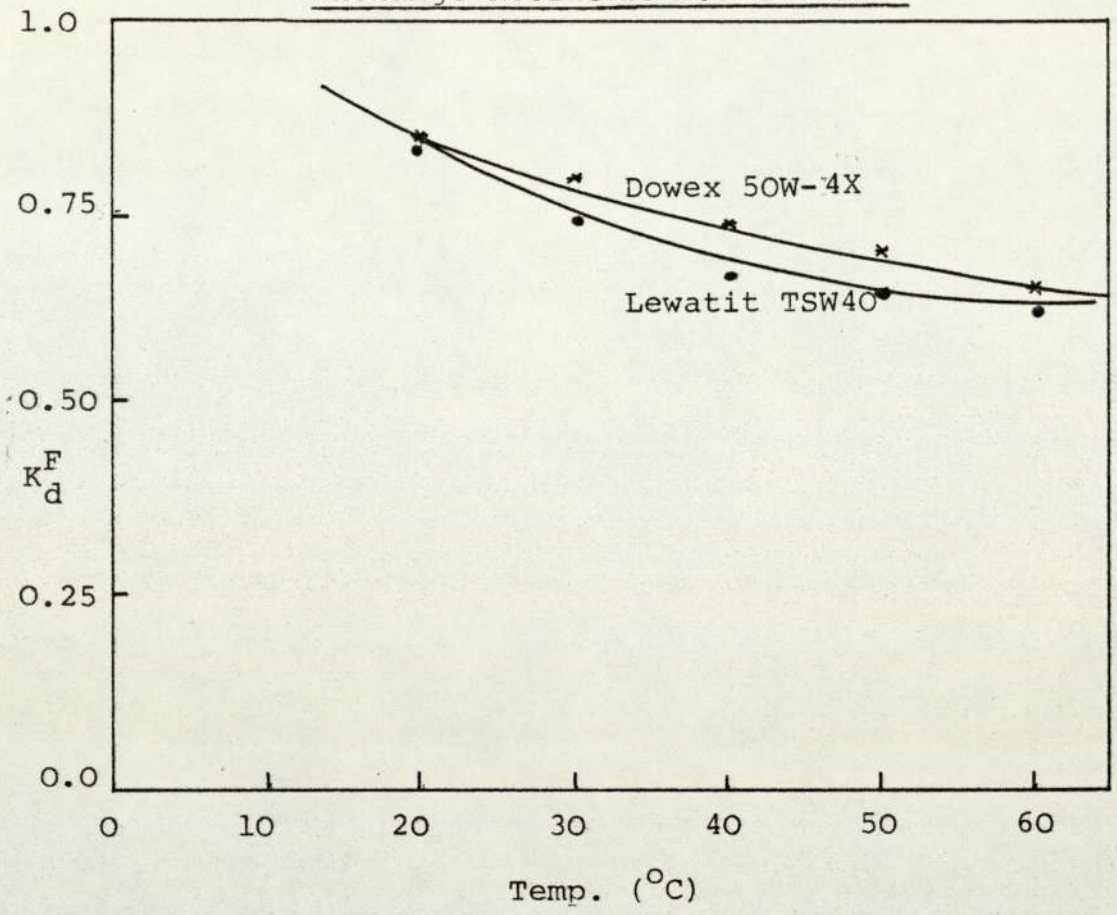

Fig. 5.4 Effect of Temperature on R_s for Cation Exchange Resins at 0.2 $cm^3 min^{-1}$

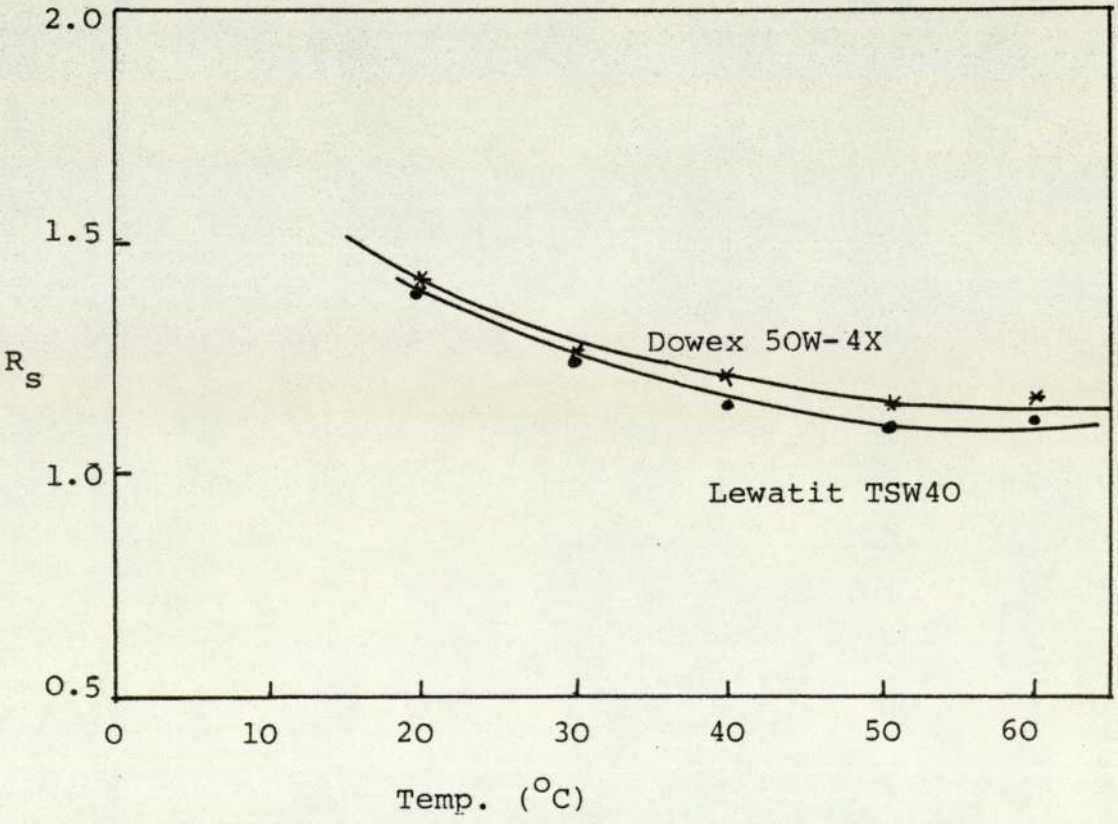

Fig. 5.5 Effect of Temperature on K_d^G for Anion Exchange Resins at 0.2 $cm^3 min^{-1}$

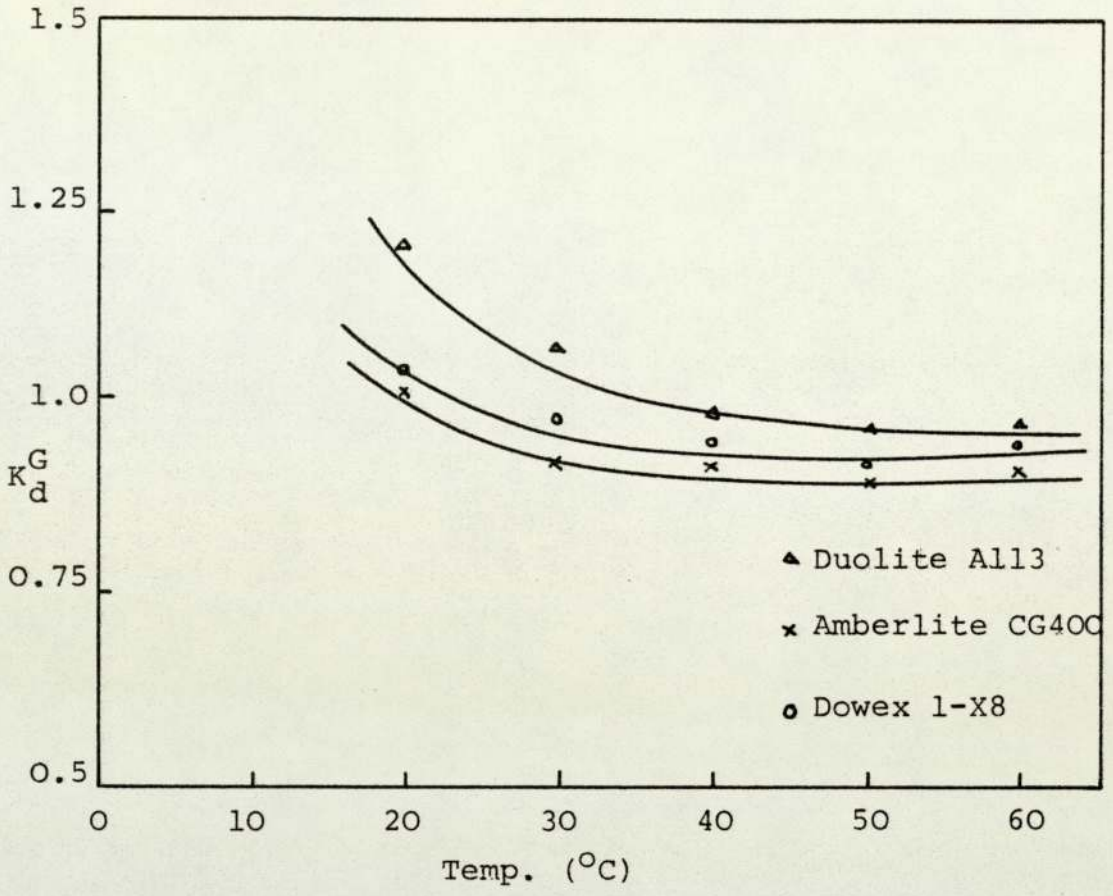

Fig. 5.6 Effect of Temperature on R_s for Anion Exchange Resins at 0.2 $cm^3 min^{-1}$

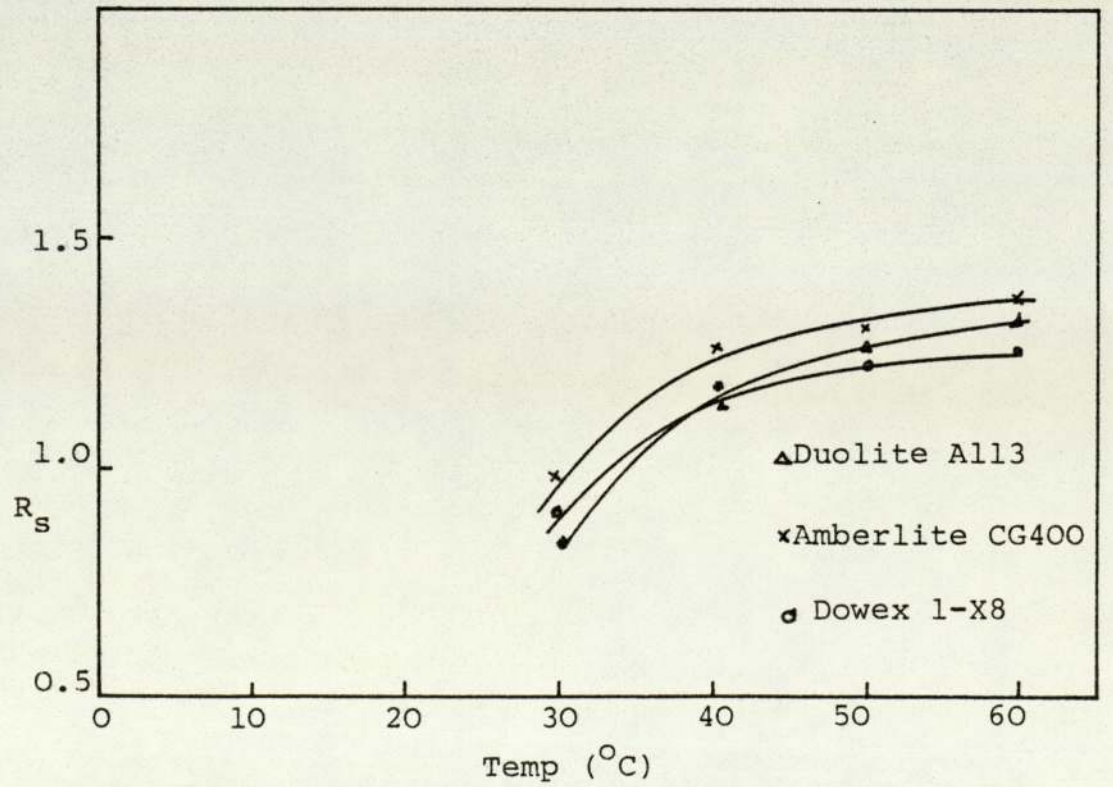

Fig. 5.7 Representation of Temperature Effect on Band Shape for Anion Exchangers

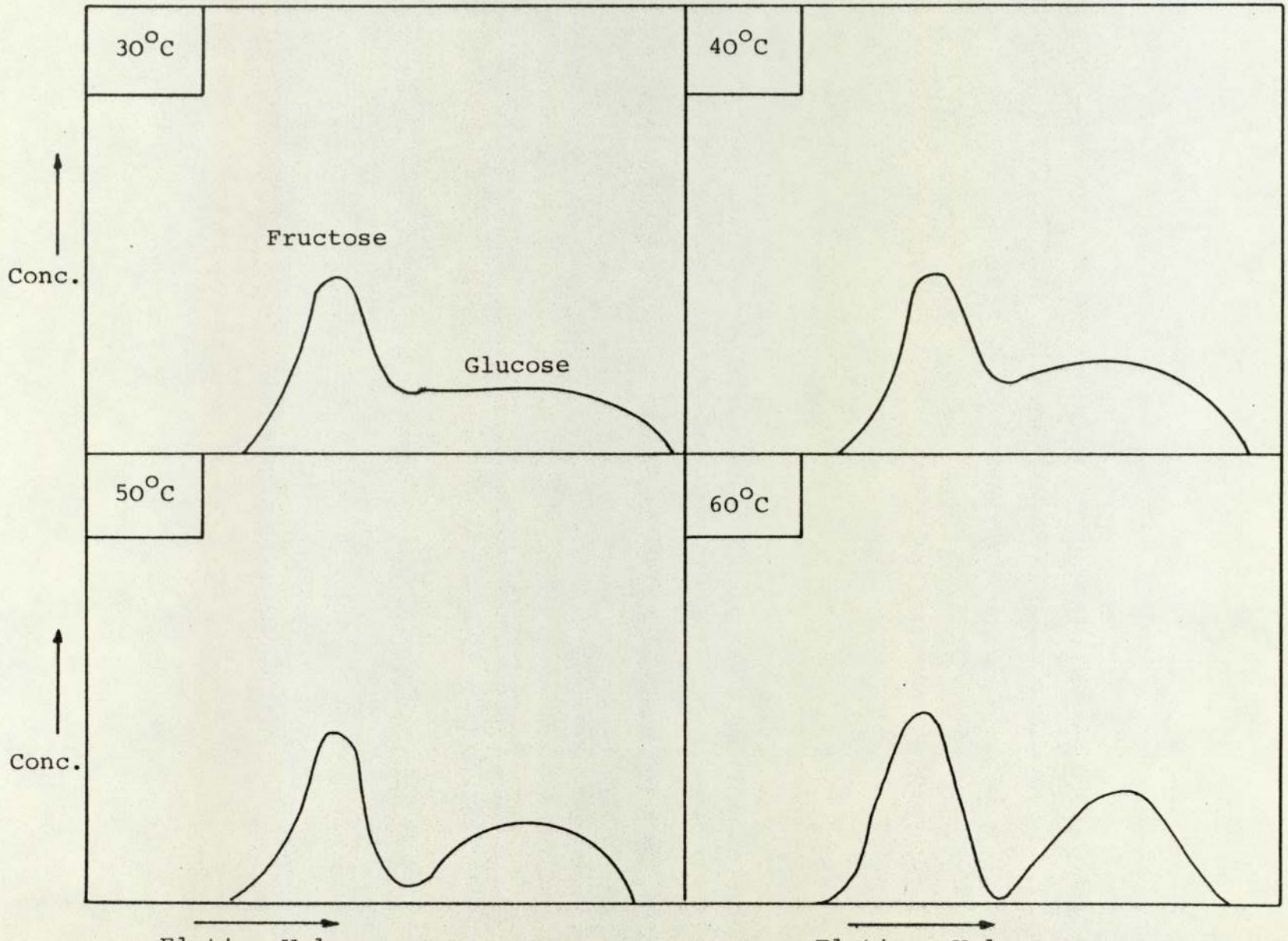

viscosity and increases the diffusivity. Giddings (79) suggested that each 10°C increase of temperature would reduce the elution volume by 10-25% due to the increase in activation energy. The reduction in elution volume will result in a sharp band with high column efficiency which will be discussed in Section 5.4.5.

5.4.4 Effect of Flow Rate on K_d and R_s

The distribution coefficient, K_d, with respect to the more retarded solute, i.e. fructose for cation exchangers and glucose for anion exchangers, is shown in Fig. 5.9 to remain constant over ranges of flow rates between (0.2-0.6). But R_s is shown in Fig. 5.10 to decrease with increase of flow rate. Measurements of the degree of separation should take into account both the degree of band overlap, i.e. the distance between the peak maxima; and the widths of the bands. A good degree of separation is obtained if the peak maxima are well-separated and the bands are narrow. By definition, R_s (equation 5.7) takes both peak maxima and widths of the bands into account. The decrease of R_s with increase of flow rate can be explained in terms of migration distance on peak maxima separation and band widths. For a Gaussian band, the peak separation ($t_{R2}-t_{R1}$) is directly proportional to the distance of migration while the bands are broadened only with the square root of distance of migration. This is because the band width is equal to 4σ, the standard deviation of the Gaussian band (26) which means that the bands separate faster than they

Fig. 5.8 Effect of Temperature on HETP at 0.2 $cm^3 min^{-1}$

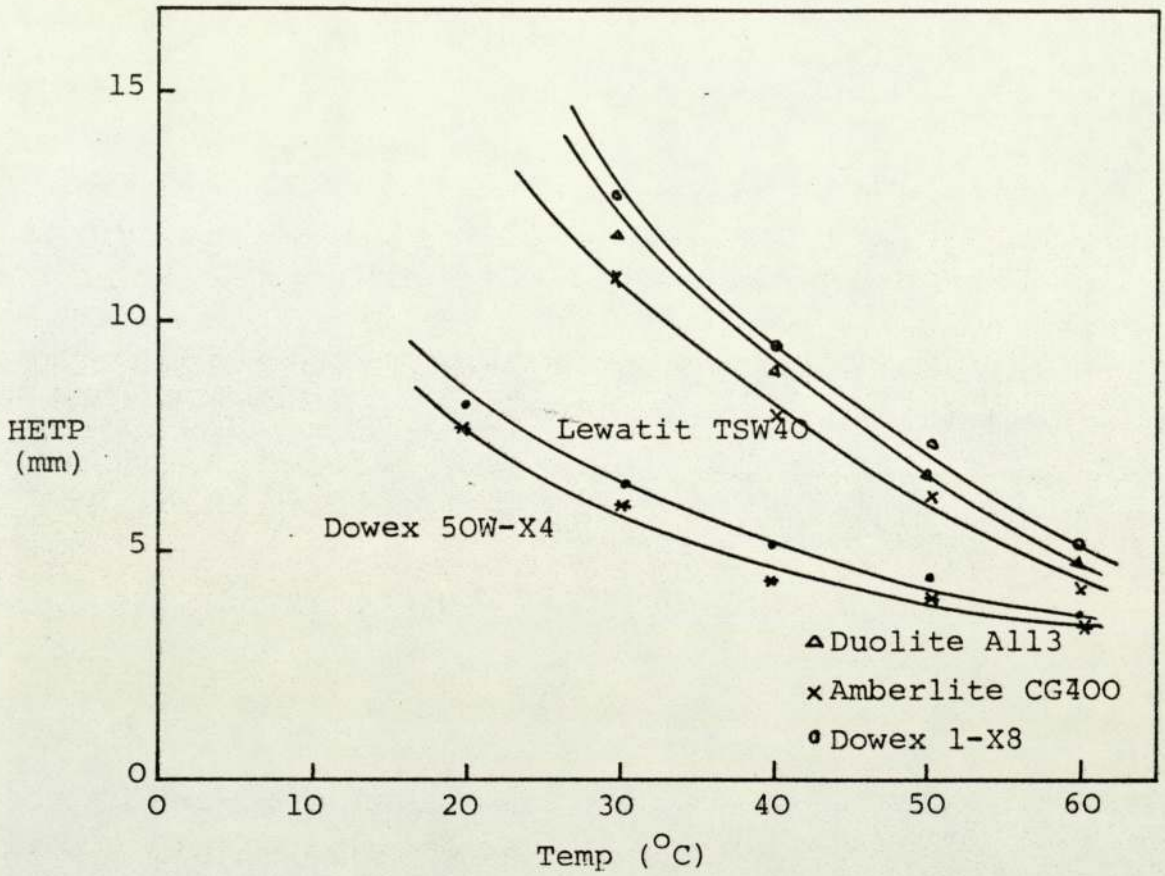

Fig. 5.9 Effect of Flow Rate on K_d at 60°C

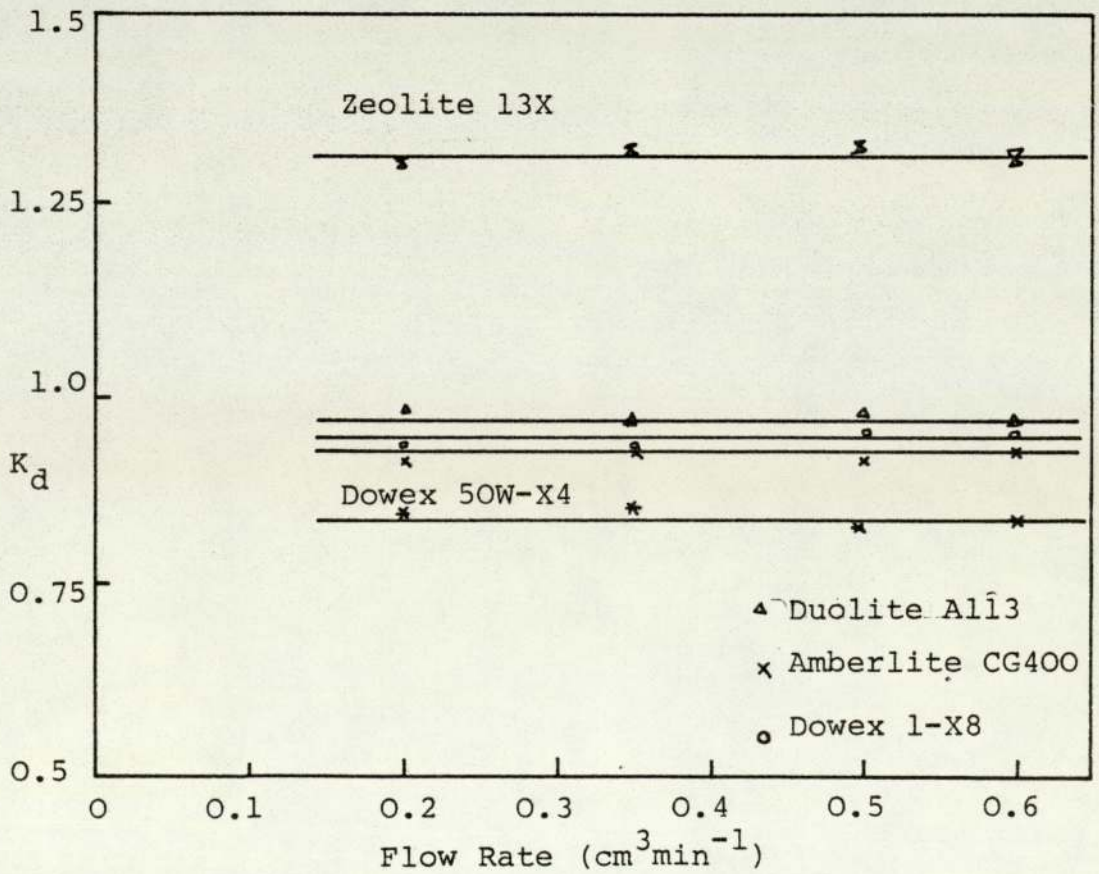

broaden. At low flow rates the distance of migration is increased and therefore the rate of increase in the numerator of equation (5.7) is greater than that of the denominator. Hence R_s increases. At high flow rates the distance of migration decreases and by the same argument, R_s decreases.

K_d, as defined by equation (5.3), does not take into account band widths, it considers only the elution of peak maxima. Since the peak maxima are directly proportional to the distance of migration, the value of K_d remains constant over ranges of flow rates.

This argument is not intended to devalue the importance of K_d. The importance of K_d arises from the fact that it relates the fundamental chromatographic bed parameters to resolution by considering the total bed volume V_T, mobile phase volume, V_M, and retention volume, V_R.

5.4.5 Effect of Flow Rate on Column Efficiency

It was found that high elution rates resulted in a smaller number of plates for all packing materials investigated. Fig. 5.11 shows that high elutuion rates are associated with high values of HETP and hence less efficiency. By examining equation (2.15), it will be observed that the numerator (t_R) is directly proportional to flow rate while the denominator ($W_{h/e}$) is proportional to the square root of the flow rate. The distance of migration is increased at low flow rates. Since the rate of

Fig. 5.10 Effect of Flow Rate on R_s at 60°C

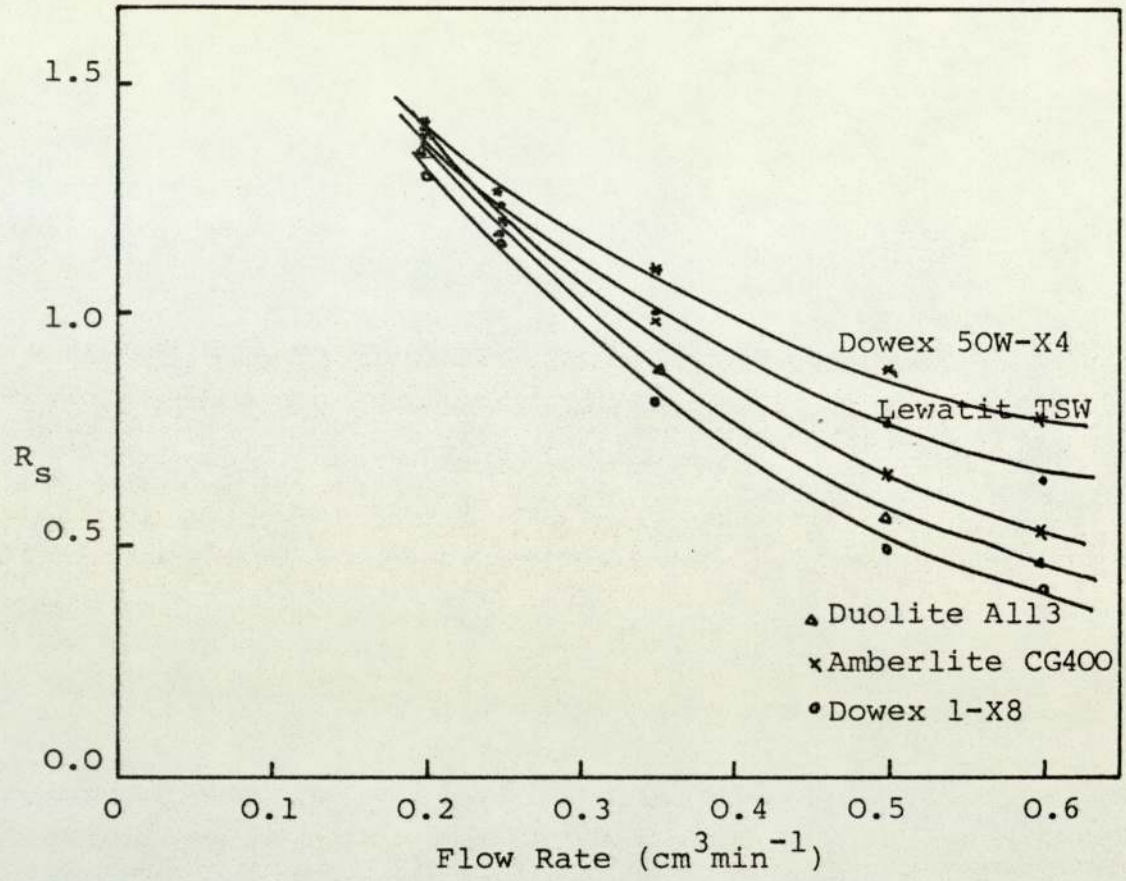

Fig. 5.11 Effect of Flow Rate on HETP at 60°C

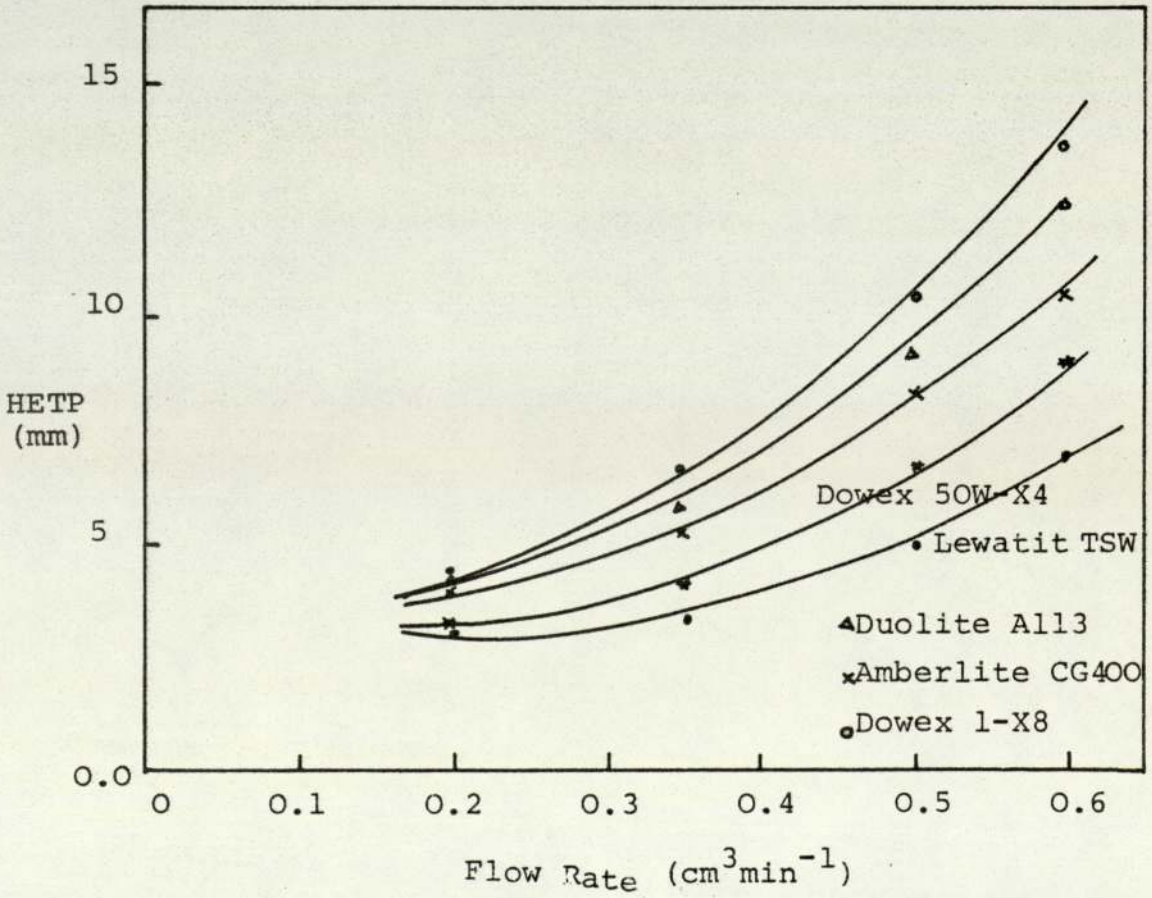

increase of the numerator is greater than the rate of increase of the denominator, then low flow rates result in high numbers of plates N, and therefore high column efficiency.

Generally the effect of elution velocity on HETP is shown by examining equation (2.18) for the plate height. Fig. 5.12 shows a plot of H vs v, the mobile phase velocity. From the curve it can be seen that there is a minimum value of H corresponding to an optimum value of the mobile phase velocity, v_{opt}. The optimum velocity which yields the best efficiency can be determined by setting the derivative dH/du equal to zero, hence

$$v_{opt} = \left(\frac{B}{C_m + C_s}\right)^{\frac{1}{2}} \quad \ldots\ldots\ldots\ldots\ldots\ldots \quad (5.8)$$

Although this optimum velocity results in the best separation and efficiency, it is disadvantageous in the very slow achievement of separation due to the low flow rate.

5.5 GENERAL CONCLUSION

5.5.1 Molecular Sieves

The results of separation of fructose-glucose mixtures using zeolites 5A and zeolite 13X in Na^+, K^+ and Ca^{2+} forms, were unsatisfactory. The only satisfactory separation was achieved with zeolite 13X in the barium (Ba^{2+}) form. The zeolites used were supplied in granulated form. Reports indicate the

Fig. 5.12 Plate Height Vs Mobile Phase Velocity

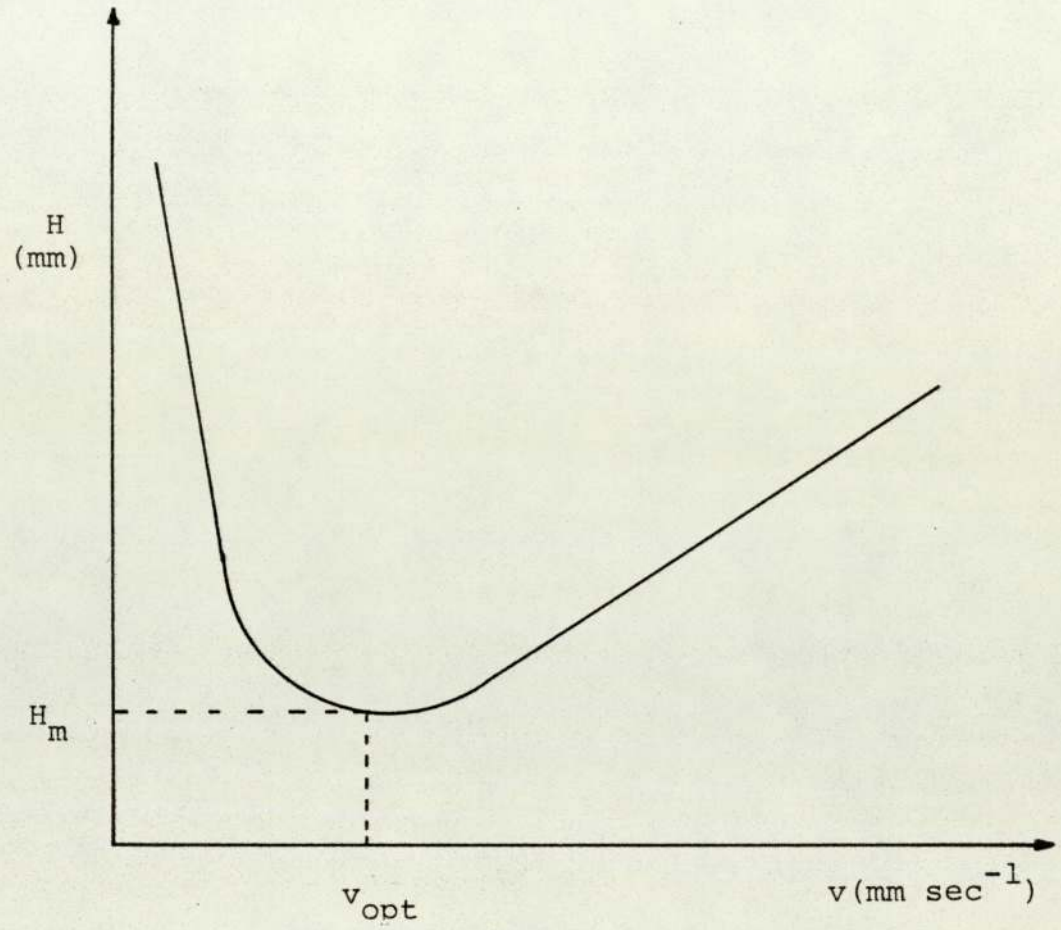

success of these zeolites in different cationic forms to separate fructose-glucose mixtures (6,16,65). These reported the use of spherical zeolite particles of (15-50) mesh compared to the irregular particles used in this work. Unfortunately it was not possible to obtain spherical particles of this size.

During the analysis, it was noticed that when water was added to the zeolites, the suspension turned turbid. Comyns (80) stated that the silica constituents of zeolites tend to dissolve gradually in aqueous systems. By the time this research work was under completion a patented process to overcome this undesirable phenomenon was disclosed. The patent (77) describes a method of coating the zeolites with a water permeable organic polymer such as cellulose acetate dissolved in an organic solvent like acetone. This coating is claimed to substantially reduce the dissolution of silica in water and the performance of the coated zeolite is remarkably increased over that of uncoated zeolites.

Since zeolites are mainly molecular sieves, this property of screening is of no use in sugar separation, because the molecular sizes of dextran, glucose and fructose are all larger than the pore sizes of zeolites 5A and 13X which are 5×10^{-7} and 1.0×10^{-6} mm respectively, and this may explain the similar elution volumes of dextran and glucose when using zeolite 13X in the Ba^{2+} form as shown in Table 5.2.

The comparatively good performance of zeolite 13X

in Ba^{2+} is attributed to the stronger complex between sugars and barium, than those between sugars and other cations. The fact that barium forms a strong complex with sugars is useful in sugar industries for desugarising molasses. The sugar in molasses is precipitated by addition of BaS to form barium saccharate (81).

However if the zeolites in barium form are to be used for separation of sugars, another problem arises. Since the separated sugars are intended for human consumption, they must be freed from any traces of barium contamination and this does not seem to be an easy task as it requires further ion-exchange treatment.

5.5.2 Synthetic Resins

In analytical chemistry, it is known that cation exchangers are more stable than anion exchangers. This fact was observed during the course of this analytical work. Columns of anion exchangers, after some batches, started to develop colouration at the top and downwards. Their performance deteriorated even when deionised water was used as an eluent. When the resin was regenerated with bisulphite, the bed volume contracted by about 10%.

Anion exchangers suffer from two main disadvantages, auto-oxidation and mechanical fouling. If however these two drawbacks are controlled, the anion exchangers for batch analytical separations seem to compete with the cation exchangers for the purpose of sugar

separation for the following reasons.

The performance of cation exchangers is better at low temperatures while that of anion exchangers is reasonable at temperatures higher than 30°C. Working at higher temperatures, say 60°C, reduces the viscosity and hence pumping cost. Another benefit of working at high temperatures is that it inhibits bacterial growth.

A further advantage offered by anion exchangers for sugar separation, and especially if fructose is desired as a main product, is that fructose is not retarded and is therefore eluted first at a higher concentration.

CHAPTER SIX

CONTINUOUS SEPARATION OF FRUCTOSE AND GLUCOSE ON THE SCCR4 UNIT

6.1 PREDICTION OF OPERATING CONDITIONS OF THE SCCR4 UNIT

The principle of operation of the SCCR unit has been described in Section 4.1. In order to use the unit for the separation of a binary mixture of fructose and glucose, a mathematical expression has to be constructed to relate the flow rates of the mobile and stationary phases to the relative elution of the solutes. Barker et al (41,82,83,84) have developed a model relating the flow rates to the distribution coefficients for different units. The model was proved to be adequate by other researchers (12,14,15). The model can be adapted to the fructose/glucose system in an SCCR unit packed with a cation exchange resin in the Ca^{2+} form.

Fig. 6.1 shows a schematic diagram of the SCCR unit. Since glucose is not adsorbed by the packing, it travels preferentially with the mobile phase while fructose travels with the stationary phase. A material balance on glucose about the feed point gives:

$$F_g = L_e Y_g + P X_g \quad \ldots\ldots\ldots\ldots\ldots\ldots\ldots\ldots \quad (6.1)$$

where F_g = mass rate of glucose input at feed point

L_e = mobile phase flow rate

P = stationary phase flow rate

Fig. 6.1 Schematic Diagram of SCCR4

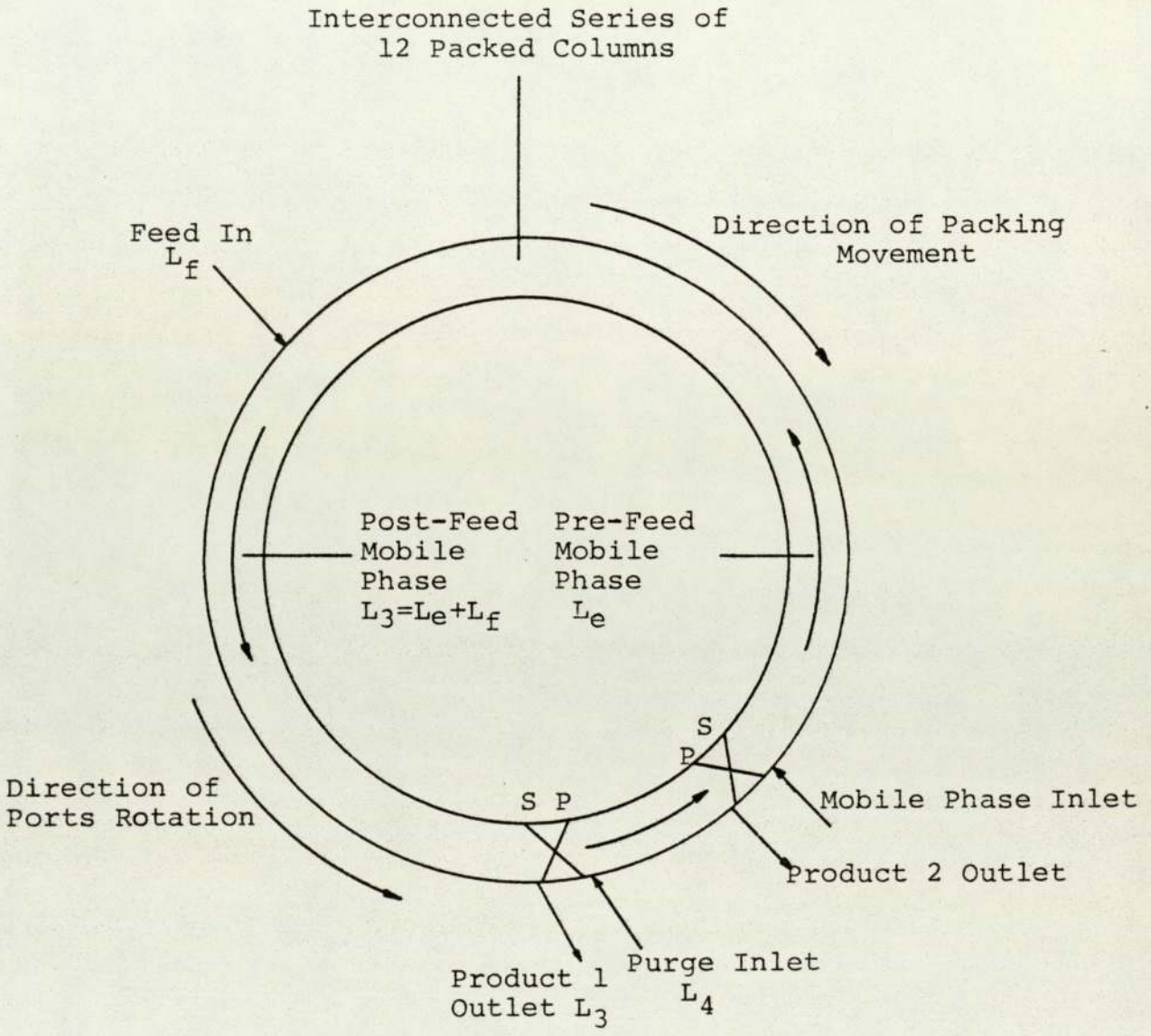

S-S Separation Section
Product 1-Glucose-Rich

P-P Purge Section
Product 2-Fructose-Rich

Y_g = concentration of glucose in mobile phase

X_g = concentration of glucose in stationary phase

If a glucose molecule is to move preferentially with the mobile phase then

$$L_e Y_g > P X_g \quad \text{..... (6.2)}$$

or $$\frac{L_e}{P} > \frac{X_g}{Y_g} \quad \text{..... (6.3)}$$

But as $$\frac{X_g}{Y_g} = K_d^G \quad \text{..... (6.4)}$$

Then $$\frac{L_e}{P} > K_d^G \quad \text{..... (6.5)}$$

Similarly for fructose to move with the stationary phase

$$\frac{L_e}{P} < K_d^F \quad \text{..... (6.6)}$$

Combining equations 6.5 and 6.6 gives

$$K_d^G < \frac{L_e}{P} < K_d^F \quad \text{..... (6.7)}$$

Equation 6.7 predicts the theoretical limits of the flow rates of the mobile and stationary phases to achieve the separation of fructose and glucose.

In the SCCR4 unit simulated stationary phase flow is achieved by the sequencing action at the end of every switch period. As each column contains mobile phase in the void volume the actual mobile phase flow rate is effectively reduced thus

$$L_e = L_i - \frac{V_o}{S} \quad \text{..... (6.8)}$$

where L_i = measured mobile phase flow rate

V_o = void volume

S = switch period

To completely purge all the fructose from the isolated column, it is necessary that

$$\frac{L_4}{P} \gg K_d^F \quad \ldots\ldots\ldots\ldots\ldots\ldots\ldots\ldots\ldots\ldots \quad (6.9)$$

where L_4 = purge stream flow rate

Equation 6.7 is a very simplified model and represents the ideal case of insignificant feed flow rate, low solute concentrations and a truly continuous mode of operation.

In practice the feed flow rate is significant. This gives rise to an increase in mobile phase flow rate at and beyond the feed point. The separation length of the unit can be considered as two sections, pre-feed and post-feed. Consequently two sets of operating conditions will exist. The difference between the two is dependent on the feed flow rate. Therefore equation 6.7 can be modified:

$$K_d^G < \frac{L_e}{P} < \frac{L_e'}{P} < K_d^F \quad \ldots\ldots\ldots\ldots\ldots\ldots\ldots \quad (6.10)$$

where $L_e' = L_e + L_f$ ..... (6.11)

and L_f = feed flow rate

If a mean value, L_m', of L_e and L_e' is taken then

$$K_d^G < \frac{L_m'}{P} < K_d^F \quad \ldots\ldots\ldots\ldots\ldots\ldots\ldots\ldots\ldots \quad (6.12)$$

where $L_m' = \frac{1}{2}(L_e + L_e')$

The distribution coefficients, K_d^F and K_d^G were determined at very low concentrations of the sample (14). The dependency of the distribution coefficient on concentration is known but there are no existing quantitative data for K_d with respect to fructose and glucose.

The mode of operation of the SCCR is not quite continuous. During a switch period the unit is operating as an elution batch chromatograph. The counter-current movement of the stationary phase is imposed by the discontinuous stepping of the inlet and outlet valves around the linked columns.

A theoretical model to account for the real effect of the concentration of the feed and the semi-continuous mode of the unit is proposed to modified equations 6.12 and 6.9 thus

$$(K_d^G + \delta_1^G + \delta_2^G) < \frac{L_m'}{P} < (K_d^F - \delta_1^F - \delta_2^F) \quad \ldots\ldots \quad (6.13)$$

and

$$\frac{L_4}{P} >> (K_d^F - \delta_1^F - \delta_2^F) \quad \ldots\ldots\ldots\ldots\ldots\ldots \quad (6.14)$$

where δ_1^G and δ_1^F are the changes due to the effect of feed concentration on the distribution coefficient and δ_2^G and δ_2^F are those due to the semi-continuous mode of operation of the SCCR4.

6.2 ANALYSIS METHOD

Fig. 6.2 shows the analytical system which was used to analyse the feed and the products of SCCR4 qualitatively and quantitatively. The system comprised a High Performance Liquid Chromatographic (HPLC) column, a micro-metering pump, a refractometer and an integrator. The HPLC was packed with Animex HPX87 in the Ca^{2+} form and was used for separating carbohydrates. The analysis was affected at 85°C. The eluent was deionised water which had been degassed at 80°C by placing the eluent reservoir in a constant temperature water bath. The micro-metering pump was used to pump the eluent at approximately 0.3 $cm^3 min^{-1}$ which gave a pressure of 7800 kNm^{-2}. The elution times of glucose and fructose at this rate were 190 ± 4 seconds and 250 ± 4 seconds respectively.

The eluate from the column was analysed by differential refractometry. The refractive index detector was electrically linked to a Servoscribe Chart recorder and a Hewlett Packard 337B integrator. The integrator printed out the time of the chromatogram developed on the recorder together with the area under the curve. The accuracy of this system was within ±4%.

6.3 EXPERIMENTAL PROCEDURE

A synthetic feed mixture was made by mixing laboratory grade fructose and glucose each of purity over 99.5% w/w. An approximate quantity of the sugars was dissolved in warm deionised water. The desired

Fig. 6.2 The Analytical System

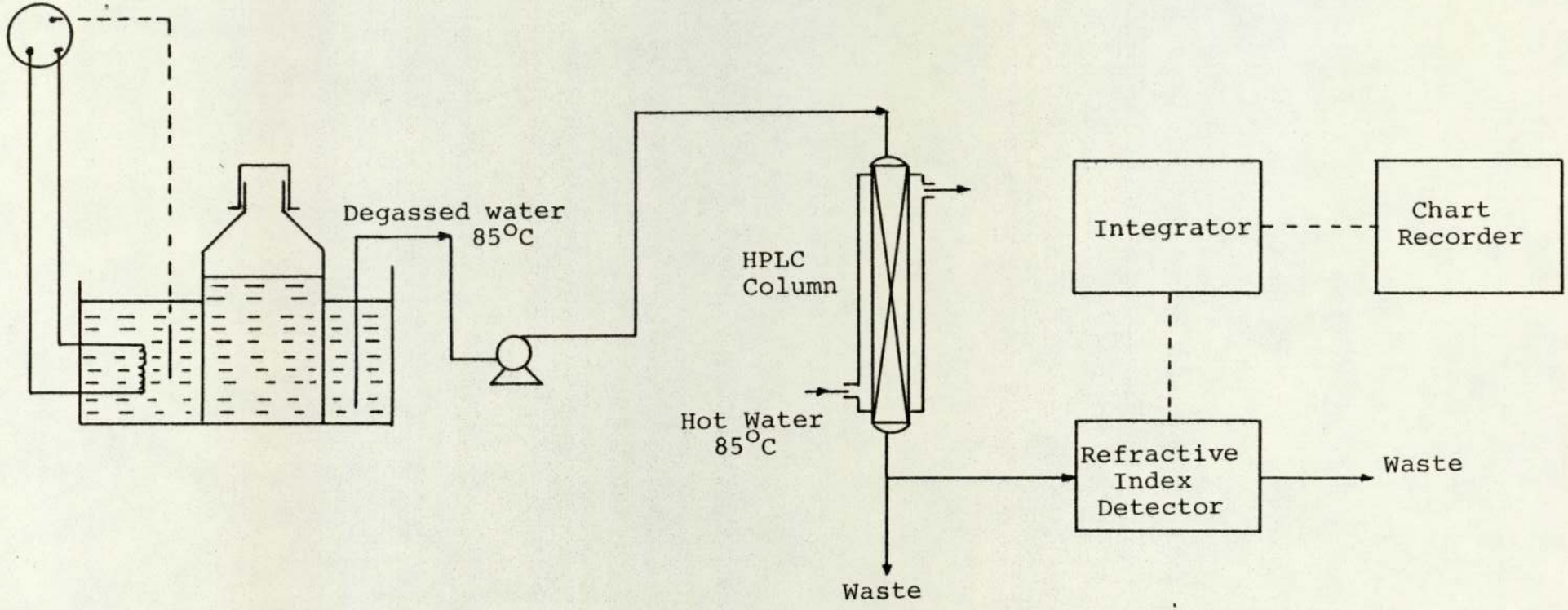

concentration of the sugars was adjusted by adding water or sugars as required and the product was analysed by the analytical unit described above.

Sodium azide of 0.02% w/v concentration was added to the feed to inhibit biological growth on the resin. The concentration of the azide was recommended by Fisons Ltd.

The following steps were taken at the start of each run with the SCCR4.

1. The functioning of the poppet valves was tested by setting the timer to a very small interval, e.g. 10 seconds and the performance of each valve was observed on the control system panel.
2. The timer was then set to a switch interval of 30 minutes.
3. The feed, eluent and purge pumps were adjusted to the required flow rates.
4. The heating devices of the liquid preheaters and the constant temperature enclosure were switched on. When the required operating temperature was achieved, the pumps were switched on.

During operation and especially on the first two cycles, frequent observations and measurements of flow rates and pressure drops of the feed, eluent and purge were carried out every switching sequence. The flow rates of the issuing products were also measured. The temperatures were monitored. Any discrepancy of these measurements from the desired valves was readjusted. Examples of these measurements are shown in Appendix (IV).

The collection of the products from each cycle was started after the fourth cycle. This was to give the unit sufficient time to reach a pseudo-steady state. The pseudo-equilibrium state was initially checked by the steady pressure drops of the feed and eluent and later by the material balance when the samples were weighed and analysed.

The SCCR4 was usually run continuously for 10-12 cycles. At the end of the final switch of the last cycle the pumps were switched off. The control system was then switched to manual to purge out each column separately. The purge pump was adjusted to a higher flow rate of 300 cm^3 min^{-1} and used to purge each column for 15 minutes. The purge product of each column was collected then weighed and analysed. This permitted the assessment of the total sugars retained by each column and thereby enabled the purge concentration profile to be drawn.

6.4 RUNS WITH SYNTHETIC FRUCTOSE AND GLUCOSE FEED

6.4.1 Objectives

A set of three runs were performed to separate synthetic mixtures of fructose and glucose at varying temperatures. The objectives were

1. To familiarise the operator with the SCCR4 unit.
2. To investigate whether the packing material of the unit had deteriorated since the previous use by Chuah (14).

6.4.2 Run Conditions

Previous work of Chuah (14) and Gould (15) had established that the best separation was obtained at the ratio of flow rate of feed to eluent of 1:3.0. Further work of Chuah showed that the best separation obtained by the SCCR4 was at 2.0 cm^3min^{-1} of feed and 6.0 cm^3min^{-1} of eluent. Throughout the work with the SCCR4, synthetic mixtures of 50% w/v sugar solution of equal proportion of fructose and glucose were used as feed.

The first run was performed at 30°C since the best separation obtained by Chuah (14) was at that operating temperature. Another run was carried out at 45°C and that was the optimum temperature to hydrolyse sucrose (14). A further run was carried out at 60°C since microbial growth would be reduced even further at this higher temperature.

6.4.3 Results and Discussion

Table 6.1 shows the results of this first set of experiments. The assigned run number was as follows.

1-50-2-6-30-30

The first digit denotes the experiment number and the second is the concentration of the feed. The third and fourth numbers indicate the feed and eluent flow rates in (cm^3min^{-1}). These are followed by the temperature (°C) and the switch period in minutes.

The concentration profiles of the runs are shown in Figs. 6.3, 6.4 and 6.5.

TABLE 6.1 RUN CONDITIONS FOR VARYING TEMPERATURES

Run Number	Flow Rate ($cm^3 min^{-1}$)			Feed Conc. % w/v		Feed Rate ($gm\ hr^{-1}$)	Temp. ^oC	Switch Period (min)	L'/P_m Ratio
	Feed	Eluent	Purge	F	G				
C*-50-2-6-30-30	2	6	30	25.0	24.0	60	30	30	0.362
1-50-2-6-30-30	2	6	30	24.3	24.8	60	30	30	0.362
2-50-2-6-44-30	2	6	30	25.6	24.9	60	45	30	0.362
3-50-2-6-60-30	2	6	30	25.7	25.1	60	60	30	0.362

RESULTS FOR VARYING TEMPERATURES

RUN NUMBER	Fructose Rich Product				Glucose Rich Product			
	Mass Bal. %	Purity %	Recovery %	Conc. % w/v	Mass Bal. %	Purity %	Recovery %	Conc. % w/v
C*-50-2-6-30-30	102	92	91	1.9	99	87	87	5.3
1-50-2-6-30-30	98	93	93	2.0	94	88	85	5.0
2-50-2-6-45-30	98	89	87	1.8	99	83	84	4.4
3-50-2-6-60-30	98	88	75	1.8	104	76	79	3.8

* Run carried out by Chuah (14)

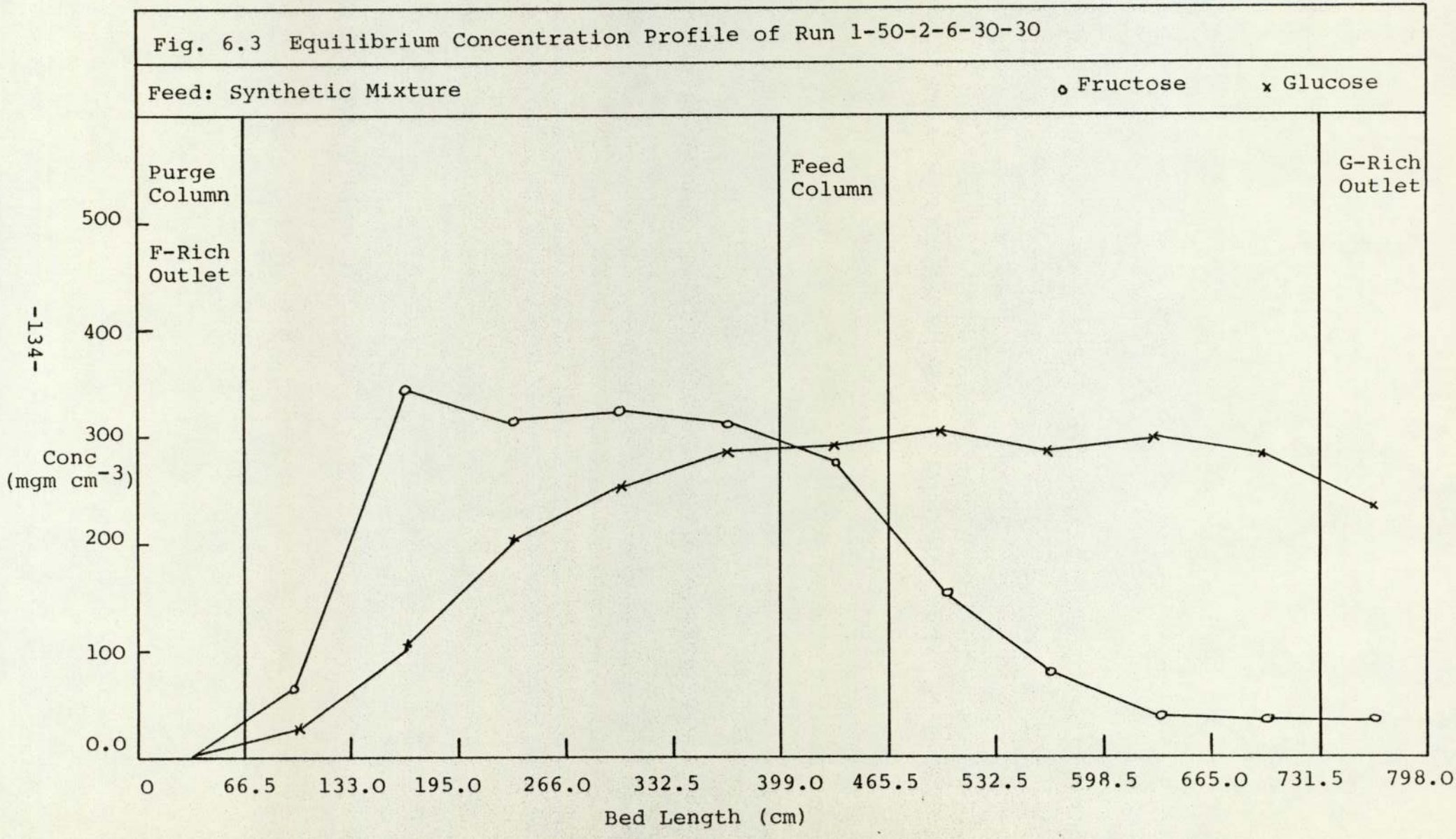
Fig. 6.3 Equilibrium Concentration Profile of Run 1-50-2-6-30-30
Feed: Synthetic Mixture
o Fructose
x Glucose
Purge Column
F-Rich Outlet
Feed Column
G-Rich Outlet
500
400
300
200
100
0.0
Conc (mgm cm-3)
0
66.5
133.0
195.0
266.0
332.5
399.0
465.5
532.5
598.5
665.0
731.5
798.0
Bed Length (cm)

Fig. 6.4 Equilibrium Concentration Profile of Run 2-50-2-6-45-30

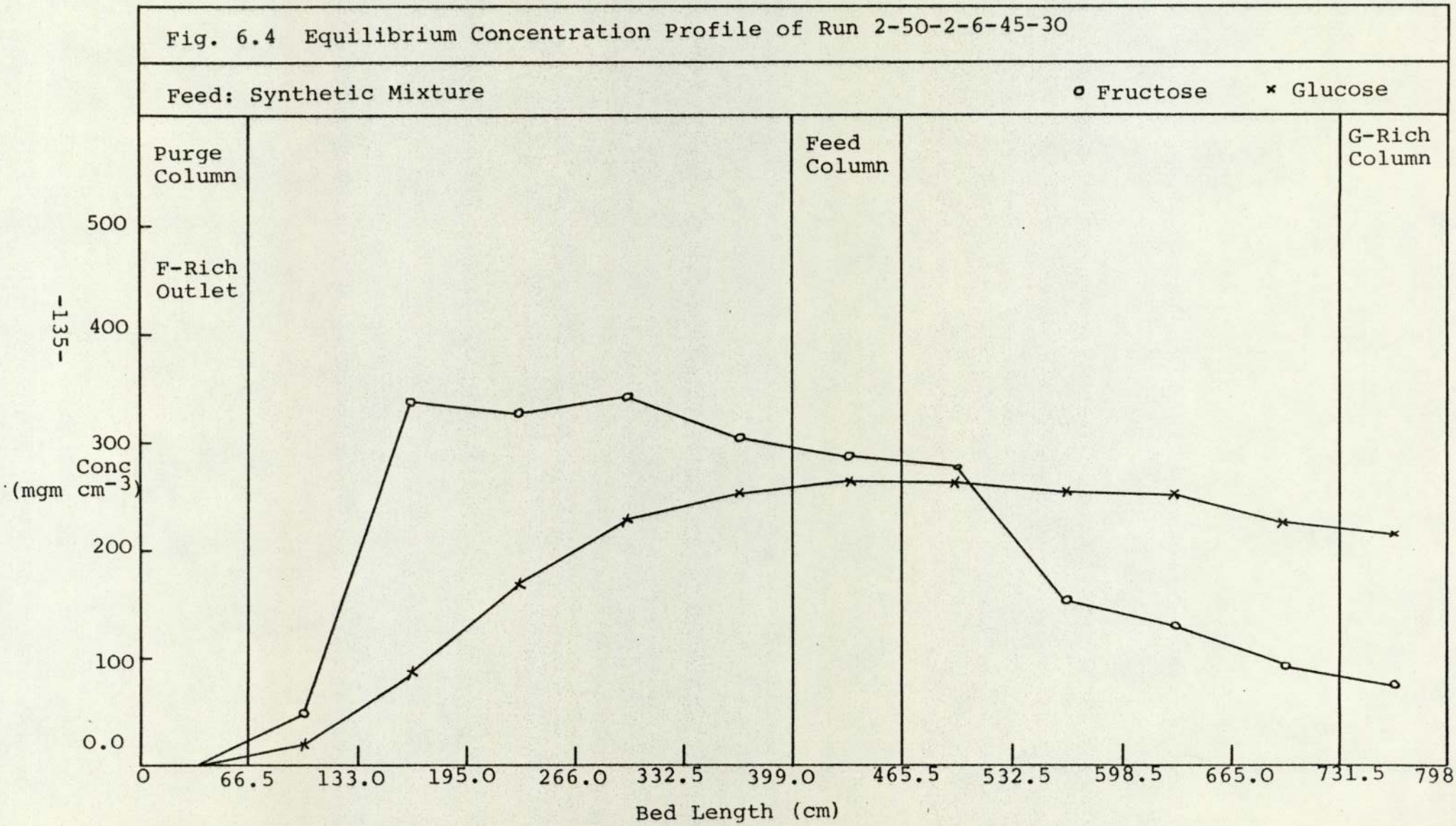

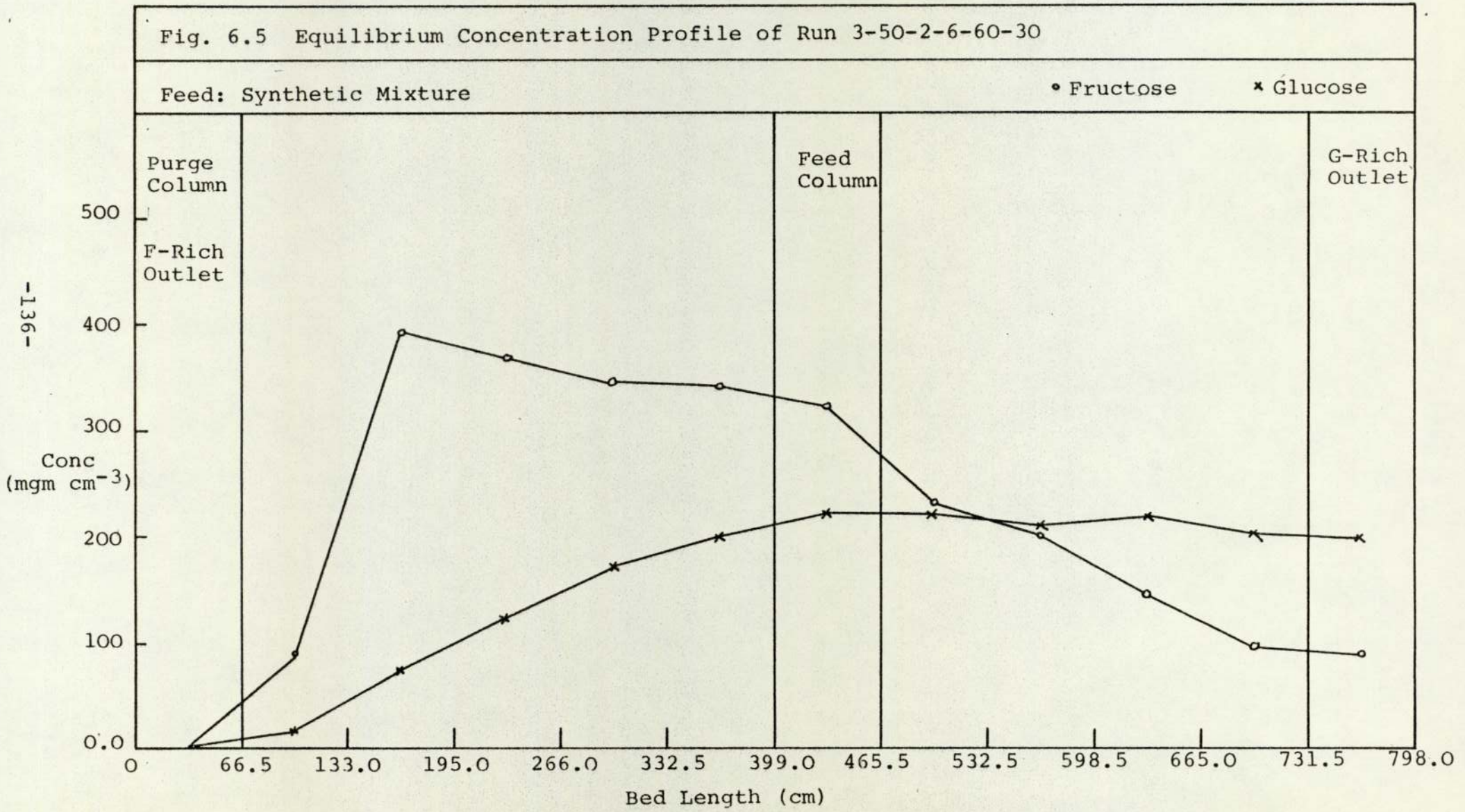
Fig. 6.5 Equilibrium Concentration Profile of Run 3-50-2-6-60-30
Feed: Synthetic Mixture
Fructose
Glucose
Purge Column
F-Rich Outlet
Feed Column
G-Rich Outlet
500
400
300
200
100
0.0
Conc (mgm cm^{-3})
0
66.5
133.0
195.0
266.0
332.5
399.0
465.5
532.5
598.5
665.0
731.5
798.0
Bed Length (cm)

Run C-50-2-6-30-30, which was carried out by Chuah (14) is included here to compare it to run 1-50-2-6-30-30 which was carried out under the same operating conditions. From the approximately similar results it was concluded that the resin had not deteriorated and it still retained its separating capacity.

The effect of temperature on the separation can be seen from the purities of the products. Although the purity of fructose remained constant, the purity of glucose dropped from 88% at 30°C to 76% at 60°C. The concentration profiles of these runs illustrate gradual shifts of the cross-over point towards the glucose-rich product outlet as the temperature increases. This means that more fructose is travelling with the mobile phase.

The shift of the cross-over point can be explained by the fact that for elution chromatography the retention volume is generally reduced with an increase of temperature and therefore the solute bands are brought nearer to each other making the separation more difficult. In addition, β-D-fructopyranose is the only form of fructose that is known to make a complex with the Ca^{2+} ions (see Chapter 3). The proportion of this form, at equilibrium to the other forms, is a function of the temperature of the solution. This has been proved by polarimetric measurements (51), n.m.r. spectrometry (85)and gas-liquid chromatography (86). As shown in Table 6.2, the proportion of β-D-fructopyranose form

TABLE 6.2 EQUILIBRIUM OF 20% FRUCTOSE AT DIFFERENT TEMPERATURES (85)

Temp. ^{o}C	α-D-Fructo Furanose %	β-D-Fructo-Furanose %	β-D-Fructo-Pyranose %
10	4	18	78
22	6	21	73
67	8	28	64
77	12	31	57

decreases with increase of temperature. This also explains the decrease of sweetness of a warm fructose solutions due to the formation of more of the less sweet furanose form.

A final observation is that although run 1-50-2-6-30-30 was considered to be performed under the most favourable conditions for separation, the purity of glucose was still only 88%. By examining the concentration profile of the run it will be observed that a significant amount of fructose is accumulating throughout the bed length and up to the glucose-rich product outlet. This was believed to be due to the hold-up liquid in the valves and the process lines.

6.5 RUNS WITH SUCROSE-BASED FEED

The objective of these runs was to investigate the behaviour of the SCCR4 when handling less expensive sources of fructose and glucose like sucrose.

6.5.1 The Hydrolysis Column

The hydrolysis of sucrose into a mixture of fructose and glucose was carried out by eluting sucrose solution through a 1" glass column packed with, Amberlite 1R-118, a cation resin provided by Rohn and Haas U.K. Ltd. The resin was used in the free H^+ ions form. The column was of similar length and had the same inlet and outlet fittings to other columns of the SCCR4 unit.

6.5.2 Run Conditions

The operating temperature for the hydrolysis of the sucrose and the separation was 45°C. That was a compromise, for low temperatures effect a better separation and high temperatures benefit hydrolysis.

The column was placed inside the constant temperature enclosure of the SCCR4. The inlet of the column was connected to the feed pump and the outlet to the feed line leading to SCCR4 columns. A T-connector fitted with a septum was placed in line just after the column outlet for frequent monitoring of the hydrolysis product.

For all the hydrolysis experiments, 50% w/v sucrose solutions were prepared by dissolving the sugar in deionised water. The exact concentration was analysed by the HPLC column described in Section 6.1.

6.5.3 Results and Discussions

Table 6.3 shows the contents of the sugars emerging from the hydrolysis column to the SCCR4 unit.

The samples were diluted and analysed as soon as they were taken. The first observation from the results in Table 6.3 is that there is no sucrose residue and this indicates that the inversion of sucrose was complete. Another observation is that the proportion of glucose in the inversion product is higher than that of fructose. The average percentage of glucose to the total sugars is 51.7% w/w while that of fructose is 48.3%. Since a molecule of sucrose contains one molecule of fructose and one molecule of glucose, the result of inversion is

Table 2 Run Conditions For Different Feed Sources

Run Number	Feed		Conc (w/v%)		Flow Rate (cm³ min⁻¹)			Temp °C	Switch Period (min)
	Source	pH	F	G	Feed	Eluent	Purge		
1-50-26-45-30	SYNTHETIC	6.8	26.0	25.4	2	6	30	45	30
2-50-2-6-45-30	SUCROSE	2.9	S 49.5		2	6	30	45	30
3-50-2-6-45-30	SUCROSE	7.2	S 50.6		2	6	30	45	30
4-50-2-6-45-30	SYNTHETIC	3.0	25.9	24.9	2	6	30	45	30

Results For Different Feed Sources

Run Number	Fructose Rich Product				Glucose Rich Product			
	Mass Bal %	Purity %	Recovery %	Conc % w/v	Mass Bal. %	Purity %	Recovery %	Conc. % w/v
1-50-2-6-45-30	98	89	92	2.0	102	87	85	4.5
2-50-2-6-45-30	102	73	87	1.8	104	88	74	4.3
3-50-2-6-45-30	98	74	88	1.9	1&2	86	72	4.2
4-50-2-6-45-30	101	88	91	1.9	100	88	85	4.9

TABLE 6.4 RUN CONDITIONS FOR DIFFERENT FEED SOURCES									
Run Number	Flow Rate ($cm^3 min^{-1}$)			Feed Conc. % w/v		Feed Rate ($gm\ hr^{-1}$)	Temp. °C	Switch Period (min)	L'/P_m Ratio
	Feed	Eluent	Purge	F	G				
4*-50-2-6-45-30	2	6	30	S 49.5		60	45	30	0.362
5*-50-2-6-45-30	2	6	30	S 50.6		60	45	30	0.362
6 -50-2-6-45-30	2	6	30	26.0	25.4	60	45	30	0.362
7 -50-2-6-45-30	2	6	30	25.9	24.9	60	45	30	0.362

RESULTS FOR DIFFERENT FEED SOURCES								
Run Number	Fructose Rich Product				Glucose Rich Product			
	Mass Bal. %	Purity %	Recovery %	Conc. % w/v	Mass Bal. %	Purity %	Recovery %	Conc. % w/v
4*-50-2-6-45-30	102	73	87	1.8	104	88	74	4.3
5*-50-2-6-45-30	98	74	88	1.9	102	86	72	4.2
6 -50-2-6-45-30	98	89	92	2.0	102	87	85	4.5
7 -50-2-6-45-30	101	88	91	1.9	100	88	85	4.9

* Sucrose-based feed

TABLE 6.3 ANALYSIS OF SUCROSE HYDROLYSIS PRODUCT

Time (hrs)	Glucose % w/v	Fructose % w/v	Sucrose % w/v
6	25.1	24.1	-
12	27.6	25.1	-
24	26.5	24.8	-
32	27.4	24.9	-
48	26.9	24.8	-
54	25.1	23.9	-
72	25.4	24.1	-

expected to be 50/50 mixture. However, it has been shown that a 50/50 mixture is obtainable only if the inversion is carried out by the enzyme Invertase (87).

The results of separation of the inverted mixtures are shown in Table 6.4. When comparing run 4-50-2-6-45-30 and 2-50-2-6-45-30 (see Table 6.1) it can be seen that both runs were carried out at identical operating conditions. The only difference was the origin of the feed. The feed for run 2-50-2-6-45-30 was a synthetic mixture of fructose and glucose and that for run 4-50-2-6-45-30 was an inverted sucrose mixture.

The products obtained by run 4-50-2-6-45-30 were of lower purities. The fructose purity dropped from 89% for the synthetic feed to 73% for the inverted sucrose feed. Further examination of the concentration profile, illustrated in Fig. 6.6, showed that the cross-over point was shifted almost two column lengths beyond the feed column, i.e. towards the purged product outlet. The shift was mainly due to an unusual accumulation of glucose on the pre-feed columns. This means that some glucose was travelling with the packing. Another observation was that the level of fructose to the left of the feed column was lower than that of run 2-50-2-6-45-30. However the total sugars retained by all the columns, determined by weighing the area under the curves, was found to be approximately the same for the synthetic and the inverted sucrose feed mixtures.

Run 4-50-2-6-45-30 was repeated to exclude the probability of analytical error and the duplicate confirmed the results obtained previously.

TABLE 6.4 RUN CONDITIONS FOR DIFFERENT FEED SOURCES

Run Number	Flow Rate ($cm^3 min^{-1}$)			Feed Conc. % w/v		Feed Rate ($gm\ hr^{-1}$)	Temp. °C	Switch Period (min)	L'/P_m Ratio
	Feed	Eluent	Purge	F	G				
4*-50-2-6-45-30	2	6	30	S 49.5		60	45	30	0.362
5*-50-2-6-45-30	2	6	30	S 50.6		60	45	30	0.362
6 -50-2-6-45-30	2	6	30	26.0	25.4	60	45	30	0.362
7 -50-2-6-45-30	2	6	30	25.9	24.9	60	45	30	0.362

RESULTS FOR DIFFERENT FEED SOURCES

Run Number	Fructose Rich Product				Glucose Rich Product			
	Mass Bal. %	Purity %	Recovery %	Conc. % w/v	Mass Bal. %	Purity %	Recovery %	Conc. % w/v
4*-50-2-6-45-30	102	73	87	1.8	104	88	74	4.3
5*-50-2-6-45-30	98	74	88	1.9	102	86	72	4.2
6 -50-2-6-45-30	98	89	92	2.0	102	87	85	4.5
7 -50-2-6-45-30	101	88	91	1.9	100	88	85	4.9

* Sucrose-based feed

Fig. 6.6 Equilibrium Concentration Profile of Run 4-50-2-6-45-30

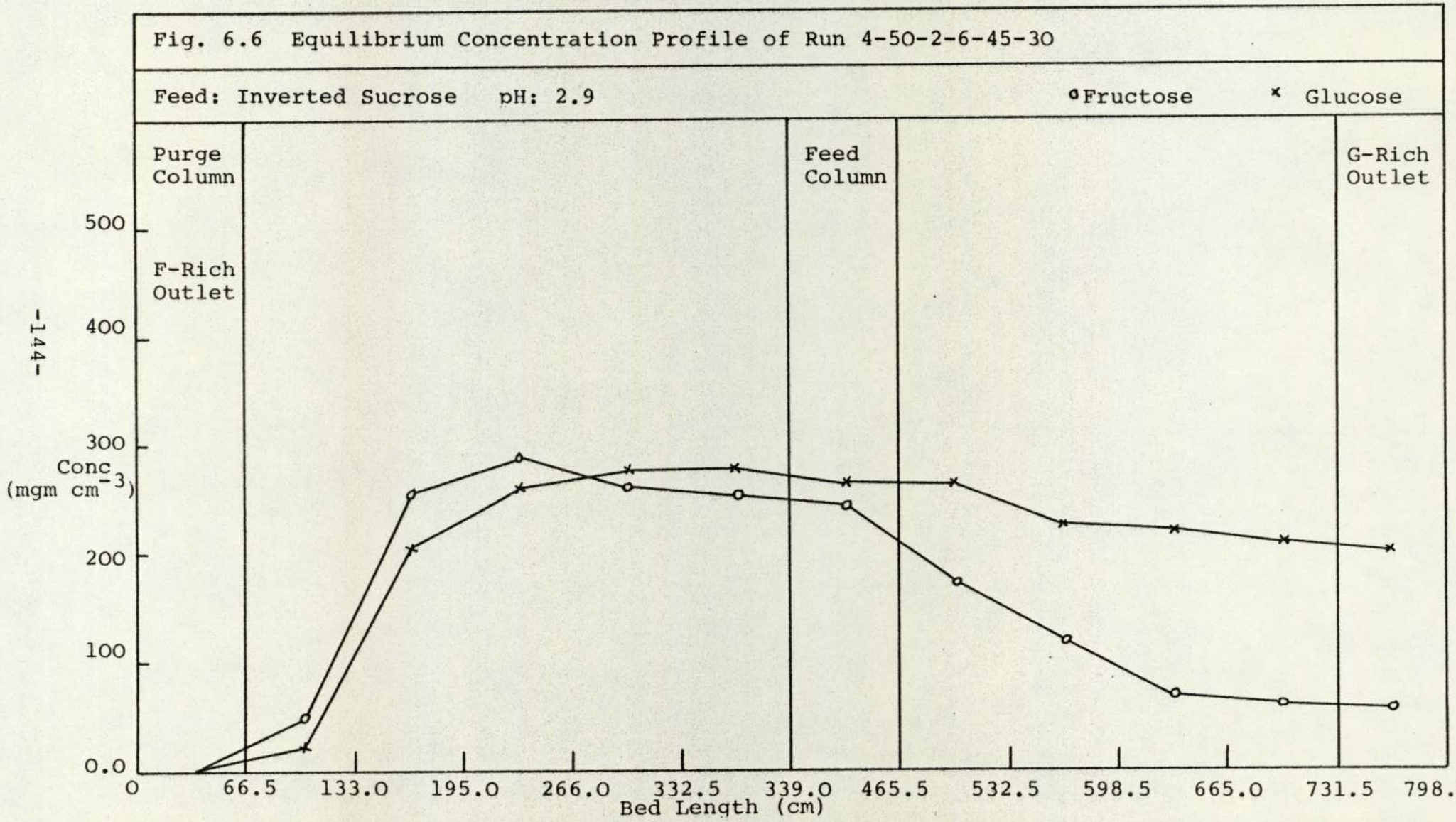

The pH of the inverted syrup was found to be 2.9 while that of a synthetic mixture was 6.8. It is known that the capacity of a weak resin is affected by the pH (88). Run 5-50-2-6-45-30 was performed to investigate whether the pH has an effect on the separation of fructose and glucose. The sucrose was inverted separately. The pH was then adjusted to 7.2 by adding dilute NaOH solution and the syrup was separated by the SCCR4. The results of this run are included in Table 6.4 and the concentration profile is shown in Fig. 6.7. It was found that the separation was not improved by adjusting the pH of the inverted sucrose syrup.

Then run 6-50-2-6-45-30 with a synthetic feed mixture was carried out. This was to eliminate the possibility of a mechanical fault having developed in the SCCR4 unit, and secondly to make sure that the resin had not deteriorated by the adverse pH ranges. The results of run 6-50-2-6-45-30 are shown in Table 6.4 and the concentration profile in Fig. 6.8, and these are in agreement with those of its replica 2-50-2-6-45-30.

A final run was carried out by separating a synthetic feed mixture that had been treated with dilute HCl to adjust the pH to 3.0. From the results of run 7-50-2-6-45-30 as presented in Table 6.4 and Fig. 6.9, it was concluded that the SCCR4 had not developed a mechanical fault and the resin was still retaining its separation capacity. The combined results of runs 5-50-2-6-45-30 and 2-50-2-6-45-30 excluded totally the contribution of pH to the abnormal behaviour of sucrose

Fig. 6.7 Equilibrium Concentration Profile of Run 5-50-2-6-45-30

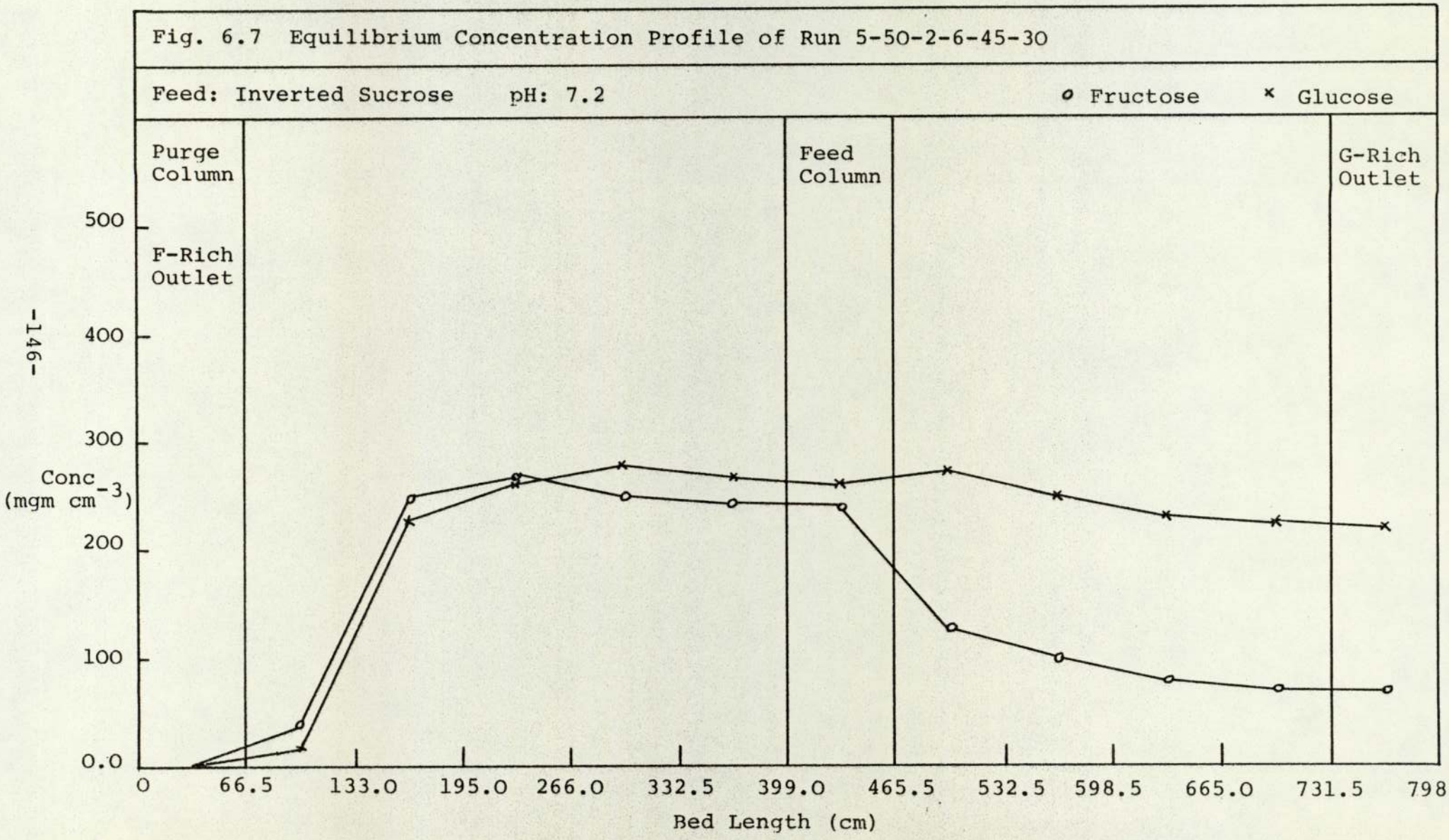

Fig. 6.8 Equilibrium Concentration Profile of Run 6-50-2-6-45-30

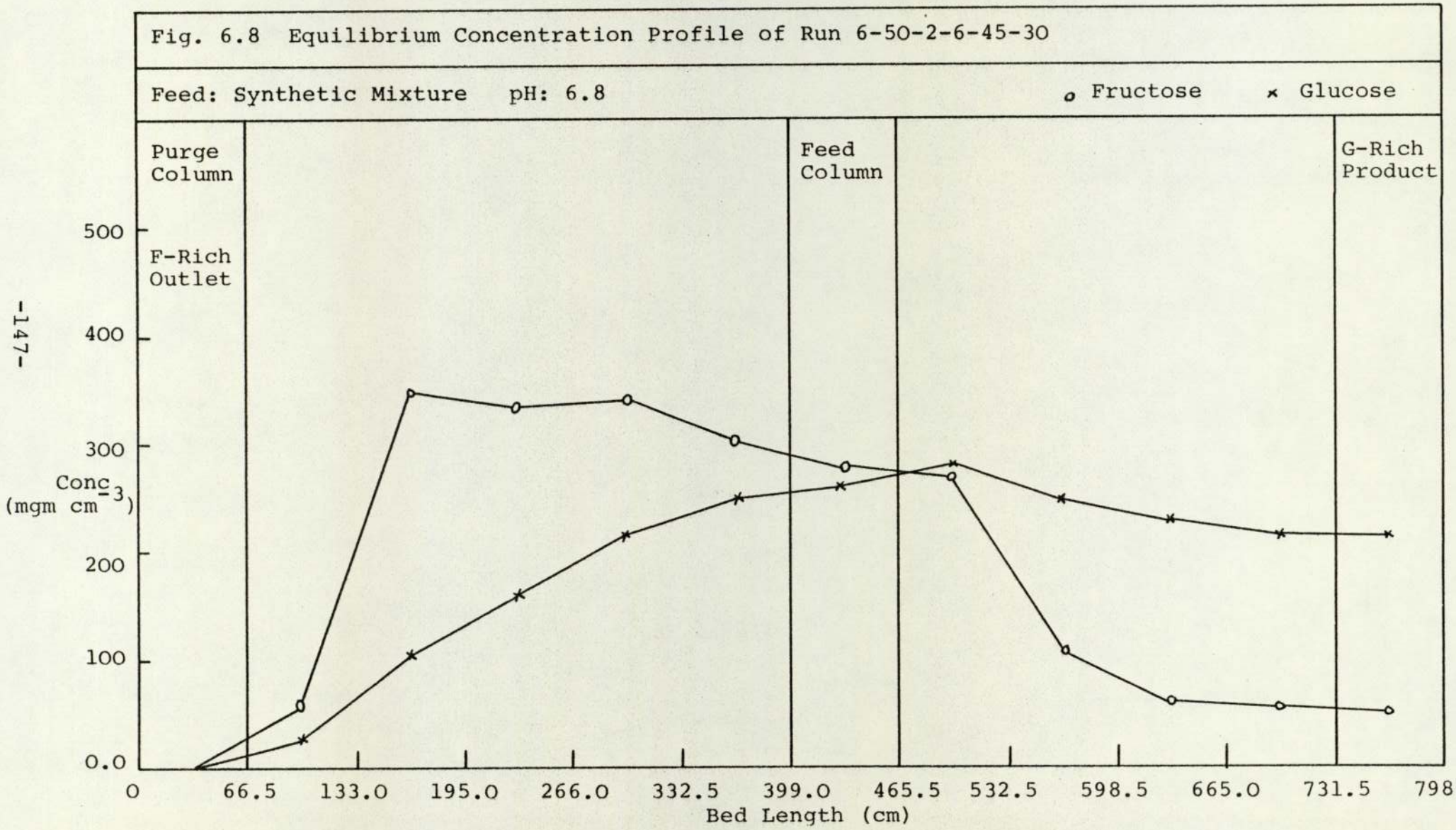

Fig. 6.9 Equilibrium Concentration Profile of Run 7-50-2-6-45-30

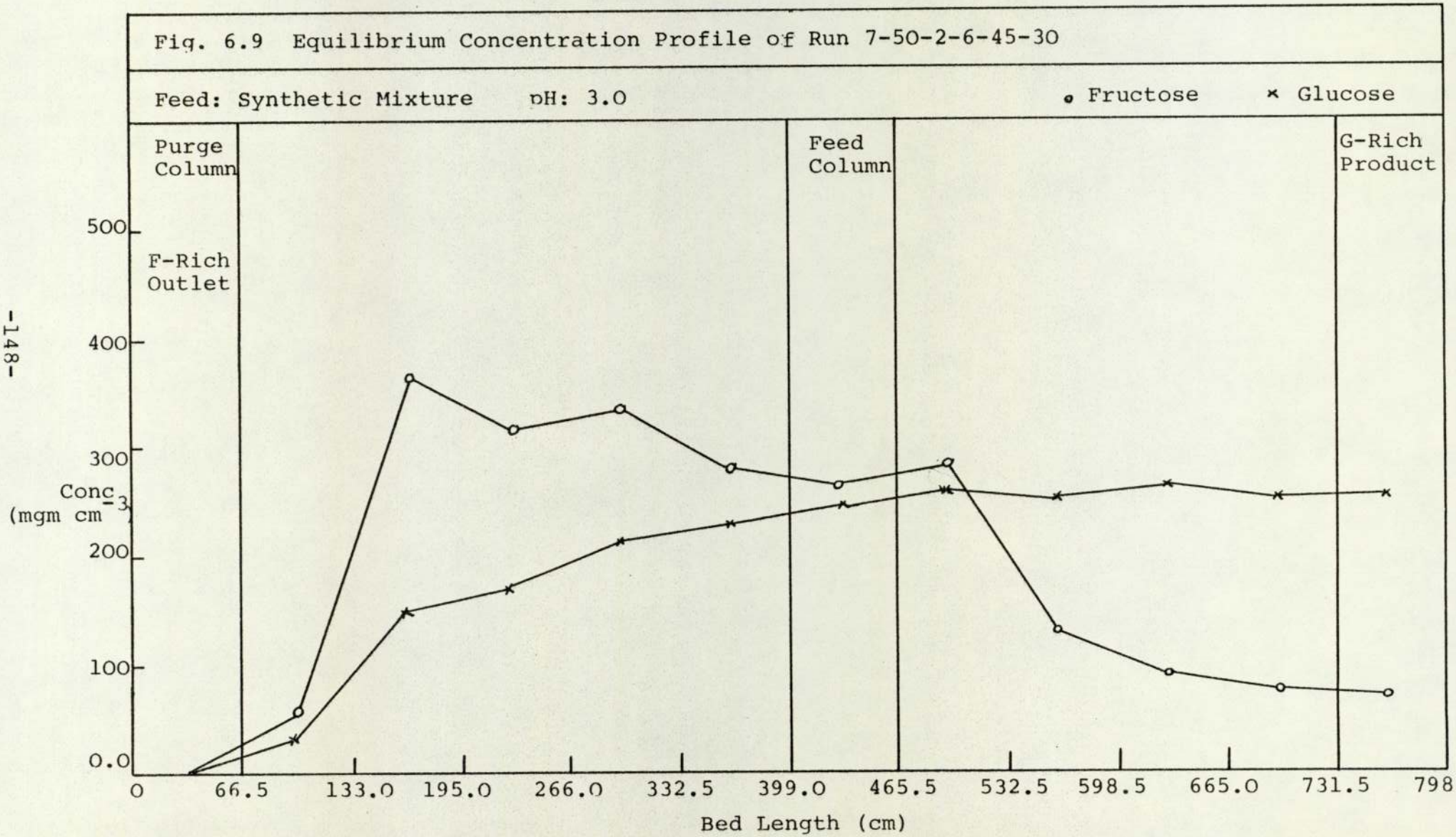

in this special system.

6.6 GENERAL DISCUSSION

In order to find an explanation for the abnormal behaviour of the SCCR4 when separating the products of inverted sucrose, several sessions of discussion were held with Barker (89) and Somers (90). The outcome of the discussion is summarised below.

The nature of the invert sugars, fructose and glucose as obtained by the acid hydrolysis of sucrose are different from the synthetic ones. As an example the fructose resulted from hydrolysis of sucrose is essentially a furanose or five-membered ring form. The process of conversion to the equilibrium forms of this sugar is quite a slow process (89).

One explanation of the behaviour of the inverted sucrose syrup on separation is that the SCCR4 might act as a convertor, to a limited extent, of fructose to glucose especially at these conditions of temperature and pH (90). This explanation is supported by the findings of Velasco et al (87). They reported that when a sucrose solution was inverted by HCl and kept at room temperature for 16 days the percentage of fructose to the total sugars decreased from 47.8% to 45.3% and that of glucose was increased from 52.2% to 54.7%. They also reported that there was no change in the proportions of fructose and glucose when a 50% synthetic mixture of these sugars was kept for 19 days at pH ranges of 4.7 and 2.4.

A further explanation is that the fructose obtained by acid hydrolysis of sucrose undergoes a degradation process to yield other stable forms of fructose such as difructose dianhydrides I and II (87). These forms could then have a similar retention time to glucose and therefore during the analysis by HPLC they could be mistaken for glucose. If that is the case then the apparent glucose proportion in the sample will be higher than the actual value because the band of these compounds overlap the glucose band.

Both the fructose conversion and the fructose-degradation suggestions can explain the low purity of fructose obtained by runs 4-50-2-6-45-30 and 5-50-2-6-45-30 and the concentration profiles of these runs.

CHAPTER 7

COMMISSIONING AND OPERATION OF THE SCCR7 UNIT FOR SUGARS SEPARATION

7.1 COMMISSIONING THE SCCR7

7.1.1 Hydraulic Testing of the Columns

During the manufacturing stage, each column underwent turning and welding processes. These processes might weaken and distort the machined parts. Therefore it was necessary to test the columns before commissioning. Each column was subjected to the following tests.

The turned part of the column was scanned by an ultra-sonic detector around the diameter. The thickness was found to be within ± 0.5 mm of the design calculations. Then after each column was fitted with all its parts, a hydraulic test was carried out. That test was performed with both compression and separation compartments of the column separately. The compartment was subjected to 2025 kN m^{-2} pressure by introducing water by a hand-pump and left overnight. Welded parts, especially the sample points, were inspected for leakage. The constant pressure indicated soundness of welding and effectiveness of the seal between the two compartments. Any defective column was rewelded and tested again.

7.1.2 Treatment of the Anion Exchange Resin

16 kg of anion exchange resin, Duolite A113-S1404, were provided by Dia-prosim Ltd. The resin was quoted

by the manufacturer to have particle size range between 50 and 100 mesh. Table (7.1) shows a sieve analysis of the resin. Other properties of the resin are included in Table (5.1).

The resin was originally in the chloride form. It was desired to convert it to the bisulphite form. First the resin was washed by a 1% w/v H_2SO_4 solution to remove the metallic ions which might be present as impurities (91). These ions and especially Fe^{2+} and Cu^{2+} might act as catalysts to enhance the destructive process of auto-oxidation, which has been discussed in Section (2.2.3.4). Then the resin was washed with deionised water and contacted with a 4% w/v NaOH solution to convert the resin to the OH^- form (16). Again the resin was washed with deionised water and treated with a 5% w/v $NaHSO_3$ solution to finally convert it to the bisulphite (HSO_3^-) form.

The resin then in the HSO_3^- form was left in the bisulphite medium without washing the unbound salt. This was done deliberately to take advantage of a technique known as in-situ charging (92). Adsorbents shrink in volume when exposed to concentrated salt solutions, and subsequently expand when washed to remove the excess unbound salt. If a column is filled to capacity with contracted resin the column can then be closed and the resin washed, causing it to swell and become densely packed.

All the treatment was carried out in a 1.2×10^{-1} m^3 plastic tank and each time after the resin was washed

TABLE 7.1 SIEVE ANALYSIS OF DUOLITE A113 (91)

B.S. Mesh	Size (μm)	Mass Fraction $x10^{-2}$
40	400	1.3
45	350	8.9
50	300	5.2
55	275	4.0
60	250	10.4
65	225	18.1
75	200	23.5
80	175	21.1
100	150	6.9
120	125	0.35
150	100	0.25

excess solution was drained by a syphoning process.

The concentration of reagents used for charging were recommended by the supplier of the resin. The amount of the reagent necessary for full conversion of the resin form was calculated from equation (2.2).

Experimentally about four times the calculated amount of reagents by equation (2.2) were used to ensure complete conversion (93).

7.1.3 Packing Technique

Slurry packing using a partial vacuum technique was adopted. The outlet assembly of the column was fitted and all the ports of the outlet head were closed. The column was supported in a vertical position and filled with deionised water. One port was then opened and connected to a vacuum pump. The vacuum pump was started and at approximately the same rate of draining of water, slurry resin was added to the column. That continued until the resin filled completely the separation chamber of the column, i.e. 650 mm of resin bed height. This procedure was thought advantageous in avoiding the segregation apparent in gravitational settling. The piston was then placed and secured in position and each packed column was weighed. The wet packing density was found to be 1.29-1.33 gm cm^{-3}. The columns were then installed.

The SCCR7 unit was commissioned with deionised water for 5 days to wash the unbound bisulphite salt and establish a uniform and stable packing.

7.1.4 Characterisation of the Packed Columns

7.1.4.1 Calibration Technique

To study the characteristics of individual columns, each column was first isolated from the system and connected to a metering pump and detector as shown in Fig. 7.1. The temperature of the enclosure was maintained at 60°C throughout the calibration. Pre-heated water was pumped to the column and when a stable base line was obtained on the recorder the sample was injected.

Three solute samples were run separately at a constant elution rate of 24 $cm^3/min.^{-1}$. The sample volumes and concentrations were

1 cm^3 of 5% w/v dextran 5500

5 cm^3 of 5% w/v fructose

5 cm^3 of 5% w/v glucose

The chromatograms obtained for each sample by different columns were analysed and the results are shown in Table (7.2). Equations (5.5) and (5.6) were used to calculate the distribution coefficients, K_d^F for fructose and K_d^G for glucose. HETP was calculated from equation (2.15).

7.1.4.2 Results and Discussion

The operating temperature at which the calibration was carried out was 60°C. This temperature was chosen because the analytical work (Section 5.0) showed that the best performance of the anion exchange resins was obtained at high temperatures. The elution rate was

Fig. 7.1 Flow Diagram for Individual Column Characterization

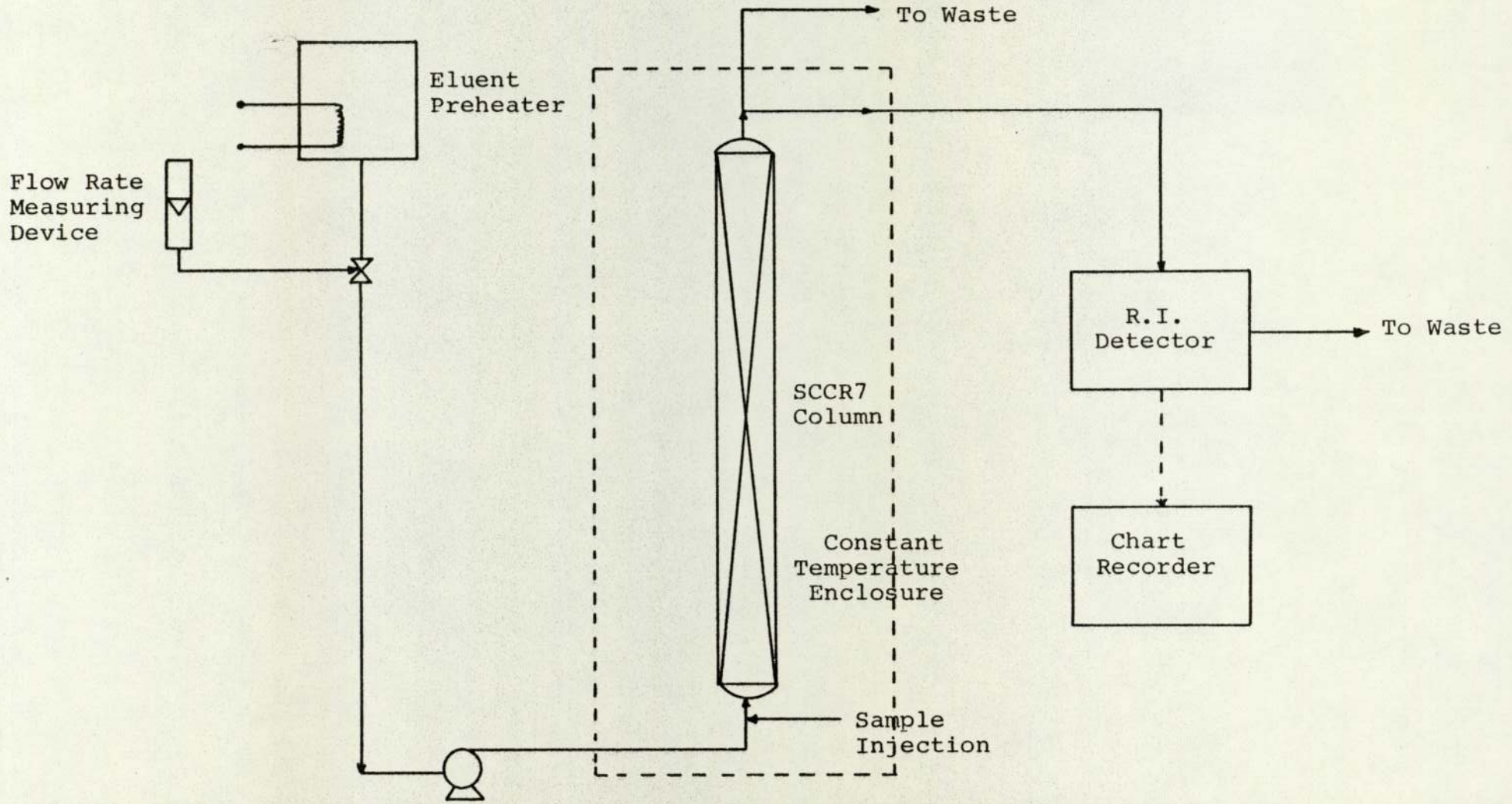

TABLE 7.2 Characteristics* of Individual Columns

Column No.	Elution Volume (cm^3)			Distribution Coefficient		No. of Theoretical Plates		H.E.T.P. (mm)			Void V_o
	V_R^D	V_R^F	V_R^G	K_d^F	K_d^G	w.r.t. Fructose	w.r.t. Glucose	w.r.t. Dextran	w.r.t. Fructose	w.r.t. Glucose	
1	442	919	1423	0.42	0.73	246	56	0.47	2.64	11.6	0.278
2	434	912	1428	0.43	0.75	249	54	0.49	2.60	11.93	0.275
3	434	888	1399	0.40	0.74	237	48	0.42	2.74	13.60	0.275
4	444	936	1409	0.43	0.73	248	53	0.47	2.62	12.25	0.279
5	453	914	1391	0.41	0.71	266	45	0.45	2.44	14.40	0.285
6	508	964	1401	0.39	0.71	227	47	0.54	2.68	13.74	0.297
7	430	919	1392	0.43	0.73	269	49	0.45	2.41	13.70	0.271
8	462	953	1439	0.43	0.75	266	46	0.50	2.44	14.20	0.291
9	457	919	1387	0.40	0.71	260	48	0.49	2.50	13.54	0.288
10	452	967	1404	0.44	0.71	265	48	0.44	2.45	13.54	0.285
11	439	999	1465	0.44	0.71	262	48	0.46	2.48	13.54	0.277
12	460	978	1398	0.44	0.70	224	44	0.46	2.80	14.86	0.289

* At 60^oC and elution rate of 24.0 $cm^3 min^{-1}$

adjusted to 24 cm^3 min^{-1}, based on previous experience with the SCCR4 unit.

It was observed that dextran 5500, of average molecular weight of 5500, emerged as a very sharp band. The fructose band was fairly sharp, but the glucose band was flattened and tailed. This is because dextran does not enter the pores of the resin due to its large molecular size, while the fructose and glucose do enter the resin pores. Moreover glucose forms a stronger complex with the bisulphite and therefore it is further retarded.

When comparing the performance of the anion resin in the SCCR7 unit to that of the cation resin used in the SCCR4 unit, it is clear that the anion resin gave higher efficiencies with respect to dextran, fructose and glucose. This is most probably due to the fact that this calibration was carried out at 60°C while the SCCR4 was calibrated at room temperature (14). Column efficiency has been shown in Section (5.4.3) to increase with the increase of temperature.

The average values of the distribution coefficient K_d^F for fructose and K_d^G for glucose were 0.43 and 0.73 respectively. These values were higher compared to the average values obtained by Chuah (14) which were 0.2 for K_d^G and 0.6 for K_d^F for the cation exchange resin. This indicates that the separation factor, α, is higher for the cation exchange resin.

The high value of K_d^F in the case of the anion exchange resin compared to the low value of K_d^G in the

case of cation exchange resin could be explained by the fact that the bisulphites are also known to complex to a lesser degree with fructose (76). But literature reports indicate no confirmation of the existence of a complex between glucose and calcium.

7.2 CONTINUOUS SEPARATION OF FRUCTOSE AND GLUCOSE MIXTURE WITH THE SCCR7 UNIT

The SCCR7 unit was operated continuously to separate mixtures of fructose and glucose. The object of the work was to establish the optimum operating conditions for the unit. Therefore runs at different flow rates of feed and eluent and different concentrations were tried.

7.2.1 Experimental Procedure

The synthetic feed mixtures were prepared in the same way as described for the SCCR4 unit. The only difference was that no sodium azide as preservative was added. Instead, the sugars were dissolved in deionised water containing approximately 60 ppm sodium bisulphite. Later the same amount of sodium bisulphite was added to the water that was used for eluting and purging the SCCR7 throughout the practical work. The sodium bisulphite served as both preservative and reducing agent to protect the anion resin against biological growth and auto-oxidation (91,94).

The start-up and shut-down procedures were similar to those described for the SCCR4 unit. Since the

pressure sensitive switch was incorporated into the SCCR7 unit, the functioning of the pumps, preheaters and liquid level control device were then automatically controlled.

The work involved during each run included

- Monitoring the flowrates and temperatures. A sample of these values is included in Appendix IV.
- Collection of samples from the columns to ensure that a steady state was achieved as will be discussed in the next Section.
- Collection of the products as will be described in Section 7.2.1.2.
- Analysis of the samples

and finally purging the columns at the end of the run.

7.2.1.1 Establishing Pseudo-Equilibrium

Due to the semi-continuous nature of the SCCR7 only a pseudo-equilibrium state can be achieved. To assess the establishment of a pseudo-equilibrium, actual samples of on-column fluid were withdrawn through the sample points. This took place from the same point on the same column at the same fixed time into each switch during the experiment. When two on-column concentration profiles of two consecutive cycles were identical, the pseudo-equilibrium state was deduced to have been reached.

Figs. 7.2 and 7.3 represent examples of the on-column concentration profiles of two consecutive cycles of one experiment. It was found that the

Fig. 7.2 On-Column Concentration Profile of Cycle 9 of Run 16-70-7-30-60-30

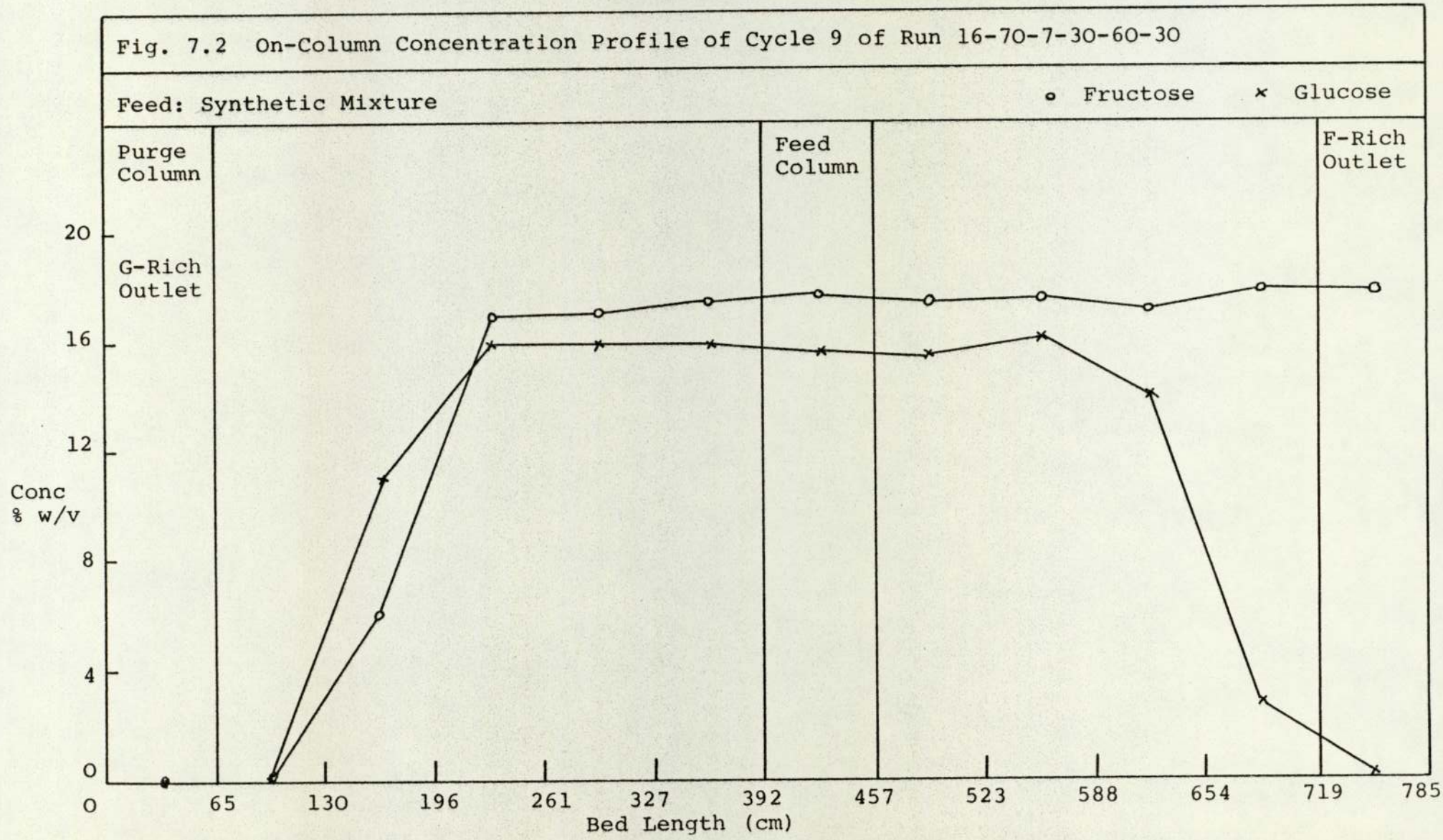

Fig. 7.3 On-Column Concentration Profile of Cycle 10 of Run 16-70-7-30-60-30

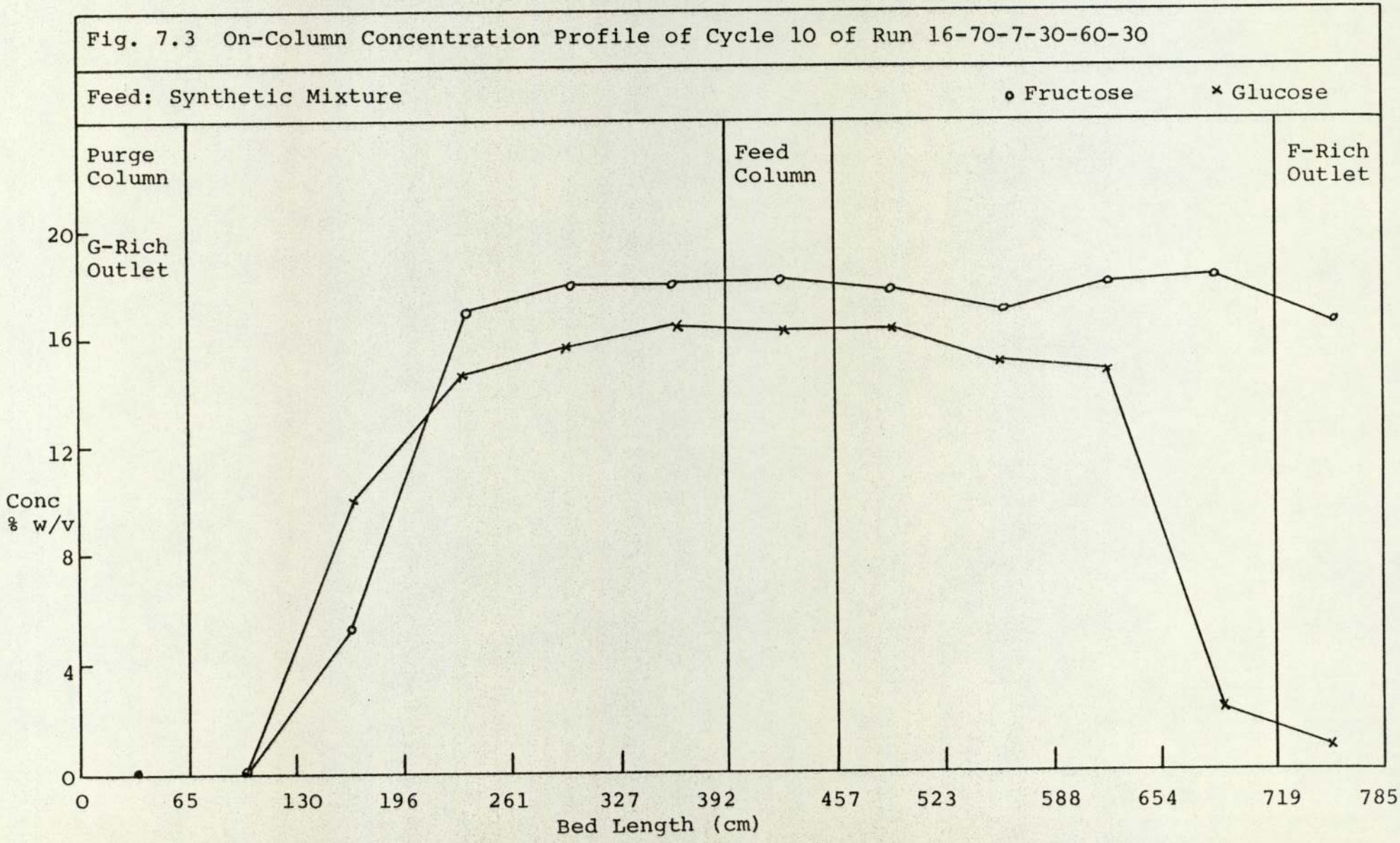

pseudo-equilibrium state was achieved after eight cycles. It is to be noticed that the on-column concentration profiles represented the concentration of sugars in the mobile phase only, while the end of run concentration profiles represented the total concentration of sugars in the column.

7.2.1.2 Fraction Collection of the Products

The concentration profiles of the issuing product streams were monitored with respect to time during a switch period. It was found that all the glucose rich product was purged in the first fifteen minutes, i.e. half the switch period. However, the fructose rich product was eluted in the last 12 minutes of the switch period. The reason for this was that the column from which the fructose product was issuing had been purged in the previous switch period and therefore it contained pure water only. This water was eluted first followed by the fructose rich product. Typical concentration profiles of the fructose rich product and glucose rich product are shown in Figs. 7.4 and 7.5.

Each product stream was split into two fractions. One fraction contained almost all the sugars and the other fraction contained water only. This fraction collection of the products was adopted in all the experiments in order to increase the concentration of the products. Examples of the analysis of the product is included in Appendix III.

Fig. 7.4 Purging of Fructose-Rich Product

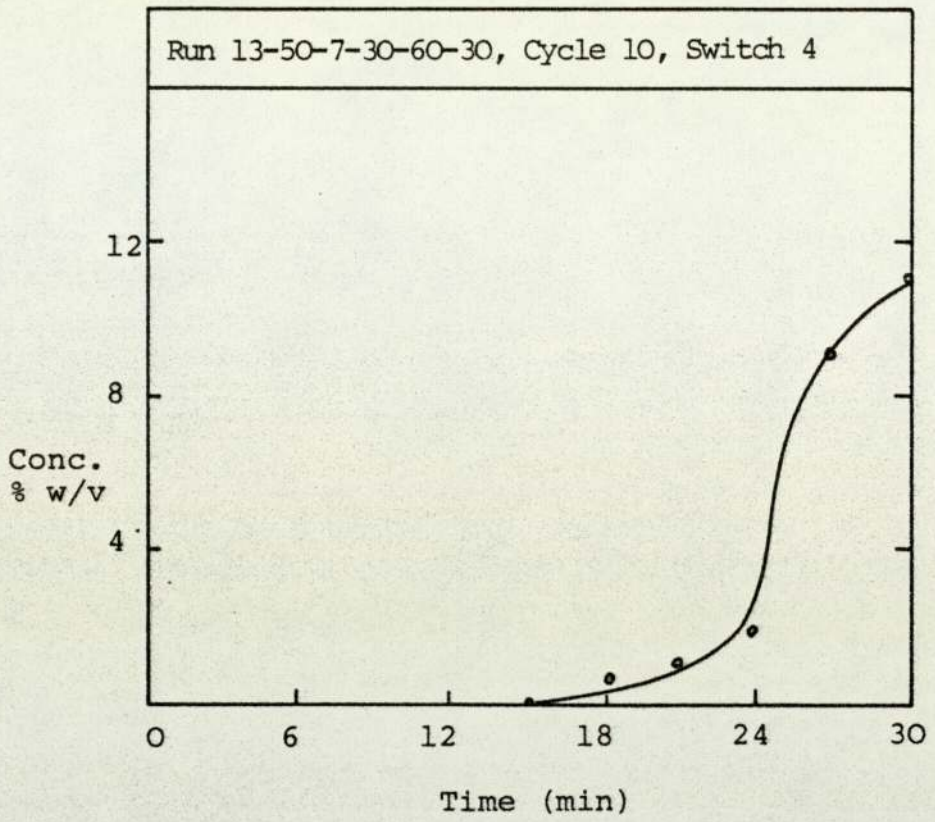

Fig. 7.5 Purging of Glucose-Rich Product

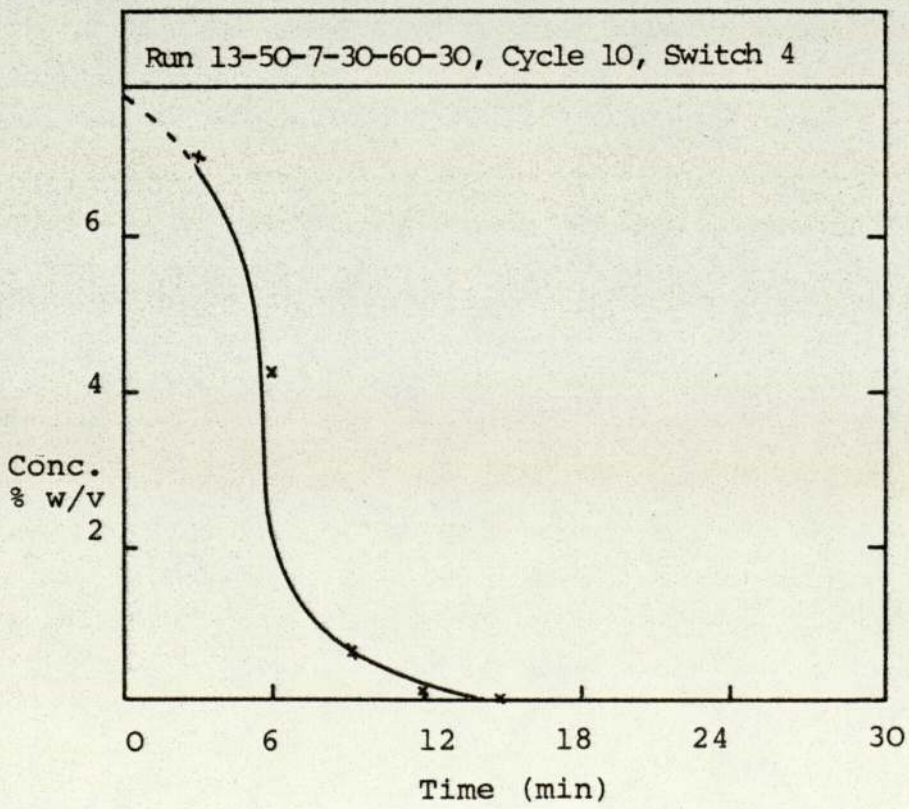

7.2.1.3 Analysis of the Products

The analytical system with the HPLC column, which has been discussed in Section 6.2, was used to analyse the products of the SCCR7 unit. However from the initial analysis it was noticed that the refractometer responded to the small quantity of the bisulphite present in the sample. The result was a small flat band with an elution time nearly equal to that of glucose. When the glucose concentration was small, the bisulphite band overlapped the glucose band. Therefore it was necessary to remove the bisulphite from the sample before analysis. A simple device was used as follows.

A small glass column of 10 mm internal diameter was packed to a height of 100 mm with a mixed bed of a cation exchange resin in the calcium form and an anion exchange resin in the acetate form (94). The sample was passed through the column at a flow rate of 0.6-0.8 $cm^3 min^{-1}$ and the sample collection started after allowing the column to be saturated with the sample. This procedure was found successful in removing both the bisulphite and sodium ions and did not change the concentration of the sugars because the residence time was too small.

7.2.2 Initial Runs with the SCCR7 Unit

A set of four runs were carried out to separate mixtures of fructose and glucose on the SCCR7 unit.

The object of these initial runs was to familiarise the operator with the SCCR7 unit. The values of the

feed, eluent and purge flow rates were chosen on the basis of equation 6.13 coupled with the previous experience with the SCCR4 unit. Three of these runs were interrupted after the first four cycles due to high pressure drops in connection with certain columns. When these columns were inspected it was found that some small particles of the resin had escaped through cavities, between the mesh and the retaining ring to block the inlet liquid ducts. Therefore the meshes of the twelve columns were cemented to the retaining rings by an adhesive. This remedy was successful in preventing the resin particle to escape.

7.2.3 Effect of Feed Rate

A set of three runs were carried out to investigate the effect of feed flow rates on the performance of the unit. These runs were carried out at similar operating conditions. The flow rates of the feed were chosen as 7, 8.5 and 10 $cm^3 min^{-1}$. The results of these runs are shown on Table 7.3 and the concentration profiles of each run are shown in Figs. 7.6, 7.7 and 7.8.

7.2.3.1 Results and Discussion

The result of the experiments are represented in a similar tabulated way to that used for presenting the results of the SCCR4 unit. However since the products of the SCCR7 were split into two fractions, the concentration of the products are presented in

TABLE 7.3 RUN CONDITIONS FOR VARYING FEED FLOW RATE										
Run Number	Flow Rate ($cm^3 min^{-1}$)			Feed Conc. % w/v		Feed Rate ($g\ hr^{-1}$)	Temp. ^oC	Switch Period (min)	L'/P Ratio	
	Feed	Eluent	Purge	F	G				Pre-Feed	Post Feed
9-50-7-28-60-30	7	28	120	26.1	25.5	210	60	30	0.374	0.577
10-50-8.5-28-60-30	8.5	28	120	25.9	24.8	255	60	30	0.374	0.620
11-50-10-28-60-30	10	28	120	25.2	24.7	300	60	30	0.374	0.664

RESULTS FOR VARYING FEED FLOW RATE										
Run Number	Fructose Rich Product					Glucose Rich Product				
	Mass Bal. %	Purity %	Recovery %	Conc. % w/v Fraction	Bulk	Mass Bal. %	Purity %	Recovery %	Conc. % w/v Fraction	Bulk
9-50-7-28-60-30	96	99	51	9.6	2.8	96	67	95	3.3	1.7
10-50-8.5-28-60-30	101	94	64	10.3	3.0	97	70	94	3.4	1.7
11-50-10-28-60-30	96	84	59	11.6	3.4	97	75	95	3.8	1.9

Fig. 7.6 Equilibrium Concentration Profile of Run 9-50-7-28-60-30

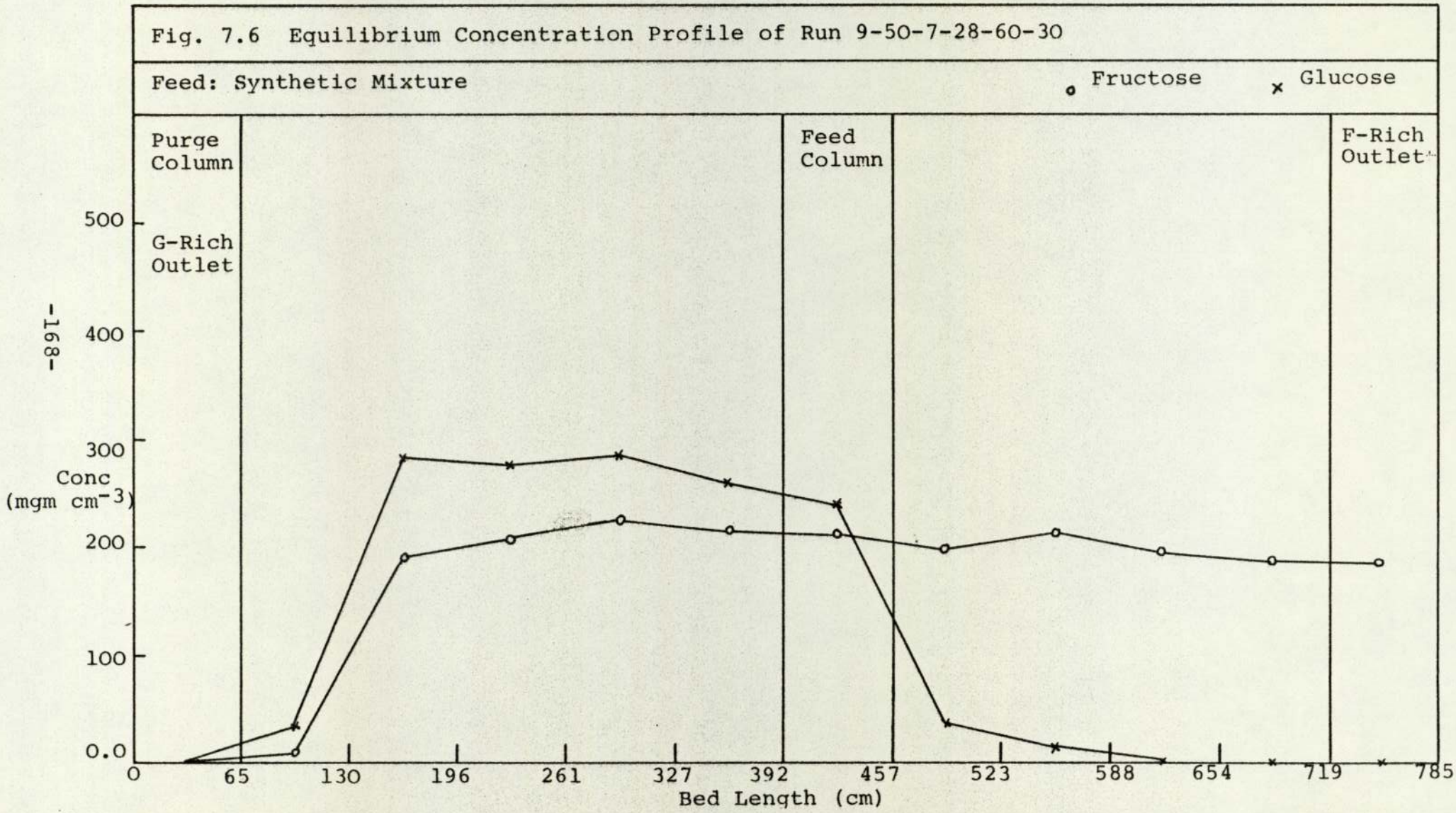

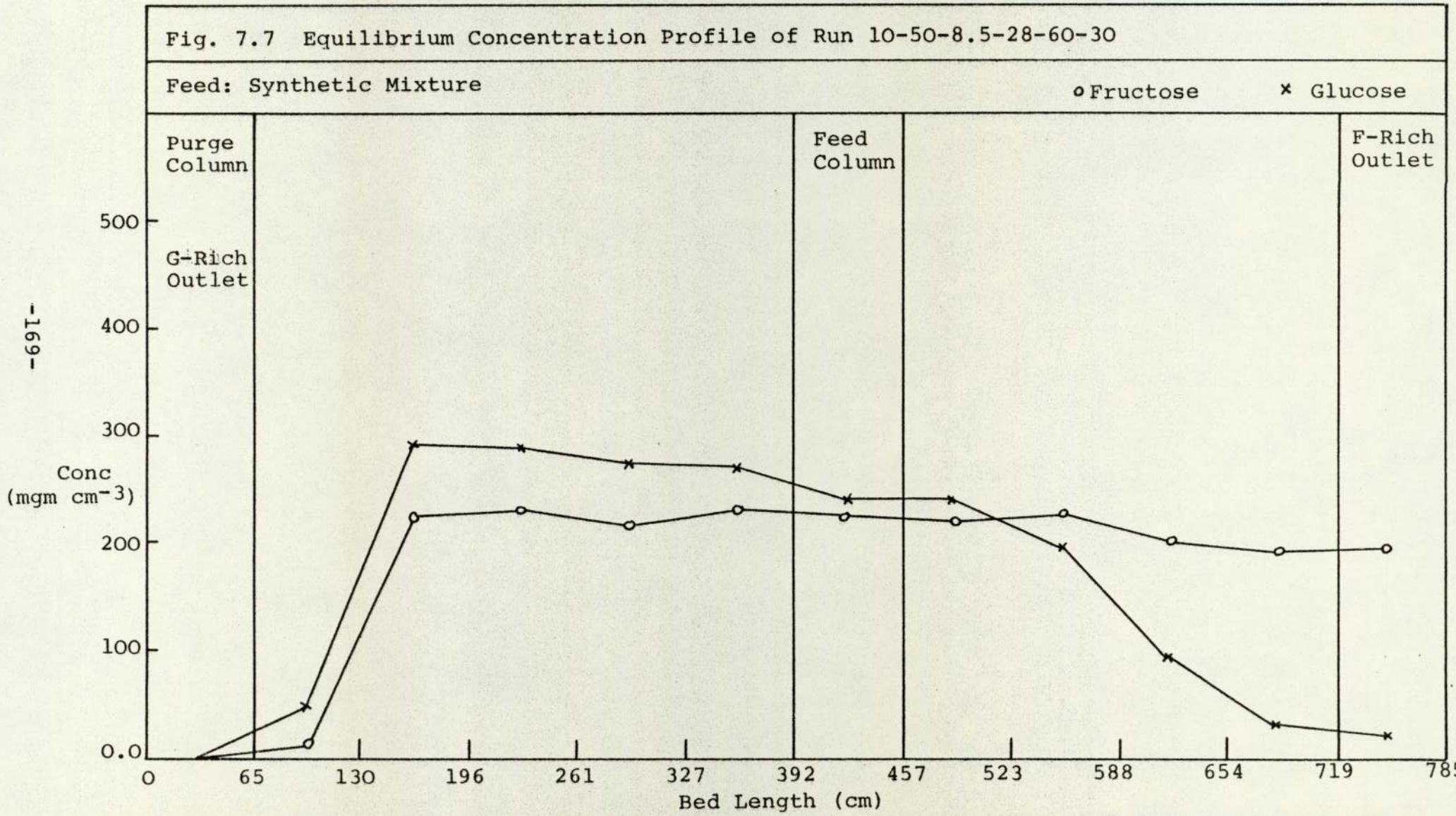
Fig. 7.7 Equilibrium Concentration Profile of Run 10-50-8.5-28-60-30
Feed: Synthetic Mixture
o Fructose
× Glucose
Purge Column
Feed Column
F-Rich Outlet
G-Rich Outlet
500
400
300
200
100
0.0
Conc (mgm cm-3)
0
65
130
196
261
327
392
457
523
588
654
719
785
Bed Length (cm)

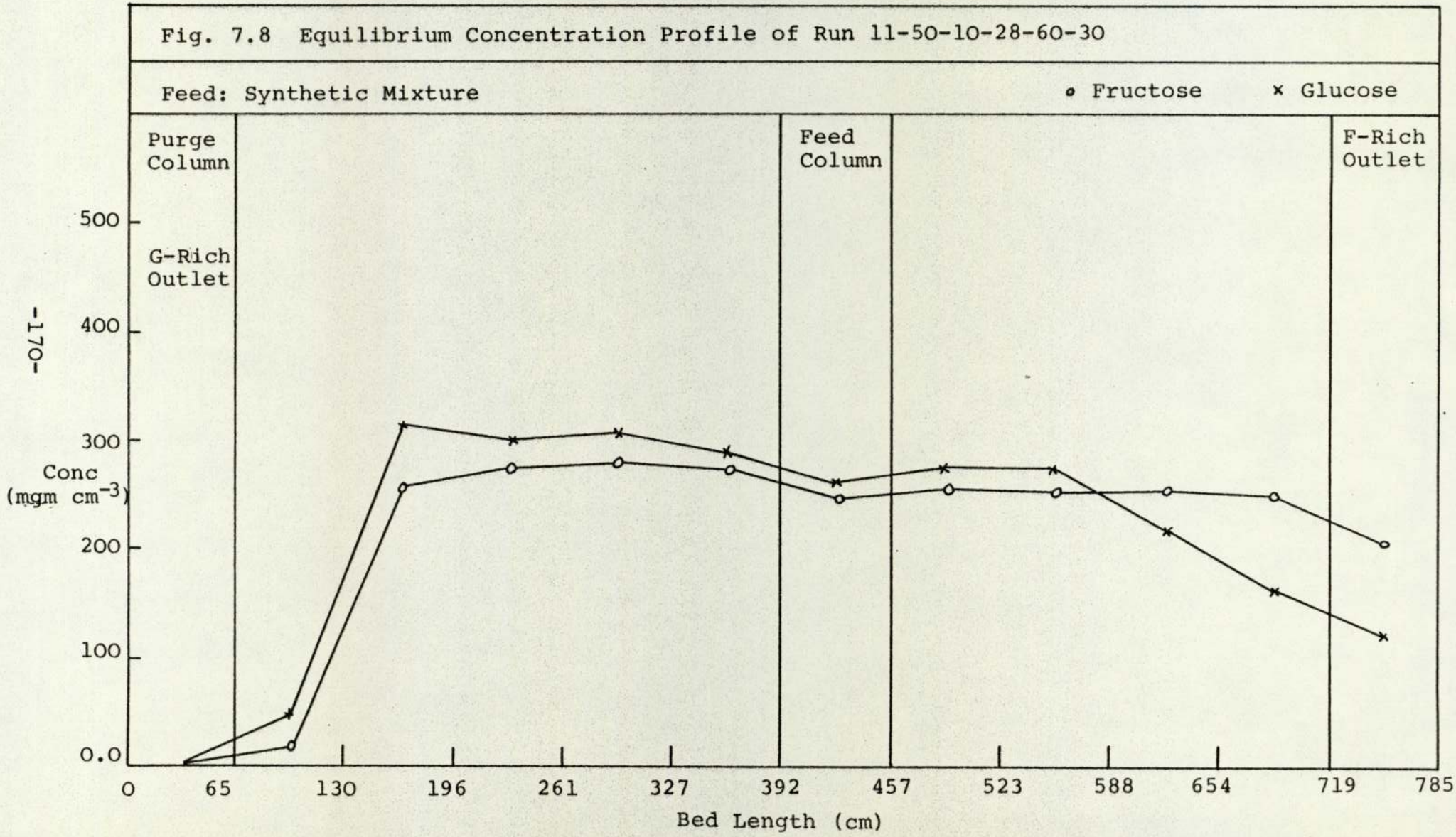
Fig. 7.8 Equilibrium Concentration Profile of Run 11-50-10-28-60-30
Feed: Synthetic Mixture
o Fructose
× Glucose
Purge Column
Feed Column
F-Rich Outlet
G-Rich Outlet
500
400
300
200
100
0.0
Conc (mgm cm^{-3})
0
65
130
196
261
327
392
457
523
588
654
719
785
Bed Length (cm)

two quantities. The first one labelled 'Fraction' refers to the concentration of the rich fraction and the second one, labelled 'Bulk' refers to the average concentration of the two fractions.

It can be seen from Table 7.3 that when the feed rate increases, the L'/p ratio in the post-feed increases while that in the pre-feed remains constant. It is also clear that as the feed rate increases the cross-over is shifted towards the fructose rich product outlet as shown in the concentration profiles. This means that more of glucose which is the retarded solute, is travelling with the mobile phase. The practical effect of this was a decrease of the purity of fructose from 99% in run 9-50-7-28-60-30 to 84% in run 11-50-10-28-60-30.

It can also be observed from Table 7.3 that the recovery of fructose is generally low which means that some fructose is travelling with the stationary phase. This is clear from the low purity of the glucose products. The reason for this is that the eluent flow rate is too slow to elute all of the fructose.

7.2.4 Effect of Eluent Rate

Two runs were conducted at 24 and 30 cm^3min^{-1} and compared to run 9-50-7-28-60-30 to investigate the effect of eluent rate. The feed rate was constant at 7 cm^3min^{-1}.

7.2.4.1 Results and Discussion

The results are presented in Table 7.4 and the concentration profiles in Figs. 7.9 and 7.10

From Table 7.4 it can be observed that by changing the eluent rate, the L'/P ratio changes in both the pre-feed and post-feed sections. This is also clear from the concentration profiles in Figs. 7.6, 7.9 and 7.10. Although the purity of fructose is slightly affected by increasing the eluent rate, the glucose purity is greatly improved by increasing the eluent rate from 24 to 30 cm^3min^{-1}. Run 13-50-7-30-60-30 was considered to be carried out at the optimum operating conditions of the SCCR7. This is because both the purity and recovery of the sugars were improved as shown in Table 7.4. From this it was concluded that the optimum feed to eluent ratio for the SCCR7 unit was 1:4.3.

7.2.5 Effect of Feed Concentration

A set of four runs were chosen to investigate the effect of the feed concentration on the separation capacity of the SCCR7. These runs were carried out at identical flow rates of 7 cm^3min^{-1} feed and 30 cm^3min^{-1} eluent since these values were shown to give the best separation. The feed concentrations were 20%, 35%, 50% and 70% w/v each containing equal proportions of fructose and glucose.

TABLE 7.4 RUN CONDITIONS FOR VARYING ELUENT FLOW RATE										
Run Number	Flow Rate ($cm^3 min^{-1}$)			Feed Conc. % w/v		Feed Rate ($g\ hr^{-1}$)	Temp. ^oC	Switch Period (min)	L'/P Ratio	
	Feed	Eluent	Purge	F	G				Pre-Feed	Post-Feed
12-50-7-24-60-30	7	24	120	25.8	24.5	210	60	30	0.258	0.461
9-50-7-28-60-30	7	28	120	26.1	24.9	210	60	30	0.374	0.577
13-50-7-30-60-30	7	30	120	25.5	24.5	210	60	30	0.432	0.635

RESULTS FOR VARYING ELUENT FLOW RATE										
Run Number	Fructose Rich Product					Glucose Rich Product				
	Mass Bal. %	Purity %	Recovery %	Conc. Fraction	% w/v Bulk	Mass Bal. %	Purity %	Recovery %	Conc. Fraction	% w/v Bulk
12-50-7-24-60-30	97	100	42	7.1	1.9	97	61	96	3.5	1.8
9-50-7-28-60-30	96	99	53	9.6	2.8	96	67	95	3.3	1.7
13-50-7-30-60-30	97	97	80	10.2	3.8	96	84	93	3.1	1.6

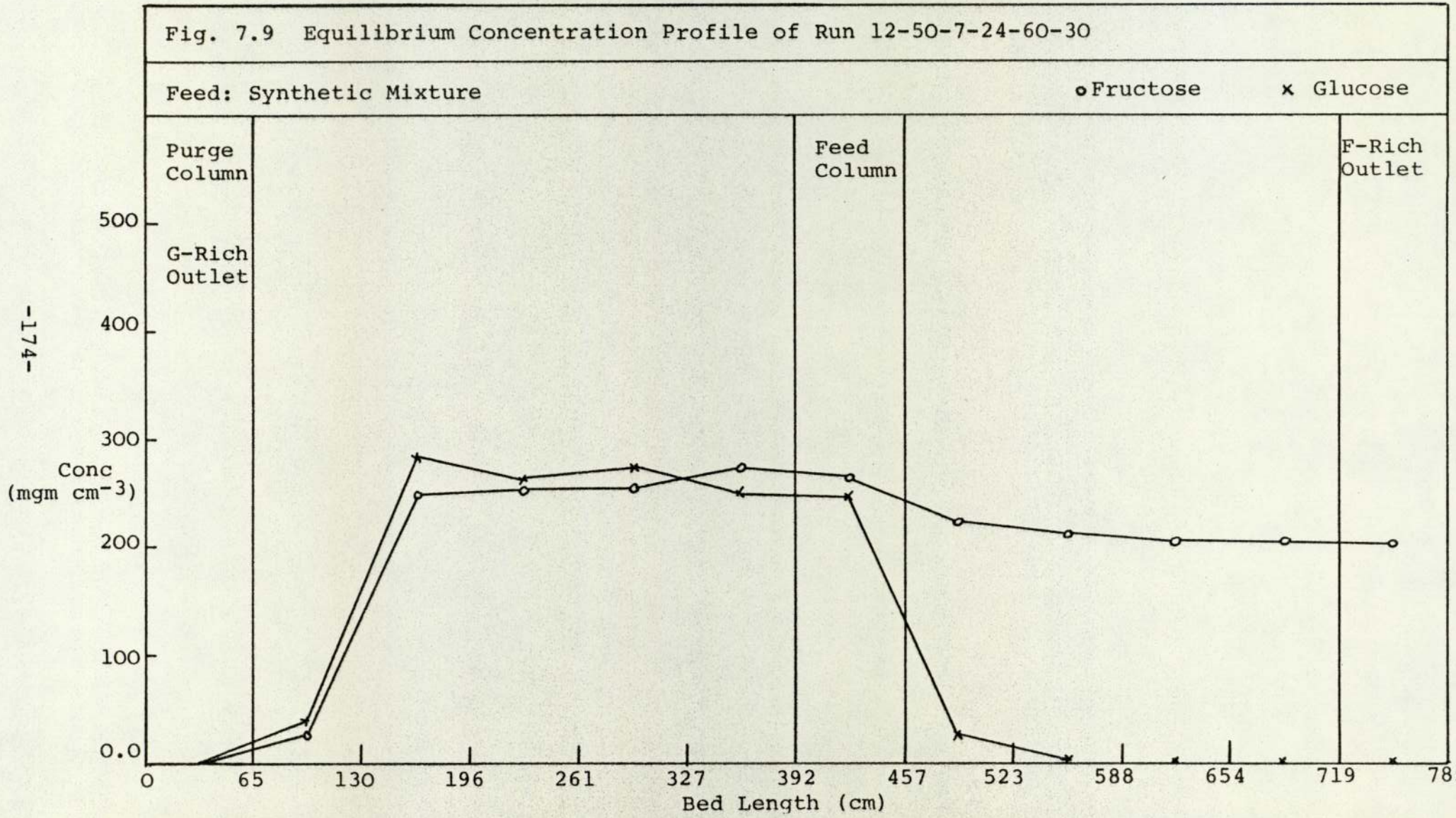
Fig. 7.9 Equilibrium Concentration Profile of Run 12-50-7-24-60-30
Feed: Synthetic Mixture
o Fructose
x Glucose
Purge Column
Feed Column
F-Rich Outlet
G-Rich Outlet
500
400
300
200
100
0.0
Conc (mgm cm^{-3})
0
65
130
196
261
327
392
457
523
588
654
719
785
Bed Length (cm)

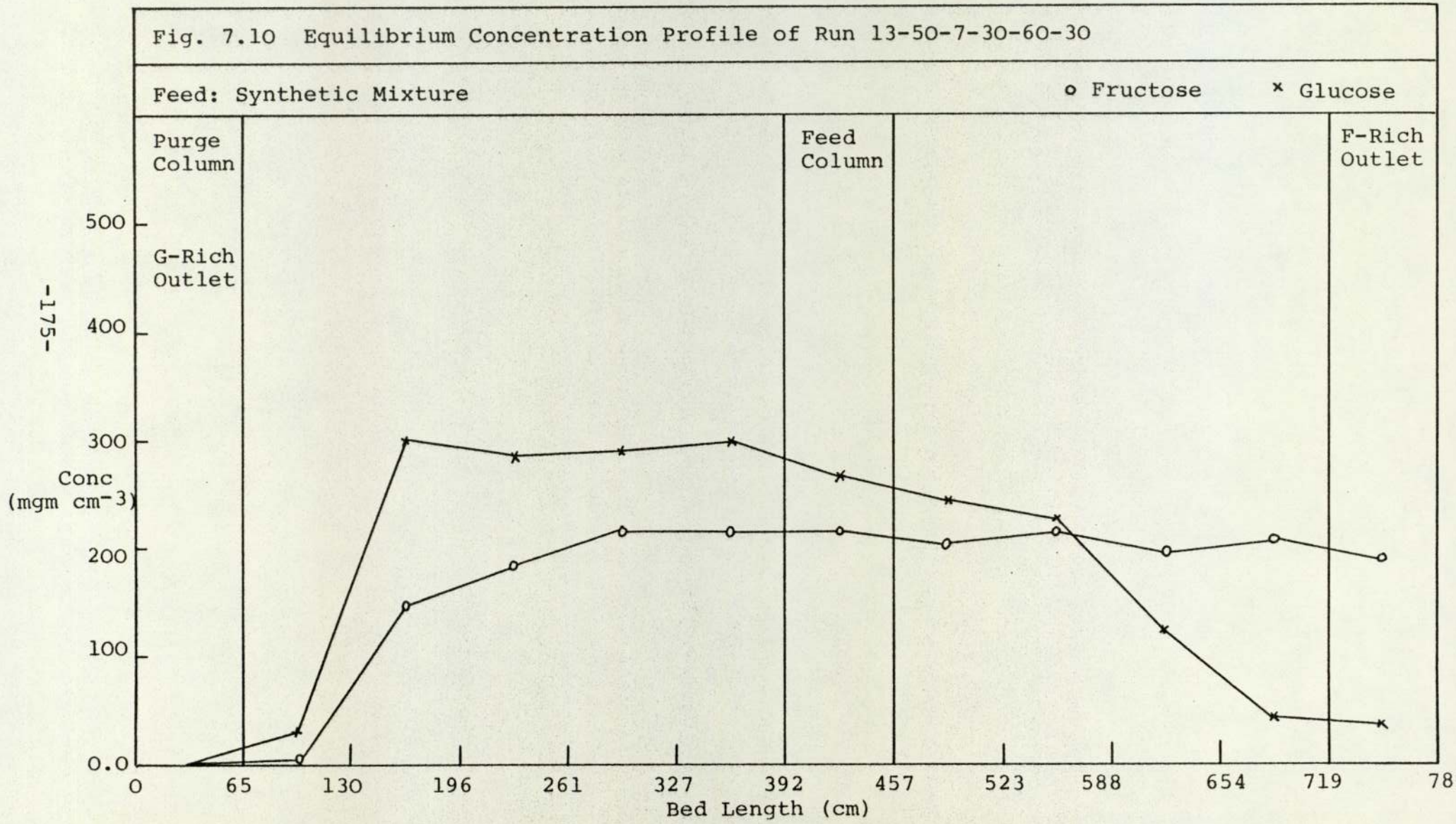
Fig. 7.10 Equilibrium Concentration Profile of Run 13-50-7-30-60-30
Feed: Synthetic Mixture
o Fructose
× Glucose
Purge Column
Feed Column
F-Rich Outlet
G-Rich Outlet
500
400
300
200
100
0.0
Conc (mgm cm⁻³)
0
65
130
196
261
327
392
457
523
588
654
719
785
Bed Length (cm)

7.2.5.1 Results and Discussion

The results of these runs are shown in Table 7.5 and the concentration profiles are in Figs.(7.10-7.13). The purity of fructose remained fairly constant for feed concentrations up to 50% w/v. However at 70% w/v the purity dropped sharply for both products. By examining the concentration profiles it can be seen that the general shape of the curves is not affected. It is only that the level of the sugars retained by each column increases with increase of the feed concentration. This is illustrated by Fig. 7.14 for fructose and Fig. 7.15 for glucose.

It can be concluded that the SCCR7 was not very sensitive to changes of concentration of the feed until a point was reached when the system was overloaded with sugars and the excess sugars then contaminated the products.

7.3 RUNS WITH SUCROSE-BASED FEED

Two runs were performed to simultaneously hydrolyse sucrose and separate the products of hydrolysis. The object of the runs was to study the performance of the SCCR7 unit when the feed was an inverted sucrose mixture.

A similar arrangement for hydrolysis to that used with the SCCR4 (see Section 6.5.1) was employed. The only difference was that a larger hydrolysis column of 2" (50.8 mm) internal diameter was used to cope with the increased capacity of the SCCR7 unit.

TABLE 7.5 CONDITIONS FOR RUNS WITH VARYING FEED CONCENTRATION

Run Number	Flow Rate ($cm^3 min^{-1}$)			Feed Conc. % w/v		Feed Rate ($g\ hr^{-1}$)	Temp. °C	Switch Period (min)	L'/P Ratio	
	Feed	Eluent	Purge	F	G				Pre-Feed	Post-Feed
14-20-7-30-60-30	7	30	120	10.5	10.4	84	60	30	0.432	0.635
15-35-7-30-60-30	7	30	120	18.0	17.8	147	60	30	0.432	0.635
13-50-7-30-60-30	7	30	120	25.5	24.5	210	60	30	0.432	0.635
16-70-7-30-60-30	7	30	120	35.1	33.6	294	60	30	0.432	0.635

RESULTS FOR VARYING FEED CONCENTRATION

Run Number	Fructose Rich Product					Glucose Rich Product				
	Mass Bal. %	Purity %	Recovery %	Conc. Fraction	% w/v Bulk	Mass Bal. %	Purity %	Recovery %	Conc. Fraction	% w/v Bulk
14-20-7-30-60-30	96	99	97	6.0	1.8	97	100	96	1.3	0.7
15-35-7-30-60-30	97	97	97	9.6	3.2	97	100	93	2.1	1.2
13-50-7-30-60-30	97	97	80	10.2	3.7	96	84	93	3.1	1.6
16-70-7-30-60-30	100	86	66	12.9	4.4	101	71	89	4.2	2.2

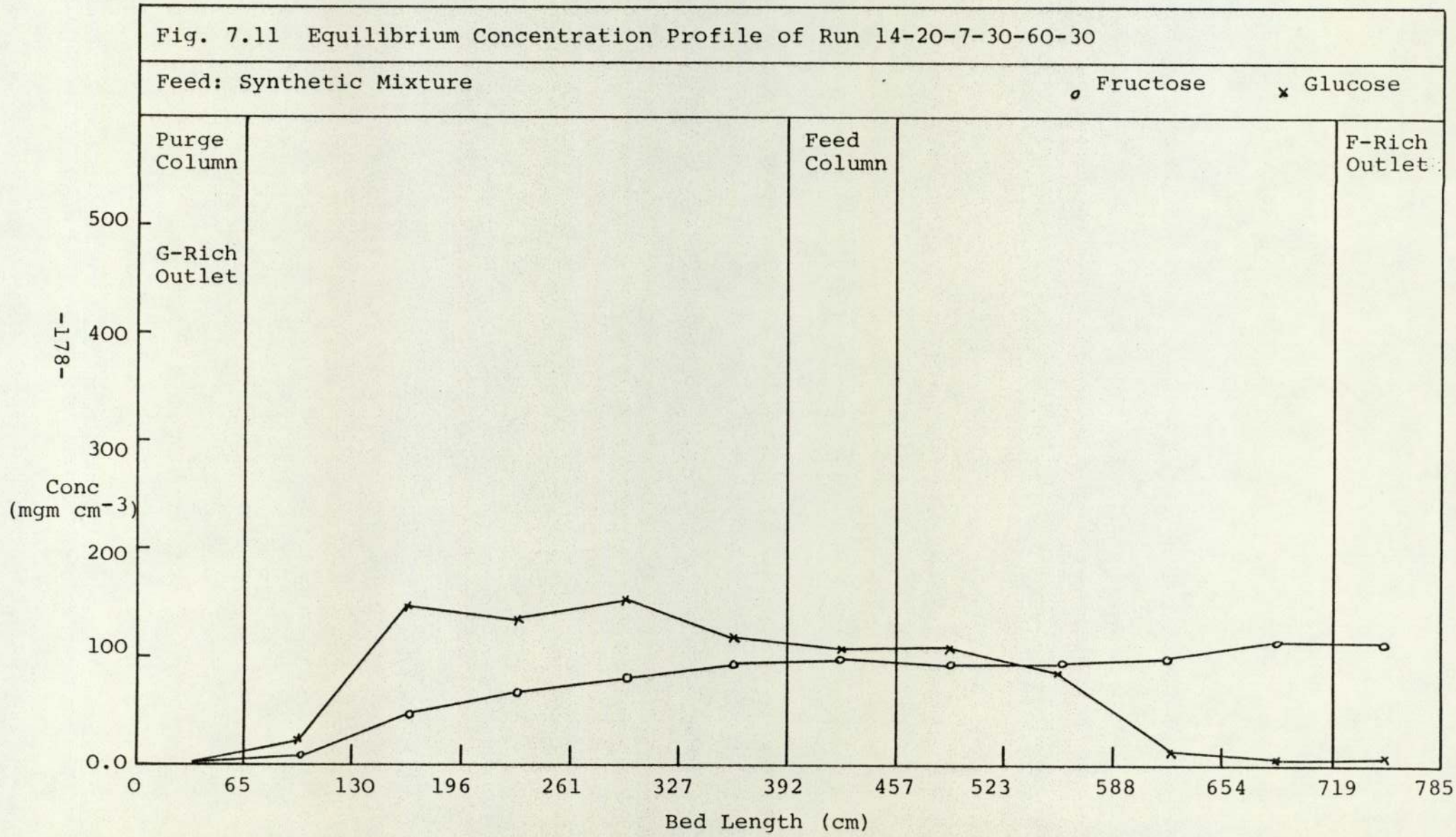
Fig. 7.11 Equilibrium Concentration Profile of Run 14-20-7-30-60-30
Feed: Synthetic Mixture
o Fructose
x Glucose
Purge Column
Feed Column
F-Rich Outlet
G-Rich Outlet
500
400
300
200
100
0.0
Conc (mgm cm-3)
0
65
130
196
261
327
392
457
523
588
654
719
785
Bed Length (cm)

Fig. 7.12 Equilibrium Concentration Profile of Run 15-35-7-30-60-30

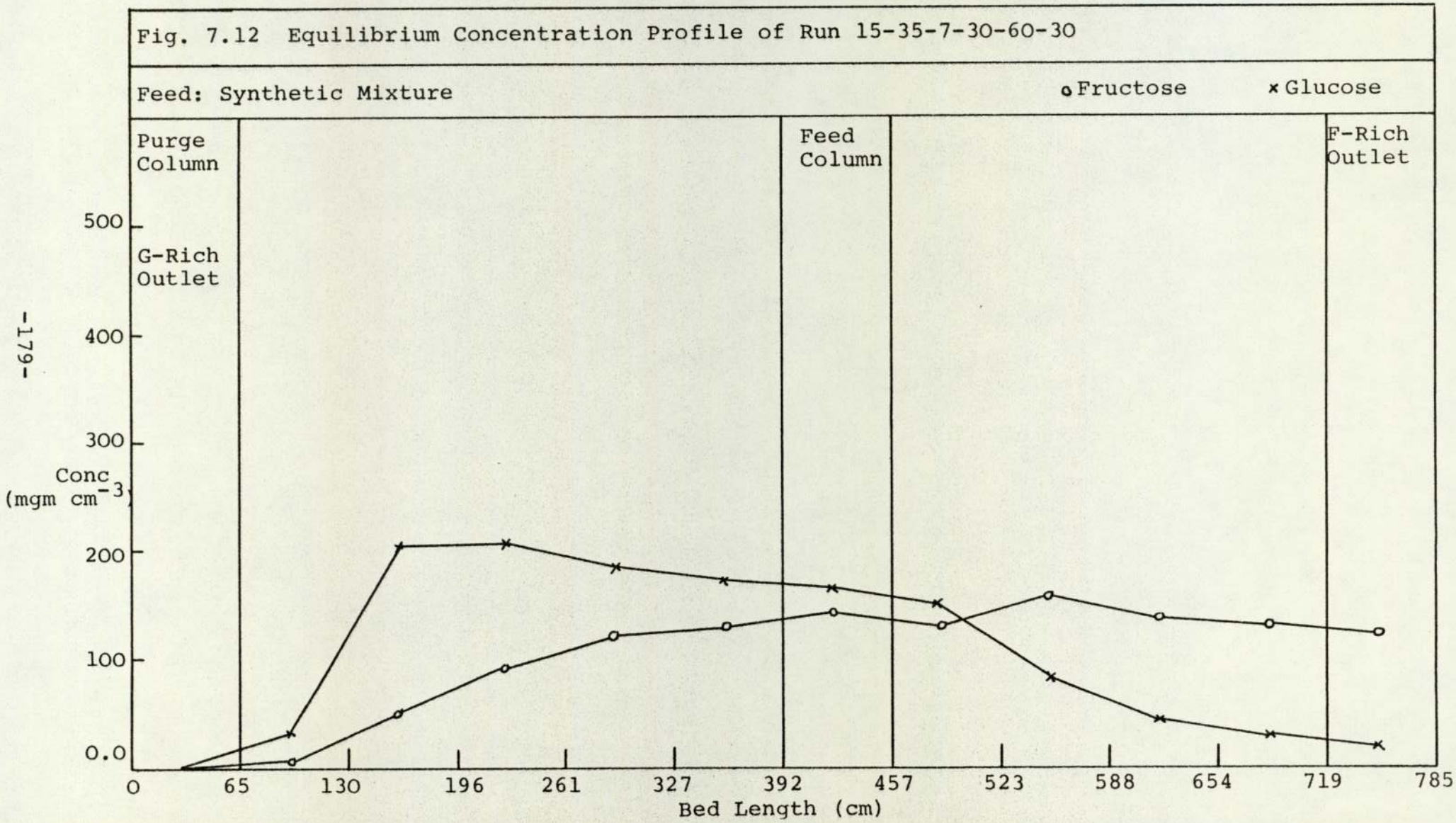

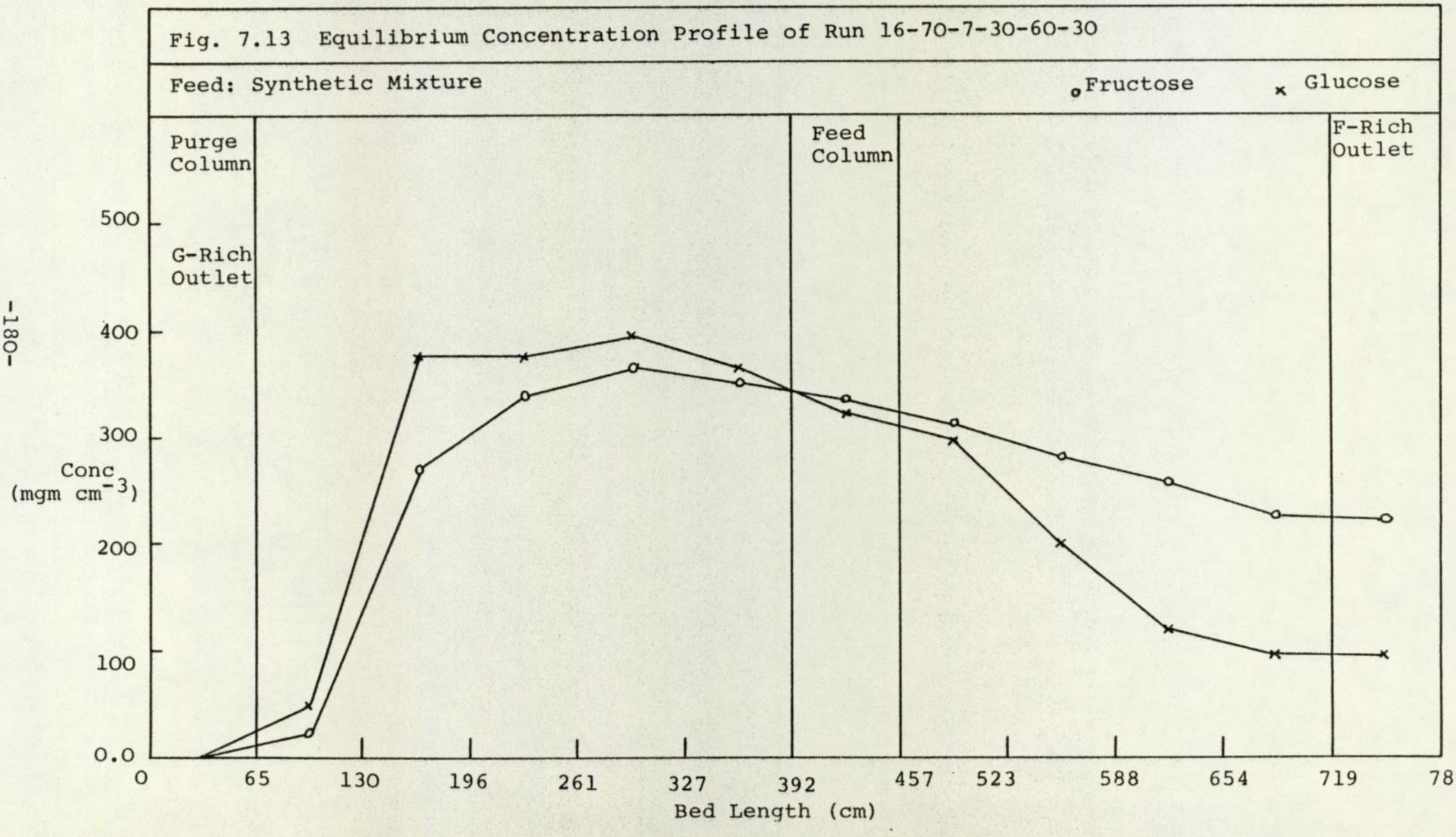
Fig. 7.13 Equilibrium Concentration Profile of Run 16-70-7-30-60-30
Feed: Synthetic Mixture
Fructose
Glucose
Purge Column
Feed Column
F-Rich Outlet
G-Rich Outlet
500
400
300
200
100
0.0
Conc (mgm cm^{-3})
0
65
130
196
261
327
392
457
523
588
654
719
785
Bed Length (cm)

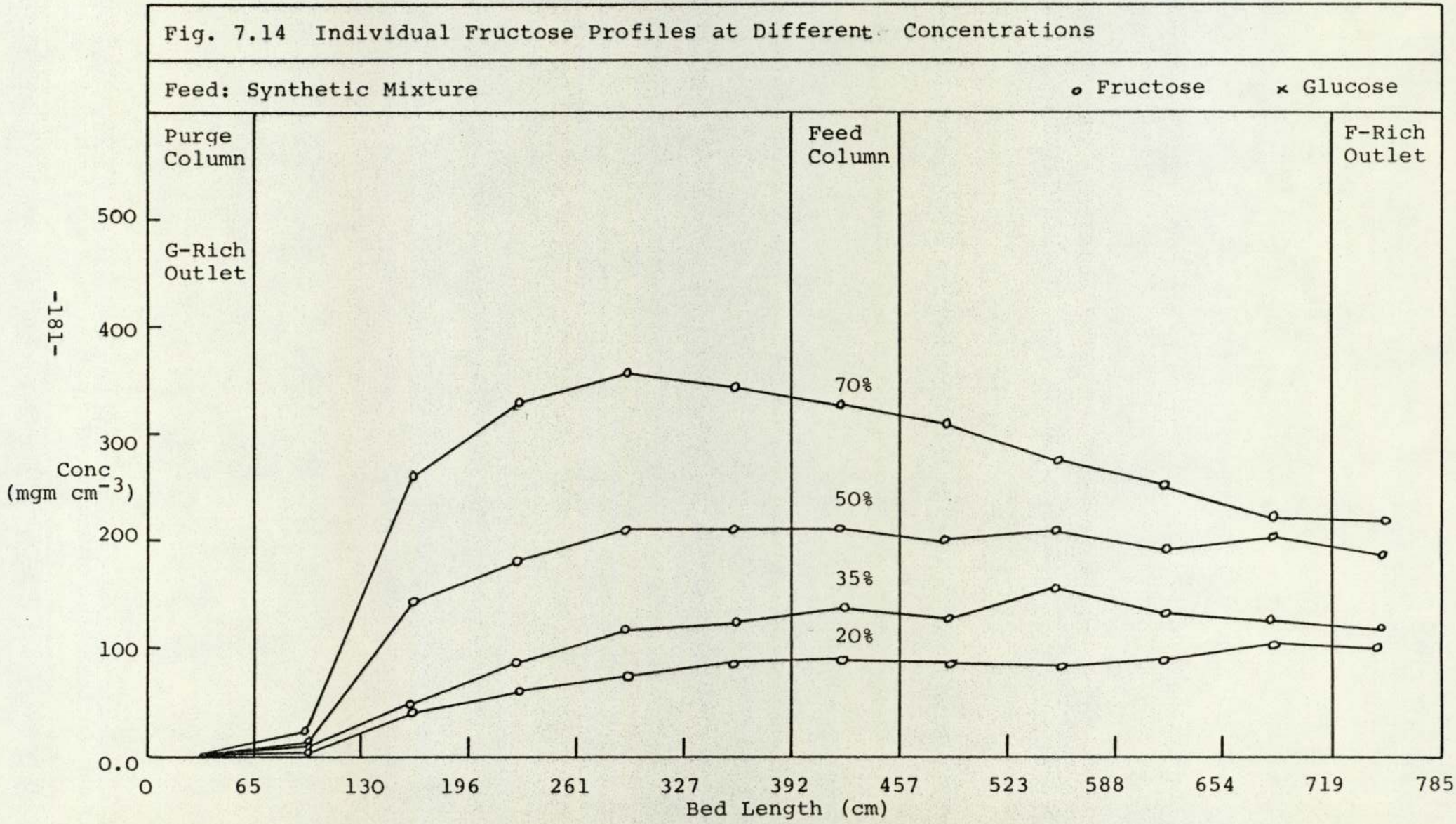
Fig. 7.14 Individual Fructose Profiles at Different Concentrations
Feed: Synthetic Mixture
o Fructose
x Glucose
Purge Column
Feed Column
F-Rich Outlet
G-Rich Outlet
70%
50%
35%
20%
Conc (mgm cm^{-3})
0.0
100
200
300
400
500
0
65
130
196
261
327
392
457
523
588
654
719
785
Bed Length (cm)

Fig. 7.15 Individual Glucose Profiles at Different Concntrations

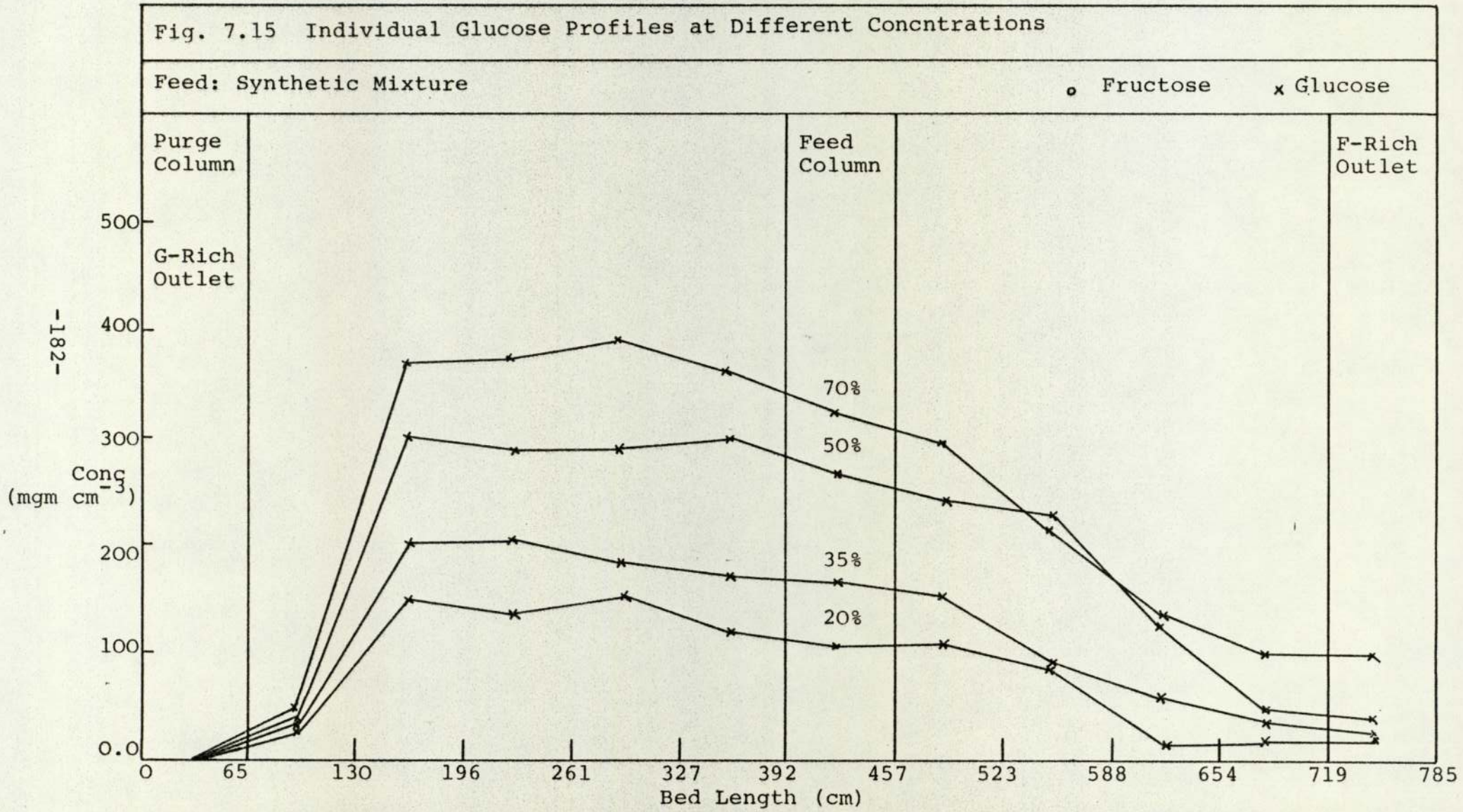

7.3.1 Results and Discussion

Table 7.6 includes runs S17-50-7-30-45-30 and S19-50-10-28-45-30 which were carried out with inverted sucrose mixtures and two identical runs 18-50-7-30-45-30 and 20-50-10-28-45-30 with synthetic fructose and glucose mixtures. It can be seen that the results of the runs with the inverted sucrose are in agreement with those carried out with the synthetic feed mixtures. Also by comparing the concentration profiles on Figs. 7.16 and 7.18 to those on Figs. 7.17 and 7.19 it can be seen that there is no change in the general shape of the curves or position of the cross-over points.

It can be concluded that the performance of the SCCR7 is not affected when the feed is an inverted sucrose mixture.

The above discussion gives further support for the previous suggestion in Section 6.6 that fructose was responsible for the abnormal behaviour of the SCCR4 when separating inverted sucrose mixtures. In the case of the SCCR7 unit the fructose was not the adsorbed solute and therefore the nature or form of this sugar had no direct effect on the separation.

7.4 REGENERATION OF THE ANION EXCHANGE RESIN

It was observed that after six consecutive runs with the SCCR7 unit, the separating capacity of the unit sharply deteriorated. The purity of the fructose product was very low, which indicated that glucose

TABLE 7.6 RUN CONDITIONS FOR VARYING FEED SOURCE

Run Number	Flow Rate ($cm^3 min^{-1}$)			Feed Conc. % w/v		Feed Rate ($g\ hr^{-1}$)	Temp. ^oC	Switch Period (min)	L'/P Ratio	
	Feed	Eluent	Purge	F	G				Pre-Feed	Post-Feed
S*17-50-7-30-45-30	7	30	120	S49.1		210	45	30	0.432	0.635
18-50-7-30-45-30	7	30	120	25.5	24.5	210	45	30	0.432	0.635
S*19-50-10-28-45-30	10	28	120	S49.0		300	45	30	0.374	0.664
20-50-10-28-45-30	10	28	120	25.2	24.7	300	45	30	0.374	0.664

RESULTS FOR VARYING SOURCE

Run Number	Fructose Rich Product					Glucose Rich Product				
	Mass Bal. %	Purity %	Recovery %	Conc. % w/v Fraction	Bulk	Mass Bal. %	Purity %	Revovery %	Conc. % w/v Fraction	Bulk
S*17-50-7-30-45-30	98	96	84	10.7	4.1	100	88	95	3.3	1.8
18-50-7-30-45-30	97	97	83	10.3	3.9	98	89	94	3.1	1.9
S*19-50-10-28-45-30	98	87	67	12.2	4.4	101	74	86	4.1	2.1
20-50-10-28-45-30	98	85	64	11.7	4.1	97	72	91	3.8	1.9

* Inverted Sucrose

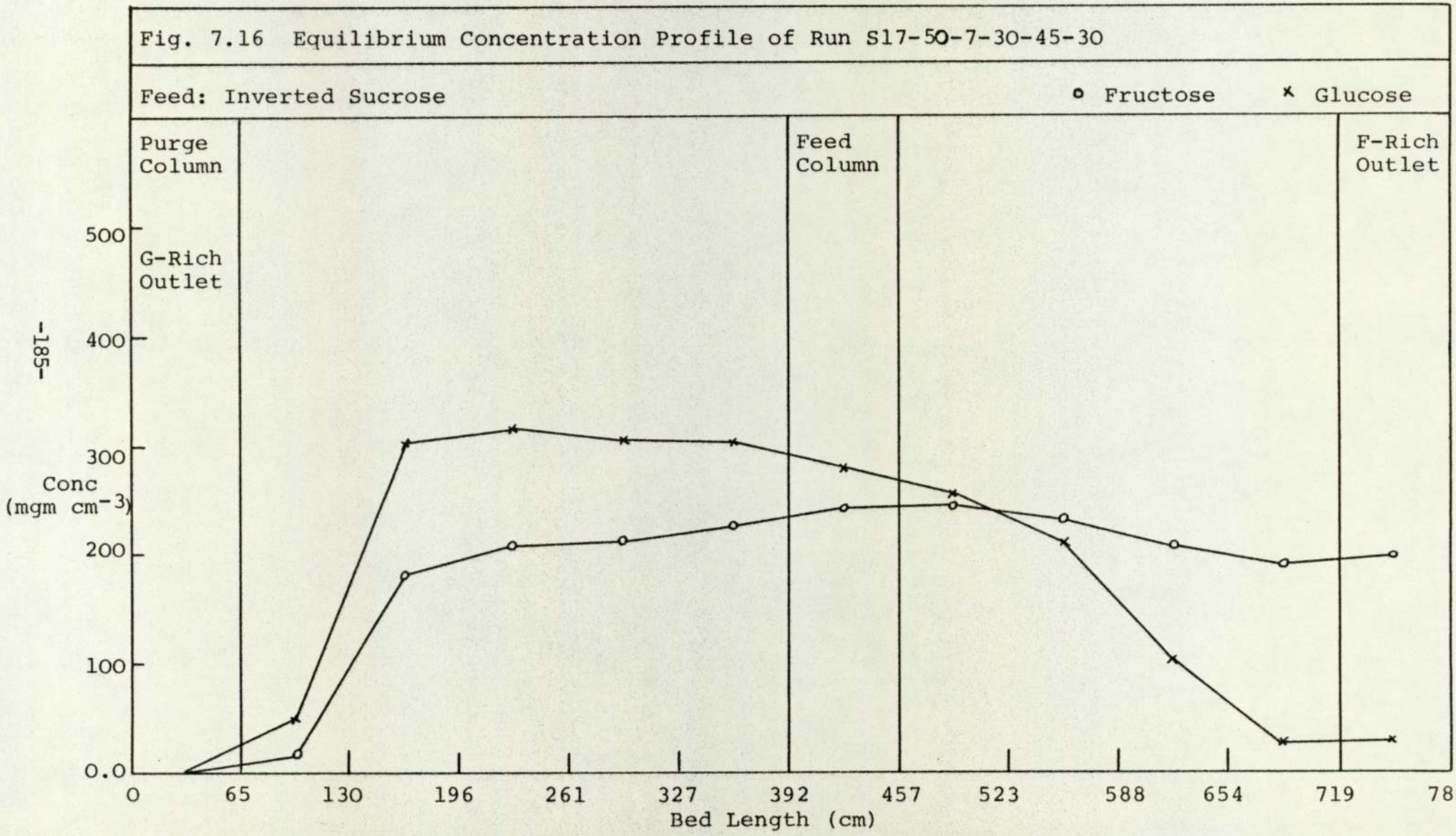
Fig. 7.16 Equilibrium Concentration Profile of Run S17-50-7-30-45-30
Feed: Inverted Sucrose
o Fructose
× Glucose
Purge Column
Feed Column
F-Rich Outlet
G-Rich Outlet
500
400
300
200
100
0.0
Conc (mgm cm⁻³)
0
65
130
196
261
327
392
457
523
588
654
719
785
Bed Length (cm)

Fig. 7.17 Equilibrium Concentration Profile of Run 18-50-7-30-45-30

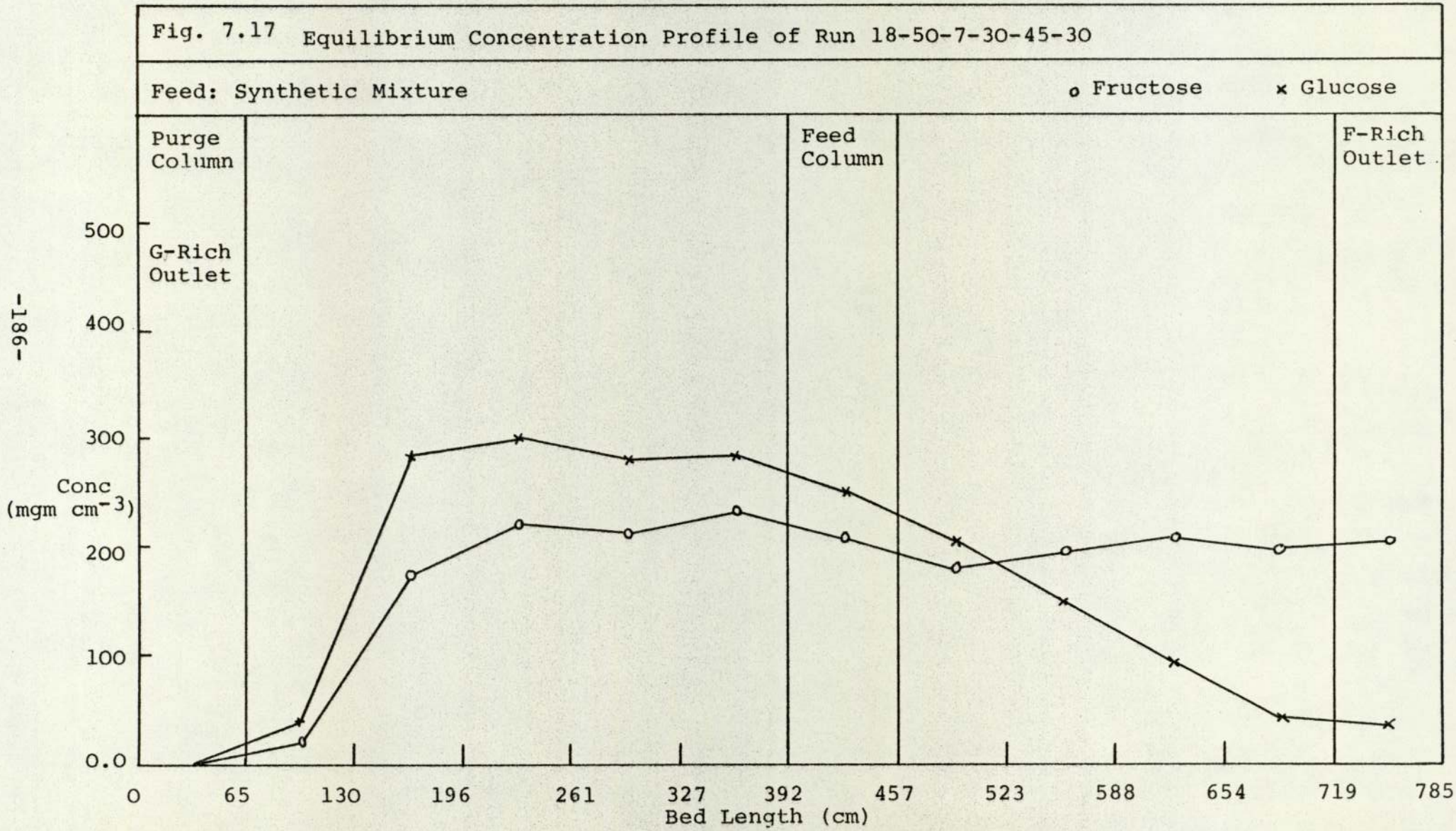

Fig. 7.18 Equilibrium Concentration Profile of Run S19-50-10-28-45-30

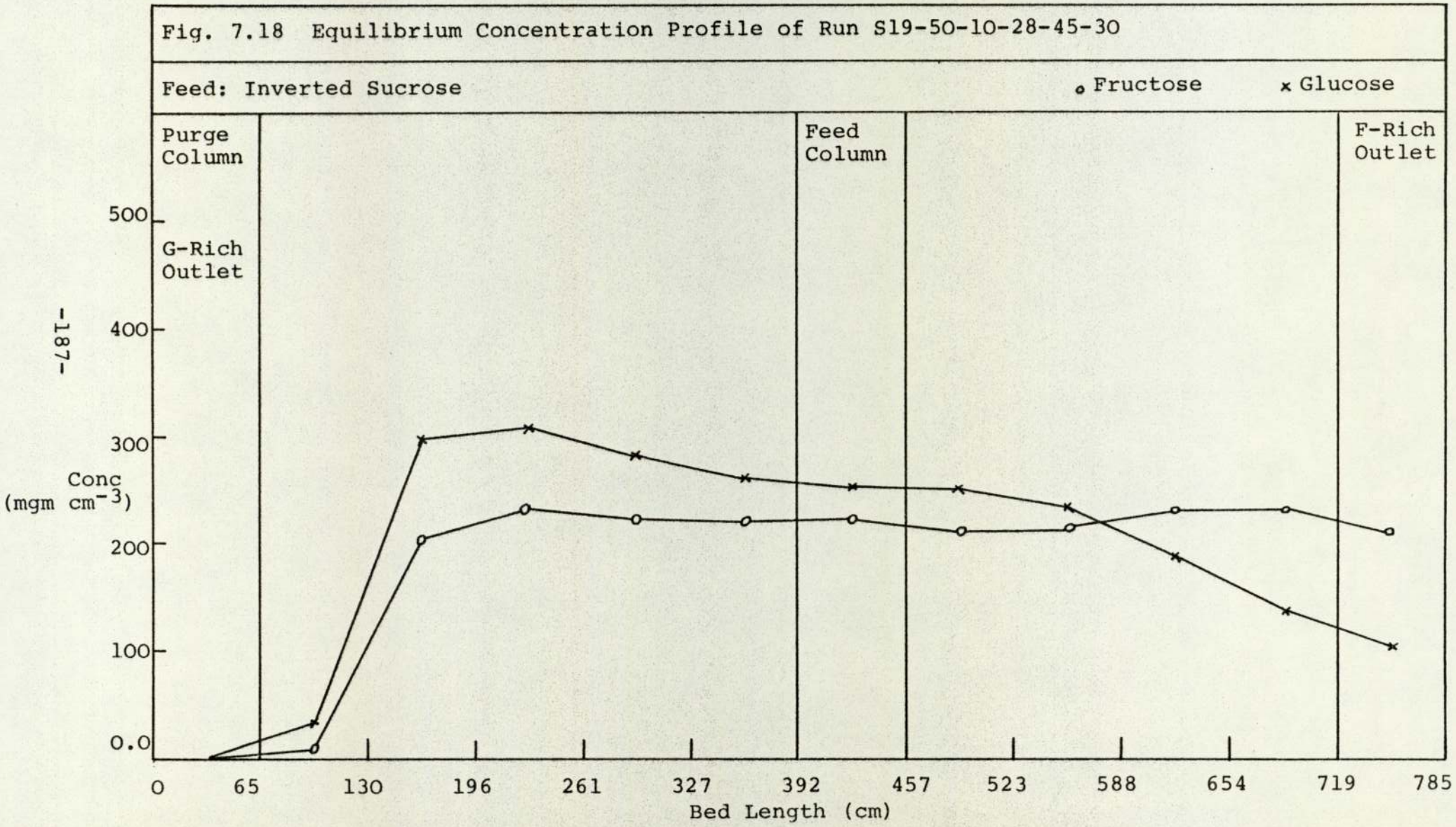

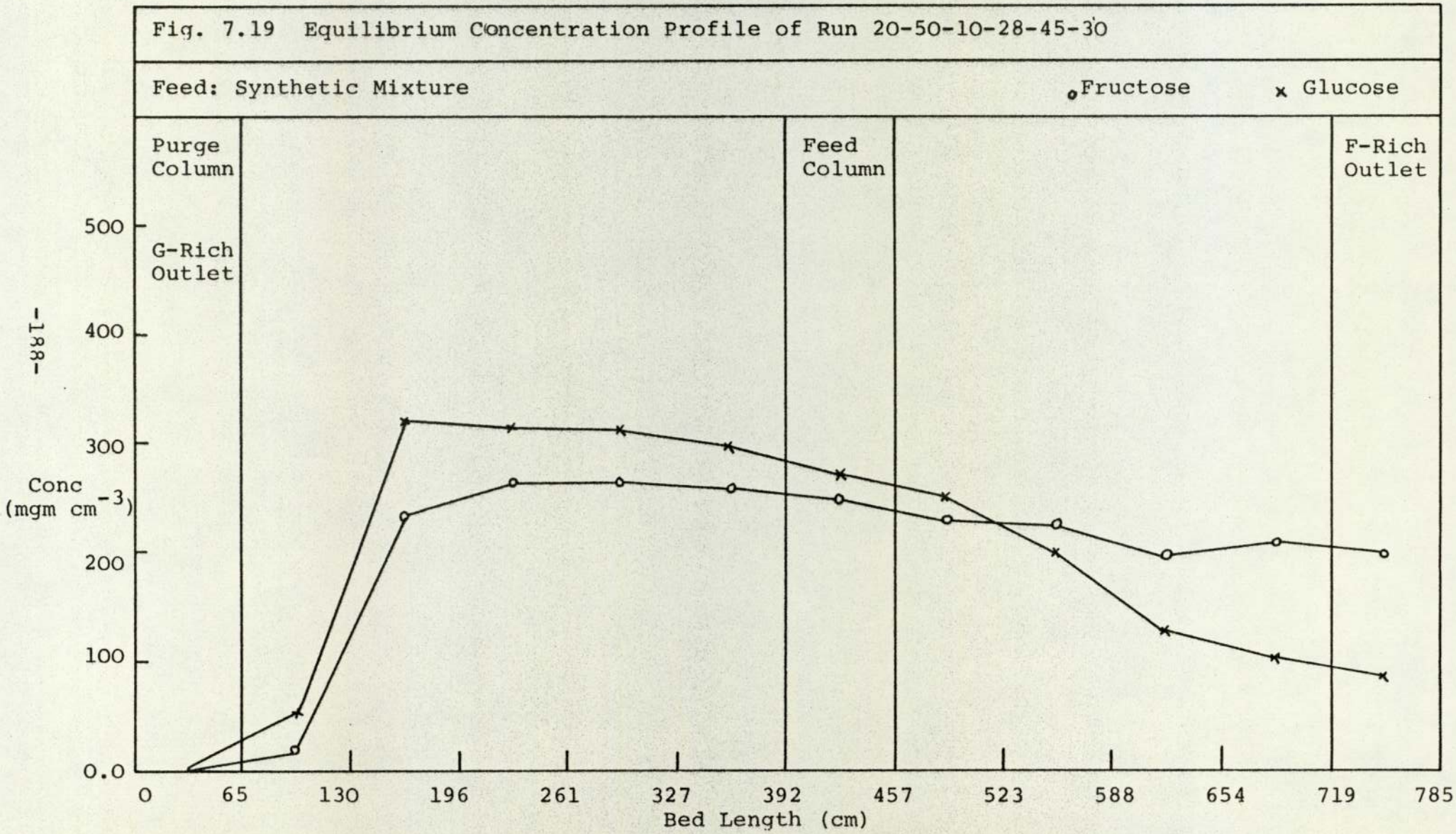
Fig. 7.19 Equilibrium Concentration Profile of Run 20-50-10-28-45-30
Feed: Synthetic Mixture
Fructose
Glucose
Purge Column
G-Rich Outlet
Feed Column
F-Rich Outlet
500
400
300
200
100
0.0
Conc (mgm cm-3)
0
65
130
196
261
327
392
457
523
588
654
719
785
Bed Length (cm)

was not effectively retarded and therefore it contaminated the fructose product. When a dilute sodium bisulphite solution was eluted through the unit, the separation capacity of the unit was restored to its initial value. This is shown by Fig. 7.20 where the glucose concentration profile is constructed for run 14-20-7-30-60-30 before and after addition of sodium bisulphite solution.

The process of regeneration of the resin was then carried out after each four runs as follows.

4% w/v sodium bisulphite solution was pumped to the unit at a rate of 50 $cm^3 min^{-1}$ for 1.5 hr. Then the pump was switched off for about an hour to allow for the exchange reaction between the resin and the bisulphite ions. The system was then washed with deionised water.

7.5 COMPARISON BETWEEN THE PERFORMANCES OF ANION AND CATION EXCHANGE RESINS

Unfortunately the results of the experimental work on the SCCR4 and SCCR7 units were unsuitable to give a fair quantitative comparison between the performances of the cation and anion exchange resins. This is because the products of the SCCR4 were substantially contaminated by the hold-up liquid. A run carried out on the SCCR6 (see Table 1.0) by Thawait (95) and run 8-40-8.5-28-60-30 which was carried out on the SCCR7, were taken as a basis for comparison. These two runs were not performed at the best operating

Fig. 7.20 Equilibrium Concentration Profile of Glucose Before and After Regeneration

Feed: Synthetic Feed (Run 14-20-7-30-60-30)

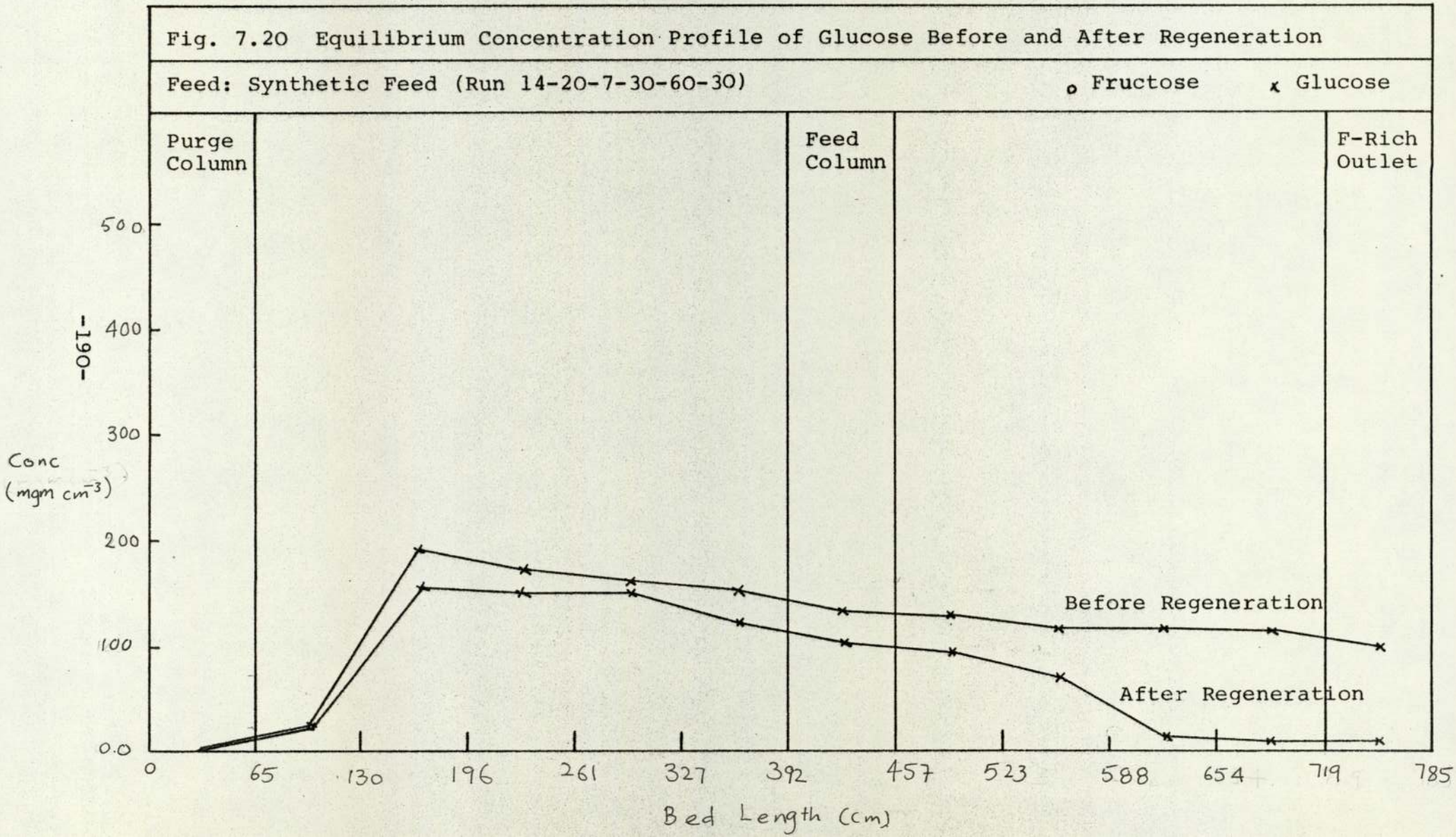

conditions of either of the units but they represented similar conditions of temperature, feed concentration and flow rate. The results of these runs are shown in Table 7.7. Considering the fructose product it is clear that the anion exchange resin in the SCCR7 gave better separation in terms of purity and concentration. On comparing the glucose products, the performance of the cation exchange resin in the SCCR6 was better in terms of both purity and concentration.

When comparing the concentration of the unretarded solutes, i.e. fructose for the SCCR7 unit and glucose for the SCCR6 unit it can be seen that the cation exchange resin gave better results. The separation factor, α of the cation resin was reported by Chuah (14) to be 3.0 while that of the anion resin was found to be 1.7. This means that the separation is easier by cation exchange resin in the calcium form.

A further qualitative comparison is that the cation exchange resin was used in the SCCR4 for more than three years and did not deteriorate or need regeneration. Although the anion exchange resin used in the SCCR7 did not deteriorate in 15 months, it needed frequent regenerations.

Finally it could be concluded that the anion exchange resin seems to qualify with the cation exchange resin especially if fructose is desired as a main product.

Table 7.7 Comparison Between the Performance of Anion and Cation Exchange Resins

Unit	Resin Form	Temp. (°C)	Flow Rates ($cm^3 min^{-1}$)			Feed Conc. (% w/v)	Fructose Product		Glucose Product	
			Feed	Eluent	Purge		Purity (%)	Conc. (% w/v)	Purity (%)	Conc. (% w/v)
SCCR7	Duolite A113 (HSO_3^{-1})	60	8.5	28	120	40	97	2.9	71	1.7
SCCR6*	Zerolit 225 (Ca^{2+})	60	35	105	500	40	84	1.4	100	4.0

* The SCCR6 unit has been described in Table (1.1)

CHAPTER 8

COMPUTER SIMULATION OF THE SCCR7 UNIT

8.1 Introduction

Many mathematical models have been constructed to describe batch chromatographic processes. These models are used to predict the elution curve and the concentration profiles (96,97,98). Most of these models involve statistical functions which are simplified and restricted to special cases. An attempt to develop a computer program which numerically simulates the actual processes taking place in chromatographic column, such as diffusion and adsorption, was tried by Jönsson (99). He simulated the process of linear chromatography with a simple computer program based on the plate theory.

Some models have also been formulated to describe continuous chromatographic processes. Sciance and Crosser (100) proposed a model for moving bed systems to relate both the degree of separation and operating conditions to the column length. The model proposes the following equations when a binary feed mixture is introduced into the mid-point of the column

$$\ln(U_Z)_A = \frac{Lk''_A}{2v} (K_A - \psi) \quad \ldots\ldots\ldots\ldots\ldots\ldots \quad (8.1)$$

and

$$\ln(1-(U_Z)_B) = \frac{-Lk''_B}{2v} (K_B - \psi) \quad \ldots\ldots\ldots\ldots\ldots \quad (8.2)$$

where

A refers to the non-retarded component

B refers to the retarded component

$(U_Z)_A$ = bottom / feed mass flow rate ratio of A

$(U_Z)_B$ = top/feed mass flow rate ratio of B

k'' = rate constant of desorption

v = average mobile phase velocity

ψ = mobile phase/stationary phase velocity ratio

L = required column length

The application of this model is very limited because it is difficult to determine experimentally the values of k''_A and k''_B and available data are scarce.

Another model for moving column gas-liquid systems was developed by Al Madfai (101) to predict the plate height

$$H = d_p \frac{2D_m}{v} + \frac{2\gamma_1\gamma_2}{(\gamma_1+\gamma_2)^2} \cdot \frac{(v+v_L)^2}{v\gamma_2 - v_L\gamma_1} \quad \text{..... (8.3)}$$

where

H = plate height

d_p = average particle diameter

D_m = mobile phase diffusivity

v = mobile phase velocity

v_L = stationary phase velocity

γ_1 = rate of transfer of molecules from gas to liquid

γ_2 = rate of transfer of molecules from liquid to gas

8.2 MODELS BASED ON THE TRANSFER UNIT CONCEPT

Barker and Lloyd (102) employed the transfer unit concept in their treatment of counter-current gas/liquid systems and derived the following relationships:

$$(N_G)_R = \frac{1}{V_G/(K_o V_L - 1)} \ln \left[\frac{E_1/K_o V_L - C_1(V_G/K_o V_L - 1)}{E_1/K_o V_L - C_2(V_G/K_o V_L - 1)} \right] \quad \text{...(8.4)}$$

and

$$(N_G)_S = \frac{1}{(1 - V_G/K_o V_L)} \ln \left[\frac{E_2/K_o V_L - C_1(1 - V_G/K_o V_L)}{E_2/K_o V_L - C_2(1 - V_G/K_o V_L)} \right] \quad \text{...(8.5)}$$

where

$(N_G)_R, (NG)_S$ = the number of overall gas phase transfer units in rectifying and stripping sections respectively

E_1 and E_2 = the mass flow rates of solute leaving in products 1 and 2 respectively

C_1 and C_2 = gas phase solute concentrations at points 1 and 2 in the column

V_G and V_L = gas and liquid volumetric flow rates

K_o = the partition coefficient

8.3 SIMULATION OF THE SCCR7 UNIT

Ching (12) developed a model which attempted to describe the SCCR4 mode of operation. The model was an adaptation of the work of Sunal (103) and Deeble (104). The concept used was that of the equilibrium stage or plate. The separating length of the unit was considered to consist of a number of theoretical

plates, each containing a volume of mobile and a volume of stationary phase. Considering a stream of the mobile phase of volumetric flow rate Q, with initial concentration C_{n-1} then a material balance over the plate will give

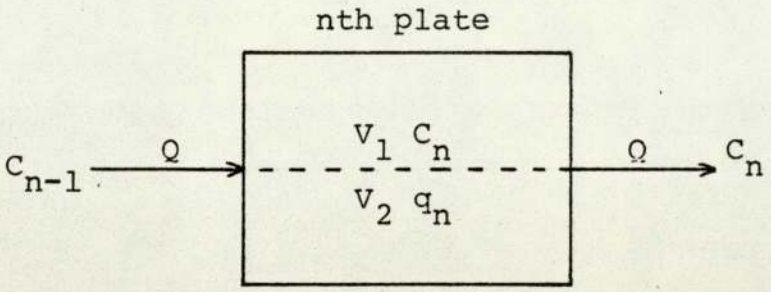

$$QC_{n-1} = QC_n + V_1\frac{dC_n}{dt} + V_2\frac{dq_n}{dt} \quad \ldots\ldots\ldots\ldots \quad (8.6)$$

where

C = solute concentration in the mobile phase

q = solute concentration in the stationary phase

V_1 = volume of the mobile phase in the plate

V_2 = volume of the stationary phase in the plate

Since the equilibrium distribution coefficient, K_d, is defined by

$$K_d = \frac{q_n}{C_n}$$

Then equation 8.6 can be rearranged to give

$$QC_{n-1} = QC_n + (V_1+V_2K_d)\frac{dC_n}{dt} \quad \ldots\ldots\ldots\ldots\ldots \quad (8.7)$$

If the time increment Δt is sufficiently small so that C_{n-1} can be considered constant, then integrating equation (8.7) yields

$$C_n = C_{n-1}\left(1-\exp\left(\frac{-Q\Delta t}{V_1+V_2K_d}\right)\right) + C_n^o \exp\left(\frac{-Q\Delta t}{V_1+V_2K_d}\right) \quad \ldots \quad (8.8)$$

where C_n^o is the initial concentration of the solute in the plate.

The first term on the right hand side of equation (8.8) represents the contribution from the (n-1)th plate and the second term represents the material already present in the nth plate.

A similar treatment for a mass balance over the feed plate will result in

$$C_n = \frac{QC_{n-1}+FC_f}{Q+F}\left(1-\exp\left(\frac{-Q\Delta t}{V_1+V_2K_d}\right)\right) + C_n^o \exp\left(\frac{-Q\Delta t}{V_1+V_2K}\right) \quad \ldots \quad (8.9)$$

where F and C_f are the feed volumetric flow rate and concentration.

This model predicts the concentration of one solute in the mobile phase leaving the plate. The simulation is repeated for every theoretical plate over a small time increment Δt. When the number of time increments simulated is equal to the length of the switch period, the sequencing action of the stationary phase is imposed by stepping the accumulated concentrations obtained backwards by one column and continuing the simulation.

The model calculates the concentration profile of only one solute at a time and the concentration profile of the other solute can be obtained by duplication of the calculations at each plate. It is also assumed that there is no interaction between the solutes present in the system and the value of

K_d is taken as constant irrespective of the concentration.

The original model used by Ching (12) to simulate the SCCR4 unit was modified by Chuah (14). The important improvements are summarised below.

Ching considered that the glucose was not retained by the resin and therefore he equated the distribution coefficient K_d^G for glucose equal to zero. However Chuah (14) and Gould (15) suggested that K_d^G had a finite value. The analytical work in Chapter 5 supported the suggestion that glucose was actually retained by the resin due to the g.p.c. mechanism and therefore a finite value was assigned for K_d^G.

Another modification was that the hold-up liquid volume has a determinate effect on the concentration profile especially on the post feed section of the SCCR4 unit. This effect was substantial for fructose because it was the more strongly adsorbed solute. A term H/V_m was added to equation 8.8 to account for this:

$$C_n = C_{n-1}\{1-\exp(\frac{-Q\Delta t}{V_1+V_2K_d})\} + C^o_{n-m} \cdot \exp(\frac{-Q\Delta t}{V_1+V_2K_d}) \cdot H/V_m \quad \text{..... (8.10)}$$

where

n = total number of plates in the system

m = number of plates in the prefeed section

H = volume of the hold-up liquid

V_m= total volume of the mobile phase

8.4 ADAPTATION AND IMPROVEMENTS OF THE MODEL FOR THE SCCR7 UNIT

The program modified by Chuah was used to simulate some of the runs carried out with the SCCR4 unit. The simulated concentration profiles were in good agreement with the experimental concentration profiles. Before using the model to simulate the SCCR7 unit, some modifications were made to adapt the model to the nature of the SCCR7 unit because of the following:

The hold-up volume associated with the SCCR7 unit was very small and therefore it was considered unnecessary to add the H/V_m term. This restored the model to equation (8.8).

In the case of the SCCR7 unit the more strongly adsorbed solute was glucose. Therefore the program was adapted to account for this by switching the values of K_d in the calculation equations. Also new values for the stationary and mobile volumes of each plates were inserted to cope with the SCCR7 unit.

From the initial applications of the program to simulate the SCCR7 unit it was noticed that the concentration profiles of glucose in the pre-feed section and those of fructose in the post-feed section were in good agreement with those obtained experimentally. However the simulated concentration profiles of fructose in the pre-feed section were found to be at a lower concentration level than those obtained experimentally. This means that practically the resin

retained more fructose than predicted by the model as shown in Figs. 8.2 and 8.3. The reason for this was believed to be because of the values of K_d used for the simulation were obtained at very low concentrations.

In order to rectify this, the simulation program was further improved to calculate the concentration profiles for each solute with two different values of K_d. One value was used for the pre-feed section and the other for the post-feed section.

A flow sheet of the program is shown in Fig. 8.1 and a listing of the program with a sample of the results printout are included in Appendix 1. The program was used to simulate various runs carried out with the SCCR7 unit. Input data for the distribution coefficients, K_d for glucose and fructose were initially taken as an average of the values obtained for characterisation of the SCCR7 columns. Then arbitrary values were chosen for the best agreement with the experimental profiles.

8.4.1 Results and Discussion of the Simulation of the SCCR7 Unit

Figs. 8.2 and 8.3 are two examples of the simulated concentration profiles together with the experimental profiles for runs 13-50-7-30-60-30 and 16-70-7-30-60-30. It can be seen that the concentration profiles of glucose obtained by the simulation are in good agreement with those obtained experimentally. When comparing the concentration profiles of fructose obtained by the simulation to those obtained experimentally

Fig. 8.1 Computer Flow Chart for the Simulation Model

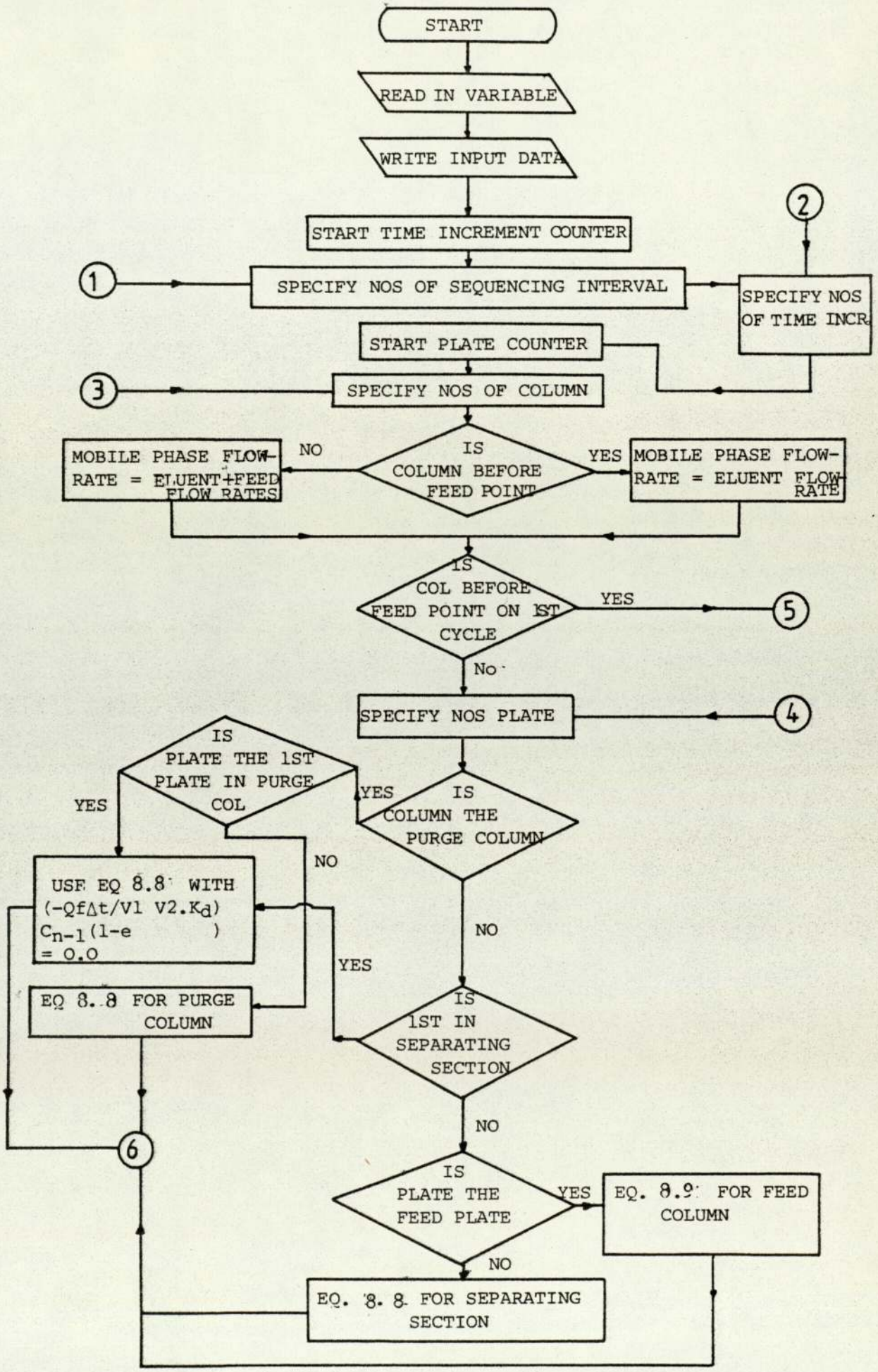

Fig. 8.1 continued .....

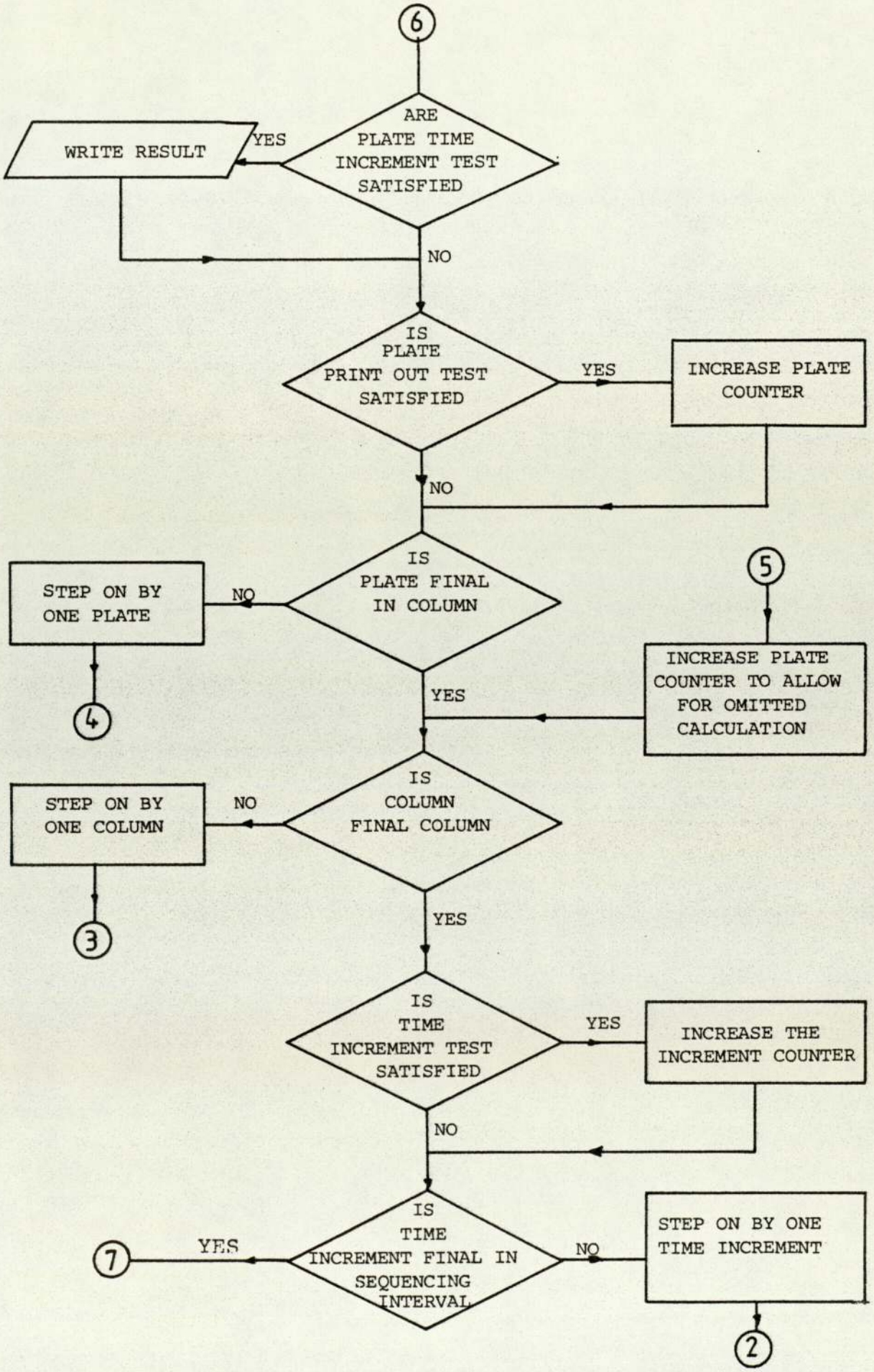

Fig. 8.1 continued .....

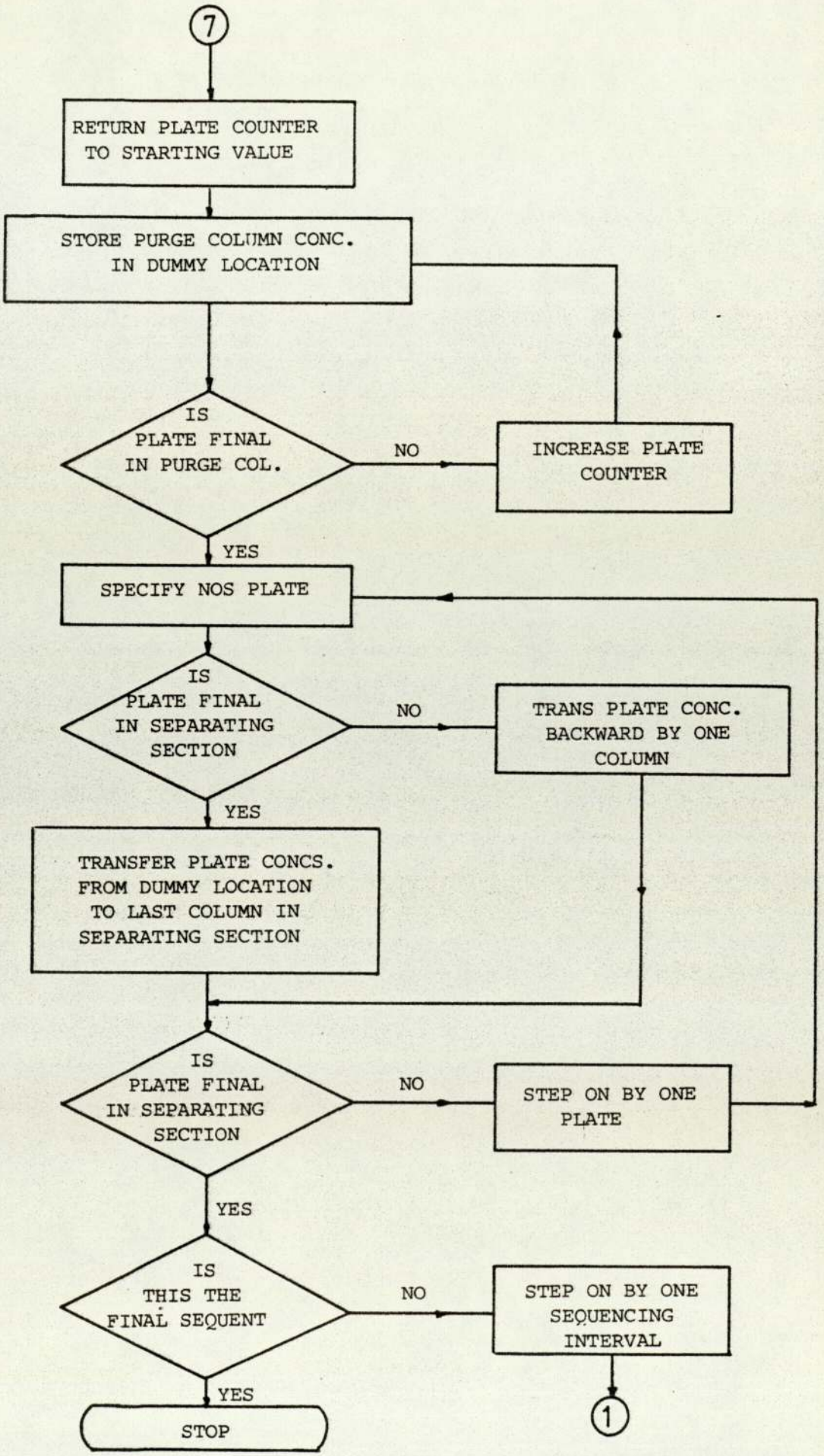

Fig. 8.2 Experimental and Simulation Profiles of Run 13-50-7-30-60-30

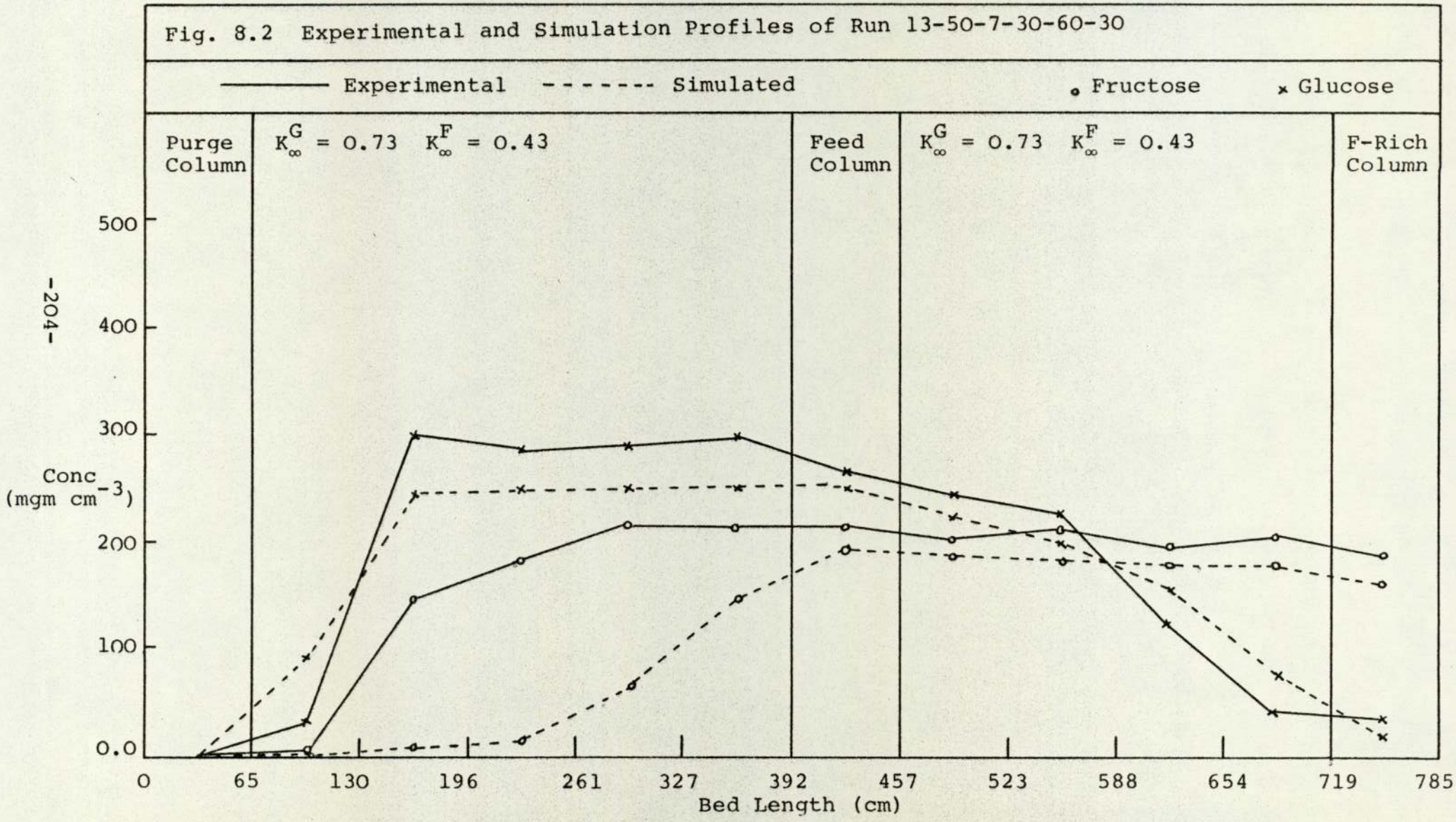

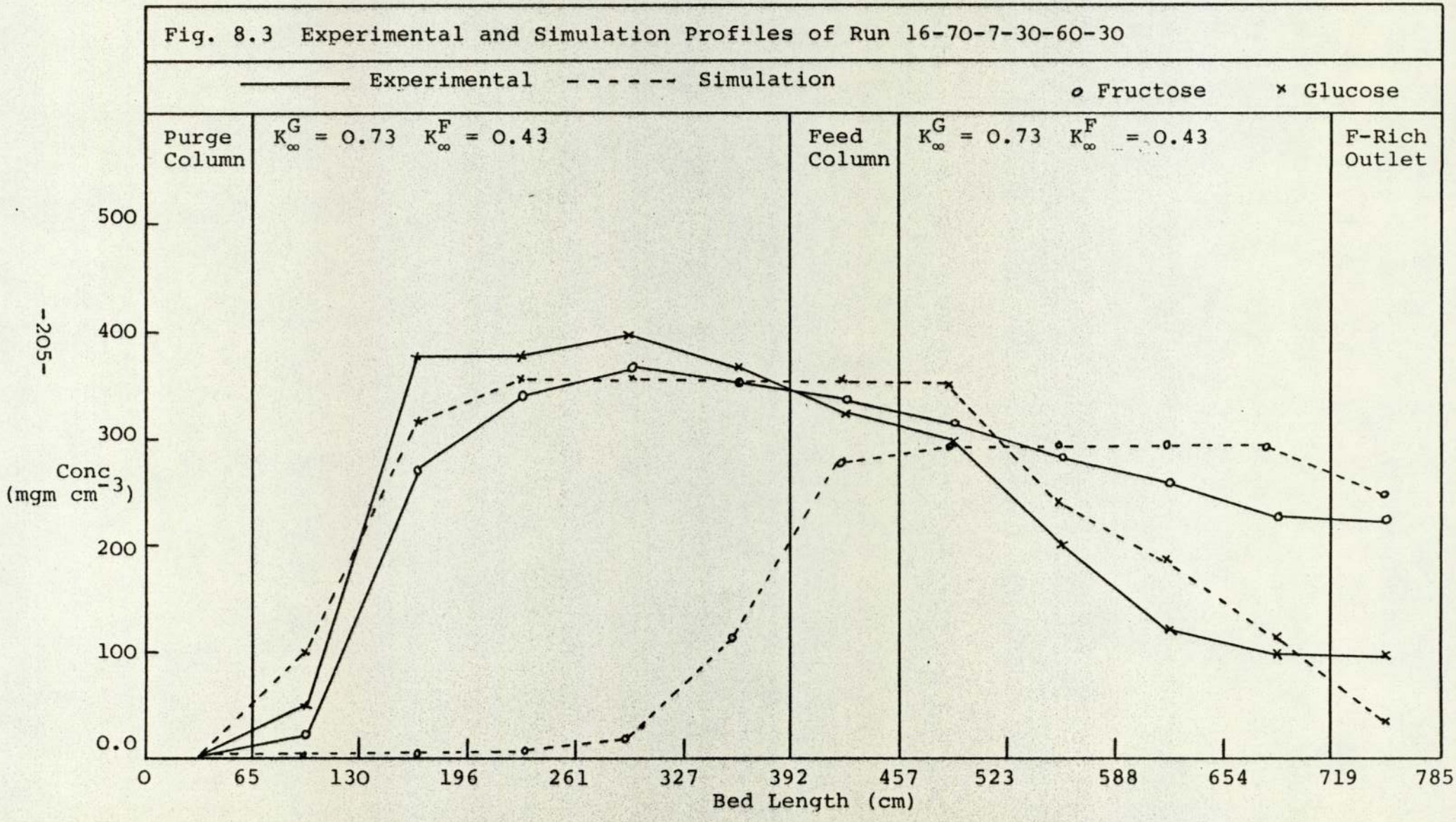
Fig. 8.3 Experimental and Simulation Profiles of Run 16-70-7-30-60-30
Experimental
Simulation
o Fructose
× Glucose
Purge Column
K_∞^G = 0.73 K_∞^F = 0.43
Feed Column
K_∞^G = 0.73 K_∞^F = 0.43
F-Rich Outlet
Conc (mgm cm^{-3})
0.0
100
200
300
400
500
0
65
130
196
261
327
392
457
523
588
654
719
785
Bed Length (cm)

there are some differences which are apparent especially in the pre-feed section. From the experimental results it was noticed that the level of fructose in the pre-feed section was higher than that predicted by the simulation. This indicated that the actual K_d^F values were greater than the values input to the model.

The simulation model calculated the concentrations of the solute according to the values of the distribution coefficient without considering the interaction of the other solute. In practice the solute was not present alone and the concentration was not constant. For this reason and when the concentration profiles were calculated with different values of K_d for the same solute in the pre-feed and post-feed sections the simulation results were in good agreement with the experimental ones. This is shown in Figs.(8.4-8.7) for runs with different concentrations and Figs. 8.8 and and 8.9 for runs with different flow rates.

It can be seen from Figs. 8.4 and 8.7 that the value for K_d^F to give the best agreement between the simulated and experimental run with 20% feed concentration is 0.46 while that for 70% feed concentration is 0.59. This indicates that the value of K_d increases with the increase of concentration. The increase of the K_d values with increase of concentrations for a cation exchange resin was proved by the analytical work of Thawait (95).

It was also found that only six cycles were necessary to achieve an equilibrium state with the

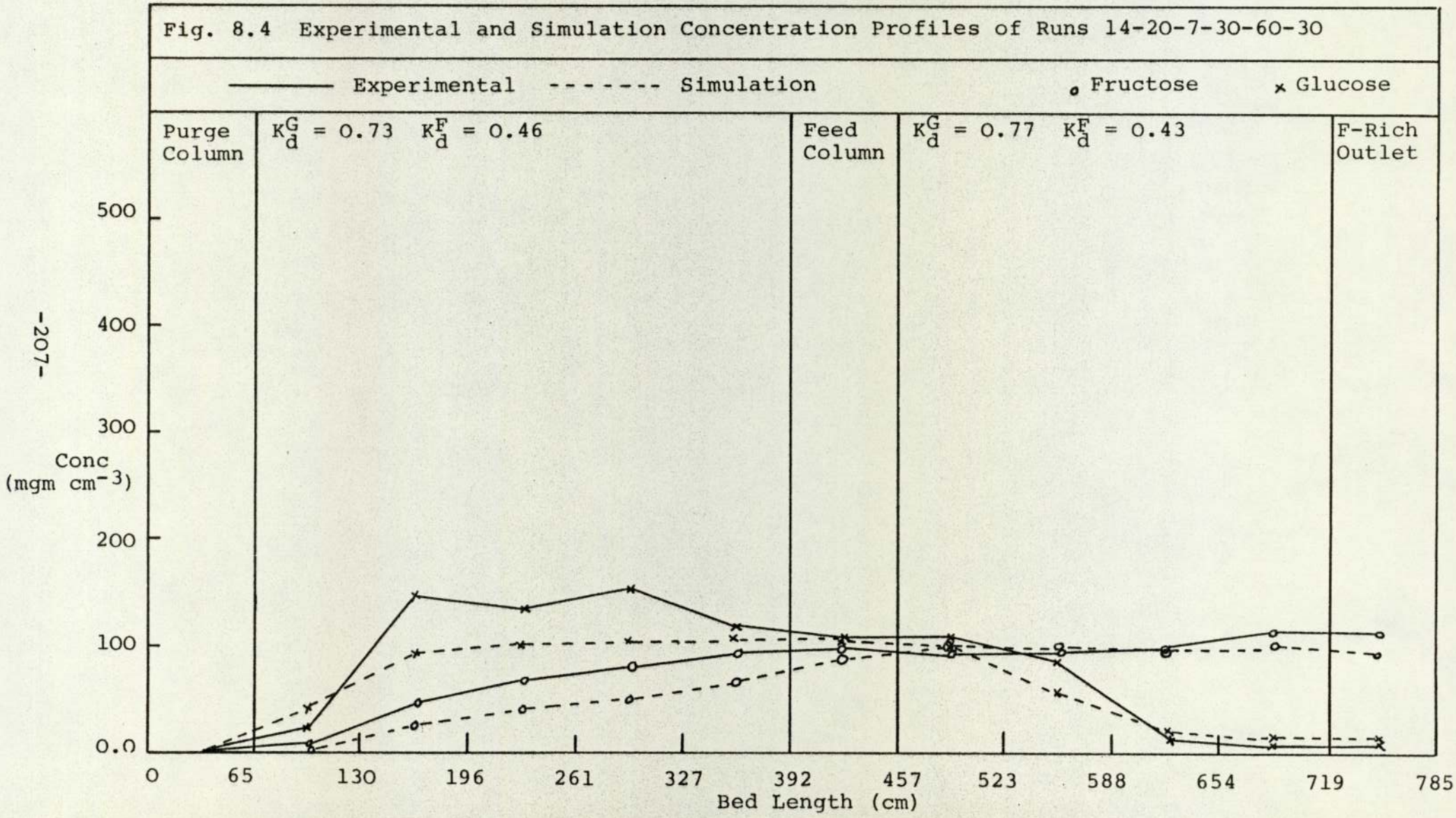
Fig. 8.4 Experimental and Simulation Concentration Profiles of Runs 14-20-7-30-60-30
Experimental
Simulation
Fructose
Glucose
Purge Column
$K_d^G = 0.73$ $K_d^F = 0.46$
Feed Column
$K_d^G = 0.77$ $K_d^F = 0.43$
F-Rich Outlet
Conc (mgm cm^{-3})
500
400
300
200
100
0.0
0
65
130
196
261
327
392
457
523
588
654
719
785
Bed Length (cm)

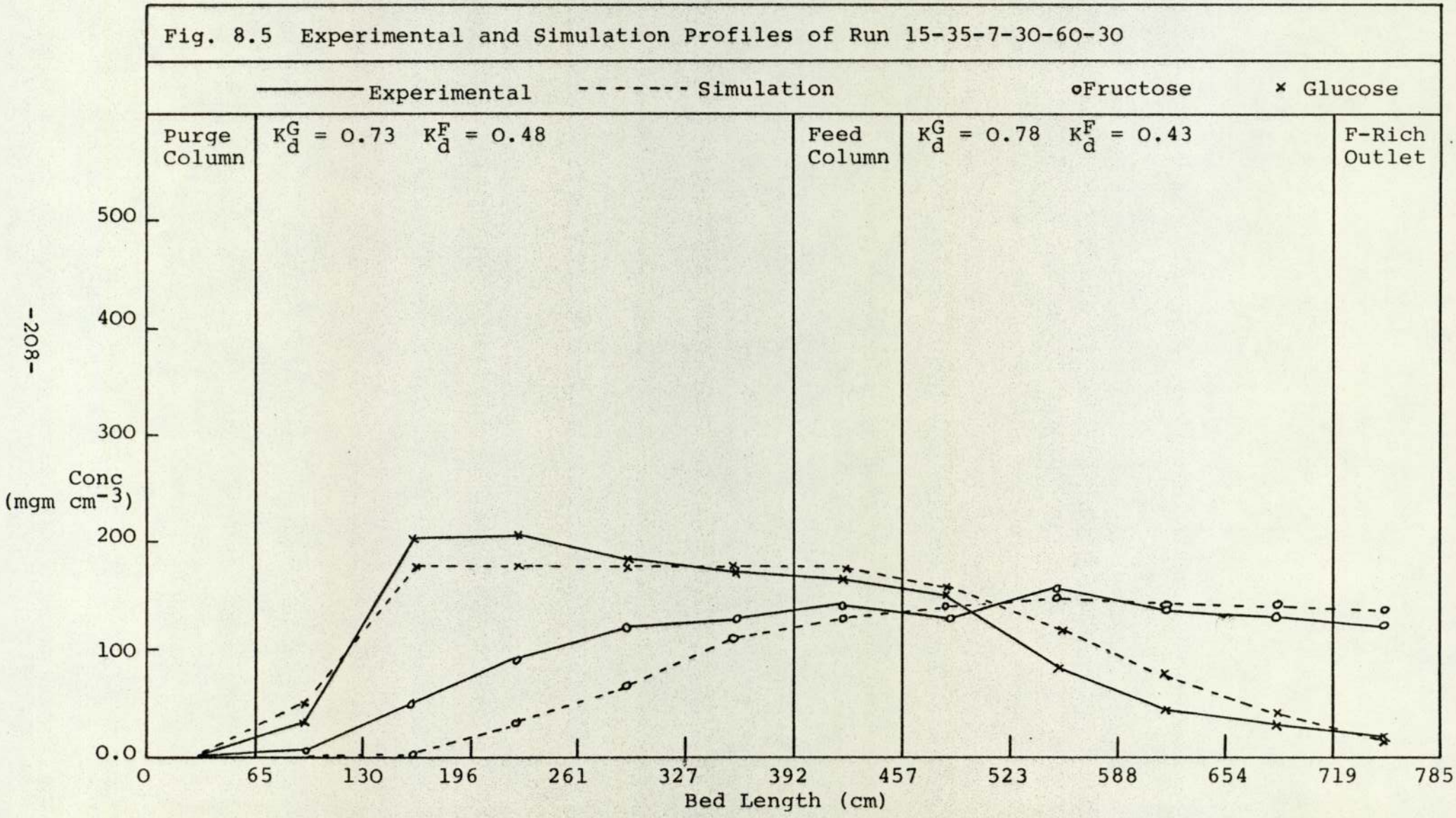

Fig. 8.5 Experimental and Simulation Profiles of Run 15-35-7-30-60-30

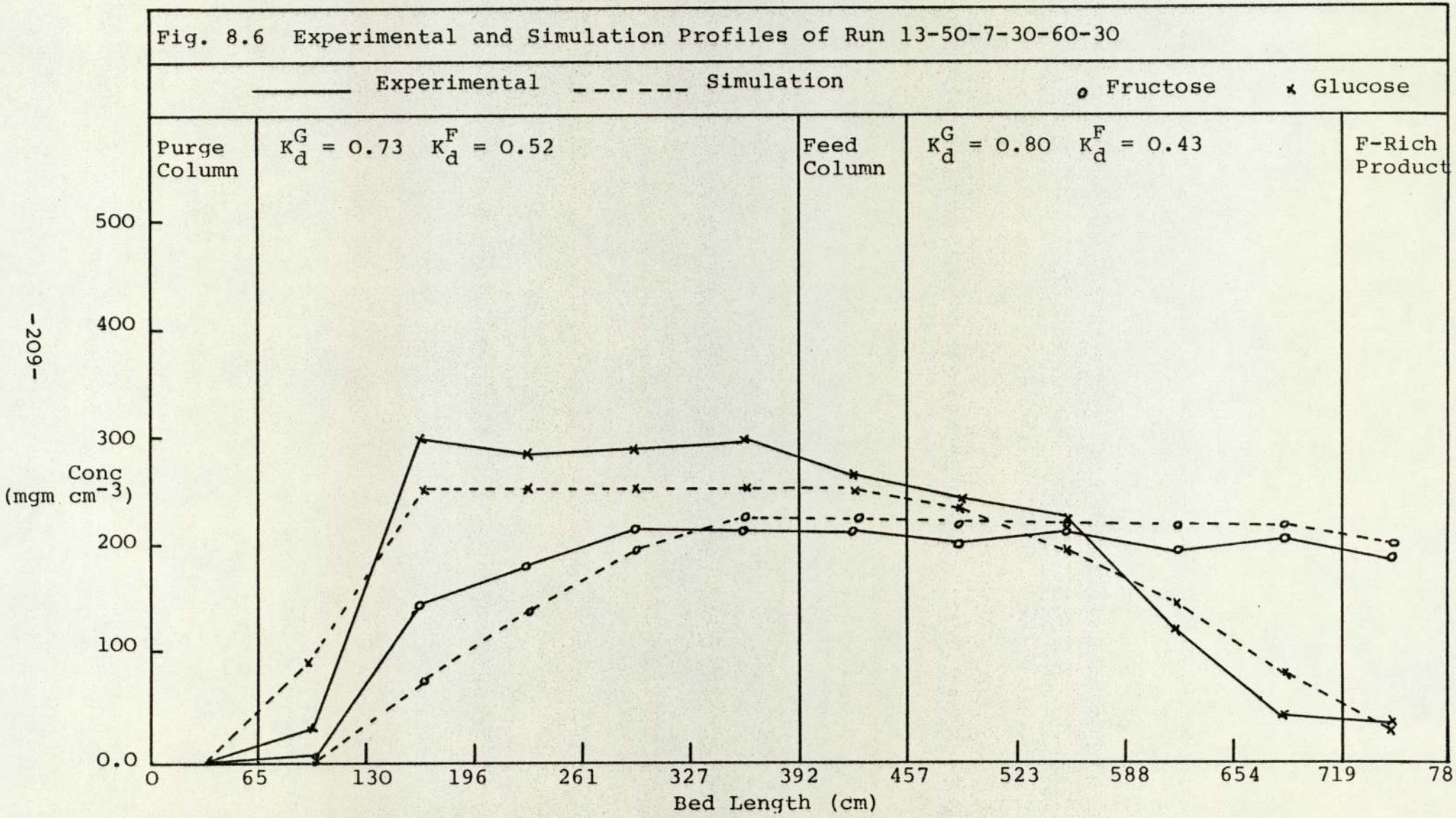
Fig. 8.6 Experimental and Simulation Profiles of Run 13-50-7-30-60-30
Experimental
Simulation
Fructose
Glucose
Purge Column
$K_d^G = 0.73$ $K_d^F = 0.52$
Feed Column
$K_d^G = 0.80$ $K_d^F = 0.43$
F-Rich Product
Conc (mgm cm^{-3})
0.0
100
200
300
400
500
0
65
130
196
261
327
392
457
523
588
654
719
785
Bed Length (cm)

Fig. 8.7 Experimental and Simulation Profiles of Run 16-70-7-30-60-30

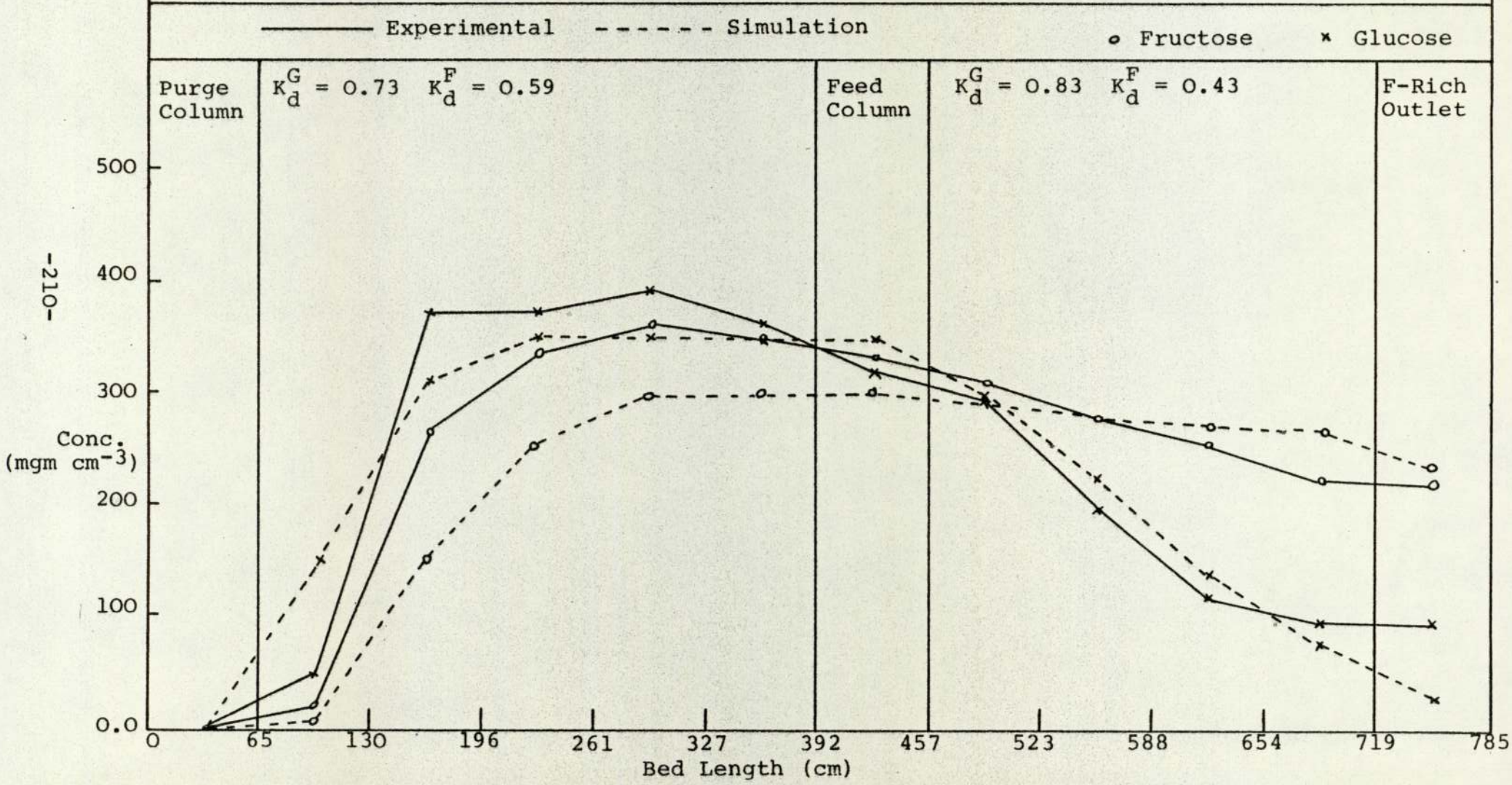

Fig. 8.8 Experimental and Simulation Profiles of Run 10-50-8.5-28-60-30

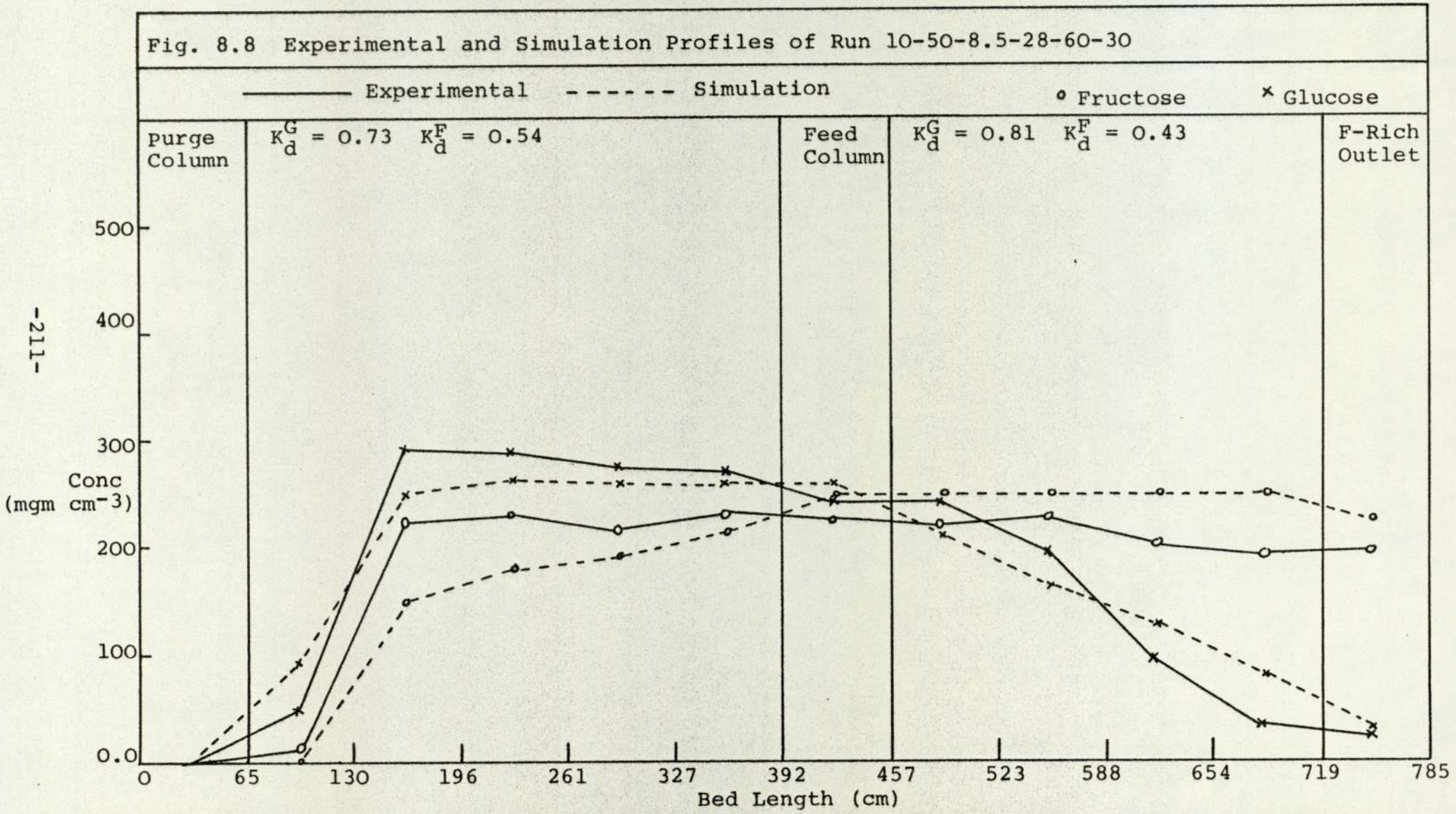

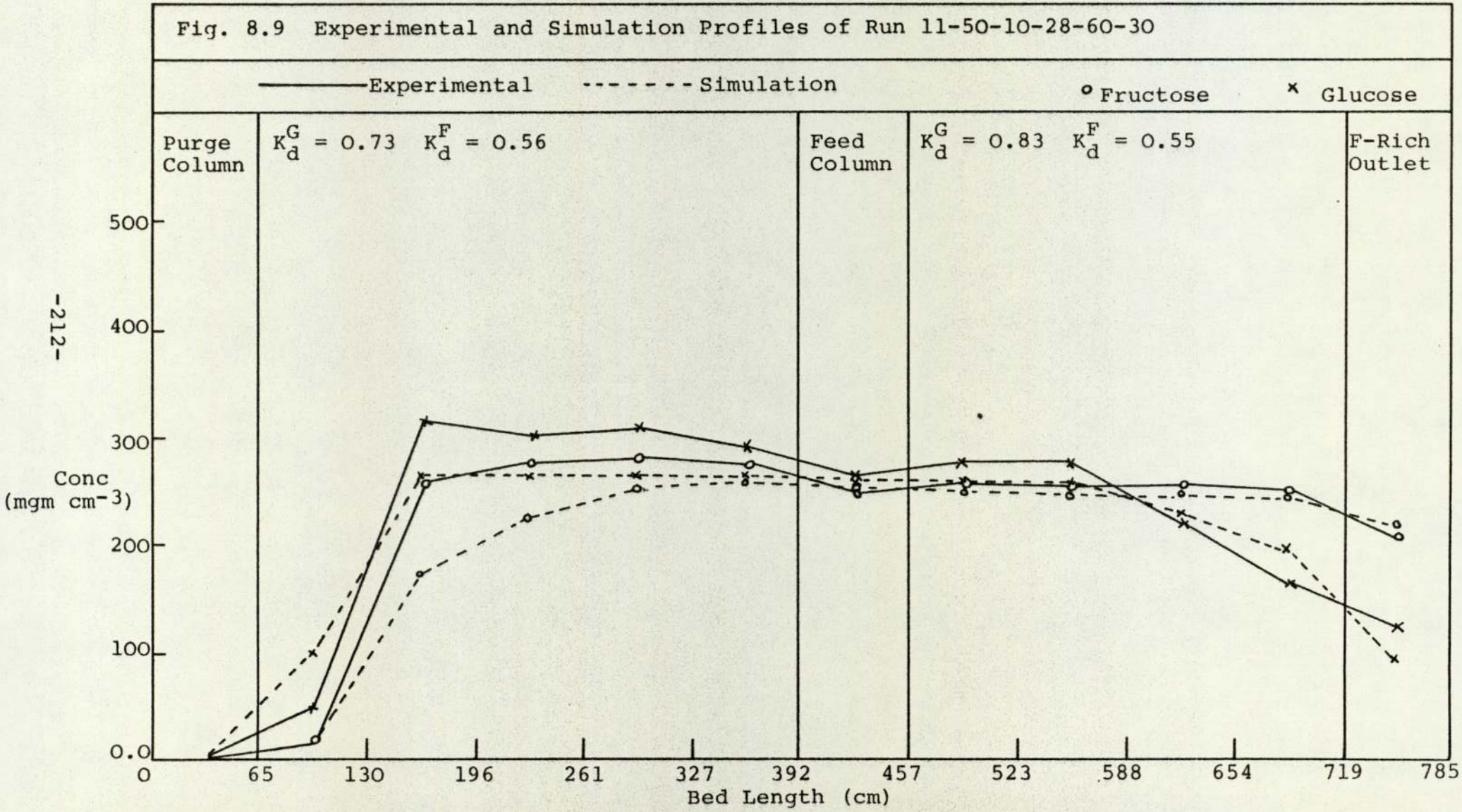

Fig. 8.9 Experimental and Simulation Profiles of Run 11-50-10-28-60-30

simulation. However experimentally eight cycles were necessary before reaching an equilibrium state. This may be because the model assumes instantaneous equilibrium conditions in each plate.

It was noticed that this simulation model required a long computer time and a large memory core, which was not available in the ICL 1904S or the HARRIS computers at the University of Aston. Therefore the program was run on the North-West Regional Computer CDCI 7600 at Manchester University which was line linked to the University of Aston.

Finally it is concluded that the model gave a better understanding of the performance of the SCCR7. It identified the effect of concentration and the interaction between the solutes on K_d. The model can be used to investigate other parameter effects. For example the effect of changing the feed position on the purity and the concentration of the products can be predicted by the model.

CHAPTER 9

CONCLUSIONS AND RECOMMENDATIONS

9.1 CONCLUSIONS

The SCCR7 unit which was used for part of this research is believed to be the largest scale unit of its kind for the separation of sugars with an anion exchange resin.

Other conclusions which are drawn from the various parts of this work are summarised in the following sections.

9.1.1 Performances of the Packing Materials on an Analytical Size Column

A comparison of the performance of different packing materials of cationic and anionic exchange resins together with the zeolites in different ionic forms were investigated to separate fructose and glucose mixtures. The results of the separation obtained at different operating temperatures and flow rates showed that:

1. The cation exchange resins perform best at ambient temperatures while anion exchange resins perform best at temperatures higher than 40^{o}C. The separation factor for the cation resin (Zerolit 225) at 20^{o}C was 2.6 while that for the anion resin (Duolite A113) at 60^{o}C was 1.8. This indicates that the separation is easier with the cation exchange resin.

2. Anion exchange resins in the (HSO_3^-) form ensured higher fructose solid concentrations than cation exchange resins.

3. While cation exchange resins showed no sign of deterioration, anion exchange resins deteriorated after only a few hours of use.

4. The different types of zeolites used in different forms gave no satisfactory separations of sugars. The only successful separation was achieved when zeolite 13X was used in the barium (Ba^{2+}) form. This result was not promising because barium is toxic.

9.1.2 Work with the SCCR4 Unit

The experimental work with the SCCR4 unit which had 25.4 mm internal diameter columns and was packed with a cation exchange resin in the Ca^{2+} form proved that:

1. The unit was capable of separating sucrose based feed mixtures as well as synthetic mixtures of fructose and glucose. Fructose and glucose products with purities of up to 93% were achieved when separating a 50% w/v equimolar synthetic feed mixture. However less pure fructose products of 75% purity were obtained when separating sucrose based feed mixtures. The contamination of the fructose products in the case of inverted sucrose feedstocks was demonstrated by a substantial shift of the cross-over point of the concentration profiles of glucose and fructose towards the fructose rich product outlet.

2. Due to the capacity of the SCCR4 unit the maximum possible sugar solids throughput was 0.06 kg hr^{-1}.

3. It was estimated that the resin had been in use for over 2000 hours, some of it using a carbohydrate effluent containing various ions. No discernable deterioration was observed over this period.

9.1.3 Work with the SCCR7 Unit

The SCCR7 unit which had 54 mm internal diameter columns and was packed with an anion exchange resin in the (HSO_3^-) form, was also used for the separation of sugars. The benefits of the SCCR7 unit over the SCCR4 unit were:

1. The sugar solids throughputs were increased from 0.06 kg hr^{-1} with the SCCR4 unit to 0.22 kg hr^{-1} with the SCCR7 unit.

2. The achievements of products with purities of up to 99% was possible with the SCCR7 unit. This is mainly because of the reduced intercolumn hold-up which was 2.7% of the total volume of the liquids in the SCCR7 unit.

3. The solids concentration of the fructose product was substantially increased from 4% w/v which was the maximum possible with the SCCR4 unit, to 12% w/v. This is because the anion exchange resin did not retard the fructose and hence emerged with the eluent stream rather than the purge stream.

4. The ability to operate the unit at 60°C decreased the viscosities of the sugars and thereby

reduced the pressure drops and pumping costs. Also working at this temperature contributed in inhibiting bacterial growth.

5. The quality of the products was similar whether the feedstock was a synthetic mixture of fructose and glucose or inverted sucrose. There was no shift of the cross-over point of the concentration profiles such as that with the SCCR4 unit containing the cation exchanger. Thus the SCCR7 unit can handle a variety of feed stocks.

6. With simple precautions like the use of pure water and addition of a small quantity of sodium bisulphite, the useful life of the anion resin was prolonged to more than 15 months. However the resin needed frequent regenerations with dilute sodium bisulphite solutions.

9.1.4 The Mathematical Model

The results of the computer model which was based on the equilibrium stage concept showed an acceptable degree of agreement with the experimental results. The model was capable of predicting the behaviour of the unit at different flow rates and concentrations.

The model also showed that the dependency of the distribution coefficient K_d needs to be quantified.

9.2 RECOMMENDATIONS FOR FURTHER WORK

The following suggestions are recommended for further work to complete various parts of this research.

9.2.1 The Analytical Work

The investigation of the use of inorganic ion-exchangers, namely the zeolites, was not completed. These packing materials offer good stability even under the severe operating conditions induced by contaminants, high temperatures and wide pH ranges. It is therefore recommended that the zeolites be coated with an organic polymer to stop the dissolution of silica and that the zeolites be used in the Ca^{2+} form for the separation of sugars.

9.2.2 Recommendations for Work with SCCR7 Unit

It is recommended that the effect of changing the feed position of the feed entry be investigated. In the present work the feed entry was the seventh column, i.e. mid-way along the separation section. It was noticed from the concentration profiles that the leading edge of the fructose spread over the pre-feed section. By shifting the feed column towards the fructose rich product outlet, it might be possible to increase the purity of glucose and the recovery of fructose.

The recycle of part of the fructose product as eluent provides another recommendation for increasing the solids concentration of the fructose product.

It was proved that the switch period of 30 minutes was more than enough to elute all the products. It is therefore recommended that the effect of reducing the switch period on the equilibrium of the system and the quality of the products be investigated. This

might reduce the necessary duration of operation. Otherwise the time saved could be used to regenerate the resin without interrupting the operation of the unit. This could be done after purging the column. It involves the passage of a dilute sodium bisulphite solution through the purge column, followed by deionized water to wash off the excess bisulphite salt. One pump head and two pneumatic valves are all that is needed to do this task.

9.2.3 Carbohydrate Feedstocks

In pursuit of less expensive sources of fructose and glucose it is suggested that the separation of HFCS be attempted. It is also recommended that molasses, a cheap by-product of sugar refineries, be used as feedstock. A pre-feed column containing a cation exchange resin mostly in the H^+ form with about 25% of the resin in the Ca^{2+} form would be sufficient to purify and desugarise the molasses and hydrolyse the sucrose.

9.2.4 The Mathematical Model

The simulation program needs further improvements. The model did not take into account the variation of the distribution coefficient, K_d with respect to the concentration of the solute. It also calculated the concentration of each solute separately, i.e. without considering the interaction of the other solute. Therefore it is recommended that improvements to model should be made to take into account these two effects.

APPENDIX 1

COMPUTER PROGRAM LISTING AND RESULTS PRINTOUT

```
      PROGRAM PROFILE(INPUT,OUTPUT,TAPE1=INPUT,TAPE2=OUTPU
     DIMENSION G(1500),F(1500),AG(150),AF(150),KD1(3),KD2(
    1KD12(3),KD22(3)
      REAL KD1,KD2,KD12,KD22
      READ(1,31)V1,V2
      READ(1,32)CFLOW,FFLOW,SFLOW
      READ(1,111)GFEED,FFEED
      READ(1,4)NFEED,NNFED,KTOTAL,KKINK,KKTYPE,NNTYPE,NNBE
      READ(1,5) (KD1(I),KD2(I),KD12(I),KD22(I),I=1,3)
      READ(1,33) DT
      DO 711 I=1,3
      DO 1 NN=1,1500
      G(NN)=0.0
      F(NN)=0.0
    1 CONTINUE
      DO 2 NN=1,150
      AG(NN)=0.0
      AF(NN)=0.0
    2 CONTINUE
      WRITE(2,210)CFLOW
      WRITE(2,211)SFLOW
      WRITE(2,212)FFLOW
      WRITE(2,213)V1
      WRITE(2,214)V2
      WRITE(2,215) NFEED
      WRITE(2,216) NNFED
      WRITE(2,217) KTOTAL
      WRITE(2,218) KKINK
      WRITE(2,219) KKTYPE
      WRITE(2,220) NNTYPE
      WRITE(2,221)GFEED
      WRITE(2,222)FFEED
      WRITE(2,223) DT
      WRITE(2,225) KD1(I),KD2(I)
      WRITE(2,226) KD12(I),KD22(I)
      NNTOT=NNBED*12
      NNNINE=NNBED*11+1
      NNFEED=(NFEED-1)*NNBED+1
      WRITE(2,12)
      KKSUM=1
      DO 100 K=1,KTOTAL
      ISTKK=KKINK*(K-1)+1
      LSTKK=KKINK*K
      DO 200 KK=ISTKK,LSTKK
      NNSUM=1
      DO 500 N=1,12
      IF(N.LE.6) GO TO 1700
      GO TO 1701
 1700 KD1(I)=KD1(I)
      KD2(I)=KD2(I)
 1701 IF(N.LE.6)CFLOWC=CFLOW
      IF(N.GE.7) GO TO 1702
      GO TO 1703
 1702 KD1(I)=KD12(I)
      KD2(I)=KD22(I)
 1703 IF(N.GE.7)CFLOWC=CFLOW+FFLOW
      IF (N.LE.(NFEED-K)) GO TO 500
```

```
      508   NNFST=NNBED*(N-1)+1
            NNLST=NNBED*N
   60       DO 400 NN=NNFST,NNLST
            IF(N.EQ.1) GO TO 80
            IF((N.EQ.2).AND.(NN.EQ.NNFST)) GO TO 40
            IF(NN.EQ.NNFEED) GO TO 50
            GO TO 60
   65    40   G(NN-1)=0.00
            F(NN-1)=0.00
            GO TO 70
         50   A=CFLOWC*DT
            IF(G(NN-1).LT.0.1E-10)G(NN-1)=0.0
   70       IF(F(NN-1).LT.0.1E-10)F(NN-1)=0.0
           RR=EXP(-A/(V1+V2*KD1(I)))
           SS=EXP(-A/(V1+V2*KD2(I)))
           G(NN)=(1-RR)*((CFLOW*G(NN-1)+FFLOW*GFEED)/
          1 CFLOWC)+RR*G(NN)
   75      F(NN)=(1.0-SS)*((CFLOW*F(NN-1)+FFLOW*FFEED)/
          1 CFLOWC)+SS*F(NN)
            GO TO 150
         60   IF(G(NN-1).LT.0.1E-10)G(NN-1)=0.0
            IF(F(NN-1).LT.0.1E-10)F(NN-1)=0.0
   80       70   A=CFLOWC*DT
           RR=EXP(-A/(V1+V2*KD1(I)))
           SS=EXP(-A/(V1+V2*KD2(I)))
      153   G(NN)=(1.0-RR)*(G(NN-1))+RR*G(NN)
            F(NN)=(1.0-SS)*(F(NN-1))+SS*F(NN)
   85    151   GO TO 150
         80   IF(NN.EQ.NNFST) GO TO 90
            IF(G(NN-1).LT.0.1E-10)G(NN-1)=0.0
            IF(F(NN-1).LT.0.1E-10)F(NN-1)=0.0
            GO TO 95
   90    90   G(NN-1)=0.0
            F(NN-1)=0.0
          95   A=SFLOW*DT
           RR=EXP(-A/(V1+V2*KD1(I)))
           SS=EXP(-A/(V1+V2*KD2(I)))
   95       G(NN)=(1.0-RR)*((G(NN-1))+RR*G(NN)
            F(NN)=(1.0-SS)*(F(NN-1))+SS*F(NN)                    ANI
         150   IF((NN.EQ.(NNTYPE*NNSUM)).AND.(KK.EQ.(KKTYPE*KKSUM))
          1 (K.EQ.KTOTAL)) GO TO 160
            GO TO 170
  100    160   WRITE(2,161)K,KK,N,NN,G(NN),F(NN)
         170   IF(NN.EQ.(NNTYPE*NNSUM))NNSUM=NNSUM+1
         400   CONTINUE
            GO TO 300
         500   NNSUM=NNSUM+NNBED/NNTYPE
  105    300   CONTINUE
            IF(KK.EQ.(KKTYPE*KKSUM)) GO TO 180
            GO TO 200
         180   KKSUM=KKSUM+1
         200   CONTINUE
  110       IF(K.EQ.KTOTAL) GO TO 131
            GO TO 132
      131   WRITE(2,190)
            WRITE(2,12)
      132   DO 1500 NN=1,NNBED
```

```
115                AC(NN)=G(NN)
                   AF(NN)=F(NN)
                1500 CONTINUE
                   DO 2000 NN=1,NNTOT
                   IF(NN.GE.NNNINE) GO TO 2010
120                NNADJ=NN+NNBED
                   G(NN)=G(NNADJ)
                   F(NN)=F(NNADJ)
                   GO TO 2000
                2010 NNADJ=NN+1-NNNINE
125                G(NN)=AG(NNADJ)
                   F(NN)=AF(NNADJ)
                2000 CONTINUE
                 100 CONTINUE
                 711 CONTINUE
130               31 FORMAT(2F10.5)
                  32 FORMAT(3F10.5)
                   4 FORMAT(7I4)
                   5 FORMAT(4F10.5)
                   6 FORMAT(2F10.5)
135             33   FORMAT(F10.5)
                210  FORMAT( 1H, 7HCFLOW= ,F5.3/)
                211  FORMAT( 1H, 7HGFLOW= ,F5.3/)
                212  FORMAT( 1H, 7HFFLOW= ,F5.3/)
                213  FORMAT( 1H, 4HV1= ,F8.5/)
140             214  FORMAT( 1H, 4HV2= ,F8.5/)
                215  FORMAT( 1H, 7HNFEED= ,I2/)
                216  FORMAT( 1H, 7HNNBED= ,I5/)
                217  FORMAT( 1H, 8HKTOTAL= ,I3/)
                218  FORMAT( 1H, 7HKKINK= ,I4/)
145             219  FORMAT( 1H, 8HKKTYPE= ,I3/)
                220  FORMAT( 1H, 8HNNTYPE= ,I3/)
                221  FORMAT( 1H, 7HGFEED= ,E13.6/)
                222  FORMAT( 1H, 7HFFEED= ,E13.6/)
                223  FORMAT( 1H, 4HDT= ,F10.5/)
150             225  FORMAT(1H,5HKD1= ,F10.5,5X,5HKD2= ,F10.5/)
                226  FORMAT(1H,6HKD12= ,F10.8,5X,6HKD22= ,F10.8/)
                227  FORMAT(1H,3HH= ,F10.5,5X,4HV0= ,F10.5/)
                 111 FORMAT(2F10.5)
                  12 FORMAT(1H ,22X,1HK,14X,2HKK,15X,1HN,14X,2HNN,5X,
155                1 14HGLUCOSE CONC. ,4X,15HFRUTOSE CONC.  )
                 181 FORMAT(1H0,21X,I2,13X,I5,12X,I2,12X,I4,6X,F12.10,5X,
                 190 FORMAT(1H1,23HNEXT SWITCHING INTERVAL)
                   STOP
                   END
```

SYMBOLIC REFERENCE MAP (R=1)

ENTRY POINTS
46 PROFILE

PROGRAM PROFILE 76/76 OPT=1 PMDMP FTN 4.8+538 10/03/83 15.56.

LOOPS	LABEL	INDEX	FROM-TO	LENGTH	PROPERTIES
201	200	KK	44 109	243B	EXT REFS NOT INNER
203	300	N	46 105	231B	EXT REFS NOT INNER
233	400	NN	60 132	172B	EXT REFS
455	1500	NN	114 117	4B	INSTACK
471	2000	NN	113 127	13B	OPT

STATISTICS
PROGRAM LENGTH 74728 3898
47000B SCM USED

CFLOW= .500

SFLOW= 7.000

FFLOW= .117

V1= 32.00000

V2= 28.00000

NFEED= 7

NNBED= 20

KTOTAL= 60

KKINK= 900

KKTYPE= 900

NNTYPE= 10

GFEED= .250000E+00

FFEED= .250000E+00

DT= 2.00000

KD1= .73000 KD2= .52000

KD12= .80000000 KD22= .43000000

K	KK	M	NN	GLUCOSE CONC.	FRUTOSE CONC
60	54000	1	10	0.0000000000	0.0000000000
60	54000	1	20	0.0000000000	0.0000000000
60	54000	2	30	.0060328121	.0000001967
60	54000	2	40	.1638301727	.0003563765
60	54000	3	50	.2382212113	.0002404386
60	54000	3	60	.2426342052	.0007837870
60	54000	4	70	.2435631273	.0021830855
60	54000	4	80	.2442454233	.0056065937
60	54000	5	90	.2448183417	.0134964231
60	54000	5	100	.2453089966	.0306894121

60	54000	6	110	.2457324083	.0663840962
60	54000	6	120	.2458727927	.1343155305
60	54000	7	130	.2449442969	.1971792716
60	54000	7	140	.2372622046	.2146093315
60	54000	8	150	.2181747879	.2173338896
60	54000	8	160	.1921453569	.2171585512
60	54000	9	170	.1614736397	.2170346952
60	54000	9	180	.1289654062	.2168995591
60	54000	10	190	.0972070563	.2167532379
60	54000	10	200	.0691353396	.2165944407
60	54000	11	210	.0461964004	.2164215758
60	54000	11	220	.0287454497	.2162306186
60	54000	12	230	.0157687067	.2156931270
60	54000	12	240	.0047862990	.1855097275

APPENDIX II

NOMENCLATURE

A	eddy diffusion mass transfer resistance term in van Deemter equation
B	axial diffusion mass transfer resistance term in van Deemter equation
C	concentration of solute in the mobile phase
C_1, C_2	gas phase solute concentration at points 1 and 2 in Barker and Lloyds H.T.U. model
C_{n-1}, C_n	concentration of solute in mobile phase of plate (n-1) and n in the simulation model
C_o	initial concentration of solute in plate n used in the simulation model
C_f	feed concentration in the simulation model
C_m' and C_s'	resistance to mass transfer in mobile and stationary phases
d_p	mean particle diameter
D_m	diffusivity of the solute
F_f	feed flow rate in the simulation model
F.R.P.	fructose rich product
G.R.P.	glucose rich product
H	plate height
HETP	height equivalent to a theoretical plate
k	capacity factor
k"	rate constant of desorption
K_d	equilibrium distribution coefficient
L	length of packed column
L_3	post-feed mobile phase flow rate
L_4	purge flow rate
L_e	pre-feed mobile phase flow rate

L_f	feed flow rate
L'_m	mean mobile phase flow rate in the pre-feed and post-feed sections
N	number of theoretical plates
P	stationary phase flow rate
ΔP	pressure drop
q	solute concentration in the stationary phase
Q	mobile phase flow rate in the simulation model
R_s	resolution
S	switch period
r_c	column radius
t_R	retention time
v	mobile phase velocity
v_{opt}	optimum mobile phase velocity
V_D, V_F, V_G	retention volume of dextran, fructose and glucose
V_M	mobile phase volume in a column
V_o	void volume
V_s	stationary phase volume in a column
V_T	total column volume
W	band width at the base line
$W_{h/e}$	band width measured at a height equal to the peak height divided by the 'e'
α	relative retention or separation factor
β	selectivity of ion exchangers
γ_1, γ_2	rate transfer of molecules from gas to liquid and from liquid to gas in Al-Madfai model
δ_1	coefficient for the effect of feed concentration on the distribution coefficient

δ_2	coefficient for the effect of semi-continuous mode of the SCCR on the distribution coefficient
ε	porosity
σ	standard deviation of the Gaussian band
μ	viscosity of the mobile phase

APPENDIX III

SAMPLES OF PRODUCTS ANALYSIS

Fig. IIIa Run 13-50-7-30-60-30

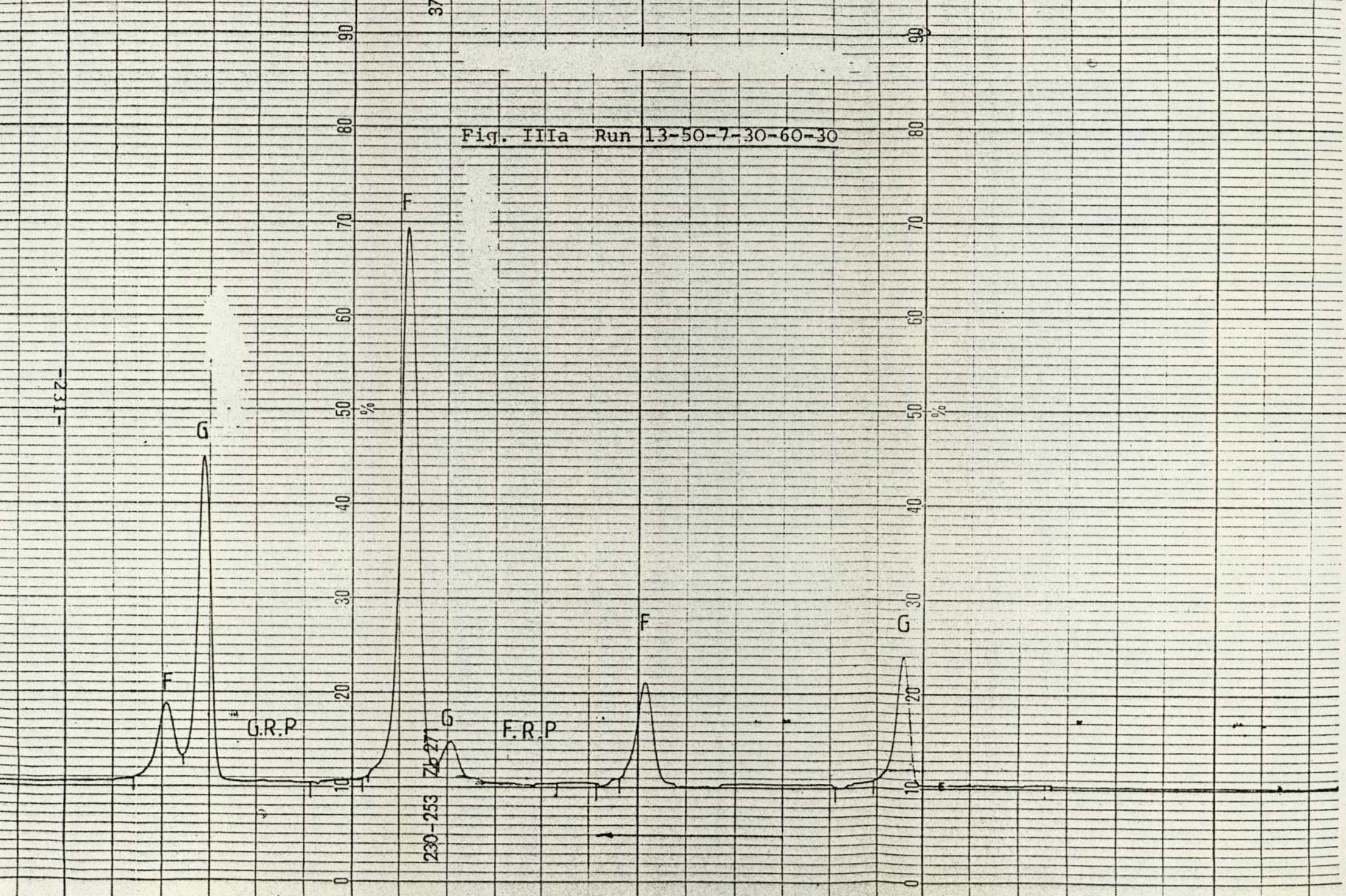

Fig. IIIb Run 16-70-7-30-60-30

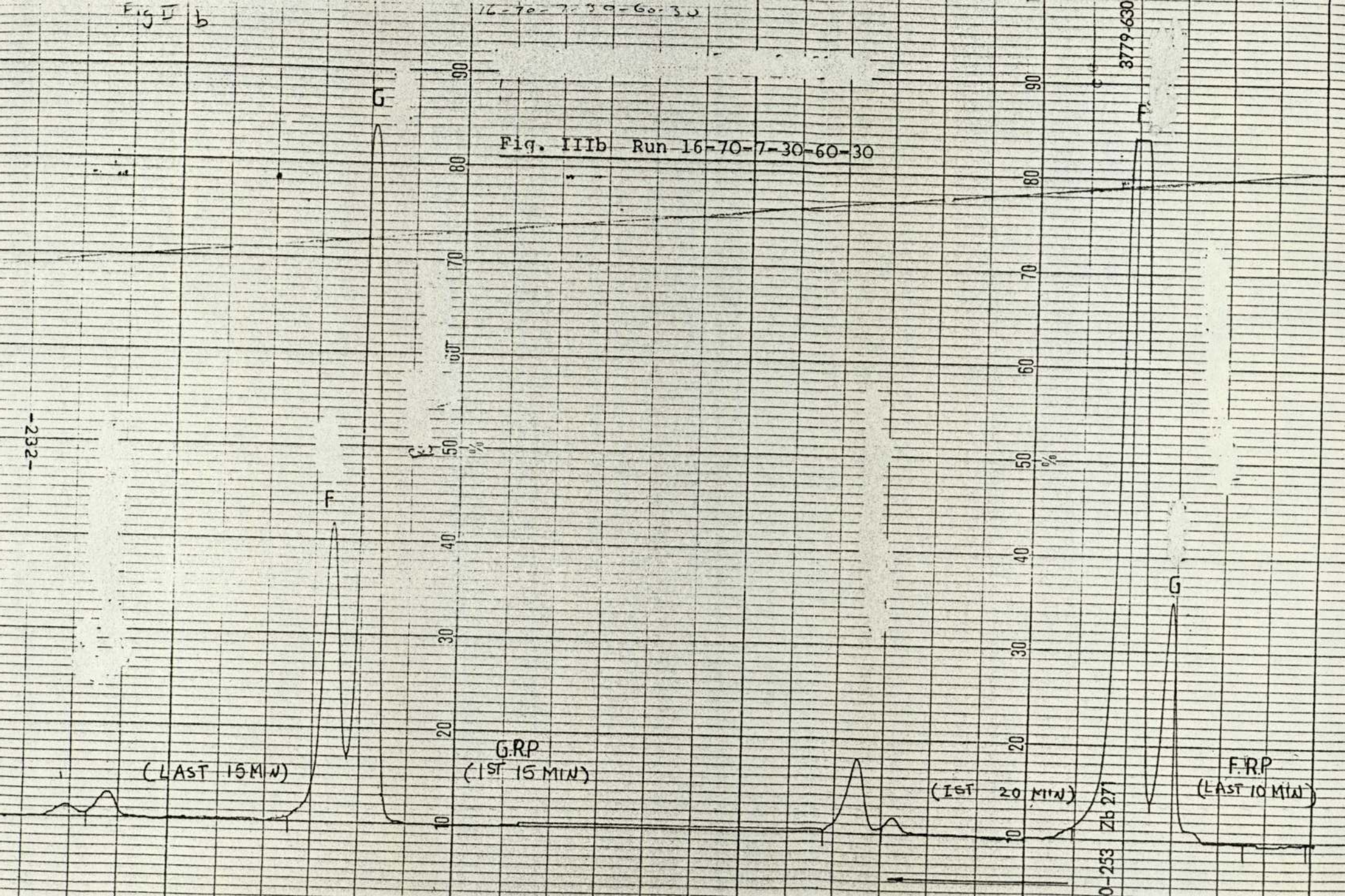

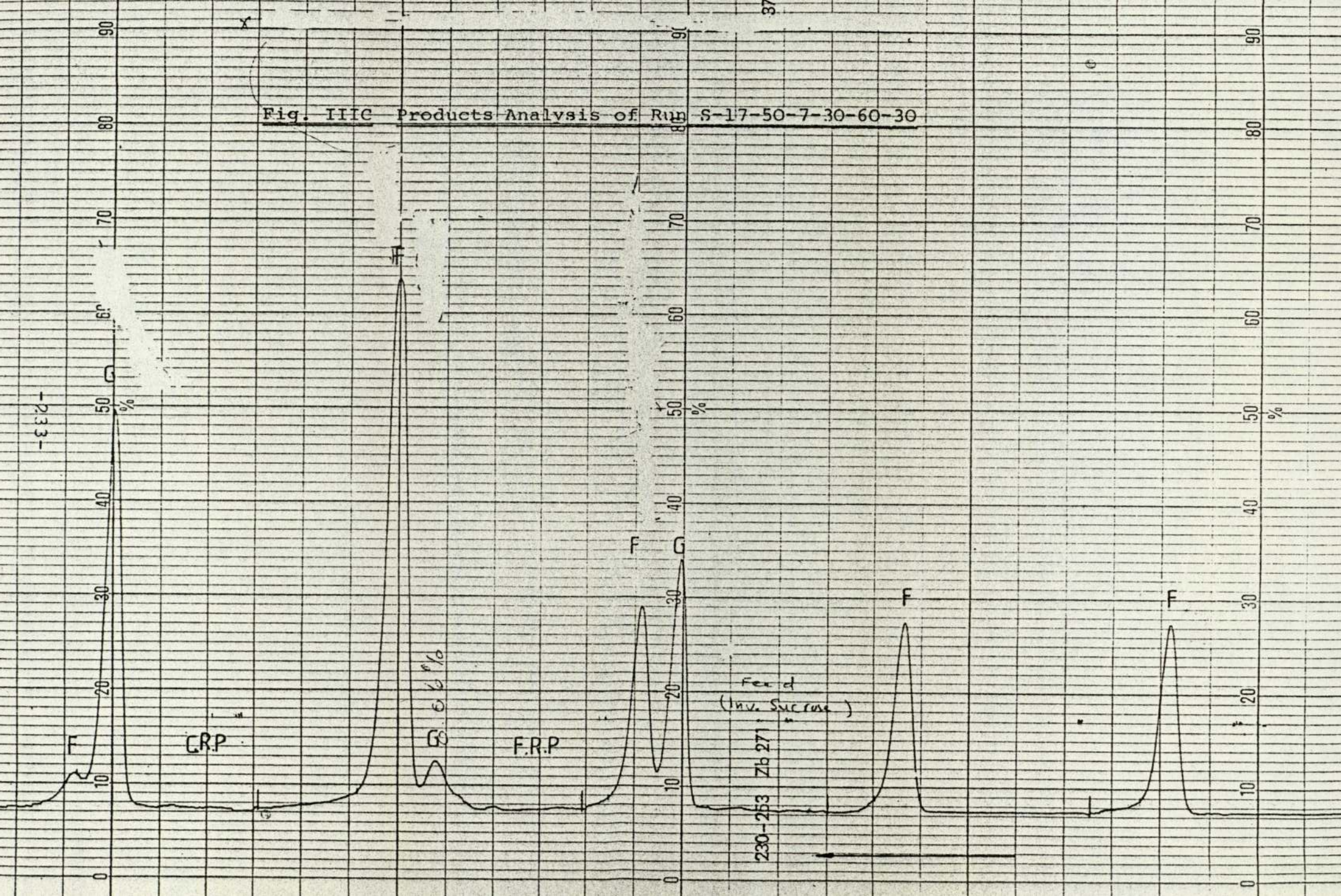

Fig. IIIC Products Analysis of Run S-17-50-7-30-60-30

APPENDIX IV

EXPERIMENTAL READINGS AND MEASUREMENTS

TABLE IVa Experimental Readings and Measurements (for SCCR7 Unit)

Run No. 13-50-7-30-60-30, Feed Concentration 50% w/v, Switch Period 30 min

Feed Column 7 Eluent Column 2 Purge Column 1

Cycle	Flow Rate ($cm^3 min^{-1}$)					Temperature (^oC)			Pressure Drop kNm^{-2}		
	Feed	Eluent	Purge	F.R.P.	G.R.P.	Pre-Feed	Pre-Eluent	Pre-Purge	Feed	Eluent	Purge
1	6.8	30	118	40	115	55	60	60	38	76	15
2	7.1	30	115	40	117	56	59	59	52	100	15
3	7.0	30	115	39	117	58	55	55	64	120	15
4	7.2	30	114	38	115	59	57	57	85	165	15
5	6.9	30	115	38	115	56	59	59	100	196	15
6	7.0	30	115	38	117	60	56	56	108	209	15
7	7.0	30	115	37	115	59	58	58	122	245	15
8	7.2	30	118	37	116	59	61	61	123	250	15
9	7.0	30	122	37	115	59	59	59	122	250	15
10	7.0	30	118	37	118	59	58	58	124	250	15

continued.....

TABLE IVa(continued)

Cycle	Temperature of Liquids Inside the Columns (°C)					
	1-2	3-4	5-6	7-8	9-10	11-12
1	57	57	58	59	59	58
2	60	55	60	60	59	60
3	55	56	57	58	59	60
4	58	57	55	56	57	60
5	58	59	58	57	60	59
6	56	57	58	58	59	58
7	58	59	57	58	58	59
8	60	60	56	58	59	60
9	59	58	59	57	60	60
10	58	57	58	58	57	59

Table IVb Experimental Readings and Measurements (for SCCR4 Unit)

Run 2-50-2-6-45-30 Feed Concentration 50% w/v Switch Period 30 minutes
Feed Column 7 Eleuent Column 2 Purge Column 1

Cycle	Flow Rate ($cm^3 min^{-1}$)					Temperature (^oC)			Pressure kN m^{-2}		
	Feed	Eluent	Purge	F.R.P.	G.R.P.	Pre-Feed	Pre-Eluent	Pre-Purge	Feed	Eluent	Purge
1	2.1	6.1	30	37.3	8.1	44	43	43	130	195	48
2	2.0	6.0	30	30.0	8.4	44	46	46	143	260	48
3	1.9	5.9	30	30.2	8.3	45	46	46	177	290	48
4	2.1	6.0	30	31.0	8.5	45	46	46	215	346	48
5	2.1	6.0	30	30.5	8.2	45	45	45	261	455	48
6	2.0	6.0	30	31.0	8.0	45	44	44	261	448	48
7	2.0	5.9	30	30.0	8.1	45	45	45	252	443	48
8	2.0	6.1	30	30.0	8.0	45	45	45	249	448	48
9	1.9	6.0	30	30.5	8.0	45	44	44	262	460	48
10	2.0	6.0	30	30.3	8.1	45	45	45	263	442	48

Table IVb continued

Cycle	Temperature of Liquids Inside the Columns (°C)					
	1-2	3-4	5-6	7-8	9-10	11-12
1	46	46	45	46	45	39
2	44	43	44	45	45	43
3	44	42	43	44	44	44
4	45	46	45	46	43	45
5	45	45	45	46	47	42
6	47	45	46	45	45	42
7	47	46	45	46	48	41
8	46	46	44	46	48	43
9	45	45	44	45	46	45
10	44	44	45	45	43	46

REFERENCES

1. Martin, A.J.P., Synge, R.L.M., Biochem. J., 35, 1358 (1941).

2. James, A.T., Martin, A.J.P., Biochem. J., 50, 679 (1952).

3. Hongisto, H.J., Int. Sug. J., 79, 100 (1977).

4. Munir, M., Int. Sug. J., 78, 100 (1976).

5. Broughton, D.B., Chem. Eng. Progr., 64, 60 (1968).

6. Bieser, H.J., de Rosset, A.J., Die Stärke, 11, 392 (1977).

7. Barker, S.A., Proc. Biochem., 10, 39 (1975).

8. Boehringer, C.F., Brit. Patent No. 1,085,696 (1967).

9. The Colonial Sugar Refining Co., Brit. Patent No. 1,083,500 (1967).

10. Sussman, M., Chem. Tech., 6, 260 (1976).

11. Odawara, H., Ohno, M., Yamazaki, T., U.S. Patent No. 4,157,267 (1979).

12. Ching, C.B., Ph.D. Thesis, University of Aston in Birmingham (1978).

13. England, K., Ph.D. Thesis, University of Aston in Birmingham (1979).

14. Chuah, C.H., Ph.D. Thesis, University of Aston in Birmingham (1980).

15. Gould, J.C., Ph.D. Thesis, University of Aston in Birmingham (1981).

16. Takasaki, Y., U.S. Patent No. 3,806,363 (1974).

17. Tiselius, A., Adv. Protein Chem., 3, 67 (1947).

18. King, C.J., 'Separation Processes', 179, 2nd Edition, McGraw Hill, New York (1980).

19. Fowkes, F.M., 'Encyclopedia of Science and Technology', Volume 1, 5th Edition, McGraw Hill, New York (1982).

20. Dorfner, K., 'Ion Exchangers Properties and Applications', Ann Arbor Science, Michigan, (1972).

21. Milton, R.M., Baffalo, N.Y., U.S. Patent No. 2,884,244 (1959).

22. Rieman, W., Walton, H.F., 'Ion Exchange in Analytical Chemistry', 224, Pergamon Press Ltd., Suffolk (1970).

23. Rodrigues, A.E., Tondeur, D.T., 'Percolation Processes: Theory and Application', 264, Sythoff and Noorhoff (1981).

24. Neuzil, R.W., Priegnitz, J.W., U.S. Patent No. 4,024,331 (1977).

25. Kulprathipanja, S., Neuzil, R.W., U.S. Patent No. 4,287,001 (1981).

26. Kirkland, J.J., 'Modern Practice of Liquid Chromatography', J. Willey, New York (1971).

27. Mikes, O., 'Laboratory Handbook of Chromatographic Methods', 190-191, Von Norstrand (1966).

28. Coulson, J.M., Richardson, J.F., 'Chemical Engineering', Volume 2, 3rd Edition, Pergamon Press, Oxford (1978).

29. Kunin, R., Ind. Eng. Chem., 49, 1365 (1959).

30. Audebert, R., Polymer, 20, 1561 (1979).

31. Purnell, J.H., J.Chem.Soc., 1268 (1960).

32. Yau, W.W., Kirkland, J.J., Bly, D.D., 'Modern Size Exclusion Liquid Chromatography', 53, J. Willey, New York (1979).

33. Giddings, J.C., 'Dynamics of Chromatography, Part 1, Principles and Theory', Chap. 1, Edward Arnold, London (1965).

34. Glueckauf, E., Trans. Faraday Soc., 51, 34 (1955).

35. Lapidus, L., Amulson, N.R., J.Phys.Chem., 56, 986 (1952).

36. Van Deemter, J.J., Zuidermann, F.J., Klinkenberg, A., Chem.Eng.Sci., 5, 271 (1956).

37. Giddings, J.C., Mallik, K.L., Anal.Chem., 38, 8, 997 (1966).

38. Badour, R.F., U.S. Patent No. 3,250,505 (1966).

39. Lauer, K., Stoeck, G., U.S. Patent No. 3,539,505 (1970).

40. Melaja, A.J., Hämäläinen, L., Rantanen, L., U.S. Patent No. 3,928,193 (1975).

41. Barker, P.E., Deeble, R.E., Chromatographia, 8, 2 (1975).

42. Barker, P.E., Critcher, D., Chem.Eng.Sci., 13, 82 (1960).

43. Barker, P.E., Barker, S.A., Hatt, B.W., Somers, P.J., Chem.Proc.Eng., 52, 64 (1971).

44. Wankat, P.C., Ind.Eng.Chem.Fundam., 16, 468 (1977).

45. Wankat, P.C., Oritz, P.M., Ind.Eng.Chem.Process Des.Dev., 21, 416-420 (1982).

46. Broughton, D.B., Neuzil, R.W., Chem.Eng.Progr., 9, 66-70 (1970).

47. Szepesey, L., Sebestyen, Z., Feher, I., Nagi, Z., J. Chromatog., 108, 285 (1975).

48. Barker, P.E., Deeble, R.E., Anal.Chem., 45, 1121 (1973).

49. Guthrie, R.D., Honeyman, J., 'An Introduction to the Chemistry of Carbohydrates', 3rd Edition, Clarendon Press, Oxford (1968).

50. Ferrier, R.J., Collins, P.M., 'Monosaccharides Chemistry', Penguin Library, London (1972).

51. Hyvönen, L.H., Varo, P., Koivistoinen, P., J. of Food Sci., 42, 3 (1977).

52. Birch, G.G., Green, L.F., Coulson, C.B., 'Sweetness and Sweeteners', Applied Science Publishers, London (1971).

53. Birch, G.G., Parker, K.J., 'Sugars: Science and Technology', Chapter 14, Applied Science Publishers, London (1979).

54. Marshall, R.O., Kooi, E.A., Science, 125, 648 (1957).

55. Takasaki, Y., Agri.Biol.Chem., 30, 1247 (1966).

56. Editors, Food Processing, 40, 74-75 (1979).

57. Richards, G.N., F. Shafizadeh, Aust.J.Chem., 31, 1825-32 (1978).

58. Herve, D., Process Biochem., 6, 31-34 (1974).

59. Hongisto, H., H. Heikkila, 'Desugarization of Cane Molasses by the Finnsugar Chromatographic Separation Process', Finnsugar Eng. Publication, Kantvik (1977).

60. Bichsel, S.E., Wang, Y., Sandre, A.M., U.S. Patent No. 4,263,052 (1981).

61. Samuelson, O., Sjöstrum, Swensk Kem. Tidski, 64, 305 (1952).

62. Serbia, G.R., U.S. Patent No. 3,044,904 (1962).

63. Leferve, L.J., U.S. Patent No. 3,044,905 (1962).

64. Leferve, L.J., U.S. Patent No. 3,044,906 (1962).

65. Odawara, H., Nogushi, Y., Ohno, M., U.S. Patent No. 4,014,711 (1977).

66. Lippman, E.O., Abstract from J.A. Rendleman Jr., Adv. in Carbohydr. Chem. and Bioch., 24, 209 (1966).

67. Vogal, H., Georg, A., Abstract from J.A. Rendleman Jr., Adv. in Carbohydr. Chem. and Bioch., 24, 209 (1966).

68. Charley, P.J., Abstract from J.A. Rendleman Jr., Adv. in Carbohydr. Chem. and Bioch., 24, 209 (1966).

69. Angyal, S.J., J. Chem., 25, 1957-66 (1972).

70. Angyal, S.J., J.Chem., 27, 1447-1456 (1974).

71. Angyal, S.J., J.Chem., 28, 1279-1287 (1975).

72. Angyal, S.J., J.Chem., 28, 1541-1549 (1975).

73. Angyal, S.J., Olis, J., James, V.J., Pojer, P.M., Carbohydr. Res., 60, 219 (1978).

74. Rendleman, J.A., Adv. in Carbohydr. Chem. and Bioch., 24, 209 (1966).

75. McKenzie, J.E., Quin, J.P., J.Chem.Soc., 951 (1929).

76. Lindberg, B., Glessor, K.N., Carbohydr. Res., 5, 286-291 (1967).

77. Kulprathipanja, S., Neuzil, R.W., U.S. Patent No. 4,319,928 (1982).

78. Wood, C.W., 'Inorganic Chemistry', 3rd Edition, Butterworths, London (1967).

79. Giddings, J.C., Anal.Chem., 40, 14, 2143 (1968).

80. Comyns, A.E., Laporte Industries U.K., Personal Communication (1982).

81. Thomson, F., U.S. Patent No. 2,938,817 (1961).

82. Barker, P.E., Huntington, D., Dechema Monographien, 62, 153 (1968).

83. Barker, P.E., Hatt, B.W., Williams, A.N., Chromatographia, 10, 7, 377 (1977).

84. Barker, P.E., Hatt, B.W., Williams, A.N., Chromatographia, 11, 9, 487 (1978).

85. Hyvönen, L., Varo, P., Koivistoinen, P., J. Food Sci., 42, 3,657 (1977).

86. Hyvönen, L., Varo, P., Koivistoinen, P., J. Food Sci., 42, 3,654 (1977).

87. Velasco, V.S., Dowling, J.F., Proc. Cane Sug. Refin. Res., 138-154 (1974).

88. Samuelson, O., 'Ion Exchange in Analytical Chemistry', 329, John Wiley and Sons, New York (1963).

89. Barker, S.A., Chemistry Dept., Birmingham University, Personal Communication, March (1981) and Sept. (1982).

90. Somers, P.J., Chemistry Dept., Birmingham University, Personal Communication, June (1981), Sept. (1982).

91. Nolan, J.D., Dia-prosim Ltd., Pontyclun, Wales, Private Communication (1981).

92. Leiser, R.S., Liaw, G.C., Brit. Patent No. 1,548,543 (1979).

93. "Ion Exchange Properties", Published by B.D.H. Ltd (1976).

94. Woodbury, R., Chemistry Dept., Birmingham University, Private Communication (1981).

95. Thawait, S., Chemical Engineering Department, Aston University in Birmingham, Private Communication (1982).

96. Glueckauf, E., J.Chem.Soc., 1302 (1947).

97. Huang, S., Wilson, J.W., Overholser, K.A., J. Chromatography, 89, 119 (1974).

98. Zhitomirskii, B.M., Agafonow, A.V., Berman, A.D., Yanowski, M.I., J. Chromatography, 94, 1 (1974).

99. Jönsson, J.A., Chromatographia, 13, 5, 273-276 (1980).

100. Scaince, C.T., Crosser, O.K., A.I.Chem.Eng.J., 12, 1, 100 (1966).

101. Al Madfai, S., PhD Thesis, University of Aston in Birmingham (1969).

102. Barker, P.E., Lloyd, D., Symposium on the Less Common Means of Separation, Inst. Chem. Eng. (1963).

103. Sunal, A.B., PhD Thesis, University of Aston in Birmingham (1973).

104. Deeble, R.E., PhD Thesis, University of Aston in Birmingham (1974).